

~~CONFIDENTIAL~~

Copy No. \_\_\_\_\_ 58

# THE VANGUARD SATELLITE LAUNCHING VEHICLE - AN ENGINEERING SUMMARY \*

(Engineering Report No. 11022)

April 1960

*reger*

(Contract No. Nonr-1817 (00))

Prepared by:

B. Klawans

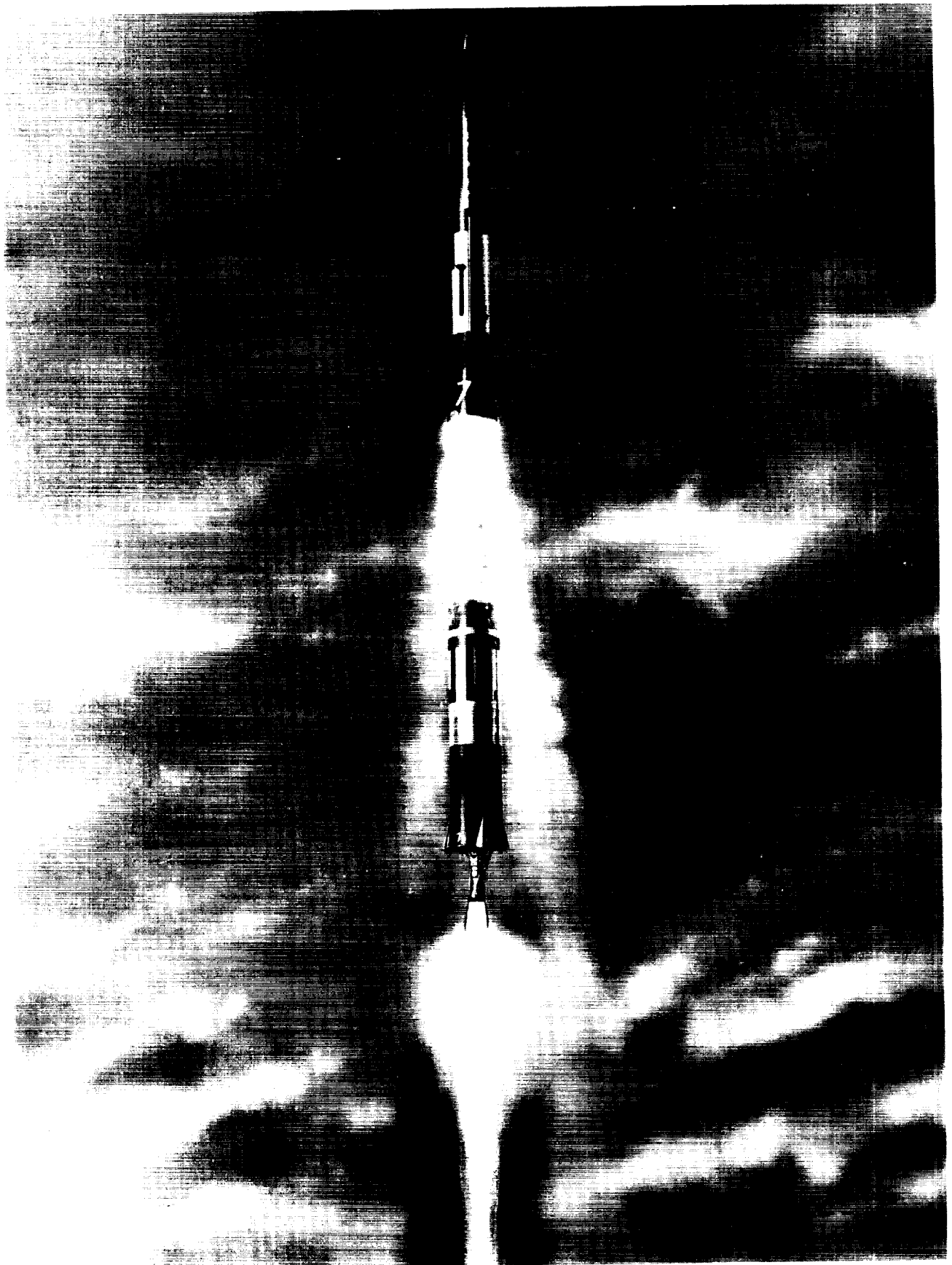
Technically Edited  
and Approved by:

J. Banghardt

5524004

THE MARTIN COMPANY, Baltimore, Md.

~~CONFIDENTIAL~~



## FOREWORD

This engineering summary for the Vanguard satellite launching vehicle has been prepared by the Martin Company for the National Aeronautics and Space Administration, in fulfillment of Item AB of Martin Specification No. 1082, under United States Navy Contract No. Nonr-1817(00).

The Martin Company acknowledges the valuable information and guidance furnished by Mr. J. M. Bridger, of the National Aeronautics and Space Administration, who instigated the report effort.

# CONTENTS

FOREWORD .....	iii
CONTENTS .....	iv
SUMMARY .....	vii
I. INTRODUCTION .....	1
II. BACKGROUND	
A. State of the Art in 1955 .....	3
B. Vanguard Program Philosophy .....	4
III. VEHICLE DESIGN AND DEVELOPMENT	
A. Mission Requirements .....	7
B. Trajectory Simulation .....	7
C. Staging and Flight Path Considerations .....	8
D. Performance Optimization .....	9
E. Aerodynamics .....	10
F. Structure .....	18
G. Weight Control .....	25
H. Final Vehicle Configuration .....	25
IV. SYSTEMS DESIGN AND DEVELOPMENT	
A. Guidance and Control .....	29
B. First-Stage Propulsion .....	40
C. Second-Stage Propulsion .....	51
D. Third-Stage Propulsion .....	62
E. Separation .....	66
F. Ordnance .....	70
G. Electrical .....	72
H. Mechanical .....	77
I. Hydraulic .....	80
J. Range Safety .....	84
K. Instrumentation .....	85
L. Systems and Payload Integration .....	86
V. RELIABILITY	
A. Requirement .....	89
B. Environmental Criteria .....	89
C. Component and System Qualification .....	89
D. Component and System Acceptance Testing .....	95
E. Vehicle Acceptance Testing .....	95
F. Reliability Follow-up .....	96
G. Observations on Reliability .....	98

VI.	FIELD OPERATIONS	
	A. Launch Complex .....	99
	B. Field Testing .....	104
	C. Range Safety Considerations .....	106
	D. Flight Loading and Performance Predictions .....	106
	E. Launch Operations .....	109
VII.	VEHICLE FLIGHT ANALYSIS	
	A. Flight Summary .....	112
	B. Vehicle Trajectories .....	118
	C. Aerodynamics .....	118
	D. Structure .....	120
VIII.	SYSTEMS FLIGHT ANALYSIS	
	A. Guidance and Control .....	123
	B. First-Stage Propulsion .....	132
	C. Second-Stage Propulsion .....	139
	D. Third-Stage Propulsion .....	150
	E. Separation .....	151
	F. Ordnance .....	156
	G. Electrical .....	156
	H. Mechanical .....	159
	I. Hydraulic .....	159
	J. Range Safety .....	161
	K. Instrumentation .....	163
IX.	SIGNIFICANT FLIGHT ANALYSIS TECHNIQUES	
	A. Philosophies .....	165
	B. Techniques .....	165
X.	PROGRAM ACCOMPLISHMENTS	
	A. Satellite Orbits .....	169
	B. Mission Capabilities of the Final Vehicle .....	169
	C. Advances in the State of the Art .....	170
XI.	REFERENCES .....	177
XII.	BIBLIOGRAPHY .....	179
	APPENDIX: PROBABILITY METHOD OF PERFORMANCE PREDICTION .....	A-1



## SUMMARY

Project Vanguard was conceived in 1955 for the purpose of establishing a scientific satellite in orbit about the earth during the International Geophysical Year (July 1957 to December 1958). It was planned and implemented as a low priority, economical effort that would not interfere with military missile development. This report has been prepared by The Martin Company to summarize the engineering of the rocket vehicle that launched the Vanguard satellites.

The Vanguard vehicle was a three-stage finless rocket with a liftoff weight of approximately 22,800 pounds; 88% of this weight was propellant. The first two stages were liquid-propellant rockets, guided by a "strapped-down" gyro reference system, and controlled by engine gimbaling and reaction jets. The third stage was a solid-propellant rocket motor, unguided but spin-stabilized. A jettisonable nose cone protected the payload. Launchings were made from the Atlantic Missile Range, Cape Canaveral, Florida.

Unique design concepts and advanced analytical techniques were developed during the Vanguard program. Significant examples are the use of structural feedback to reduce structural loads, trajectory matching for flight analysis, and a remarkably accurate statistical approach to performance prediction.

The established goal was at least one satellite orbit in six attempts. Actually, the number of attempts was increased to eleven by the use of five vehicles initially programmed for flight development testing. Three satellites were placed in orbit, containing four of the six scientific experiments originally planned for Project Vanguard. The success of the satellite launching vehicle is further manifested by the continuing use of Vanguard hardware, design concepts and analytical techniques in other advanced rocket programs.



# I. INTRODUCTION

The concept of launching small earth satellites for scientific purposes during the International Geophysical Year (IGY) was recommended for the consideration of the participating nations in October 1954 by the planning committee of the International Council of Scientific Unions. The U.S. National Committee for the IGY investigated the feasibility and scientific value of such a project and in March 1955 reported favorably to their parent organization, the National Academy of Sciences, and to the National Science Foundation. On 29 July 1955, the White House announced that the United States would construct and launch a small instrumented earth satellite as a part of its contribution to the IGY.

The Department of Defense (DOD), directed by the President to implement the program, had already under consideration several proposals from the military services for the development of satellite launching vehicles. The recommendations of the DOD Advisory Group on Special Capabilities (Stewart Committee) and the DOD Policy Council resulted in a decision on 9 September 1955 to proceed with the Navy's proposal. This plan contemplated a three-stage launching vehicle, based on the Viking and Aerobee-Hi rockets, which would not interfere with concurrent military missile programs. The Navy proposal included specific scientific uses for the payload, and an international ground tracking system (Minitrack) to trace the orbit and obtain data from the satellite.

A tri-service program was accordingly set up under Navy management and designated Project Vanguard. The Office of Naval Research retained contractual authority but delegated technical responsibility to the Naval Research Laboratory (NRL). The Stewart Committee retained an overall monitoring function for DOD. On 23 September 1955, The Martin Company was awarded the prime contract for design, construction, test and preparation for flight of the satellite launching vehicles. A detailed discussion of the history and organization of the Vanguard program is given in Ref. 1.

The above organizational structure remained in effect until May 1958, at which time the DOD monitoring function was shifted to the Advanced Research Projects Agency. On 1 October 1958, the overall responsibility for Project Vanguard was transferred from DOD to the newly created civilian agency, the National Aeronautics and Space Administration (NASA).

This engineering summary report presents a documentation of the design, development, test and flight analysis of the Vanguard satellite launching vehicles. Special emphasis is placed on basic design decisions, significant development tests, major development problems and their solutions, performance prediction methods, flight analysis techniques and program results.



## II. BACKGROUND

### A. STATE OF THE ART IN 1955

When the earth satellite program became a reality in 1955, the state of the art of rocketry (in the Western world, at least) was barely ready for it. The early work of Goddard and the other pioneers had been accorded little recognition until the startling appearance of the German V-2 late in World War II. Post-war rocket development, based largely upon the German work, had been sporadically promoted and financed. The Navy had enjoyed success with the Viking single-stage research rocket and was considering advanced versions of this vehicle. The Army had successfully developed the single-stage Corporal and Redstone ballistic missiles and had initiated design of the Jupiter IRBM. The Air Force Atlas ICBM was approaching the hardware stage, although the first flight was still about two years away. The Thor and Titan programs were just getting under way, essentially concurrent with Vanguard.

### 1. VEHICLE SYSTEMS

Specific vehicles that preceded Vanguard had more or less avoided the loads problem by accepting relatively high structural safety factors ( $> 1.5$ ), with correspondingly low ratios of propellant to loaded weights. In fact, the Viking, with a value of 0.8, had the highest mass ratio of any vehicle flown to date.

**Aerodynamics**—Considerable hypersonic wind tunnel data and theoretical analysis had been developed, and there was some flight experience on vehicles such as V-2, Viking, Aerobee, and ordnance shells. Transonic flow was not well understood. Little was known about heat transfer, since flight data were meager and theories were unconfirmed.

A general study of wind shear and gust probabilities had been made by the Air Force (Ref. 2) to be used for the design of operational military missiles on a 99% probability basis. However, this criterion was considered too severe for a scientific research vehicle. The Air Force Air Weather Service had accumulated and analyzed a body of data on upper atmosphere winds and gusts at Patrick Air Force Base for a two-year period. Some White Sands Proving Grounds data were also available. Theoretical extrapolations of upper atmosphere density, temperature and pressure to high altitudes had been computed, but required almost constant revision as later data became available. Wind-induced oscillations while the vehicle was on the launch stand had not been considered in previous designs.

**Separation**—There was little experience with tandem staging; some tandem staging had been done on the Bumper-Wac V-2 in 1949, the much smaller (1500-pound) Aerobee and various small rockets (using solid-propellant motors). Some preliminary designs had been conceived for large tandem stage separation of liquid-propellant rockets. The Atlas 1-1/2 stage concept had progressed to the detailed design phase, but the problem of ignition at altitude had been avoided by starting all engines before launch.

### 2. GUIDANCE AND ATTITUDE CONTROL

**Control configurations**—Carbon jet vanes and aerodynamic surfaces were used for powered flight control on the V-2 and later on the Redstone rocket. The Viking had pioneered the use of a gimbaled rocket engine, but still retained fixed fins and control tabs, although a finless configuration had been studied. The gimbaled engine approach was considered superior from the performance and reliability standpoints, because carbon vanes added drag and often burned or broke off, while electro-hydraulic gimbal actuation systems were rapidly reaching high levels in efficiency and reliability. The background for coasting flight control was primarily that of the Viking "tumble-jet" system. There was no other approach then available that was remotely competitive in terms of weight and demonstrated performance.

**Reference systems**—The attitude reference for Viking was provided by a conventional medium-precision, vertical-directional gyro combination with drift rates on the order of  $\frac{1}{8}$  degree per minute. Appreciably lower drift vertical-directional gyro units capable of performing in the rocket environment were not in existence. Gimbaled inertial platforms with greater precision were in development, but weighed in excess of 100 pounds, including electronics. However, low-drift, single degree of freedom integrating rate gyros were becoming available.

**Autopilots**—The Viking autopilot used d-c lead circuits, a-c gyro pickoffs, d-c transfer valve and follow-up excitation and miniature vacuum tube circuits for the proportional channels. The arrangement was more or less standard for contemporary missile systems, although many used rate gyros for lead compensation. For the periodic or "bang-bang" controls channels of Viking during coasting flight (pitch, yaw and roll jets) the implementation was similar—except that threshold amplifiers, relays, and on-off valves were used instead

of transfer valves and follow-ups. There had been very little use of reaction jets as "bang-bang" controls prior to the Viking program.

At the inception of the Vanguard program, two new approaches to autopilots were being considered by the missile industry—magnetic amplifiers and transistor circuits—to replace tubes. Magnetic amplifiers promised longer life and greater reliability. Transistors promised smaller weight and volume as well as reliability, but the state of development of basic transistor circuits was behind both vacuum tubes and magnetic amplifiers.

### 3. PROPULSION

**Liquid rocket propulsion**—Probably the largest rocket in flight status in 1955 was the Army Redstone, with a takeoff thrust of about 75,000 pounds. The smaller Navy Viking had a takeoff thrust of about 20,000 pounds. Both rockets utilized liquid oxygen and alcohol as propellants, and delivered sea level specific impulse in the 190- to 220-second range, during burning periods up to 110 seconds. Engines were under development, using hydrocarbon fuels, which would increase specific impulse to the 240- to 250-second level.

**Solid rocket propulsion**—In general, operational solid rockets in 1955 were restricted to relatively short burning times and comparatively low specific impulse (of the order of 210 seconds). Mass ratios as high as 0.85 were exceptional. Since their operation had been generally as boosters within the sensible atmosphere, where aerodynamic attitude control was feasible, little or no development had occurred in thrust vector control. Similarly, there was little knowledge of the operational environment at very high altitudes.

## B. VANGUARD PROGRAM PHILOSOPHY

The Vanguard program was planned from the outset as a comparatively low priority, economical effort, which would not be allowed to interfere with concurrent military ballistic missile development. The schedule was predetermined by the fixed dates of the IGY (July 1957 through December 1958) which required completion of the entire program in about three years. The combination of these factors introduced basic design and test philosophies which set the pattern for the project.

**Vehicle program**—In order to achieve the established goal of orbiting a satellite during the IGY, it was decided that six launching vehicles of the final configuration (SLV) should be provided—a significant measure of the initial reliability concept. The flight test program originally planned for development of the SLV configuration was the minimum considered ade-

quate for the attainment of such reliability and consisted of six test vehicles (TV) and three backup vehicles (TV-BU). The first two test vehicles were basically Viking rockets. These were used because they were available and well suited for initial checkouts of the launching and tracking facilities and personnel and for early flight testing of some Vanguard components. Subsequent test vehicles introduced the actual Vanguard configuration in increasing stages of completeness (see Chapter VII, Section A). Each backup vehicle was an identical replacement for one of the Vanguard test vehicles, to be used as such only in the event of a major deficiency in the primary test.

Plans for an instrumented nose cone for TV-3 were changed in the summer of 1957 in favor of a small satellite payload that was also to be used in TV-4. The change was made because a successful orbit would permit ground checks of the world-wide tracking system (Minitrack). This was felt to be potentially more valuable than additional third-stage data in view of the success with the TV-1 instrumented nose cone flight. A small (four-pound) payload was chosen over a full size (21.5-pound) satellite to increase the performance margin. A consequence of this change was that the firing of the *first* three-stage Vanguard test vehicle became a formal satellite launching attempt.

**Production philosophy**—While Vanguard could hardly be termed a "production" program from a quantity standpoint, the schedule did not permit the "experimental," one-vehicle-at-a-time pace of the earlier Viking program. Production engineering, and even fabrication of vehicles, had to proceed concurrently with design, development, and qualification.

**Component and system selection**—Another significant effect of the schedule and budget was to dictate the utilization, wherever feasible, of previously developed components and systems for the launching vehicle. Obviously, mission requirements, weight, environmental criteria, materials compatibility, and reliability were the primary considerations, but this "off-the-shelf" concept profoundly influenced early Vanguard design decisions. In retrospect, it must now be conceded that the "shelf" provided relatively little of the ultimate hardware.

**Performance and weight control**—The critical nature of orbital velocity and injection angle requirements (see Fig. 1), combined with the state of the art of rocketry at the time, necessitated a conservative approach to the design of the launching vehicle from a performance standpoint. Design calculations were based upon "minimum" or "maximum" extremes of performance, which assumed all known tolerances accumulated in the most unfavorable direction. In fact, since it could never be guaranteed that

*all* possible tolerances had been considered, some additional performance margin was generally provided. The extreme conservatism of this approach became more apparent as flight experience accumulated, and the vehicle ultimately demonstrated capability considerably in excess of the original mission requirements (see Chapter X, Section B). This philosophy, combined with the launch weight limitations imposed by first-stage thrust available, required that critical attention be given to vehicle weight control (see Chapter III, Section G).

***Test philosophy***—The minimal nature of the flight test program dictated considerable emphasis upon ground testing, although extensive reliability testing of components and systems in quantity was incompatible with both schedule and budget. But this very fact—the absence of formal reliability data—placed additional reliance on development, qualification and acceptance tests for components and systems, and on plant and field functional checkout procedures for the assembled rocket. The subject of reliability is treated at length in Chapter V.



### III. VEHICLE DESIGN AND DEVELOPMENT

#### A. MISSION REQUIREMENTS

The Vanguard contract was awarded on the basis of a joint NRL-Martin preliminary study which indicated that a three-stage vehicle of the order of 20,000 pounds gross weight would be capable of imparting orbital velocity to a payload of 21.5 pounds. This payload weight was written into the original design specification (Ref. 3). An improved third stage permitted a payload increase to 55 pounds for the last vehicle.

An orbit lifetime of at least two weeks was considered necessary to provide sufficient data for the scientific experiments. Although the uncertain composition of the atmosphere at extreme altitudes precluded an accurate determination, it was estimated that an initial orbit perigee of not less than 200 statute miles would ensure adequate lifetime, and this figure was specified. To provide a workable margin for angular and velocity errors at the point of injection into orbit, a "nominal" injection altitude of 300 statute miles was established. Originally, the orbit apogee was considered to be limited by the requirements of the scientific experiments to not more than 800 statute miles. However, the stringent flight path demands imposed by the apogee limitation (illustrated in Fig. 1) caused reconsideration of this requirement, which was relaxed to 1400 statute miles and was subsequently eliminated altogether.

The specification required capability for a maximum of 45 degrees inclination of the orbit to the equator, although the required easterly launch from Cape Canaveral would result in inclinations of the order of 30 degrees. A tolerance of two and one-half degrees was established for deviation of the initial orbit from the prescribed inclination angle.

The external configuration of the Government-furnished 21.5-pound satellite payload was chosen as a sphere for numerous reasons, the primary ones being optimum light reflection for optical tracking and elimination of the attitude variable from calculations of atmospheric density based on decay of the orbit. The sphere diameter was desired to be as large as possible to facilitate optical tracking. It was originally contemplated as 30 inches, but early design studies established 20 inches as the maximum consistent with the vehicle configuration and performance.

#### B. TRAJECTORY SIMULATIONS

Many special calculation programs were derived for simulating the vehicle's trajectory on both analog and digital computers. The most comprehensive of these

was the three-dimensional, six-degree-of-freedom, digital (IBM 704) trajectory program, designed to give the details of the complete system at any time, as well as the overall picture of the flight history. This program numerically integrated differential equations of motion for the vehicle, which included atmospheric variations and second-order effects, such as earth oblateness and forces generated by the action of the gimballed engines. Information was also provided for use in evaluating range safety and radar tracking. Those items in the program, but not directly concerned with the vehicle performance, included radar look angles, down-range distance, cross-range distance, altitude, etc., as functions of vehicle performance and time.

The Vanguard 3-D trajectory program was probably the most important single tool of the project in defining and solving the design and flight problems, especially in the areas of trajectory optimization, trajectory matching, range safety determinations, and preflight performance predictions. The trajectory program also provided Keplerian satellite information and was at times required to follow the satellite for one or two orbits after injection.

A two-dimensional digital trajectory program with a spherical earth, and a two-dimensional analog trajectory program were available, and were of great value in the early days of the project. The digital 2-D program survived the completion of the Vanguard 3-D program as an experimental tool to provide an economical, faster, but less detailed, look at a given trajectory. In this manner, the gross effects of a wide range of parameters could be examined before more critical studies were made.

In addition to these full-trajectory programs, others were devised to provide more detailed knowledge of the system at critical points of the trajectory. The launch-stand clearance program was a digital study to determine vehicle position during the few seconds following ignition. First-stage separation was examined in an analog study with and without hardware. Third-stage separation was analyzed by a digital solution. The two-body spin problem for the heavy ( $\approx 190$ -pounds) nose cone of TV-1 was never rigorously solved. However, analytical work by the NORC group at the Naval Proving Grounds, Dahlgren, Virginia and The Martin Company was sufficiently complete to satisfy range safety requirements. A digital program was derived for investigation of the two-body spin history and flight path deviations for the heavy ( $\approx 50$ -pounds) payload of TV-4BU.

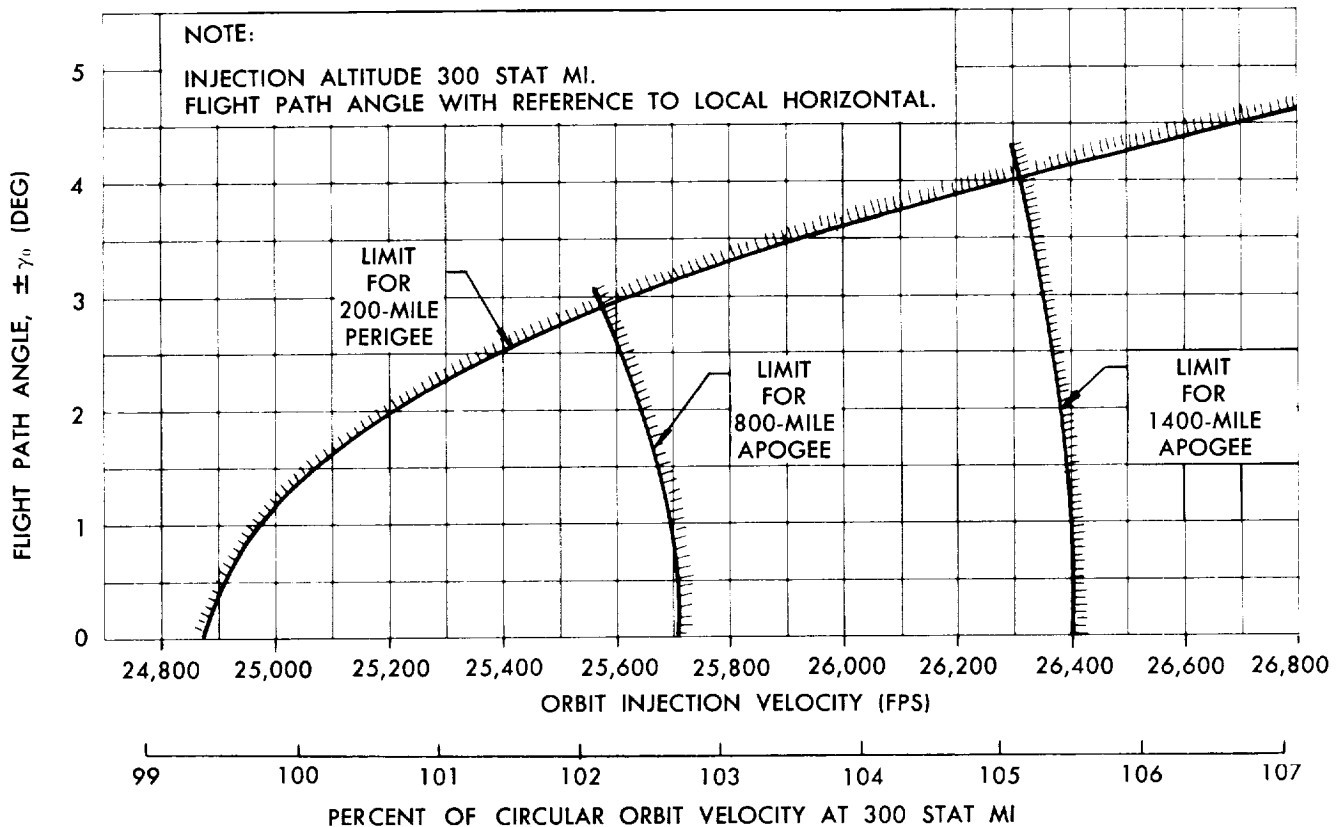


Fig. 1 Orbit Injection Tolerances for Vanguard Mission

### C. STAGING AND FLIGHT PATH CONSIDERATIONS

The number of stages and the trajectory to be used were perhaps the most basic decisions affecting performance and guidance in the design of a satellite launching rocket vehicle to fulfill given orbit requirements. The actual selections influenced and were influenced by the character and size of the individual stages, their type of guidance, complexity, and types of propulsion system and propellants (liquid or solid) to be used.

**Staging combinations**—Single- or two-stage vehicles offered much in simplicity and reliability but would have made great demands upon propulsive efficiency and guidance accuracy. The possible three-stage combinations fell into three categories which depended upon the extent of guidance chosen. A vehicle having guidance in all three stages would alleviate stringent accuracy requirements, but the weight of the guidance in the final stage would require an excessively large vehicle. On the other hand, vehicles having unguided second and third stages would require that the first-stage coasting apogee be, for all practical purposes, the maximum orbit perigee obtainable, regardless of the velocity contribution of the upper stages. Although

this system offered simplicity in the later stages, it did so by using an inefficient trajectory and by placing a high premium on first-stage guidance precision. A three-stage vehicle with two guided stages and an unguided but spin-stabilized third stage, fired at second-stage apogee, represented the most efficient vehicle combination consistent with rocket technology at that time. Such a combination was reasonably compatible with the "off-the-shelf" concept—rocket engines existed which, with some modification, would be suitable for at least the first two stages. This configuration was selected for the Vanguard vehicle prior to formal initiation of the program.

**Trajectory**—The Vanguard trajectory had to achieve the required injection conditions at 300 statute miles while fulfilling various requirements. The initial vertical flight was limited to ten seconds by range safety considerations, and the azimuth had to be such that impact could never occur on a land mass and command control capability could be maintained throughout flight.

Aerodynamic forces in flight had to be minimized to avoid excessive structural weight and consequent loss in performance. For this reason, a near zero-lift trajectory was chosen during the portion of powered flight

when atmospheric forces were appreciable. Since a perfect zero-lift trajectory was not practical because of probable wind disturbances and gross guidance system complications, a simplified ascent trajectory was used, employing several constant rates for changing the pitch gyro attitude reference. This caused the vehicle to approximate a zero-lift trajectory through a still atmosphere. The magnitudes and insertion times of the pitch rates were determined by approximating, with a series of carefully chosen straight lines, the attitude history of the computed trajectory that best satisfied the flight requirements.

The third-stage trajectory was limited by the constant attitude of the spin-stabilized third stage. Third-stage ignition time and attitude were programmed toward achieving a horizontal flight path at third-stage burnout. The resultant flight path was therefore dependent on the flight-realized performance of the propulsion and guidance systems.

The Vanguard flight plan that resulted from the design studies is shown in Table 1. This basic plan was used throughout the program.

**Table 1**  
**Vanguard Flight Plan**

- (1) Vertical flight for 10 seconds to attain forward velocity and ground clearance before introducing any significant lateral motion.
- (2) Thereafter, gradual inclination of the flight path toward the horizontal, approximating a zero-lift trajectory at least until aerodynamic forces were no longer significant.
- (3) Second-stage powered flight immediately following first-stage burnout and separation.
- (4) Nose cone jettison shortly after second-stage ignition, when aerodynamic effects on the exposed payload would no longer be critical.
- (5) Following second-stage burnout, coasting flight along a ballistic trajectory, with vehicle attitude controlled to attain proper third-stage launching angle.
- (6) At or near apogee of the coast trajectory, spinup of third stage, separation of second stage and ignition of third to provide the final velocity increment in a direction such that the resultant velocity at burnout would be parallel to the local horizontal.
- (7) After burnout, third stage may or may not be separated from the satellite.

## **D. PERFORMANCE OPTIMIZATION**

### **1. WEIGHT DISTRIBUTION AMONG STAGES**

An optimization study was made to determine, for a given overall weight, the weight of each stage which would yield the greatest velocity at the time of injection of the satellite into orbit at an altitude of 300 miles. Calculations confirmed that maximum second-stage apogee velocity was to be expected for the lowest practical takeoff thrust-to-weight ratio (T/W). At the time, the lowest known design T/W at which a large rocket had been successfully launched was approxi-

mately 1.34 (Viking). Considerations of satisfactory control of the vehicle during the initial phase of flight led to the selection of a lower design limit for T/W of 1.20. Since minimum takeoff thrust was already established at 27,000 pounds, this corresponded to a design launch weight of 22,500 pounds.

**Selection procedure**—The weights of propellant outages as functions of usable propellants and burning times, the weights of propellants and tankages per unit change in tankage length, and current configuration information were used to determine the burning times for the first two stages as functions of their weight. In consideration of design trends, burning times in terms of stage weight were also determined based on configurations with the first-stage dry weight 200 pounds lighter, and the second-stage dry weight 100 pounds heavier, than the current configuration. With the burning times as a function of stage weight, it was then possible to determine the performance of vehicles with specific stage weights.

A number of configurations, with various third-stage weights and various ratios of second - plus third-stage weight to gross weight, were arbitrarily chosen. Trajectories were computed for each configuration to determine the velocity at the 300-mile second-stage apogee. The appropriate third-stage velocity increment was added at apogee to obtain the injection velocity. Various assumptions were made regarding the third-stage mass ratio variation with total impulse, which showed that optimum third-stage weight was critically dependent on the assumptions chosen. The expected mass ratio variation, as a function of the total impulse, was therefore carefully estimated on the basis of data available from prospective vendors of the solid rocket.

**Design weight values**—The results of these calculations were graphically analyzed to determine the stage weight distribution that resulted in maximum injection velocity. On the basis of this optimization, design gross weight values of 17,830, 4286 and 484 pounds, respectively, were chosen for the three stages. The actual stage weights of the first of the Vanguard satellite launching vehicles to be flown (SLV-1) were 17,892, 4419 and 453 pounds, respectively.

### **2. TRAJECTORY OPTIMIZATION**

The optimum trajectory pitch program varies according to a vehicle's propulsive efficiency and ability to control the payload injection angle. The estimated characteristics of the Vanguard vehicle indicated that a wide range of pitch programs and combinations of injection velocity and flight path angle could attain an initial orbit perigee of at least 200 statute miles. The number of variables affecting the velocity capability appeared to be greater than the number affecting the attitude control capability. It was therefore decided

to give more emphasis to uncertainties in the propulsion system performance. The object of the trajectory optimization, then, was to select the trajectory that maximized the injection velocity margin over that velocity needed for a 200-statute mile perigee with subminimum performance vehicles having a fixed maximum injection angle error.

**Powered flight pitch program**—A “performance map” of injection altitude as a function of injection velocity needed to orbit with a perigee of 200 statute miles, for various injection flight path angles, is shown in Fig. 2. Because of external disturbances and tolerances on the vehicle parameters, it was inevitable that there would be some finite injection angle. A maximum expected angle of 2.1 degrees, determined by simply adding all known tolerances, was used in the trajectory optimization study.

Also in Fig. 2 are curves called performance lines that show the relationship between injection altitude and injection velocity of vehicles of constant propulsion performance with varying zero-lift pitch programs. The lowest performing vehicle that can achieve an orbit with a 200-mile perigee with an injection angle of 2.1 degrees is the one whose performance line is tangent to the orbit requirement line for 2.1 degrees. This subminimum performance vehicle has orbit capability only with the particular pitch program represented by this point of tangency. The pitch program may be used to generate a “pitch-line” which is a line for a given pitch program and varying vehicle performance (Fig. 2). This line is curved below minimum performance vehicles because the performance in this range was downgraded by increasing propellant outage.

The actual pitch program used during first and second-stage powered flight for the Vanguard design was slightly modified to increase the overall probability of an orbit. This pitch program was the one on the performance line midway between the minimum and subminimum performance lines, at the point where the performance line was tangent to a constant flight path angle line.

**Coasting flight pitch program**—The rate times for the pitch programs during powered flight, as determined by the performance map method, fix the flight path through third-stage ignition. Flight path angle at third-stage ignition is therefore a function of ignition time only, once coasting flight has been established. Studies indicated that a coasting pitch trim rate of approximately  $-0.03$  degrees per second was required as the last continuous rate to correct for the changing local horizontal with third-stage firing times at or near second-stage apogee.

Reduction in the magnitude of the trim rate lessened the sensitivity of injection angle errors to firing time

errors. Thus, the tolerances in the coasting time computer (see Chapter IV, Section A) contributed less to injection angle uncertainty, and errors due to imperfect relationships between firing times and indicated velocities were reduced. However, this reduction in trim rate had the effect of increasing the spread of firing times, so longer periods of reliability were required for the control jet gas reserves and rocket components operating during the coasting phase. A balance of these coasting phase design considerations yielded a trimming pitch rate and coasting time computer constants, which in combination furnished minimum satellite injection angles and nearly optimum third-stage firing times over the entire expected range of vehicle performance variations.

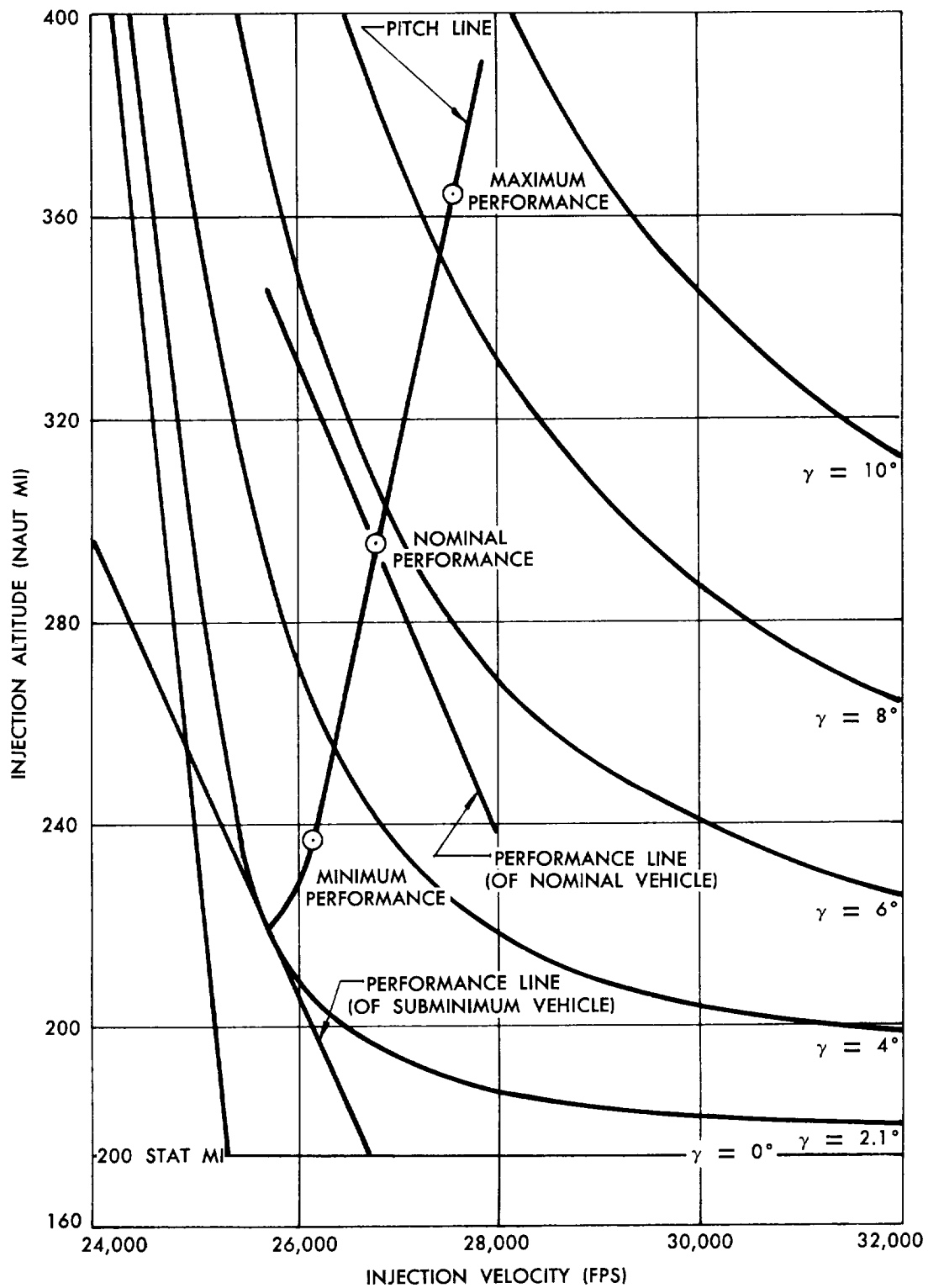
**Later optimization studies**—Later in the program, a study was conducted to determine the optimum Vanguard trajectory for maximum satellite lifetime. Satellite lifetime curves, based on injection parameters, were supplied by NRL for use in this analysis. The first phase of this study was determining the optimum powered flight pitch program. This was initiated by determining the zero-lift trajectory that maximized the orbit lifetime of the minimum vehicle selected. The existing Vanguard SLV pitch rates could be made to match this optimum zero-lift trajectory by changing insertion times only. The results of this optimization did not differ drastically from those of previous optimizations; hence the SLV pitch programs were not altered.

### 3. EQUIVALENCES

By computing numerous zero-lift trajectories, with constant second-stage apogee but variable weights, it was possible to determine changes in injection velocity as functions of stage burnout weight. The usefulness and numerical values of the stage weight equivalences are discussed in Chapter III, Section G. Values of change in injection velocity for varying values of second-stage specific impulse were also computed. These values ( $\Delta I_{sp_2}$  vs  $\Delta V_a$ ), cross-plotted against the burnout weight variation ( $\Delta w_2$  vs  $\Delta V_a$ ), resulted in a curve showing the variation of  $I_{sp_2}$  with  $\Delta w_2$  which was useful in establishing design criteria for the second-stage propulsion system. Similar computations for increased drag indicated that a 1% increase in drag ( $C_D=0.5$ ,  $M\approx 1$ ) resulted in an injection velocity decrement of 6 feet per second.

## E. AERODYNAMICS

Accurate data on air loads and aerodynamic characteristics of the external configuration were required to predict the trajectory, to design the structure and to verify the control system design criteria of the Vanguard vehicle.



**Fig. 2 Performance Map for 200-Statute Mile Perigee Orbits**

## 1. WIND TUNNEL TESTS

Three basic velocity ranges—subsonic, transonic, and supersonic — were investigated. The results of these tests (summarized in Fig. 3) were used to determine (or verify preliminary estimates of) aerodynamic coefficients, pressure distributions, center of pressure locations and running loads for the vehicle. Aerodynamic parameters based on the wind tunnel tests were also used to derive the aerodynamic transfer functions used in the vehicle dynamic stability analysis.

The first series low speed tests were made on a 12% model in the University of Maryland wind tunnel to determine the subsonic aerodynamic characteristics of the vehicle at angles of attack from zero (approximate flight path) to 90 degrees (launch stand condition). Several nose configurations were tested, along with various orientations of first- and second-stage external conduit fairings. The tests (Ref. 4) were made at a Reynolds number of  $11.27 \times 10^6$  (based on body length) and an equivalent air speed of 150 miles per hour. The lift, drag and pitching moments were appreciably increased by the fairings, whereas the different nose configurations tested had no appreciable overall effect.

A second series of low speed wind tunnel tests, using the same model and tunnel, were made to determine the Reynolds number effect on the aerodynamic characteristics. A Reynolds number range from  $4 \times 10^6$  to  $16 \times 10^6$  was examined, which corresponded to a velocity range between 50 and 200 miles per hour. The results (Ref. 5) showed a pronounced Reynolds number effect upon the aerodynamic characteristics of the complete vehicle at angles of attack above 30 degrees. Lift, drag and pitching moment increased as the Reynolds number increased. These test data were also used to verify the aerodynamic data from the first series of low speed tests.

A transonic test, in the WADC 10-foot tunnel at Wright Field, used a 7% force model and a 4.5% pressure model in several configurations, one of which included roll jet shields. In addition, tests were made with a boundary layer trip to artificially induce transition of the boundary layer from laminar to turbulent flow. The Mach number range was from 0.80 to 1.20 at a maximum Reynolds number of  $3.75 \times 10^6$  for the 7% model. These tests (Ref. 6) determined the aerodynamic characteristics and pressure distributions at low angles of attack during transonic flight conditions. Roll jet shields were found to increase lift and pitching moment over the Mach range tested.

Preliminary supersonic wind tunnel tests were made on a 3.1% scale model at the Aberdeen Proving Ground. The models used for these tests differed somewhat from the final configuration. The test results (Ref. 7) were used as the basis for the preliminary air loads

in the supersonic regime. Later supersonic wind tunnel tests were conducted in the tunnels at the Naval Air Missile Test Center at Point Mugu, California, using a 1.75% scale model of the final configuration to investigate aerodynamic characteristics and pressure distributions at Mach numbers from 1.61 to 3.5 (Ref. 8). Roll jet shields produced slight increases in lift, drag and pitching moment. The addition of a boundary layer trip behind the model nose produced no significant change in lift or pitching moment but did increase the drag somewhat. Conduit fairings could not be added to this model because of the small scale.

## 2. AERODYNAMIC LOADS

The derivation of Vanguard air loads is described in detail in Ref. 9. Critical design conditions occurred when dynamic pressure reached a maximum value, when transonic velocities were experienced, and when maximum wind shears were encountered. For the maximum performance Vanguard trajectory, these events occurred practically simultaneously at a Mach number of about 1.4 and at an altitude of 39,000 feet, after about 78 seconds of flight.

The preliminary running loads for structural design were based on the pressure distributions and force data determined from the Aberdeen supersonic wind tunnel tests. The maximum dynamic pressure condition used for design was established early in the design phase by estimating the maximum performance of the vehicle. At that time, the maximum dynamic pressure was expected to be 590 psf and the maximum angle of attack for this flight condition was expected to be 5.5 degrees. This angle of attack was composed of a 4-degree steady-state contribution, resulting from flying through a specified wind profile, and a 1.5-degree dynamic contribution, the result of a 20-fps true-velocity gust. New running loads (Fig. 4) were estimated as the configuration changed and better estimates of the performance (Fig. 5) became available. The total loads used for the basic design criterion were found to be conservative as later performance data became available.

The factors which influenced the shears and bending moments imposed upon the vehicle included such items as mass distribution and internal tank pressures which varied during the trajectory. Thus, to design the structure and controls system, it was deemed necessary to investigate conditions other than the maximum aerodynamic load condition. The aerodynamic loads were determined for the launch and burnout conditions of the first stage, representing the extreme limits for the load analysis, and for the condition at a flight time of 40 seconds, to represent a condition approximately halfway between launch and maximum dynamic pressure. In addition, a pre-launch study was included to determine the wind criteria and structural requirements to prevent vehicle toppling while on the launch stand with the

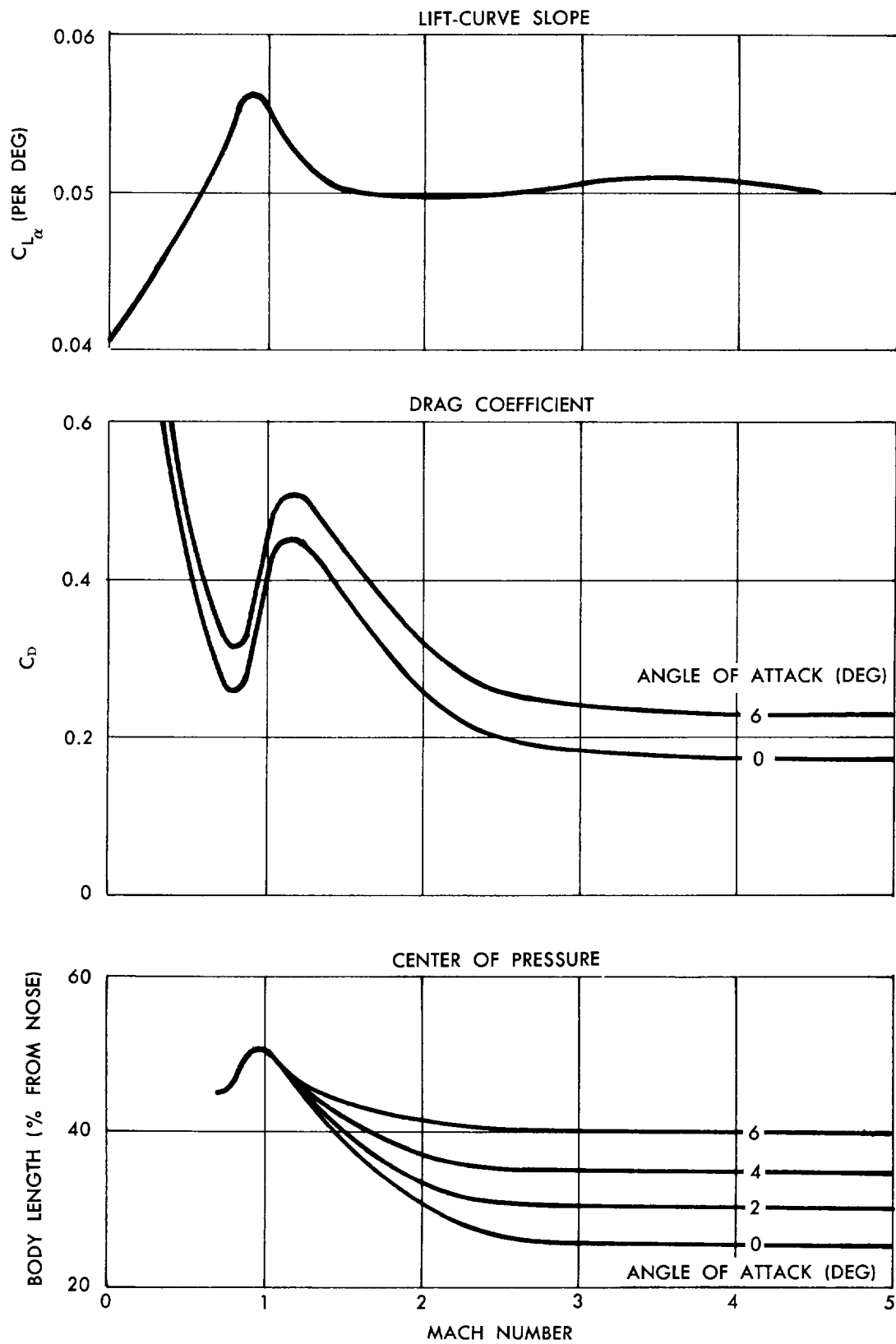


Fig. 3 Vehicle Lift, Drag Coefficient and Center of Pressure vs Mach Number

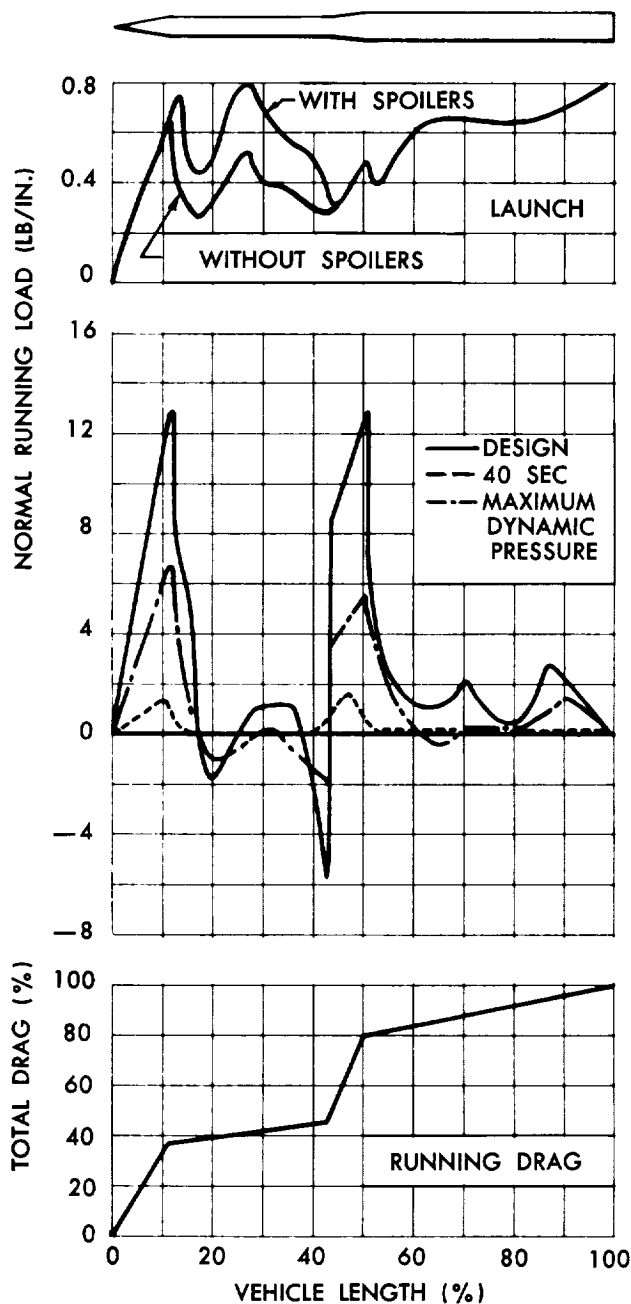


Fig. 4 Running Airloads

gantry removed. The maximum allowable wind for this condition, with all propellants aboard, was 48 miles per hour (Ref. 9).

### 3. AERODYNAMIC HEATING

Because of the vehicle's rapid ascent velocities while still within the earth's atmosphere, the effects of aero-

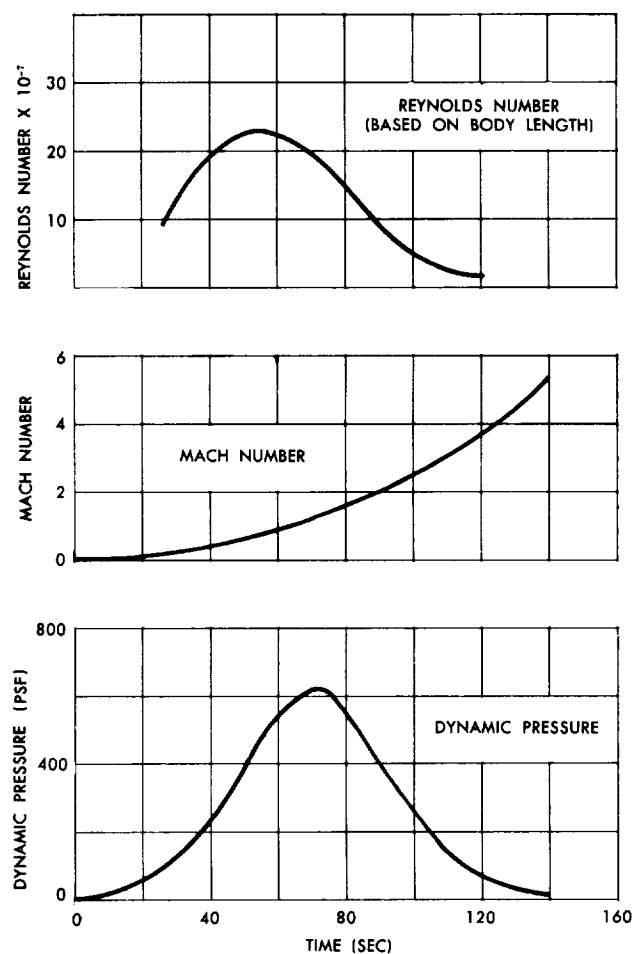


Fig. 5 Time Histories of the Design Reynolds Number, Mach Number and Dynamic Pressure

dynamic heating were investigated. The results were needed for the selection of skin materials and thicknesses, to determine whether heating would cause the nose cone tip to melt, to determine the optimum time to dispose of the nose cone, and to analyze the aerodynamic heating of external antennas, conduits, etc., and the conduction, convection, and radiation heating of the internal equipments.

To do this without the benefit of experimental data, some of the more complex relationships were reduced by calculating an upper-limit temperature which was not expected to be exceeded during actual flight. The vehicle experienced three different flow regimes during its flight through the atmosphere. The first regime, continuum flow, during which the fluid can be considered homogeneous, exists when  $\frac{Re}{M_1} > 100$ , where  $Re$  is Reynolds number, based on distance from the nose, and  $M_1$  is local Mach number. Slip flow, which is influenced by the molecular structure of the air, exists when  $100 > \frac{Re}{M_1} > 1$ . Free molecular flow, in which the mean free path of the air molecules is of a magnitude

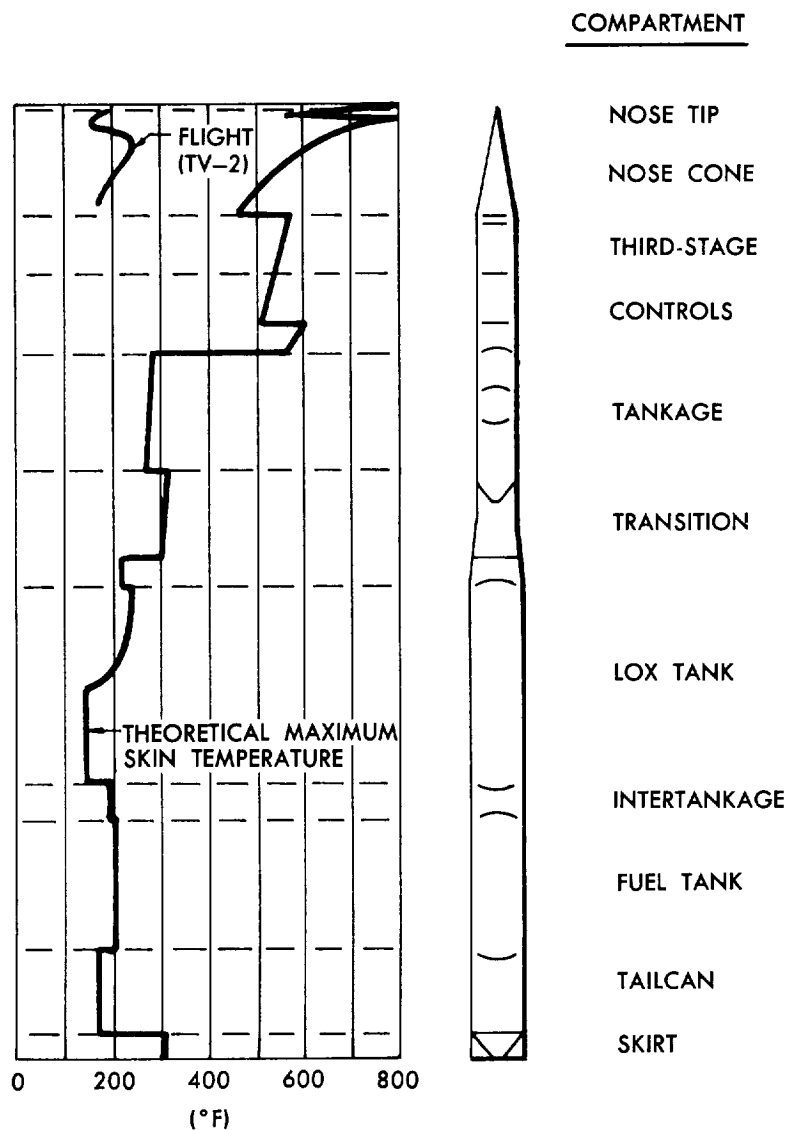


Fig. 6 Theoretical Maximum Skin Temperature due to Aerodynamic Heating

greater than the thickness of the boundary layer, exists when  $\frac{Re}{M_1} < 1$ .

The heat transfer equation was solved for the continuum flow regime. Following this, changes were made to the equations to accommodate slip flow. These changes were believed important, since it was in the slip flow regime that peak temperatures occurred. Free molecular flow was experienced beyond this peak, therefore it was not necessary to further modify the analysis for this third regime.

The method developed for the calculation of aerodynamic heating was successful, in that it provided a simplified method which was readily programmed on automatic digital computation equipment. It evaluated an upper-limit temperature which could not be exceeded

in actual flight and still permitted the use of reasonable materials and thicknesses. Calculations made by other methods for the heating of blunt bodies showed that the solid nose tip would not melt during ascent, that the outer skin of the satellite would not exceed 300°F if the nose cone were ejected 30 seconds after first-stage burnout, and that the antennas, heat shields and conduits were of sufficient strength to withstand the effects of aerodynamic heating. Further investigation revealed that no internal equipment would be damaged by heat transfer from the outer skin. The design maximum temperatures are shown in Fig. 6.

#### 4. SMOOTHNESS AND ALIGNMENT

The Vanguard vehicle was manufactured in keeping with smoothness and flushness requirements established

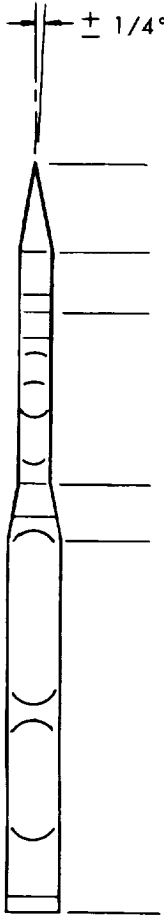
	ALL DIMENSIONS IN INCHES					
	GAPS	FASTENERS	WAVINESS	OBLATENESS	DIAMETER AT JUNCTION	LONGITUDINAL STEPS
	1/32	+0 -0.005	0.010 LONG. 0.005 LAT.	1/16	±0.015	+0 -0.015
	1/32	+0 -0.005	1/16	1/16	±0.03	+0 -0.015
	1/16	1/8	1/16	1/16	±0.03	±0.03
	1/32	+0 -0.01	0.01	1/16	±0.015	±0.015
		1/8	1/8	1/8	±0.03	±0.04
		0.21 (TAILCAN BOLTS)				
EXTERNAL INSTALLATIONS	1/32	+0 -0.005	0.01	....	....	+0 -0.015

Fig. 7 Summary of Smoothness and Flushness Requirements

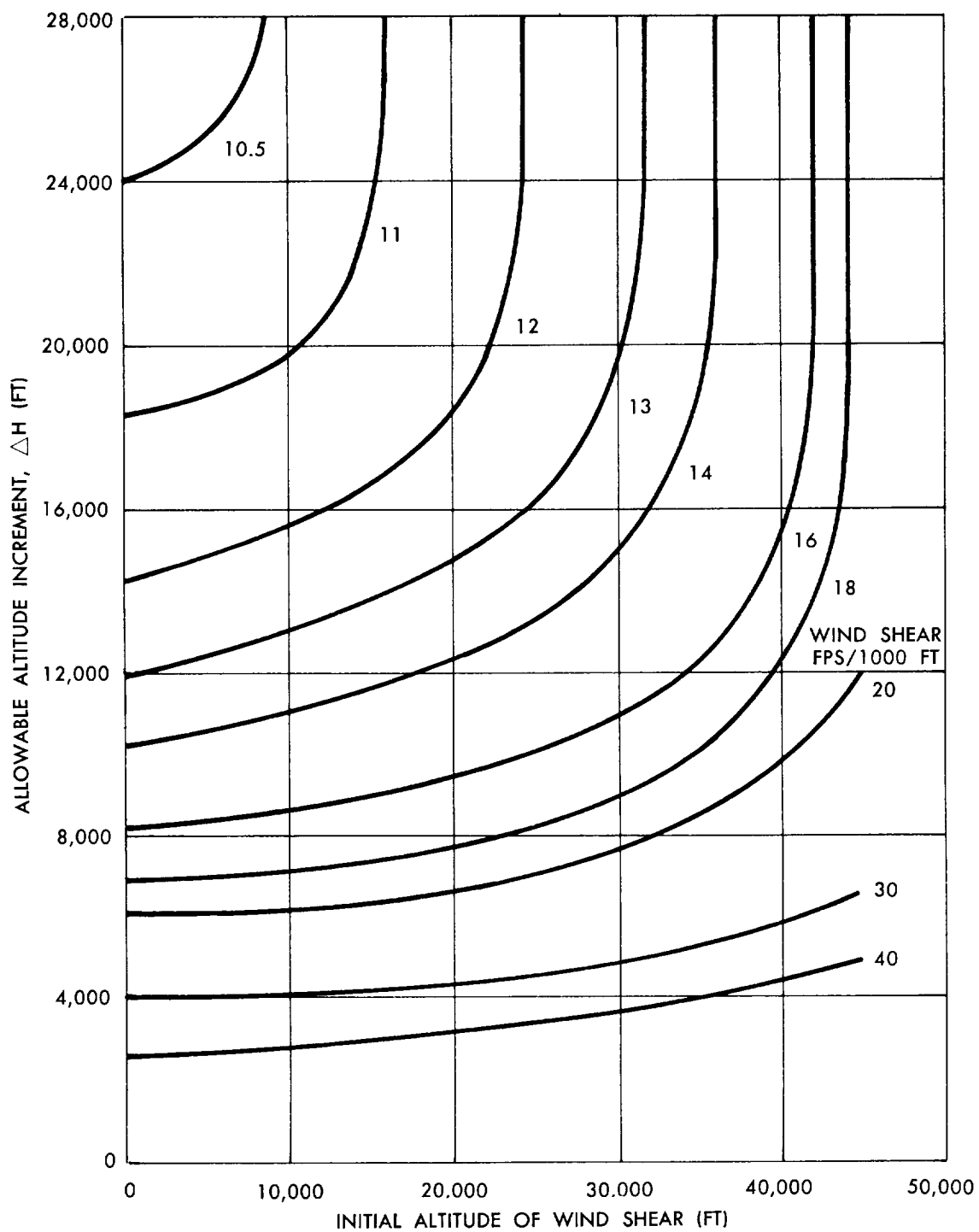
to prevent excessive aerodynamic heating, roll disturbances and drag. Vehicle alignment tolerances were established in order to maintain the center of gravity position within limits required for launch stand clearance and flight control. The basic specifications for these requirements and tolerances are shown in Fig. 7.

##### 5. IN-FLIGHT WIND SHEAR CRITERIA

Structural design of the Vanguard vehicles was based on a profile of the average winds measured by the Air Force Air Weather Service above Cape Canaveral during February (the month for which largest average altitude wind speeds had been measured) and superimposed gust loads equivalent to a 40-fps true-velocity gust (later changed to 20 fps). Direct comparison of a measured prelaunch wind profile with the average profile used for design did not necessarily indicate that the measured profile was either more or less severe

than the design profile. To solve this problem, a wind shear criterion was established which enabled calculation of the condition at which design limits were reached and which, in turn, permitted interpretation of meteorological data taken prior to flight.

Trajectories were calculated with various combinations of initial wind velocities, constant wind shears and initial altitudes of these shears (Ref. 10). The moments produced by these shears were found to increase approximately linearly with altitude until some peak value was obtained. The altitude increments ( $\Delta h$ ), over which these shears would have to act to produce the design limit aerodynamic moment of 20,600 foot-pounds, were plotted as a function of initial altitude for different initial wind conditions. With these plots, the effect of a compound wind profile could be quickly estimated. The compound profile was divided into a series of shears, acting over an altitude increment



**Fig. 8 Maximum Allowable Wind Shear Duration — No Steady Winds**

( $\Delta a$ ). The altitude increment ( $\Delta h$ ) over which each shear would have to act to reach the design limit was obtained from the appropriate curve. The vehicle could fly through any wind profile that had  $\sum \left[ \frac{\Delta a}{\Delta h} \right] < 1$  over all consecutive altitude increments for which the slope of the wind profile had the same sign.

Additional investigation of environmental conditions indicated that the critical gusts to be expected were about 20 fps instead of 40 fps. The specification was changed accordingly. In the winter of 1957, successful flights were made under wind shear conditions that had been previously considered marginal. This, coupled with an enhanced knowledge of the dynamic loads as a result of the TV-3BU flight malfunction investigation, and with revised estimates of the aerodynamic moments based on the SLV-1 flight, warranted re-examination of the wind shear criteria. This re-examination indicated that the vehicle was capable of withstanding about 30 percent higher continuous wind shears than those previously defined. The wind shear criteria as modified to agree with these relaxed requirements are shown in Fig. 8.

## 6. WIND-INDUCED OSCILLATIONS

During the second series low speed wind tunnel tests, the model experienced low frequency vibrations at angles of attack near 90 degrees. Because of the low design margin and high flexibility of the Vanguard, there was concern that vehicle structural failure might occur on the launch stand. Further investigation was therefore required to define the origin of the oscillations. Wind tunnel tests on a dynamic model were conducted at the Massachusetts Institute of Technology to measure the alternating forces and to evaluate the effectiveness of a method to suppress them. These tests (Ref. 11) confirmed that the origin of the forces was the periodic shedding of vortices, arising from a steady wind stream passing the vehicle.

The tests indicated that wind-induced oscillations could be expected to exist in the Reynolds number range of interest for the Vanguard, and that the magnitude of the alternating forces acting at resonance could result in structural failure of the vehicle if a steady wind of the appropriate velocity (16 fps) occurred for a sufficient time (several seconds). To suppress the phenomenon, a number of spoiler arrangements were tested in the tunnel at various angles to the wind. A spiral arrangement was found to be most successful in minimizing the lateral oscillations for all wind directions.

Twelve rubber spoilers were therefore mounted in a spiral pattern on the second stage of each vehicle. Drag cones ("scuppers") were attached to aid in separating the spoilers after liftoff, in order to minimize weight, drag and rolling moment penalties.

## F. STRUCTURE

### 1. STRUCTURAL CONFIGURATION

The primary structure of the three-stage Vanguard vehicle is shown in Fig. 9. The design criteria for this structure are given in Table 2.

**First stage**—The first stage was basically a 45-inch diameter cylinder. The tail can, located at the base of the first stage, was a semimonocoque cylinder consisting of 0.040- and 0.080-inch thick magnesium skin and an all-aluminum chassis of four equally spaced full-length longerons, several frames, two bulkheads, four end support fittings and four engine mount fittings. Access was provided by six structural doors and one large oval nonstructural door.

The kerosene tank, located forward of the tail can, was an integral semimonocoque, all-aluminum (6061-T6) cylinder. It consisted of 0.063-inch external skin, two 0.040-inch thick domes (spherical segments), dome chords, intermediate frames for ease of manufacturing, and a 0.049-inch thick reinforced internal conduit for the liquid oxygen feed line. A 6-inch diameter nonstructural cleaning and inspection door was provided on the upper dome. The tank spacer, located between the two propellant tanks, was a monocoque cylinder of 0.090-inch magnesium sheet. Accessibility was provided by two 14-inch diameter structural doors. The liquid oxygen tank was similar in construction to the fuel tank, but had 0.050-inch external skin and a conical 0.050-inch forward dome to withstand second-stage engine exhaust loads.

The transition section, which included portions of both first and second stages, was a semimonocoque truncated cone of 0.080-inch magnesium skin and an all-aluminum chassis of six equally spaced longerons (full length but discontinuous at the separation plane), 12 splice-bolt fittings, several frames, and a 1/8-inch thick blast shield to deflect the second-stage engine exhaust. This section was spliced in the center by six steel, tension-type, explosive bolts. The aft portion included two 14-inch nonstructural "blast" doors which also served as access ports.

**Table 2**  
**Structural Design Criteria**

Minimum factor of safety—yield .....	1.10
Minimum factors of safety—ultimate .....	1.25
Where personnel safety was involved	
during handling .....	1.50
Pressure vessels where personnel	
safety was involved .....	2.00
Margin of safety—minimum .....	0
Maximum permanent set at design loads .....	0.2%
Maximum ground handling loads—vertical .....	$\pm 2g$
fore and aft .....	$\pm 2g$
lateral .....	$\pm 1g$
Static firing tie-down equipment safety factor .....	5.0

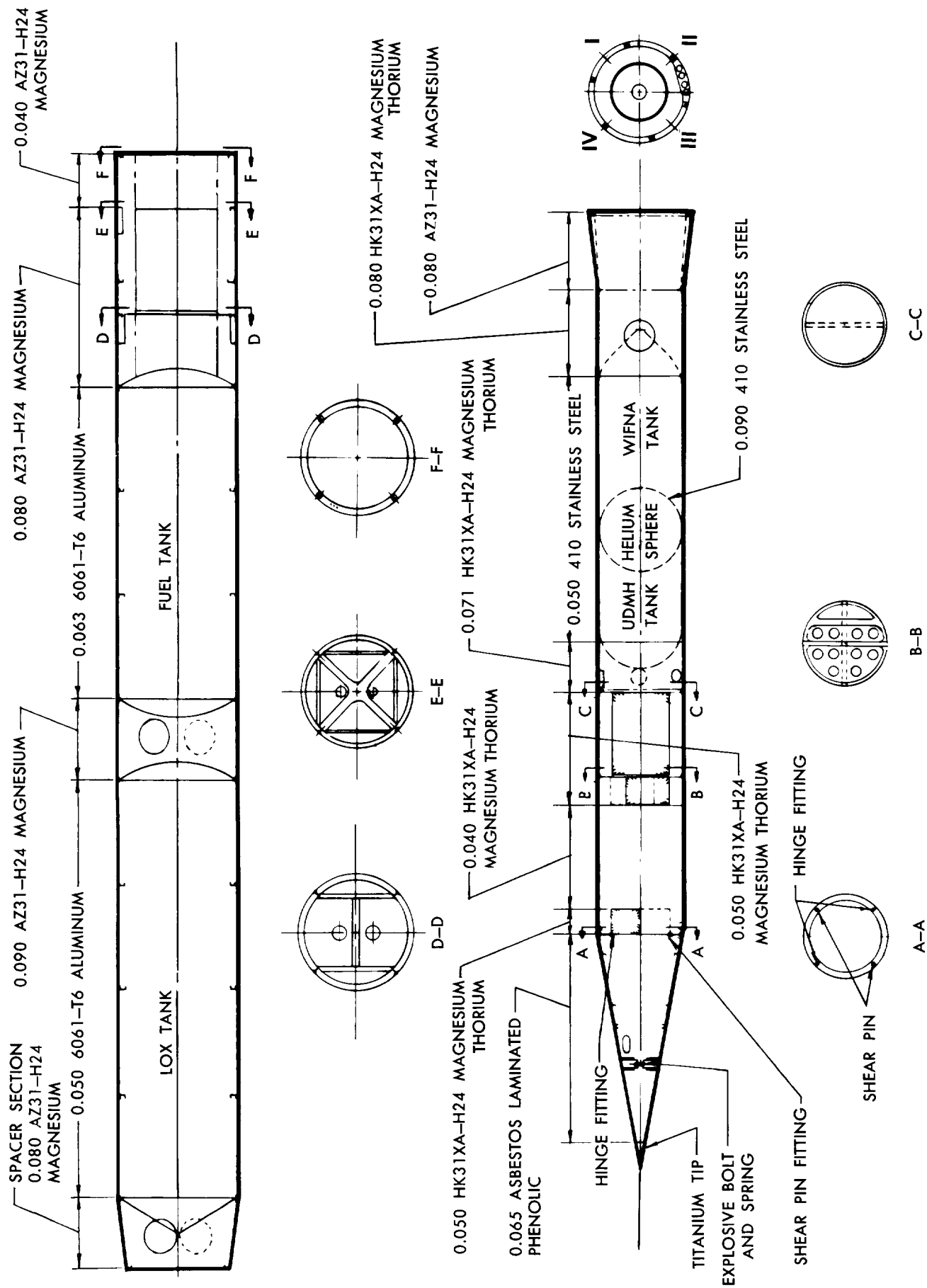


Fig. 9 Vanguard Primary Structure

**Second stage**—The second stage was basically a 32-inch diameter cylinder. The aft skirt, located between the transition section and the second-stage propellant tanks, was a monocoque cylinder of 0.080-inch temperature-resistant magnesium-thorium sheet, fastened with Monel rivets. Access was provided by two 12-inch diameter structural doors.

The propellant tankage was a 410 corrosion-resistant steel integral structure, consisting of a 0.050-inch thick monocoque oxidizer tank with a "conuckle" shaped aft dome and a 0.050-inch thick monocoque fuel tank with a hemispherical forward dome, joined together by a 32-inch diameter, 0.090-inch thick helium sphere.

The forward skirt, separating the propellant tankage from the equipment compartment, was a monocoque cylinder of 0.071-inch temperature-resistant, magnesium-thorium sheet, fastened with Monel rivets. Access was provided by three structural doors. The equipment compartment was a semimonocoque cylinder with 0.050-inch temperature-resistant magnesium-thorium skin, bound by aluminum bulkheads at each end. Further reinforcement was derived from a full-length, full-width, aluminum honeycomb vertical shear shelf. Accessibility was provided by two full quadrant, full-length, removable, structural skin panels.

The third-stage motor compartment consisted of a semimonocoque cylinder of 0.040- and 0.050-inch temperature-resistant magnesium-thorium skin, and an all-aluminum chassis of four equally spaced stringers, two intermediate frames, and two nose cone hinge fittings. The forward end frame was 17-7 PH steel. Access to this compartment was provided by two rectangular structural doors at the top and two at the bottom.

A disposable nose cone protected the satellite against aerodynamic heating and pressures during flight through the atmosphere. The nose cone was made in halves, each hinged at the base, and included 0.065-inch asbestos phenolic skin, a titanium tip attached to one cone half, aluminum longitudinal edge members with shear pins, a bottom closing frame with shear pins and intermediate frames. An explosive bolt latch and a jettison assembly, consisting of an explosive tension bolt and a compression spring, were incorporated near the tip.

**Third stage**—The third stage could be either of two solid-propellant rocket motors. The Grand Central Rocket Company motor consisted of a thin skin (0.030-inch) steel cylinder with a hemispherical forward dome and an aft dome fairing into a steel exit nozzle. A shaft was provided at the forward dome center to act as the forward spin axis and to support the satellite. The Allegany Ballistics Laboratory motor was similarly shaped, but with both case and nozzle made of glass-reinforced plastic.

## 2. STATIC LOADS

The initial approach, based on experience gained with the Viking rocket, considered those static loads imposed by aerodynamics (including gusts), inertia, and corrective engine deflections (except at burnout where a static hard-over engine deflection was considered). Concern later developed over the possibility of an inadvertent hard-over engine deflection at any time during powered flight, a condition incompatible with the original vehicle strength and weight criteria. Further controls studies, however, indicated that the maximum first-stage engine deflections could be reduced from  $\pm 5$  to  $\pm 3$  degrees. This new limit did not violate the existing structural design loads.

In the all-out effort to maintain a minimum-weight structure, a philosophy was established to control ground handling equipment design so that no weight penalties would be imposed on the vehicle. The vehicle was designed to be critical for flight loads only. This philosophy contributed to and affected the design and use of ground support equipment such as vehicle snubbers, spoilers, static firing tie-down structure and wind shields. The mode of transporting the vehicle was also affected.

## 3. DYNAMIC LOADS

The Vanguard vehicle structure was highly elastic. The outstanding problem from the standpoint of dynamics, therefore, was to find a solution to the intricate interdependence of the structure and the control system, since angular displacements caused by structural elastic deformations (as well as rigid body attitude changes) generated flight control system commands. The engine response to these commands set up further bending deformations which, under certain conditions, could combine to break up the structure. (The problem is generally referred to as structural feedback.)

**Development of analysis methods**—Preliminary dynamic analyses were required at the start of the vehicle design phase. The immediate need for these analyses demanded a simplified hand solution which ignored all second-order effects, nonlinearities and cross-coupling, as well as the effects of structural feedback on the bending moment distribution. The results indicated that transverse oscillatory loads resulting from aerodynamic and control system disturbances could, when superimposed upon the static loads, be of sufficient magnitude to cause vehicle structural failure. The condition was remedied by minor reinforcement in the marginal areas.

The limitations of the hand solution were overcome by the later development of an analog solution that permitted an extensive mathematical study of the gov-

erning equations of motion. The equations considered included:

- (1) Rigid body degrees of freedom (pitch, translation and motor motion).
- (2) Flexural motion degrees of freedom (with all linear and nonlinear coupling effects).
- (3) Complete aerodynamic forces (with external gusts and wind shears).
- (4) Engine thrust forces.
- (5) Servomechanical engine actuation system forces.

wherein the apparent viscous damping forces were added to the structure equations based on damping values which are classical for this type of structure. All further dynamic load determination used this newly developed analog solution.

**Analog results**—The flexibility of the analog solution permitted examination of numerous items. For example, a study of the effect of variations in the control system lag-circuit parameters was used to reduce the dynamic loads from this source to a minimum. In effect, the feedback phenomenon was employed to advantage, since it caused structural oscillations to damp out faster than would have been the case had system feedback not been present. It is apparent, therefore, that the representation of the complete analytical closed loop solution in the analog facilities not only verified the overall structural integrity of the design, but provided a tool for optimizing control system parameters as well. The rigid body stability was purposely slightly decreased, as a result of the analog analysis, to accelerate the effective decay rate of the structural oscillations. This design practice has been referred to as load control.

**Engine noise**—The effects of an oscillatory motor motion at varying amplitude and frequency on the overall vehicle load distribution were studied. The source of this possible motor motion lay within the control system itself and consisted of both feedback and control system noise. The noise was passed on to the servo, which translated it into small amplitude motor motion. Filtering out this noise would have been expensive and impractical from a weights and system reliability point of view. The maximum allowable motor motion due to noise, therefore, was based on the bending moment available after having subtracted all other contributions from the design moment envelope. Actual measurements, as obtained from operating hardware, indicated that the motor motion was so small that the resultant loads were still safely within the moment envelope.

**Launch misalignment**—Because of the possible occurrence of an accumulation of manufacturing tolerances and launch stand misalignments, a transient load

environment at launch was also considered. Such misalignments could produce enough gyro tilt to cause an initial error signal; this error signal would then result in an initial motor deflection, causing a suddenly applied lateral force at the gimbal point at the instant the rocket left the launch stand. The resultant loads were found to be insignificant.

**Propellant slosh**—The problem of propellant sloshing is basically concerned with the effects of the motion of liquids with free surfaces which arise from the motion of the containing structure. Sloshing can change the characteristic system response to control commands to the point where it results in completely misleading control stability predictions. The frequency associated with sloshing on the Vanguard, however, was found to lie in the rigid body frequency band. Because of the high elasticity of the structure and the differences in frequency between structural motion and propellant slosh, the representation for sloshing amounted to a correction to the rigid body dynamics acted upon by the aerodynamic forces.

**Extensional motion**—Dynamic loads in the longitudinal direction due to the oscillatory thrust vector were found to be negligible because the structure contained many joints and other characteristics which tended to damp high frequency oscillations.

**Summation**—The structural design of the Vanguard was unique in that about two-thirds of the design bending moment envelope arose from the elastic dynamics of the vehicle. Most of the bending moment arising from this source was generated by the interaction of the elastic structure and the vehicle's autopilot system through the gimbaling motion of the rocket engines.

#### 4. LOAD SUPERPOSITION

The various structural loads were superimposed (Fig. 10) in order to determine the total load on the structure. That is, the maximum bending moments due to wind shear transients, motor hard-over and engine noise were assumed to occur simultaneously, and were assumed to be added to the flight static loads. The launch condition assumed the superposition of the misalignment, motor hard-over, engine noise and static loads. This conservative approach was adopted for the Vanguard because of insufficient data on local wind shear gradients and their distribution. The probability of a control system malfunction in which the motor moved hard-over to its limits and returned in time to regain control was not studied. A more sophisticated approach would have been to determine the probability of occurrence of the various loads at some given instant. This approach could have been used if sufficient statistical data of the required type had been available.

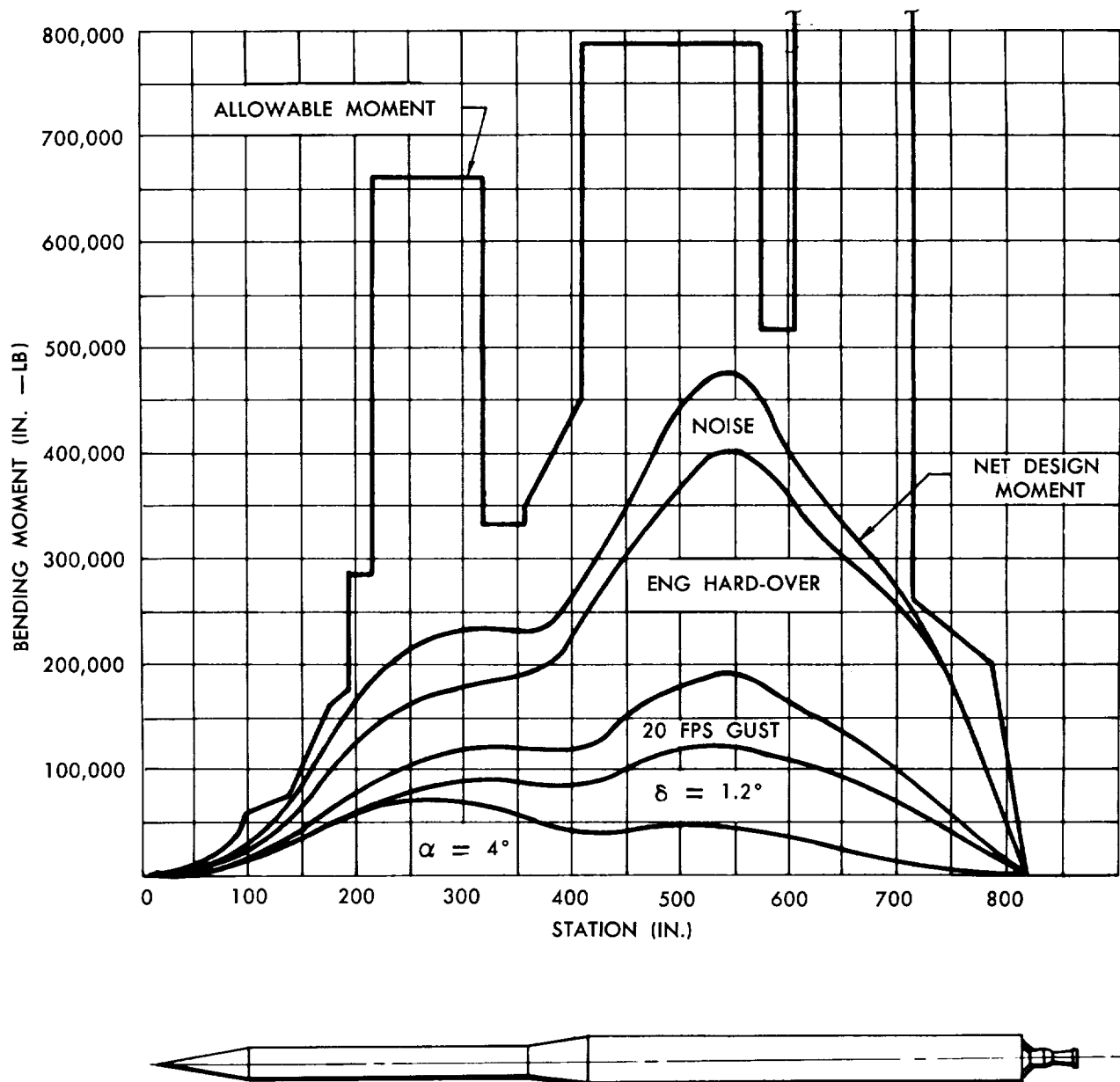


Fig. 10 Design Limit Bending Moment at Maximum Dynamic Pressure

## 5. STRUCTURAL TEST PROGRAM

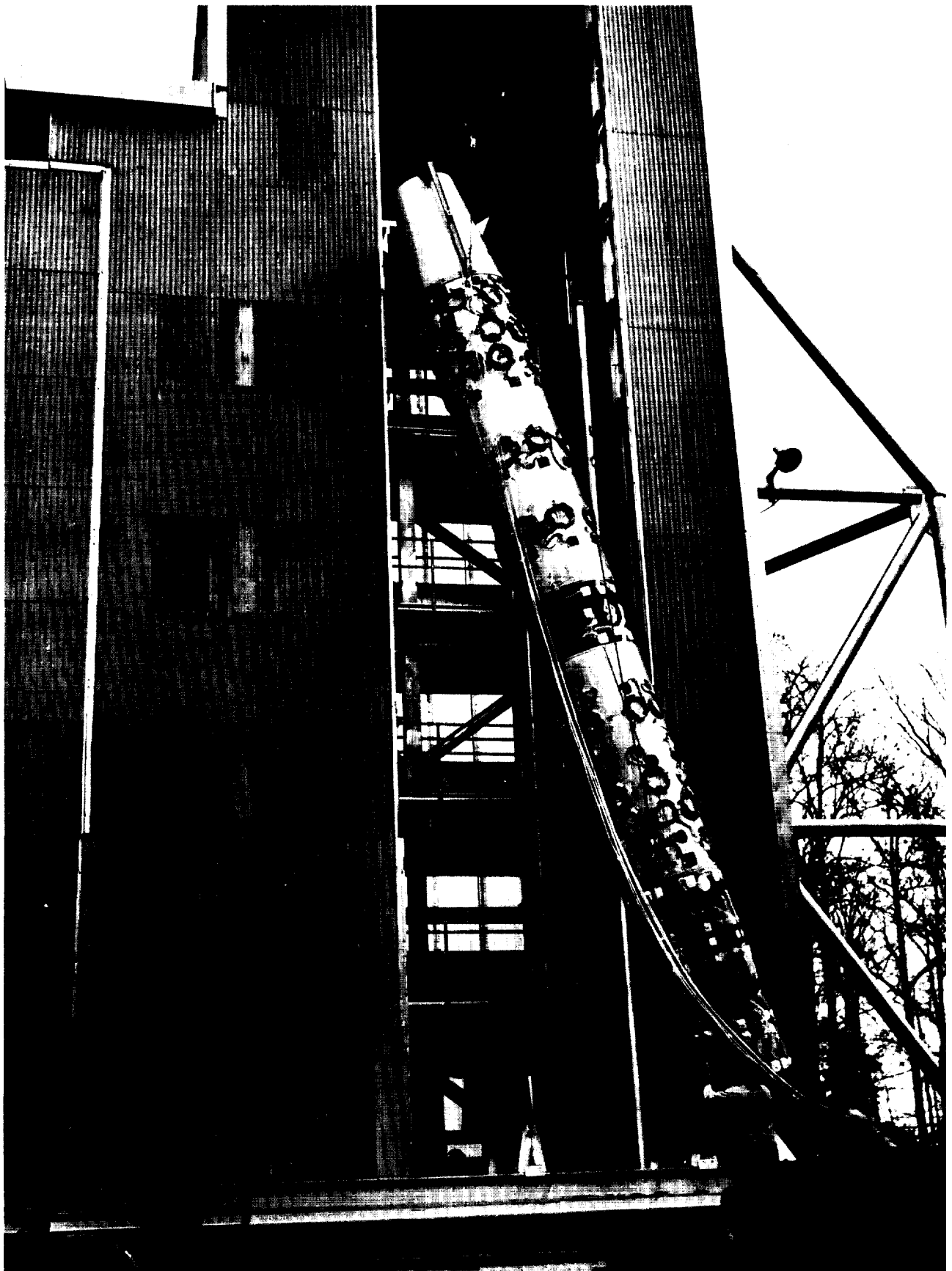
Any structure designed to the small margins of safety used for Vanguard requires extensive structural tests. In addition, verification is required on new, unproven methods of analysis as well as newly developed structural configurations. The test program used for Vanguard is described in detail in Ref. 12.

**Coupon tests**—Coupon tests were performed to supply design information in critical stress areas. These included tests on the longitudinal joint of the first-stage propellant tankage, the structural door attachments, the

chem-milled first-stage helium spheres (including surface finish effects), and slings, webbing and webbing stitching.

**Element test program**—The element test program made invaluable contributions to the successful structural design of the Vanguard. This test phase permitted optimization and verification of structural configurations, repairability evaluation, verification of the methods of design and evaluation of various redundant parameters. The program included:

- (1) Preliminary configurations of the first-stage



**Fig. 11 Structural Test Fixture**

tail can, propulsion tanks, firewall bulkhead, tank spacer, engine mount and gimbal ring.

- (2) Development program and final design of the first-stage helium spheres and hydrogen peroxide tank.
- (3) Preliminary configuration and final design of the transition section.
- (4) Preliminary configuration of the second-stage equipment bay and forward structure.
- (5) Second-stage propane tank and installation.
- (6) Third-stage support structure (spin table and forward support arms).
- (7) Nose cone heat and load tests.
- (8) Explosive bolts (steel and aluminum).

**Production article tests**—Production article tests were performed in the structural test facility (Fig. 11) on:

- (1) First-stage overall structure, and installations of the helium sphere and peroxide tank.
- (2) Second-stage lower dome and engine and gimbal support.
- (3) Third-stage support structure installation.

There was also a third-stage motor stress program by Grand Central and a second-stage propulsion tank-age stress program by Aerojet.

## 6. SPECIAL PROBLEMS AND TECHNIQUES

**Nose cone**—There were large local thermal deflections of the skin, poor positive locking of the hinge assembly, and misalignment problems associated with the early nose cone design. The local thermal deflection problem was rectified by the addition of a forward-located explosive latch. The remaining problems were corrected through utilization of a "shim, trim and jig locate" technique in final installation and assembly, in conjunction with a proof load test.

**Structural door attachment**—Repeated removal and installation of structural doors during shop and field handling created oversized holes in the doors and coamings, thus degrading the load carrying capability of these structural members. To ensure structural integrity, ground handling and field procedures were amended to include comprehensive instructions for periodic inspection and repair of all structural door installations.

**Controls bay equipment panel**—Vibration levels monitored on the vertical honeycomb controls bay equipment panel on TV-3BU and TV-4 indicated that the level was higher than had been predicted. As a result, the equipment panel and controls can mounting structure were modified and the controls can requalified, using test vibrations based on spectral density curves obtained from vehicle measurements. Test results were satisfactory with the incorporation of a minor

modification; i.e., the installation of rubber mounts under the chassis mounted in the controls can. Other marginal areas were strengthened and another random vibration test was performed on the controls can. The effectiveness of the new modifications was demonstrated by the improved performance of the controls can. Vibration levels monitored on TV-5, with the modified panel, were considerably lower than those measured on the earlier vehicles. Hence, it was concluded that the modified controls can would perform satisfactorily in the vehicle vibration environment, with a considerable margin of safety.

**Ground wind restrictions**—Because of the variety of parameters affecting the strength of the vehicle structure, field operations had to be governed by comprehensive and specific instructions limiting these parameters. These instructions took the form of maximum allowable ground wind placards for varying conditions of overall vehicle configuration (stage combinations), propellant loading, vortex spoiler usage, snubber usage, vehicle shielding configuration, structural door usage, type of operation (static firing or launch) and usage of the work platform inserts. Typical wind placards with the gantry retired were: 30 miles per hour with kerosene and UDHM loaded, 33 miles per hour after addition of WIFNA and 48 miles per hour fully loaded.

**Nose cone heat tests**—A radiant heat test facility was used to study the combined effects of thermal and applied load stresses during rapid nose cone transient heating. Maximum temperatures varied from 500°F at the base to 950°F near the tip of the nose cone. In the final test, the two halves of the nose cone were successfully separated by igniting the explosive bolt shortly after maximum heat input and temperatures were reached. The nose cone heat tests may be considered as typical of the scope of Vanguard structural tests.

**Stress corrosion**—Initial qualification tests at Aerojet revealed, by virtue of helium sphere failures, that the structural configuration was sensitive to stress corrosion cracking (material deterioration under the combined effects of high stresses and of exposure to white inhibited fuming nitric acid). This critical condition was remedied, after extensive testing of specimens and test spheres, by reducing the tempering temperature from 825° to 600°F. The resulting reduction in the ultimate strength from 180,000 to 170,000 psi did not violate the design ultimate safety factor of 1.25. Stress corrosion is discussed in detail in Chapter IV, Section C.

## 7. SPECIAL TECHNIQUES

**Tank wall design**—A method of analysis was developed for designing monocoque tank walls subjected to compression stresses with or without internal stabilizing pressure. The method is applicable to cylindrical and truncated conic sections, and includes pro-

cedures for establishing both allowable and actual stresses. The method was verified to a high degree of accuracy by a comprehensive full-scale element test program. A detailed presentation of this technique may be found in Ref. 12.

**Structural deflection due to thermal radiation—**

Structural deflections were caused by differential solar heating while the vehicle was on the launch stand. Such deflections changed the vehicle center of gravity, introducing another variable in the vehicle launch environment. A simplified analytical method for evaluating these deflections (Ref. 12) was developed and verified by measurements made on TV-2 at Cape Canaveral.

**Second-stage helium sphere design—**Comprehensive studies resulted in the submerged helium sphere configuration for the second-stage propulsion system. Submergence of the sphere reduced the differential pressure across the sphere walls by the amount of the propellant tank pressures (approximately 340 psi, or 20%), which resulted in a sizable weight reduction of about 55 pounds.

## G. WEIGHT CONTROL

Vehicle design criteria, as set forth in the specification (Ref. 3), included the following:

“Weight considerations—Because of the penalty that weight imposes on performance, every effort shall be made to reduce the weight of the vehicle.”

The significance of the penalty is best appreciated by considering the “rules-of-thumb” for the estimated reduction in final satellite injection velocity caused by the addition of one pound to the burnout weight of a given stage:

First Stage:	1 fps
Second Stage:	8 fps
Third Stage:	80 fps

These original criteria, or current variations thereof, were applied many times during the design phase of the project for evaluating compromises involving weight.

Some of these compromises are worthy of note. There were cases where additional system complexity was accepted in return for a substantial weight saving. Aerojet studies indicated a saving of 71 pounds in

structural weight through the use of a heating charge in the second-stage helium sphere which reduced the maximum sphere pressure required. Aluminum, rather than steel, was used for the second-stage thrust chamber at the price of manufacturing problems and, ultimately, a marginal chamber lifetime, for another 60 pounds. In other areas, substantial weight saving was accomplished by the deliberate interrelation of independent systems. Instances of this were:

- (1) The use of residual second-stage helium, trapped under pressure at burnout, to power the vehicle attitude control jets during coasting flight.
- (2) The utilization of turbopump exhaust to power the first-stage roll jets.
- (3) The basic design technique (not original with Vanguard) of using integral propellant tankage as vehicle structure.

To achieve the necessary emphasis, a formal and active weight control program was conducted throughout the design phase. Optimistic goals were established, IBM tabulations were maintained, weekly status reports were issued, and weight saving suggestions were solicited, evaluated and followed up. The result was a vehicle with an overall mass ratio (total propellants to gross weight) of 0.88.

Actual weight data for the Vanguard SLV's are summarized in Table 3. A more detailed weight breakdown by system for the “average SLV” is presented in Table 4. As a matter of interest, these final weights are compared in both tables with those established at the outset of the program in the Design Specification (Ref. 3) and also with the intentionally optimistic goals originally set for the weight control program.

## H. FINAL VEHICLE CONFIGURATION

The final configuration of the complete Vanguard satellite launching vehicle is shown on the inboard profile drawing, Fig. 12. This drawing specifically represents the configuration of the last vehicle, TV-4BU. With the exception of the third-stage rocket motor and a few minor details, however, Fig. 12 is representative of the configurations of the preceding six SLV's as well. Detailed descriptions of the individual systems are presented in Chapter IV.

**Table 3a Vanguard Weight Summary**

	EMPTY WEIGHT (lb)			PAYLOAD Weight (lb)	VEHICLE DRY WEIGHT <sup>①</sup> (lb)	PROPELLANT WEIGHT (lb)	VEHICLE WEIGHT AT FIRE SIGNAL <sup>②</sup> (lb)
	First Stage	Second Stage	Third Stage				
SLV-1	1587	1017	48.7	22.0	2718	20047	22,823
SLV-2	1578	1020	48.8	22.9	2713	20046	22,817
SLV-3	1590	1034	47.7	23.9	2739	20070	22,867
SLV-4	1604	1009	47.8	23.7	2728	20062	22,848
SLV-5	1614	1005	48.2	24.0	2734	20030	22,822
SLV-6	1611	1005	48.0	24.4	2731	20188	22,977
TV-4BU	1599	1013	50.9	52.3	2756	20329	23,143
Mean SLV	1598	1013	48.4	—	2727	20057	22,843
Standard deviation	± 13	± 10	± 0.5	—	± 9	± 59	± 69
Spec. Target	1740	973	67.5	21.5	2823	19756	22,600
	1552	865	—	—	—	—	—

① Includes 13 lb first-stage helium, 17 lb second-stage helium and charge, and 13 lb second-stage propane (11 lb propane on TV-4BU)

② Includes 18 lb spoiler weight and estimated 40 lb ice on LOX Tank

**Table 3b Loaded Propellant Weight Summary**

	FIRST STAGE		SECOND STAGE (lb)			THIRD STAGE (lb)
	LOX	Kerosene	Peroxide	WIFNA	UDMH	
SLV-1	10857	5095	340	2475	897	382.5
SLV-2	10845	5100	340	2478	900	383.4
SLV-3	10936	5087	340	2475	848 <sup>①</sup>	384.4
SLV-4	10923	5122	340	2433	862 <sup>①</sup>	382.3
SLV-5	10867	5103	340	2446	891	383.5
SLV-6	11066	5072	340	2450	877	383.4
TV-4BU	11077	5088	340	2477	892	454.6 <sup>②</sup>
Mean SLV	10914	5097	340	2464	894	383.0
Standard deviation	± 107	± 13	0	± 18	± 8	± 0.8

① Off-loaded, not included in the determination of the mean and standard deviation value

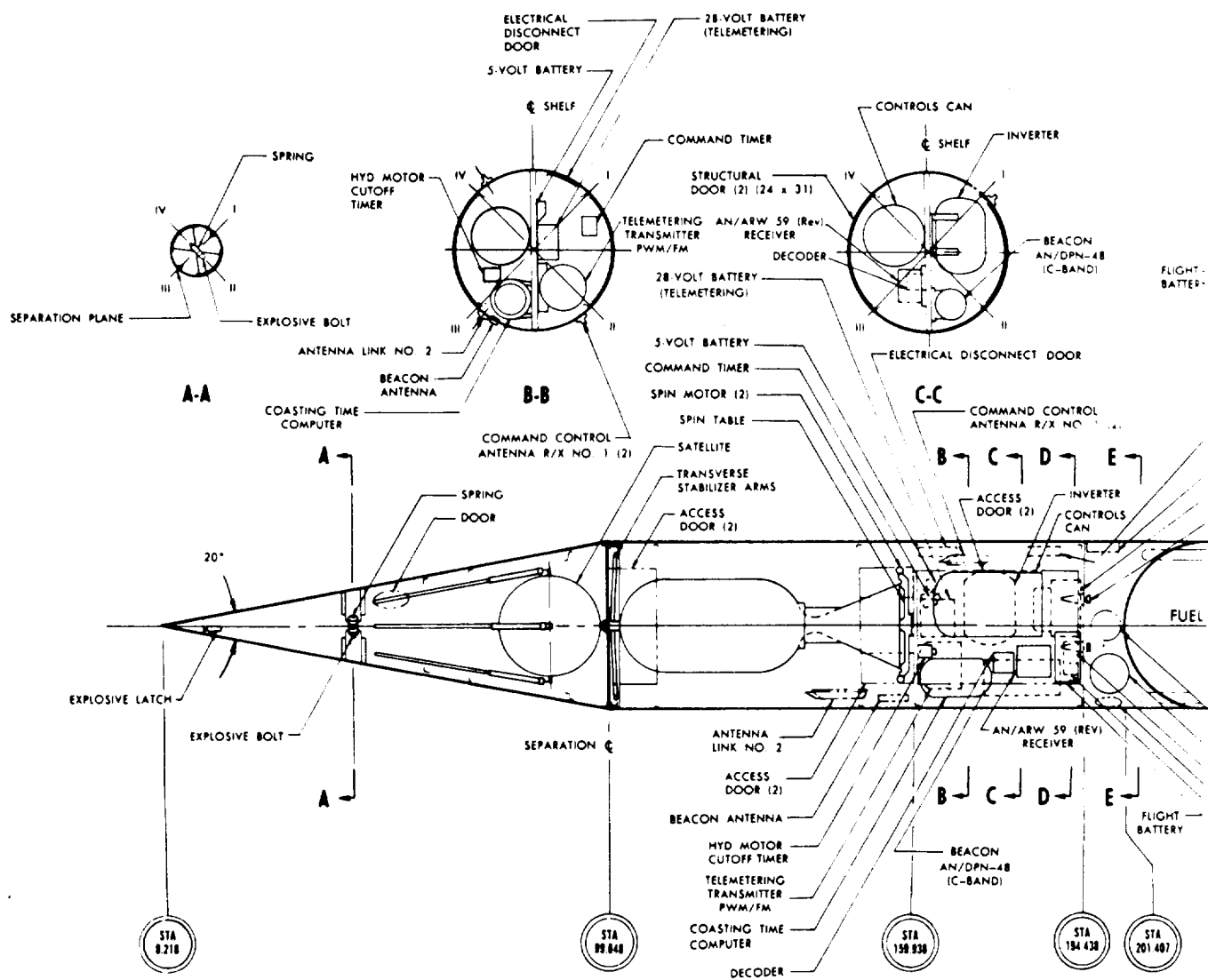
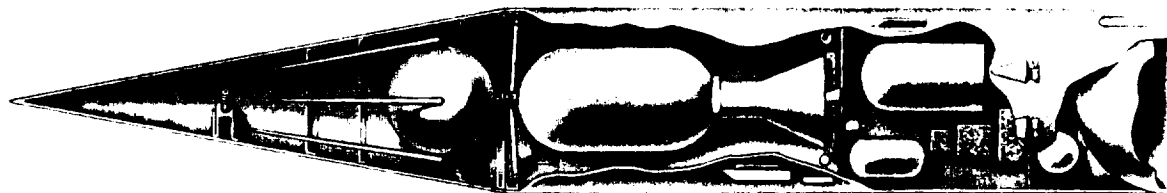
② ABL rocket motor, not included in mean and standard deviation

**Table 4 Detailed Weights Breakdown**

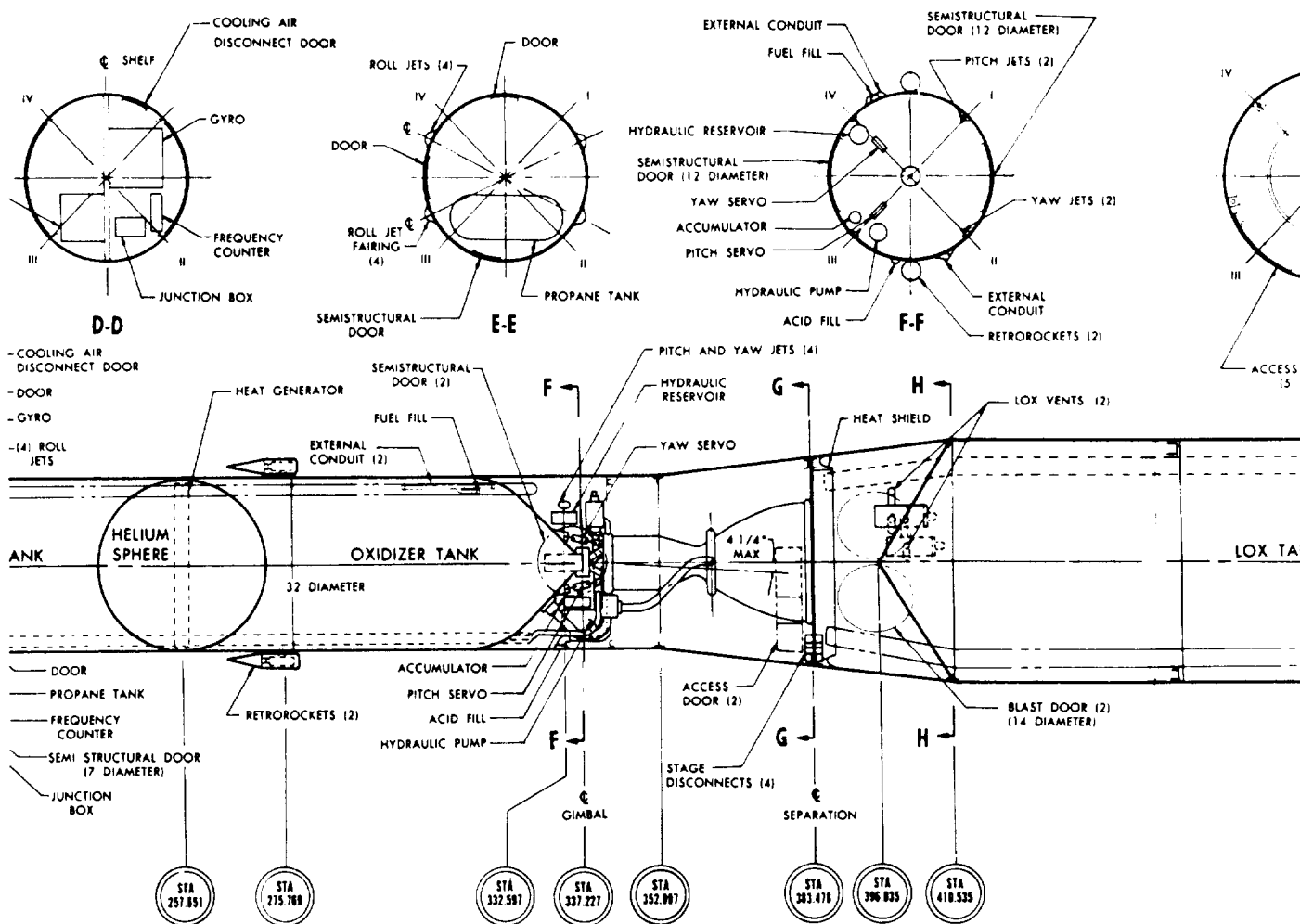
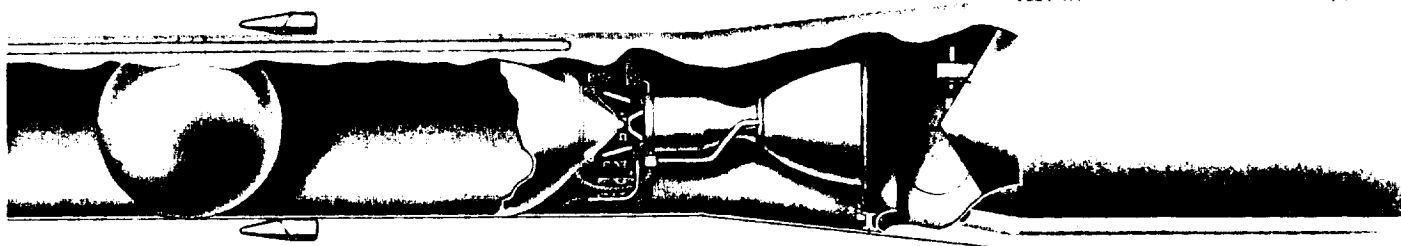
	FIRST STAGE			SECOND STAGE			THIRD STAGE			COMPLETE VEHICLE	
	Mean SLV	Spec.①	Target②	Mean SLV	Spec.	Target	Mean SLV	Spec.	Target	Mean SLV	Spec.
<b>TOTAL DRY WEIGHT (lb)</b>	1598	1769	1565	1013	973	865	48.4	67.5		2659	2810
Structure	591	667	642	156③	134	126	0.5	12.5	12	747	814
Powerplant	734	850	770	386	458	446	47.9	55		1168	1363
Guidance & control	108	120	79	269	237	187				377	357
Electrical	84	57	54	100	85	54				184	142
Instrumentation	81	75	20	69	59	45				150	134
Nose Cone				33		7				33	
<b>UNEXPULSED FLUIDS (lb)</b>	200	512		71	73					271	585
Helium	13	13		17④							
Propane for Roll Jets				13	17						
Propellant outage	55	321		7	56						
Trapped propellants	77	108		34							
LOX boil-off	55	70									
<b>CONSUMED PROPELLANTS (lb)</b>	16190	15549		3317	3240		383.0	395.0		19890	19184
Oxidizer	10830	10459		2430	2387						
Fuel	5060	4754		887	853						
Peroxide	300	336									
<b>TOTAL (lb)</b>	17988	17830		4401	4286		431.4	462.5		22820	22579
							SATELLITE PAYLOAD (lb)			23	22.1
							TOTAL WEIGHT AT FIRE SIGNAL (lb)			22843	22601

- ① Specification 4100-1  
 ② Weight Control Program Target Values  
 ③ Includes 18 lb of Spoilers on Second Stage  
 ④ Helium plus Heat Generator

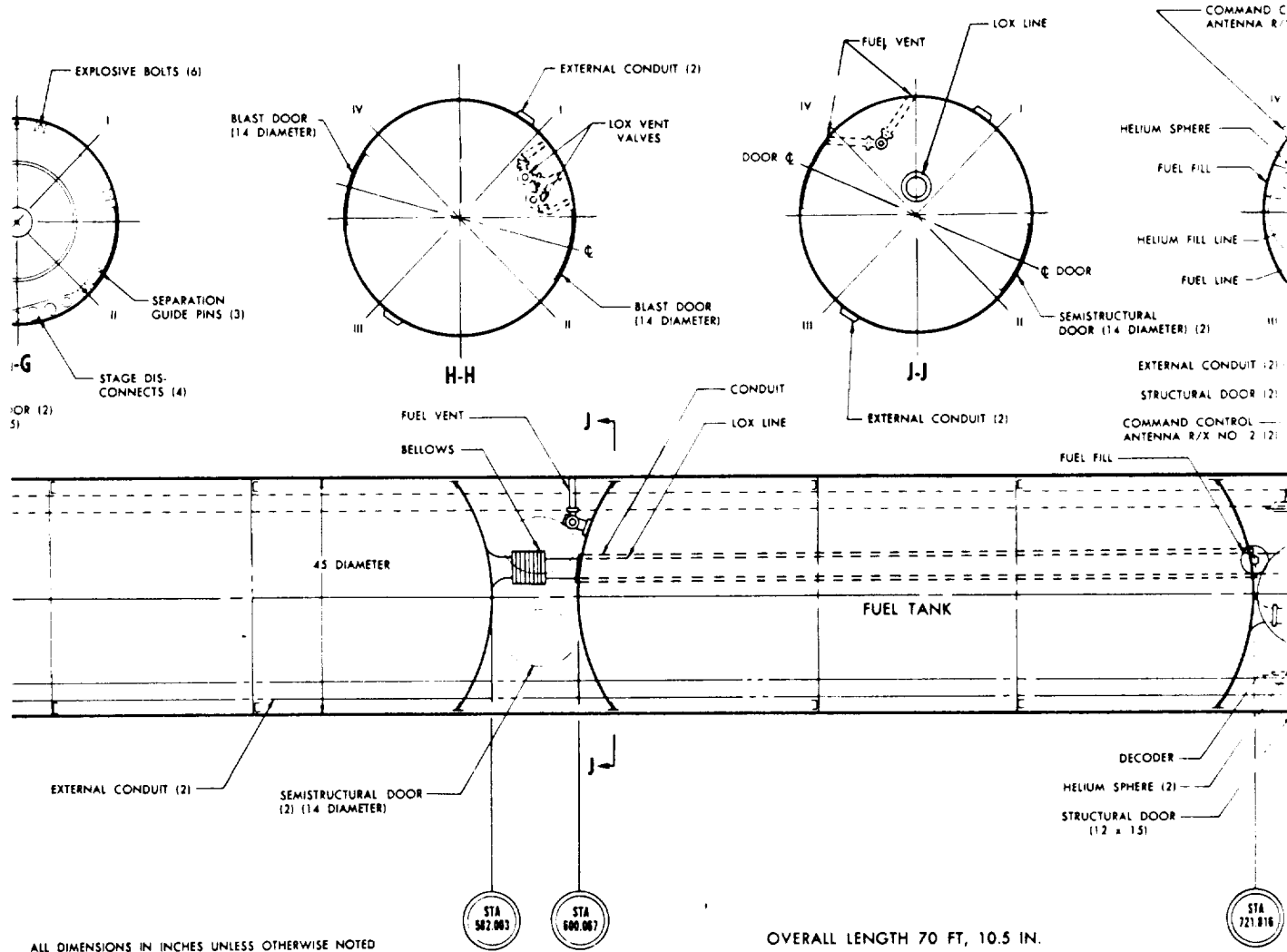
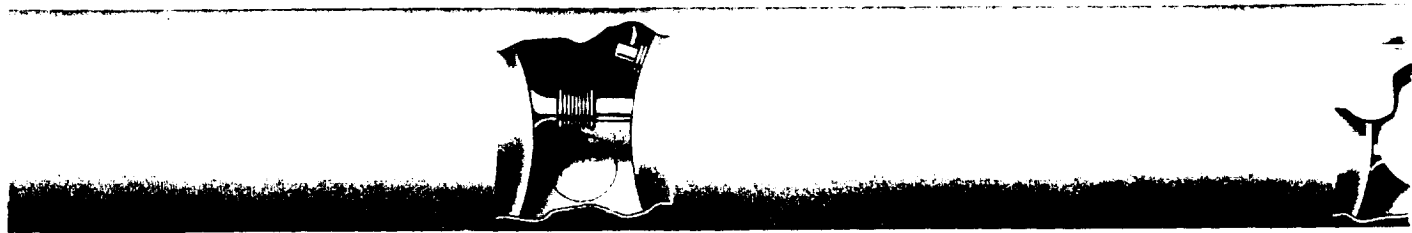














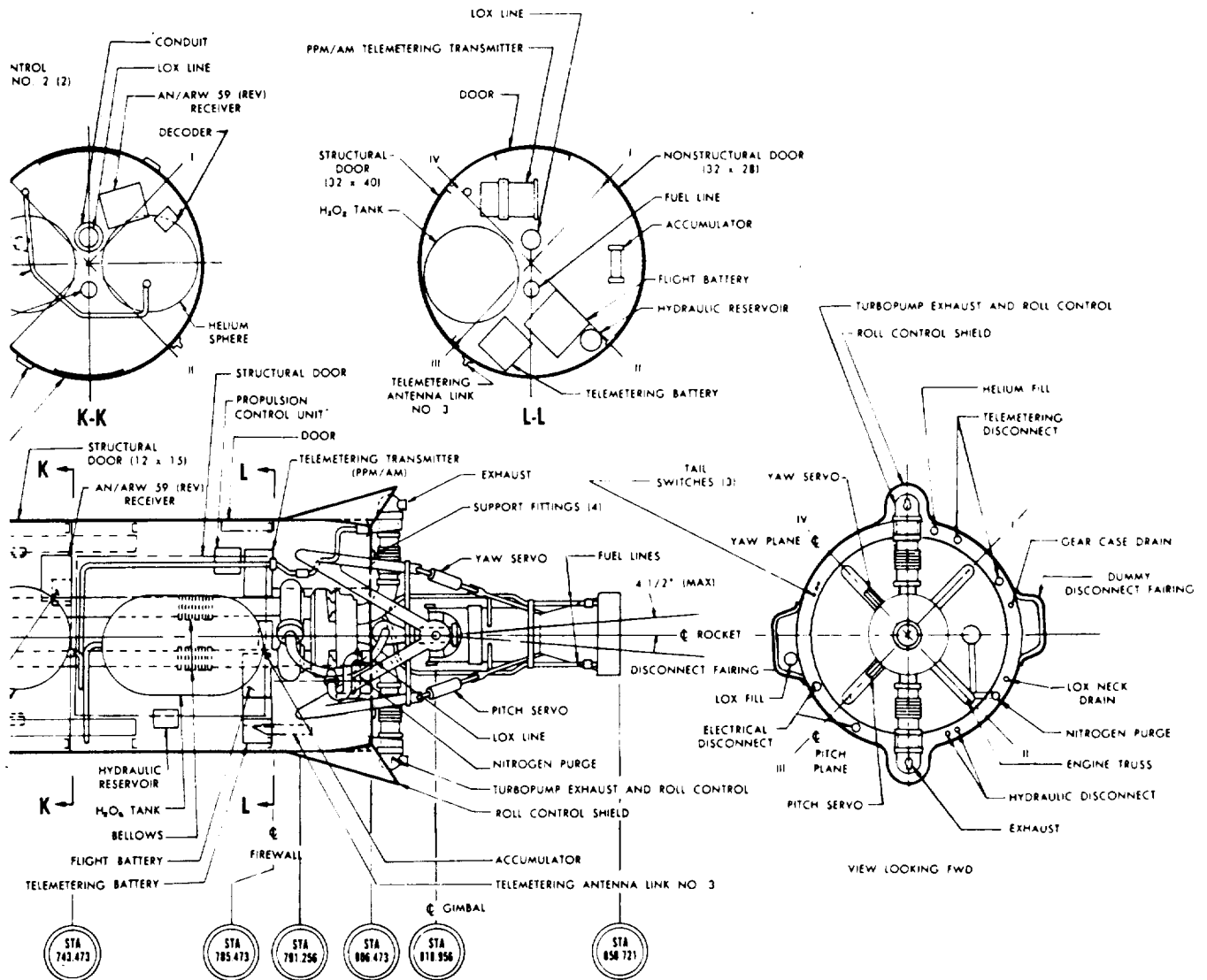
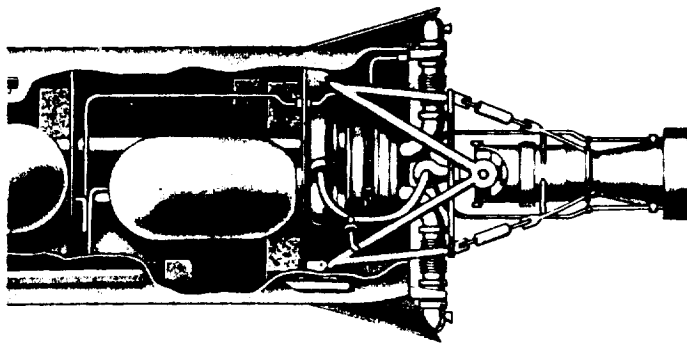


Fig. 12. Inboard Profile



## IV. SYSTEMS DESIGN AND DEVELOPMENT

### A. GUIDANCE AND CONTROL

The Vanguard guidance and control system was designed to stabilize the vehicle flight attitudes in a controlled fashion and to determine the proper time to fire the unguided third stage to obtain the optimum third-stage injection angle. The mechanism of changing flight path was supplied by changing the vehicle attitude references according to plan during first- and second-stage powered flight. A complete description of the design and operation of the Vanguard guidance and control system may be found in Refs. 13 and 14. Quantitative parameters for the system are given in Table 5.

#### 1. AIRBORNE GUIDANCE

Airborne guidance (shown in Fig. 13) consisted of the gyroscope reference system, the program timer, and the airborne third-stage firing system. An airborne guidance system block diagram is shown in Fig. 14. This diagram shows the pitch axis guidance system in detail. The yaw axis diagram was identical except that there was no yaw program such as that in pitch. The roll axis diagram is not shown, but was quite similar to those in pitch and yaw.

**Gyroscope reference system**—A Minneapolis-Honeywell "strapped-down" gyroscope reference system and a gimballed inertial platform were the only available systems that could operate with an angular accuracy of one-half degree in ten minutes in the Vanguard environment. The Minneapolis-Honeywell system was selected because it appeared to offer a weight advantage of 70 pounds. The assembly consisted of three modified HIG-6 gyros, a three-channel isolation amplifier, three gyro temperature control amplifiers, a frequency-corrected torquer current supply, a drift trim regulator, and a regulated d-c power supply. These ten major components were mounted along with all necessary circuitry in a container, 14 x 14 x 13 inches in size; the package weighed about 30 pounds. This system, shown in Fig. 13, provided accuracy better than required, yet was the simplest, lightest and one of the most economical available.

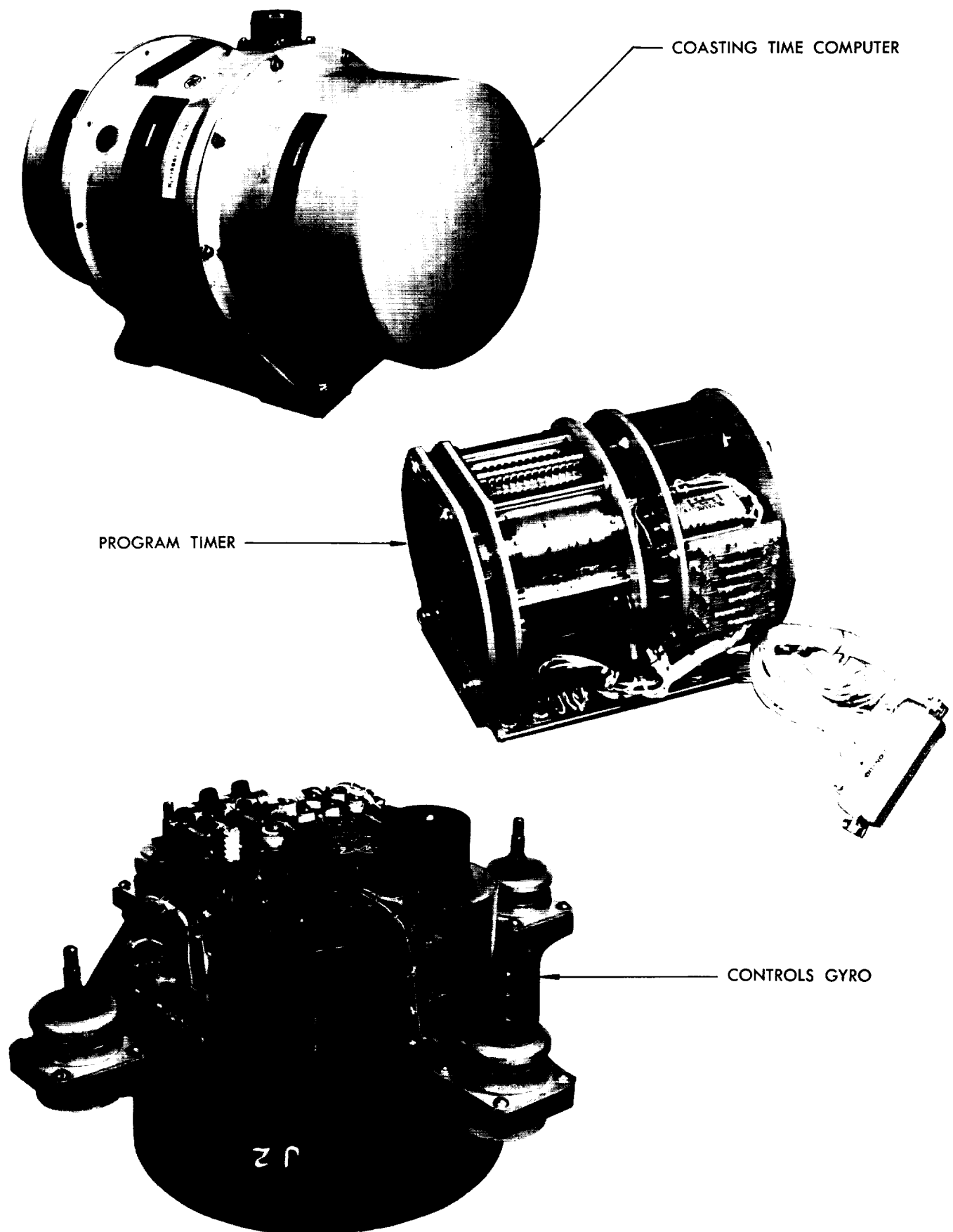
The design included modification to the HIG-6 gyro to reduce the spin motor angular momentum by a factor of two, in order to permit response to larger input angles (about  $\pm 12$  degrees) before hitting the

mechanical stops. An isolation amplifier was used at the pick-off output to permit controlled loading to compensate for gyro flex lead elastic restraint effects, which maintained uniform drift over wide input angles. An a-c to d-c converter circuit was used for the gyros instead of a precision three-phase 400-cycle power supply, in order to provide a d-c output proportional to the frequency of the input and to compensate for variations in input voltage and operating temperature. This feature was necessary because the torquing current required for a precise rate was proportional to the synchronous speed of the gyro spin motor but was independent of input voltage.

The gyroscope reference system performed two functions in the Vanguard vehicle: as an integral part of the control system, it sent error signals to the control elements to attitude-stabilize the vehicle; as part of the guidance system, it directed the vehicle along a predetermined trajectory by means of a highly accurate pitch program. The basic sensing components of the Vanguard reference system were the three rigidly mounted (strapped-down), single-axis, hermetically sealed, integrating gyros. The output signals from the reference system (pitch, yaw and roll) were fed to the control system in the form of a-c voltages proportional to angular displacement from the desired reference axes. Departure of the vehicle from the reference produced a gyroscopic torque about the output axis. This torque was opposed by the viscous damping torque of the flotation fluid, resulting in a proportional rate of motion and a gimbal angle of rotation that was proportional to the angle of vehicle departure from reference. The deflection resulted in a proportional voltage being generated by the gyro signal generator, which was transmitted to the autopilot through isolation amplifiers.

The pitch reference axis was changed by introducing current controlled by precision resistors through the torquer coil of the gyro. This produced a precession of the gyro spin axis. The precision resistors for the pitch program were mounted in a separate plug-in chassis located in the controls can. The pitch program could be easily modified by changing the plug-in chassis.

The pitch and yaw gyros were capable of being torqued at command control rates of 1 degree per



**Fig. 13 Major Components, Airborne Guidance System**

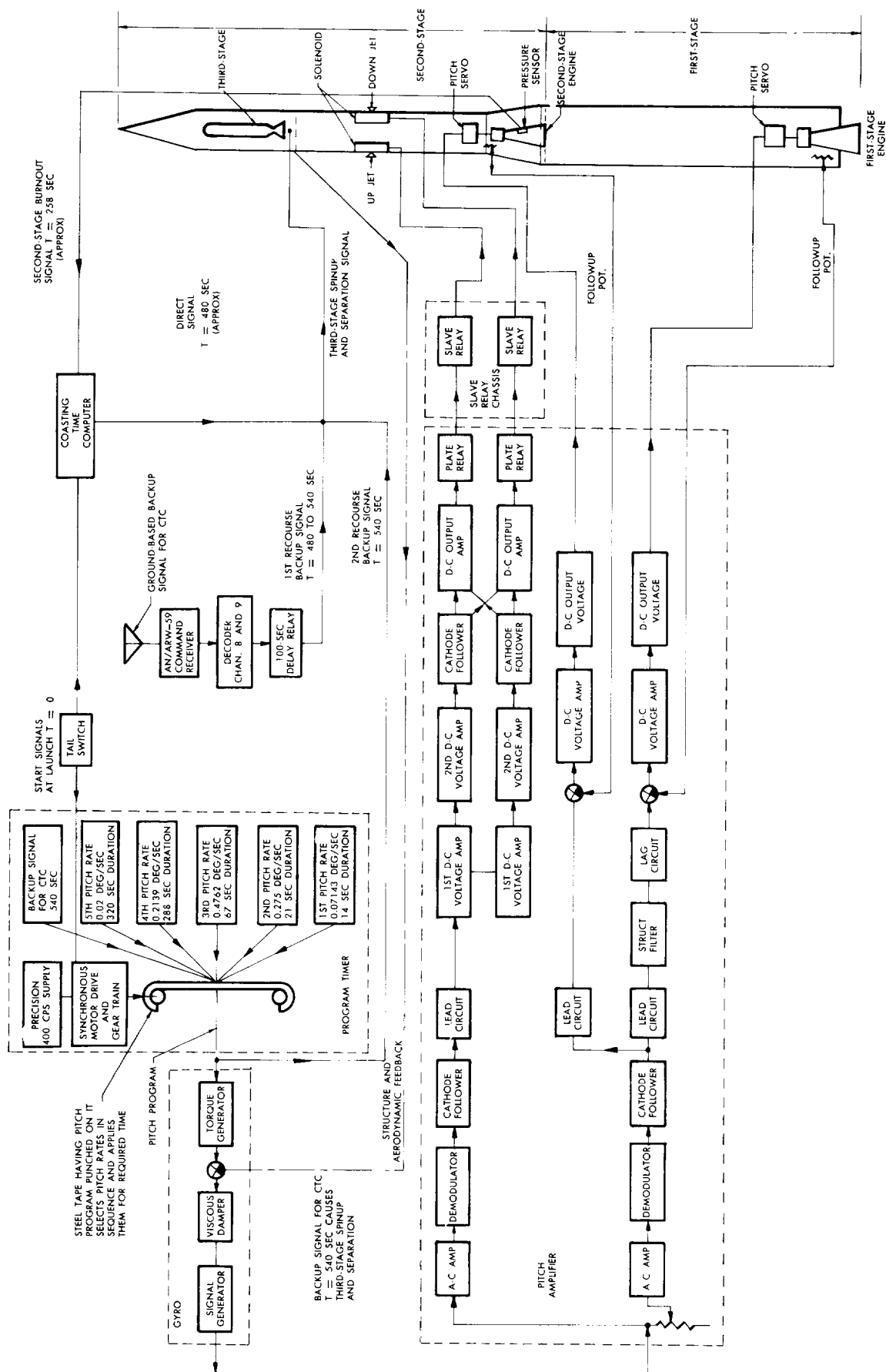


Fig. 14 Airborne Pitch Guidance and Control System

**Table 5. Guidance and Control System Parameters**

**GYRO SYSTEM**

Rotor angular momentum	$0.500 \times 10^8 \text{ gm-cm}^2/\text{sec}$
Torquer: rate sensitivity	0.00665 deg/sec/ma
Scale factor	58 dyne-cm/ma
Command rate	$\pm 1.0 \text{ deg/sec}$
Gyro time constant	1.5 ms
Minimum gyro input axis freedom	$\pm 10 \text{ deg}$
Maximum signal phase shift	$\pm 5.0 \text{ deg}$
Transfer function	200 mv/deg
Positive error signal + X roll	ccw
+ Y pitch	up
+ Z yaw	right
Isolation amplifier load impedance	3000 ohms
Gain	1
Initial gyro alignment	$\pm 0.1 \text{ deg pitch}$ $\pm 0.125 \text{ roll and yaw}$
Overall angular accuracy	$\pm 0.5 \text{ deg pitch}$ $\pm 2.0 \text{ deg roll and yaw}$
Cooling air flow (gyro package)	40 cfm (40°F)
System cooling air flow	70 cfm (40°F)
Power	
28-v dc	150 watts
115-v ac—400 cps	105 watts

**PROGRAM TIMER**

Output frequency	$400 \pm 0.04 \text{ cps}$
Output power	45 mw
Input power	27.5-v dc

**COASTING TIME COMPUTER**

Gyro: Unbalanced moment	10.30 gm-cm
Torque summing member inertia	56.7 gm-cm <sup>2</sup>
Angular momentum	10,000 dyne-cm-sec
Signal generator constant	27.9 volt/rad
Damping constant	10,000 dyne-cm-sec
Motor: Torque constant	890 dyne-cm/volt
Damping constant	52 dyne-cm/sec
Motor inertia	1.07 gm-cm <sup>2</sup>
Load inertia	17,800 gm-cm <sup>2</sup>
Power Required:	
(a) 27.5-v dc	100 watts
(b) 115-v, 400 cps	15 watts

**PITCH AND YAW CONTROL SYSTEMS**

Engine Servo Systems	<i>First Stage</i>	<i>Second Stage</i>
Static gain (engine deflection/gyro deflection)	1.2	0.375
Servo system response	50 rad/sec	50 rad/sec
Servo moment arm	13.54 in.	6.0 in.
Follow-up potentiometer		
Length	3.05 in.	1.36 in.
Resistance	5,000 ohms	5,000 ohms
Follow-up potentiometer calibration	0.201 volts/deg	0.672 volts/deg
Lead circuit transfer function	$\frac{3 (1 + 0.444S)}{40 (1 + 0.0333S)}$	$\frac{3 (.1 + 0.444S)}{40 (1 + 0.0333S)}$
Lag circuit transfer function	$\frac{1}{1 + 0.040S}$	
Filter circuit resonant frequencies	12.1 cps, 18.0 cps	
Propellant slosh frequency	2.1 cps	2.0 cps

**POWER REQUIREMENTS**

	<i>Pitch or Yaw Amplifier</i>	<i>Roll Amplifier</i>
27.5-v dc	1.5 amp	0.8 amp
150-v dc	0.06 amp	0.08 amp
115-v ac, 400 cps	0.03 amp	0.010 amp

**Table 5. Guidance and Control System Parameters (Cont.)**

**JET SYSTEMS**

**Tumble Jets (Pitch and Yaw)**

Pull-on signal	$\pm 0.40$ deg
Drop-out signal	$\pm 0.36$ deg
Lead circuit transfer function	$\frac{1 (1 + 0.5S)}{30 (1 + 0.0167S)}$
Thrust	7.2 lb
Moment arm	16 in.
Limit cycle	14 sec
Jet time per cycle	1.5%

**Roll Control Systems**

Pull-on signal	$\pm 3.0$ deg
Drop-out signal	$\pm 2.7$ deg
Lead circuit transfer function	$\frac{1 (1 + 0.2S)}{40 (1 + 0.005S)}$

**Roll jets: Minimum thrust (vacuum)**

Moment arm	25 in.
Limit cycle	—
Jet-on time per cycle	—

<i>First Stage Powered Flight</i>	<i>Powered Flight</i>	<i>Second Stage Coasting Flight</i>
115 lb	8.0 lb	7.0 lb
25 in.	17 in.	17 in.
—	3.9 sec	4.1 sec
—	7%	7%

second in the event that some external disturbance forced the vehicle to deviate from the desired trajectory. The torquer current supply for this function was located in the controls can. In addition to pitch program flexibility, the flight path azimuth could be changed from the launch azimuth by means of a roll program. This feature was employed on SLV-6 when a roll program rate of about 3 degrees per second was implemented between 5 and 22 seconds after liftoff. The flight path of this vehicle was changed after being launched at 100 degrees azimuth to an effective flight azimuth of 48 degrees.

A study was made to determine the magnitude of the errors introduced by gyro cross coupling due to gimbal deflections during flight. Results indicated that compensation was unnecessary because all errors were small. There were major problem areas in vibration isolation, the a-c to d-c converter circuit, and temperature controls in the amplifiers. The original vibration isolation system produced drift rates beyond those allowed in the specification. These drift rates stemmed from a coning effect produced by small differences in shock mount resonant frequency and transmissibility. The problem was solved by using silicone rubber vibration isolators (matched to eliminate coning) with very low transmissibility.

The precise pitch rates required imposed an accuracy requirement of  $\pm 0.1\%$  on the output linearity of this converter circuit, independent of input voltage and ambient temperature. Additional compensating circuits were added after initial design to correct for voltage and temperature characteristics. The

accuracy was finally obtained by using hand-wound resistors for final adjustment during the calibration of each circuit in final assembly.

The transistorized switching circuit used to control gyro temperature had a high failure rate. An analysis disclosed that the major fault was due to the components used and to insufficient rating of the output transistor. The amplifiers were redesigned and the new units were retrofitted in all gyroscope packages.

**Program timer**—The Vanguard program timer was designed and built by Designers for Industry, Incorporated. Most conventional methods to provide high accuracy timers in 1955 required the use of a large rotating drum. However, to save space and weight, the proposed Vanguard timer used a synchronous motor to drive a punched film. The tape was later changed from film to stainless steel to prevent stretching and a possible wear problem. A fast-rewind d-c motor was eliminated from the package to save space and weight.

The ten-channel program timer, with an accuracy better than  $\pm 0.1$  out of 720 seconds, used a 25.6-kc crystal oscillator as the primary frequency standard. This was divided through a transistor network to 400  $\pm 0.04$  cps. A transistor output stage then supplied the required power to drive a synchronous motor which, in turn, drove a tape through an appropriate gear train and clutch mechanism. Before launch, the programmer was turned on to allow the oscillator and motor to reach stable operating conditions. At liftoff, a first motion switch at the base of the vehicle sent a signal to the clutch which connected the motor to the gear

**Table 5a Program Timer Functions**

Channel	Function	Rate (deg./sec)	Time (sec)
1	First pitch rate	0.07143	10-24
2	Second pitch rate	0.2750	24-45
3	Third pitch rate	0.4762	45-112
4	Fourth pitch rate	0.2139	112-400
5	Arm critical functions	—	127-720
6	Backup for second-stage shutdown arming and nose cone separation	—	240-250
	Start third-stage spinup and separation sequence	—	540-720
	Nose cone separation	—	172-190
7	Telemetry	—	Every 10
8	Fifth pitch rate	0.02	400-720
9	Arm second-stage shutdown and backup for nose cone separation	—	240-720

train. This set the tape in motion and microswitches and relays picked off the appropriate functions. The program timer performed the functions shown in Table 5a on the flight of TV-4BU.

Some program timers were rejected early in the program because the units did not meet the required accuracy specifications. The trouble was due to failure of an oscillator to hold frequency. This oscillator was replaced by a new design that performed satisfactorily.

**Airborne third-stage firing system**—The airborne third-stage firing system contained an accelerometer that integrated (from liftoff to second-stage burnout) the longitudinal acceleration resulting from external forces other than gravity. Thus, the system had the function of determining overall first- and second-stage performance by computing a gravity-free "indicated" velocity increment imparted by the first two propulsion systems. This indicated velocity was fed into a mechanical coasting time computer (CTC) which then set a coast time such that the injection angle error would be minimized for minimum and nominal performance vehicles.

The original concept for the CTC was to produce a second-stage engine shutdown signal when the vehicle attained a preset velocity. Then the device was to send another signal to the vehicle,  $t$  seconds later, to start the third-stage spinup and separation sequence. The CTC operational concept was later changed to have the unit integrate vehicle acceleration until second-stage shutdown occurred due to either fuel or oxidizer exhaustion. All coasting time computers were manufactured and tested for the latter method of operation, with provisions to easily change back to the first method if desired.

The coasting time computer, designed by Electronics Communications, Incorporated, consisted of four major components: a velocity indicator; a time indicator; a computer; and a precision power supply.

The velocity indicator utilized a HIG-type unbalanced gyro, which was sensitive to linear accelerations along the axis of the vehicle. Its output was an angular shaft position proportional to velocity. The time indicator was a hysteresis synchronous motor and gear train, and provided an output shaft position proportional to time. The two shaft positions were combined in a mechanical analog computer to solve a linear equation. The 400-cps precision power supply ensured that the gyro wheel and motor rotated at constant speed.

The CTC received a start signal from a first motion switch at liftoff. The integrating accelerometer started calculating vehicle velocity by continuously integrating its acceleration. This process continued throughout both first- and second-stage powered flight, resulting in the rotation of a velocity arm in the coasting time computer. At second-stage burnout, a signal was sent to the unit, stopping further movement of the velocity arm and starting the timing mechanism. The timing mechanism rotated a timing arm until it came into contact with the stationary velocity arm after an elapsed coasting period that was directly related to the velocity at second-stage burnout. At this instant of contact, a signal from the computer started the third-stage spinup and separation sequence.

Major development problems were encountered during vibration and temperature testing of the CTC. Several undesirable resonances were discovered in the velocity arm and timing arm when the unit was subjected to vibration. The two arms were redesigned and stiffening plates were added to the assembly to overcome this problem. A severe resonance was also noted in the pendulous gyro assembly at a frequency of 135 cps. This resonance was eliminated by supporting the gyro assembly at the upper end with an additional bearing.

The gyro table would not revolve freely when the unit was subjected to the cold temperature test. Analysis indicated that this condition was caused by

contraction of the outer race of the bearing supporting the gyro assembly. Thermal isolation between the gyro block and the mounting table, in the form of phenolic washers between the two surfaces, provided proper unit operation at 20°F.

The sensitivity of the velocity measurement from the coasting time computer was increased to provide more accurate telemetering data for the ground-based third-stage firing system. This was accomplished by loading the velocity potentiometer with a fixed resistor.

## 2. GROUND-BASED THIRD-STAGE FIRING SYSTEM

An independent ground-based firing system was provided for the Vanguard vehicle as an alternate means of initiating the third-stage firing sequence (Ref. 15). An IBM-704 digital computer was used to predict second-stage apogee time based upon C-band radar tracking data obtained during the 30-second interval just after second-stage burnout. A coast time,  $T_s$ , was then calculated, using a quadratic conversion function based on preflight estimates of vehicle performance.  $T_s$  was compared to the coast time indicated by the airborne computer,  $T_A$ , which was obtained through a telemetry link. These two coast times and their absolute difference were used by the ground-based operator in deciding which system should fire the third stage. The decision criteria (e.g., Ref. 15) used by the ground-based system operator included a display radar roughness number, which was indicative of radar data reliability. If a decision was made to use the ground-based system, command control transmitters were employed to activate circuits in the vehicle which initiated the third-stage firing sequence after a 100-second delay. A direct command with no delay was also provided.

The airborne system, because of its simplicity, was allowed to fire all vehicles where a margin of performance existed. The inherently more accurate ground-based system was favored in most operational plans for initiating spinup of minimum performance vehicles.

## 3. CONTROL SYSTEM

The control system was required to maintain vehicle attitude control to close limits about all three axes. Powered flight control was maintained by gimballed engine motions in the pitch and yaw planes and by reaction jets about the roll axis. Reaction jets were used exclusively during second-stage coasting flight. The third stage had no control system; attitude was maintained by spin stabilization. Control system hardware consisted primarily of pitch, yaw and roll amplifiers and their associated circuitry. (See Fig. 15.)

**Design**—The plan at the start of the program was to develop a magnetic-amplifier autopilot as the

primary control system, with an electronic autopilot (Viking circuits with subminiature tubes) as a backup system. The transistor approach, though appealing, was not considered because of the rudimentary state of its development at the time. The vehicle wiring was designed so that either system could be used by simply installing in the vehicle either a mag-amp controls can or an electronics controls can. The mag-amp autopilot program was cancelled in July 1957, when it became evident that production flight units would not be available for flight testing in the early test vehicles. The Martin-designed subminiature vacuum tube electronic autopilot was then used as the control system for Vanguard.

Additional design considerations included the utilization of only one roll amplifier for control of both the first- and second-stage roll jet systems. This approach allowed one compensating network to stabilize both the first- and second-stage roll jet systems, but made the deadspot and hysteresis the same for both stages. Pressurized containers were used for mounting the control system components to avoid environmental problems and for ease of maintenance and testing.

A high natural frequency of the thrust chamber supporting structure was maintained to preclude a frequency resonance instability problem. A relatively low control system external gain (1.2 for the first stage) was used to avoid a structural feedback and engine noise problem.

The second-stage engine gimbaling system was activated prior to launch. This allowed a final check to be made while the rocket was on the ground and, even more important, it avoided the use of an in-flight hydraulic pump motor starting system and associated electrical starting transients.

**Pitch and yaw control, powered flight**—Pitch and yaw attitude control during first- and second-stage powered flight was achieved by means of gimballed engines. The engines were positioned by servos which were commanded by the gyro reference system through electro-hydraulic null-type control devices. The pitch and yaw autopilot amplifiers were identical. Displacement of the vehicle from the desired gyro reference axis produced an output signal from the gyro. This signal passed through a gain control and was then amplified and demodulated, resulting in a d-c signal. The signal passed through a cathode follower and then took two paths. One path was through a structural feedback filter, lead network and lag network on to the first-stage internal loop; the other was through a lead network on to the second-stage internal loop. The internal loop for each stage contained d-c amplifiers that converted the d-c signal into a differential current which was applied to the hydraulic transfer valve (see Chapter IV, Section I). This valve allowed hydraulic

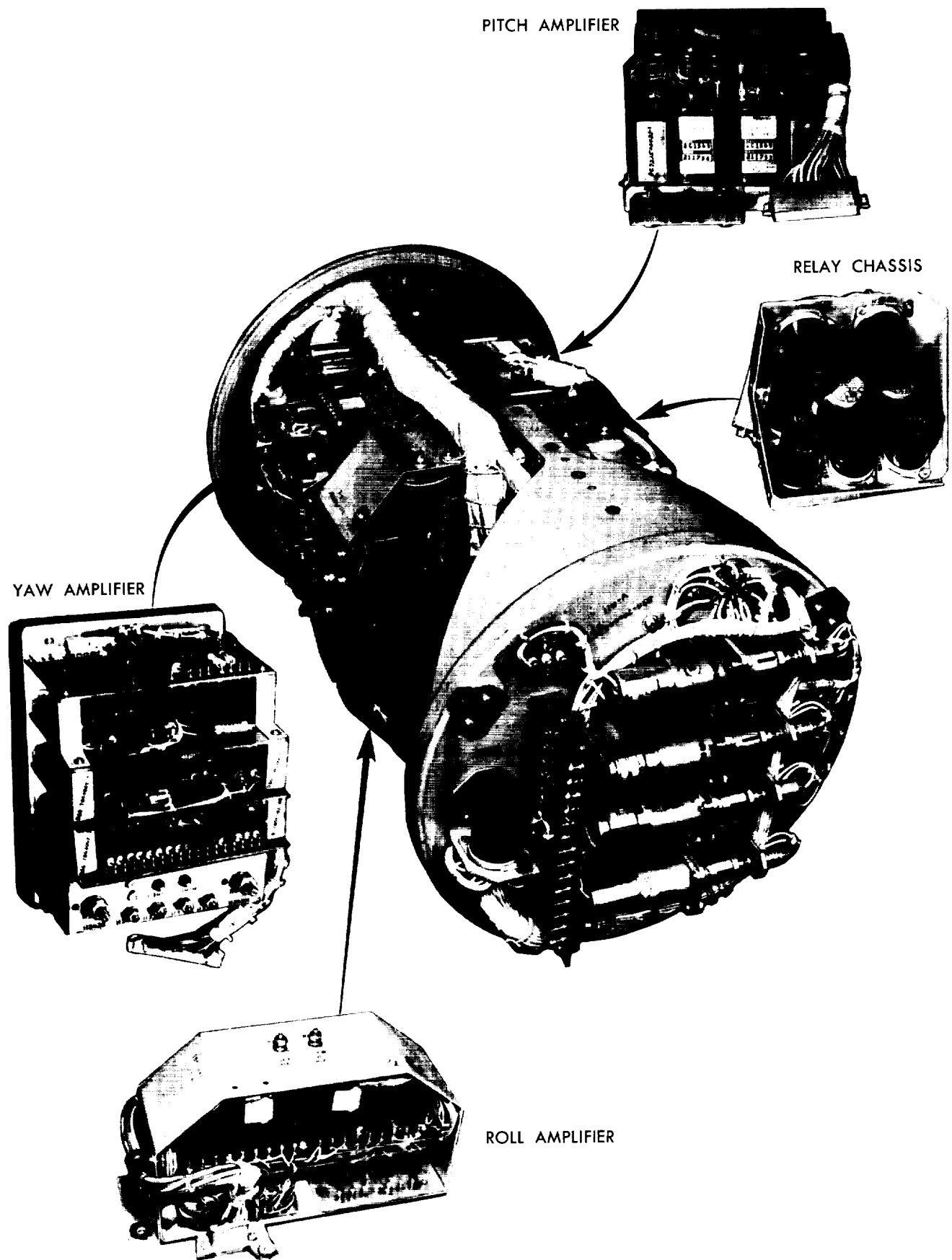


Fig. 15 Airborne Controls Can

fluid to flow in the proper direction to move an actuator piston which deflected the rocket engine. The engine continued to move until the feedback voltage from the follow-up potentiometer attached to the piston equaled the compensated gyro signal voltage at the internal loop input.

**Pitch and yaw control, coasting flight**—Coasting flight control in pitch and yaw was accomplished by means of on-off reaction jet control. The four pitch/yaw jets used the residual helium in the second-stage oxidizer tank as an energy source. The pitch and yaw jet amplifiers were identical and were contained on the same chassis as their respective engine gimbaling units. The jet amplifiers were operating during powered flight but did not actuate the jets since the slave relays, and hence the jet solenoids, were not armed until second-stage burnout.

The jet amplifiers were of the on-off type, having a system dead-zone of 0.4 degree. As in the case of the servoamplifiers, the gyro signals were amplified, demodulated and modified by an R-C lead network. The resulting signals were then amplified by high-gain d-c differential amplifiers containing output plate relays in their final stages. The amplifiers operated linearly up to the output stage containing the relay. The relay tube was biased considerably below cutoff so that a zero-rate gyro signal of 0.4 degree would just energize the relay. Changing the bias point (pull-in point) did not change amplifier gain, and therefore did not affect hysteresis. The plate relay operated a slave relay located on the relay chassis in the controls can, which, in turn, operated the jet solenoid. A slave relay was required because the plate relay could not handle the high current requirements of the jet solenoid. A condenser was added across the slave relay contacts to prevent high arcing currents from welding relay contacts.

Flow of helium through the jet nozzles provided correcting thrust, regulated to the design value of 7.2 pounds per jet by an orifice at each solenoid valve. When the attitude error decreased to a specified value, the plate relay dropped out, de-energizing the slave relay and jet solenoid. The rocket then rotated about the cg at a constant velocity until the gyro error signal activated the opposite jet. This on-off process continued throughout coasting flight. A high  $\alpha$  lead network ( $\alpha = 30$ ) was used to provide a short jet-on time ( $\approx 0.1$  second) and a long jet-off time ( $\approx 7$  seconds) for the pitch/yaw jet systems, so that consumption of residual helium would be minimized.

**Roll control**—First-stage roll control was obtained by utilizing the first-stage engine turbine exhaust to provide the correcting moment. The two exhaust nozzles (Fig. 32) normally pointed aft, providing a small additional forward thrust, but were differentially

rotated 45 degrees in either direction to provide roll control when the vehicle attitude error exceeded 3 degrees. Minimum design roll jet thrust was 50 pounds per jet at sea level and 115 pounds per jet at altitude. Residual helium gas, vented through these same jets, augmented roll control during first-stage separation.

Second-stage roll control was achieved by ejecting gas from four fixed reaction jets, two for a clockwise and two for a counterclockwise correcting moment. A separate propane system was used during powered flight to keep the control system isolated from the propulsion system. Liquid propane was stored in an aluminum tank and heated to 120°F and 240 psia by an electric heater blanket. Opening of the roll jet solenoid valves by the control system allowed gaseous propane to flow from the tank. The gas supply was replenished by further evaporation of liquid propane within the tank. A regulator reduced the upstream pressure at the nozzles to 62 psia, corresponding to a thrust level of 8.5 pounds per jet. At second-stage burnout, the roll system was switched from propane to the residual helium remaining in the fuel tank by actuating a solenoid-operated three-way valve.

The one roll amplifier actuated the first-stage, second-stage powered flight, and second-stage coasting flight roll systems. The operation of the roll jet amplifier was similar to that previously described for the pitch/yaw jet amplifier. However, the roll amplifier required less gain than the pitch/yaw amplifier because the system deadspot in roll was  $\pm 3$  degrees. Again, a high  $\alpha$  lead network ( $\alpha = 40$ ) was used to provide the least amount of jet-on time ( $\approx 0.1$  second) and the maximum jet-off time ( $\approx 2.2$  seconds) commensurate with adequate system stability. The roll amplifier output plate relay also operated a slave relay. One set of slave relay contacts actuated the first-stage system, while the second set actuated the second-stage system after an arming signal was received at second-stage ignition.

**Third-stage control**—No controls equipment was employed in the solid-propellant third stage. Disturbing moments would normally result from thrust vector and principal axis misalignments, and changes in mass, pitch and roll inertias, and cg position during burning. These disturbing moments were overcome by spinning the third stage about its longitudinal axis. Various spin studies were conducted to establish requirements for the third-stage design which would maintain the flight path error within tolerable limits and achieve desired orbit injection conditions.

A special problem arose with the TV-1 configuration, where the third-stage rocket motor carried a 180-pound instrumented nose cone. The stability of this configuration during third-stage burning, with the motor spin inertia being transmitted to the heavy non-

rotating nose cone, was open to serious doubt. Also, the re-entry velocity was sufficiently low to present a range safety problem in case of azimuth deviation. This two-body spin problem was never rigorously solved, but studies indicated that the stability deterioration was not of a serious magnitude and that range safety would not be jeopardized.

Initial Vanguard configuration studies were based on the arbitrary requirement that the flight path should not deviate more than 0.25 degree during third-stage powered flight. Equations of motion used for these early studies were for a rigid, spinning symmetric body with the disturbing moments fixed with respect to the body axes. The assumption of rigidity between motor and payload was considered adequate on the basis of a payload considerably lighter than the initial motor weight. The resulting minimum spin rate requirement was 150 rpm. However, since the TV-4BU flight used a different motor and carried a heavier payload, it was felt necessary to investigate the expected flight path deviations considering the two-body spin problem. Arbitrary pitch and roll moments to simulate the effect of the spinning satellite were included in the new study. The maximum possible third-stage flight path deviation during powered flight was found to be 0.43 degree for the TV-4BU configuration. This deviation was considered acceptable.

**Auxiliary devices**—Auxiliary electronic devices required by the control system and contained in the controls can include a B+ voltage supply, slave relay chassis and auxiliary chassis. The B+ power supply produced 150 volts dc, used as a plate supply voltage for the electronic autopilot. The final design of this unit (flown on the last two vehicles) was a transformer-rectified, Zener-diode regulated voltage supply. The unit received three-phase 115 volts ac at 400 cps from the inverter as the primary input voltage. This voltage was then converted to dc by a full-wave rectifier. The d-c output voltage was next filtered by a  $\pi$  type L-C filter and regulated by a 50-watt, 150-volt Zener diode. This system replaced a dynamotor and electronic noise filter combination that was used on previous vehicles.

The slave relay chassis contained the six pitch, yaw and roll slave relays, the pitch/yaw power relay and the helium dump relay. The pitch/yaw power relay armed the pitch/yaw jets at second-stage burnout, actuated the three-way pilot valve, and sent a signal to the coasting time computer to start the timing mechanism. The helium dump relay, when activated, energized the pitch, yaw and roll jets and the three-way pilot valve to dump helium from the second stage.

The auxiliary chassis contained the engine remote centering motor-driven potentiometers, the command control relays and voltage supply, the command con-

trol telemetering circuit, the fifth pitch program relay and the program timer test relay.

#### 4. DEVELOPMENT TESTING AND PROBLEMS

Engine and control jet mockups were used for dynamic testing and problem investigations of control system components.

**Engine mockup development tests**—The engine mockups were used to dynamically test system operation and performance, using prototype hardware. The first-stage pitch/yaw engine mockup consisted mainly of a thrust chamber mounted in its supporting structure. This entire assembly was inverted from its normal position and bolted to the floor. A first-stage hydraulic servo was used with the mockup. The pitch amplifier, power supplies and test equipment were located on a bench near the mockup. Hydraulic pressure was supplied to the actuator by an external Greer hydraulic unit. Some of the more important tests performed on the first-stage mockup (Ref. 14) were: servo loop frequency responses; servo loop transient responses; complete system frequency responses; complete system transient responses; complete system linearity tests; complete system drift tests; and closed-loop analog computer tests.

Servo loop frequency responses showed that the response was substantially independent of 10% variations in hydraulic pressure or B+ voltage. Tests also verified that the gain and stability of the loop were adequate. Transient response tests verified that loop damping, overshoot and stability were adequate. Complete system frequency responses verified that the actual first-stage hardware had the same characteristics as those predicted for the lead network, structural feedback filter and lag network. Tests also showed that response characteristics were substantially independent of 10% variations in hydraulic pressure, B+ voltage or a-c voltage. Complete system transient responses, linearity tests and drift checks all produced results well within the predicted and specification limits.

Analog computers were used extensively with the first-stage mockup to simulate vehicle dynamics and structure dynamics. Tests performed with the analog computers were chiefly transient response and noise tests. Results indicated satisfactory closed-loop system operation.

The second-stage pitch/yaw engine mockup consisted of a mass, simulating engine inertia, mounted on top of a tank duplicating the second-stage oxidizer tank. The tank was pressurized to 100 psig to simulate actual flight conditions so that the effect of structural resonances would be taken into account. The test setup was the same as that described for the first stage. Tests performed on this mockup were similar to the first-stage mockup tests. Test results demon-

strated that system performance was more than adequate (Ref. 14).

The engine mockups were maintained in an operating condition throughout the program. This proved worthwhile, since troubleshooting could conveniently be done during factory, field and flight tests without causing the schedule delays that would have accompanied troubleshooting on the vehicle. The mockups were also used to check any changes made to the system.

**Jet mockup development tests**—Three jet mockups were used to dynamically check operation of the systems using prototype hardware. Tests were made on the first-stage roll system, second-stage roll system and second-stage pitch/yaw coasting system. The first-stage roll mockup was supported from an A-frame by a chain and was free to rotate in the horizontal plane. Included on the mockup were helium pressurization tanks, a hydrogen peroxide tank, a catalyst chamber, a plenum chamber, two rotatable roll jets and a HIG gyro. The roll amplifier, power supply, slave relays, control panel, gyro panel and recording oscillograph were located in a blockhouse near the mockup. System performance was checked as simulated flight disturbing moments were imposed and as parameters such as deadspot, 28-volt dc, B+ voltage, initial mockup direction and displacement were varied. System stability and performance were adequately demonstrated in the more than 20 tests made on the first-stage roll jet system (Ref. 14).

The second-stage roll jet mockup was also supported from an A-frame by chains. Propulsion controls, a propane tank, a helium tank, roll jet solenoids, four fixed roll jets and a HIG gyro were located on the mockup. Propane or helium could be fed to the roll jets by simply actuating a three-way valve from the blockhouse. Control and instrumentation devices were located in the blockhouse. Tests similar to those performed on the first-stage roll system were performed on the second-stage system. Constant disturbing moments were also imposed on the mockup to check system stability for simulated thrust misalignment and engine shutdown disturbances. A test was made on the propane system to check flow rates, total jet-on time and the total amount of fuel that would be used during powered flight. Results showed that a more than adequate amount of fuel was available for powered flight roll control. Proper solenoid valve and slave relay opening and closing times were also checked and agreed closely with those used previously in a phase plane analysis. System stability and performance were verified by the 35 test runs made on the second-stage roll jet system (Ref. 14).

The second-stage pitch/yaw coasting flight mockup utilized an 18-foot beam to simulate vehicle inertia.

The mockup rotated in a vertical plane on bearings to lessen friction effects. Included on the mockup were a helium supply, jet solenoids, two fixed jets and a HIG gyro, with the controls and instrumentation equipment in the blockhouse. Preliminary tests revealed that system damping and overshoot was not adequate when tests were made at large initial mockup displacements. An investigation indicated that vacuum tube saturation was the problem. Proper jet amplifier operation was attained by decreasing the a-c amplifier gain to prevent saturation, while increasing the d-c amplifier gain to maintain the specified 90% hysteresis. Also, the Filtor slave relay did not have a high enough contact current rating to prevent pitting and eventual welding of contacts. The Filtor relay was replaced with a Hart relay. Discovery of these two problems early in the program certainly justified the mockup tests. This early awareness of problems avoided schedule delays and possibly flight difficulties.

System tests made on the redesigned pitch/yaw jet system were similar to those performed on the roll systems. For pitch/yaw tests, a 254 foot-pound disturbance for 0.5 second was imposed on the mockup to simulate the engine shutdown disturbance. Adequate system stability and performance were demonstrated in the 35 tests performed on the pitch/yaw coasting flight system (Ref. 14).

**Development problems**—The major autopilot problem on Vanguard was "structural feedback" (see Chapter III, Section F). The solution to this problem was to stabilize the structural loops so that the control system would perform its normal task in the presence of body-bending vibrations. The problem on Vanguard was particularly difficult because the autopilot natural frequency was quite close to the first-mode bending frequency, and the engine gimbaling control system response was appreciable at the second bending mode frequency. This problem was further aggravated by the extremely low inherent structural damping.

Stability analyses showed that the autopilot was unstable near both first- and second-mode bending frequencies. Stability was achieved by attenuating the control system response near the second-mode frequency with a double-notch rejection filter, and by phase-shifting the control system response near the first-mode frequency with a simple lag network. This solution produced loop stability and enabled the control system to effectively damp out vibrations induced by gusts, wind shears, etc.

Two minor development problems encountered during the program were engine noise due to gyro heater cycling and slave relay contact failures. In the early vehicles, an engine drift or movement was observed whenever the gyroscope heaters cycled. The

magnitudes of these shifts ranged from 0.1 to 0.3 degree in the pitch and yaw axes. This problem was eliminated by shortening the 28-volt d-c leads, by shielding the 400-cps leads, and by placing the dynamotor input on the second-stage battery and the gyroscope heaters on the first-stage battery. Heater cycling effects were negligible during second-stage powered flight, when both the dynamotor and heaters were on the second-stage battery. Here all wire runs were short, the second-stage control system gain was low and, by this time, less heater cycling occurred because the gyros had warmed up.

Several pitch/yaw relays failed during controls ground tests when the contacts on the slave relays became welded together. Steps taken to eliminate this problem were the addition of capacitors across the slave relay contacts to prevent arcing and welding, and revision of all plant and field test procedures to keep the vehicle pitch/yaw solenoids disconnected for all tests except polarity checks.

## B. FIRST-STAGE PROPULSION

### 1. BASIC DESIGN DECISIONS

The Vanguard first stage was originally envisioned as a "modified Viking," and indeed the concepts and experience (if not the actual hardware) of the successful earlier program were conspicuous in its design. Whenever possible, proven Viking concepts were used for Vanguard, with refinements introduced to obtain maximum weight economy and full integration of the engine with the propellant supply systems.

**Engine selection**—The original satellite vehicle design studies by the NRL and The Martin Company had established first-stage propulsion requirements that were considered beyond the reach of the existing Viking powerplant. However, advanced design studies for another application of Viking had considered the use of the General Electric Hermes A-3B engine, which appeared capable of development to meet the Vanguard requirements. There was actually no other existing rocket engine in this performance range, so that the "off-the-shelf" concept dictated selection of the improved Hermes engine, designated X-400, to be developed for the Vanguard first stage.

A purchase order was issued to the General Electric Company on 1 October 1955 to develop, test and deliver calibrated engine packages in accordance with a Martin Development Specification (Ref. 16). The new engine was designated X-405. The first production unit was scheduled for delivery within one year, which was not considered unrealistic, since only a modest development program was anticipated to verify the necessary modifications.

**Propellants**—The original Hermes engine had burned liquid oxygen and alcohol, as was fairly

standard for its day. The X-400 was proposed, and had some firing history, using gasoline as the fuel, which provided a significant increase in specific impulse. Early in the X-405 design phase, a decision was made to use kerosene instead of gasoline, primarily because of its higher and more predictable density, which would allow a weight saving in smaller tankage and permit more accurate prediction of fuel loadings to minimize outage.

**Engine package concept**—Viking experience indicated the necessity for an "engine package" concept, whereby the vendor-supplied engine was a fully integrated, tested and calibrated unit which would mate properly with Martin-built tankage and pressurization systems. To assure proper integration, specifications were established for engine pump inlet pressures and temperatures (Table 6). The engine manufacturer was required to maintain these conditions while demonstrating engine performance and compliance with other specification requirements. The Martin tankage and pressurization systems were designed to comply with the same pump inlet conditions. This concept also simplified the interchange of engine packages from one vehicle to another.

**Table 6. X-405 Rocket Engine Propellant Inlet Specifications**

	<i>Oxidizer</i>	<i>Fuel</i>	<i>Peroxide</i>
Temperature, °F	$-294.7 \pm 2$	$60 \pm 30$	$60 \pm 30$
Operating pressure, psia	$49 \pm 5$	$24.9 \pm 5$	650 (670 max)
Maximum lockup pressure, psia	61	39.9	690

**Tankage and pressurization systems**—The principal design philosophy for the Martin portion of the first stage was similarity to proven Viking systems, except where refinements were introduced for weight saving or reliability reasons, or to meet the more stringent Vanguard requirements.

Serious consideration was given to using an automatic propellant utilization system to minimize outage, but it was finally concluded that careful design of the pressurization system, accurate engine calibrations and precise propellant loading would provide mixture ratio accuracy such that nominal outage would not exceed 2%. On this basis, the complexity and weight of the propellant utilization system could not be justified. Vanguard flight results (Chapter VIII, Section B) testified to the soundness of this decision.

### 2. SYSTEM DESCRIPTION

The general arrangement of the first stage is shown in Fig. 12 and a schematic diagram of the propulsion system is given in Fig. 16.

**Propellant tankage**—The main propellant tank diameters were 45 inches, the same as Viking. This permitted the use of some existing Viking tooling, with

slight modification as to length, for tank fabrication. Average tank volumes and capacities are shown in Fig. 16. The liquid oxygen tank was located forward of the kerosene tank in order to keep the vehicle center of gravity forward, to take advantage of the greater liquid head, to economize on pressurization gas and to maintain a higher liquid oxygen density by stabilizing the bulk temperature through increased oxygen boiloff due to the lower gas pressure. The LOX tank top was conical in order to better withstand high external pressures from the second-stage engine during the separation sequence. The LOX tank top was capped with a plastic laminant and insulating blanket for thermal protection during second-stage ignition and separation, and also to reduce the cooling effect of the LOX on the second stage. A quick-disconnect fill fitting was provided in the side of the fuel tank.

The hydrogen peroxide tank was mounted above the firewall, off center in order to prevent interference with the propellant feed lines and to allow room for other equipment.

All first-stage propellant tanks contained baffles to prevent vortexing. Baffle design was very similar to that of Viking, the only changes being the addition of an extra vane and a slight increase in baffle depth in the LOX and kerosene tanks. Peroxide tank baffles were the same as Viking. The purpose of the inlet baffle on the peroxide tank was to prevent pressurization gas from striking the peroxide directly and causing frothing or bubbling.

All propellant tanks were vented to the atmosphere during propellant servicing and throughout the count-downs by normally open vent valves. The vents were locked closed electrically just prior to launch by remotely operated solenoid pilot valves. All three tanks had mechanical vents to relieve overpressurization. The LOX and fuel vent reliefs were set at  $30.1 \pm 1.5$  psig and  $21 \pm 1.5$  psig, respectively. The peroxide vent relief was adjustable.

**Pressurization system**—Helium was selected as the pressurization gas because of the tremendous weight advantage that it offered. Considerations of leaking and handling had little bearing on its choice. The helium was contained in two high-pressure spheres, manufactured by the A. O. Smith Company; these were located in the aft section just below the fuel tank. The high-pressure gas was regulated to a lower value by a single-stage, dome-loaded, normally closed, solenoid-operated regulator, which supplied pressure to all the propellant tanks and pneumatically operated valves. Orifices in the fuel and LOX tank lines further reduced the regulated helium pressure. Average tank pressures are shown in Fig. 16.

**Engine package**—The General Electric X-405 rocket engine (Fig. 17) is described in the manufac-

turer's Model Specification (Ref. 17). It used liquid oxygen and kerosene as propellants, at a nominal mixture ratio (O/F) of 2.2, and was capable of operation for a minimum of 150 seconds at a nominal sea level thrust rating of 27,835 pounds. Other pertinent design parameters are listed in Table 7.

**Table 7. First-Stage Rocket Engine Design Parameters**

	Minimum	Nominal	Maximum
Burning time—sec	150		
Thrust at sea level—lb	27,000	27,835	28,670
Specific impulse at sea level (overall average between 90% rated thrust points)—sec	248	254	
Oxidizer flow rate—lb/sec		73.6	
Fuel flow rate—lb/sec		33.5	
Optimum mixture ratio (O/F, by weight)		2.2	
Hydrogen peroxide flow rate— lb/sec		2.2	2.4
Chamber pressure—psia		616	700
Throat area—sq in.		31.8	
Combustion chamber volume— cu in.		616.5	
Characteristic chamber length (L*)—in.		19.4	
Thrust chamber expansion ratio		5.5	
Thrust coefficient (C <sub>r</sub> )		1.42	
Characteristic exhaust velocity (c*)—fps		5750	
Turbine speed—rpm		31,000	
Turbine exhaust pressure—psia		30	
Gimbal deflection in pitch or yaw plane—deg			$\pm 5$
Thrust vector alignment tolerances:			
Distance from center of engine mounting points—in.			0.0625
Angular deviation from engine geometric axis— deg			0.4
Thrust chamber support frequency—cps	30		
Engine package dry weight—lb			425
Engine package wet weight—lb			450
Oxidizer—Liquid oxygen, Federal Specification BB-0-925, Type II			
Fuel—Kerosene, Shell Oil Co., Jet Fuel, Grade B, No. 16185, UMF			
Hydrogen Peroxide—BECCO, 90	+1	-0%	

The engine package was located below the peroxide compartment firewall and was attached to the airframe at four thrust structure attachment points. The thrust structure assembly consisted of four identical thrust struts and two actuator support struts, welded together and supported around a central hub assembly. Four support brackets on the thrust struts supported the turbopump.

The thrust chamber assembly was attached to the thrust structure by means of the gimbal ring and yoke assembly. The gimbal ring attached to the bottom of the hub on the thrust structure by two gimbal bearings, while the yoke assembly was attached to the gimbal

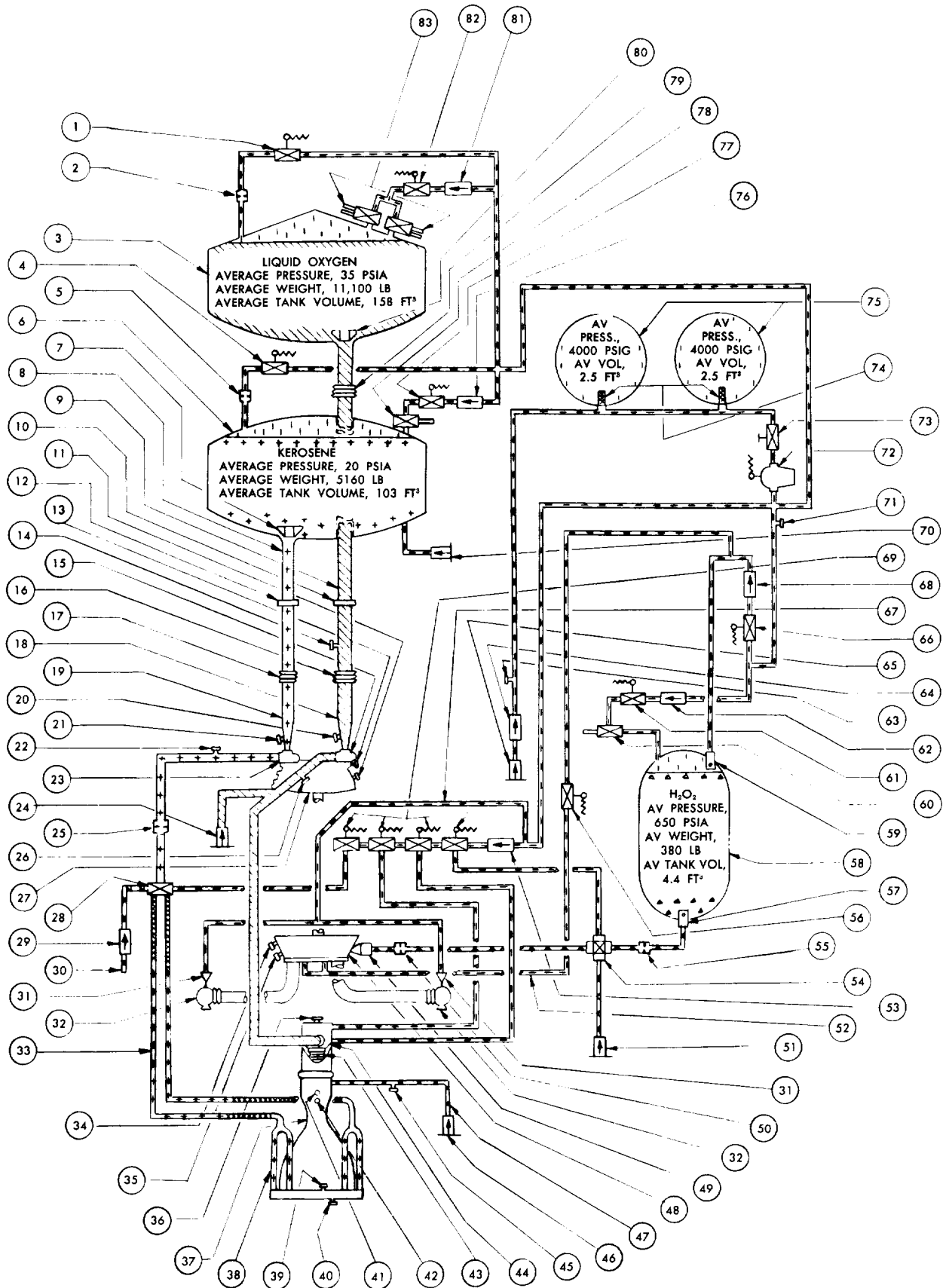


Fig. 16 First-Stage Propulsion System Schematic

## PARTS LIST

- |                                        |                                                 |
|----------------------------------------|-------------------------------------------------|
| 1. LOX TANK HELIUM FLOW CONTROL VALVE  | 43. LOX BELLOWS                                 |
| 2. LOX TANK ORIFICE                    | 44. LOX CONTROL VALVE (WITH ORIFICE)            |
| 3. LOX TANK                            | 45. FUEL INJECTOR PRESSURE SENSOR               |
| 4. FUEL TANK HELIUM FLOW CONTROL VALVE | 46. ETHANE FILL DISCONNECT                      |
| 5. FUEL TANK ORIFICE                   | 47. ETHANE LINE                                 |
| 6. FUEL TANK                           | 48. TURBOPUMP NOZZLE BOX                        |
| 7. FUEL TANK OUTLET BAFFLE             | 49. HYDROGEN PEROXIDE DECOMPOSER AND CATALYST   |
| 8. FUEL FEED LINE                      | 50. HYDROGEN PEROXIDE SYSTEM ORIFICE            |
| 9. LOX FEED LINE                       | 51. HYDROGEN PEROXIDE FILL AND DRAIN DISCONNECT |
| 10. LOX FLOWMETER                      | 52. HELIUM AUGMENTATION LINE                    |
| 11. GEAR CASE BREATHER                 | 53. CHECK VALVE                                 |
| 12. FUEL FLOWMETER                     | 54. MAIN HYDROGEN PEROXIDE VALVE                |
| 13. LOX PUMP SEAL PRESSURE SENSOR      | 55. CAVITATING VENTURI ORIFICE                  |
| 14. LOX LINE TEMPERATURE SENSOR        | 56. HELIUM THRUST AUGMENTATION VALVE            |
| 15. LOX PUMP                           | 57. HYDROGEN PEROXIDE TANK OUTLET DIFFUSER      |
| 16. LOX LINE BELLOWS                   | 58. HYDROGEN PEROXIDE TANK                      |
| 17. FUEL LINE BELLOWS                  | 59. HYDROGEN PEROXIDE TANK INLET DIFFUSER       |
| 18. LOX LINE TRANSITION SECTION        | 60. HYDROGEN PEROXIDE TANK VENT LINE            |
| 19. FUEL LINE TRANSITION SECTION       | 61. HYDROGEN PEROXIDE VENT PILOT VALVE          |
| 20. LOX LINE PRESSURE SENSOR           | 62. HYDROGEN PEROXIDE VENT CHECK VALVE          |
| 21. FUEL LINE PRESSURE SENSOR          | 63. HELIUM LINE PRESSURE TAP                    |
| 22. FUEL PUMP OUTLET PRESSURE SENSOR   | 64. HELIUM FILL CHECK VALVE                     |
| 23. FUEL PUMP                          | 65. HELIUM FILL DISCONNECT                      |
| 24. LOX FILL AND DRAIN DISCONNECT      | 66. HYDROGEN PEROXIDE SYSTEM PRESSURIZING VALVE |
| 25. FUEL SYSTEM ORIFICE                | 67. ROLL JET ACTUATOR PRESSURIZATION LINE       |
| 26. LOX PUMP OUTLET PRESSURE SENSOR    | 68. HELIUM LINE CHECK VALVE                     |
| 27. GEAR BOX ASSEMBLY                  | 69. ENGINE CONTROL PILOT VALVES                 |
| 28. FUEL CONTROL VALVE                 | 70. FUEL FILL AND DRAIN DISCONNECT              |
| 29. NITROGEN PURGE CHECK VALVE         | 71. PRESSURE REGULATOR ADJUSTMENT TAP           |
| 30. THRUST CHAMBER NITROGEN PURGE      | 72. MAIN PRESSURE REGULATOR                     |
| 31. ROLL JET ACTUATOR ASSEMBLY         | 73. MANUAL SHUTOFF VALVE                        |
| 32. ROLL CONTROL JET                   | 74. HELIUM SPHERE STRAINER                      |
| 33. FLEXIBLE FUEL LINES                | 75. HELIUM SPHERE                               |
| 34. TURBINE NOZZLE BOX PRESSURE        | 76. FUEL VENT CHECK VALVE                       |
| 35. TURBINE EXHAUST HOOD PRESSURE      | 77. FUEL VENT PILOT VALVE                       |
| 36. LOX INJECTOR PRESSURE SENSOR       | 78. FUEL TANK VENT VALVE                        |
| 37. ENGINE THRUST CHAMBER              | 79. LOX LINE BELLOWS                            |
| 38. REGENERATIVE COOLING LINES (FUEL)  | 80. LOX TANK OUTLET BAFFLE                      |
| 39. FUEL PRIMING BOSS                  | 81. LOX VENT CHECK VALVE                        |
| 40. DRAIN PLUG                         | 82. LOX VENT PILOT VALVE                        |
| 41. THRUST CHAMBER PRESSURE SENSOR     | 83. LOX TANK VENT VALVE                         |
| 42. FUEL INJECTOR TEMPERATURE SENSOR   |                                                 |

## LEGEND

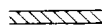
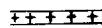
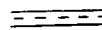

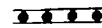
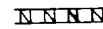
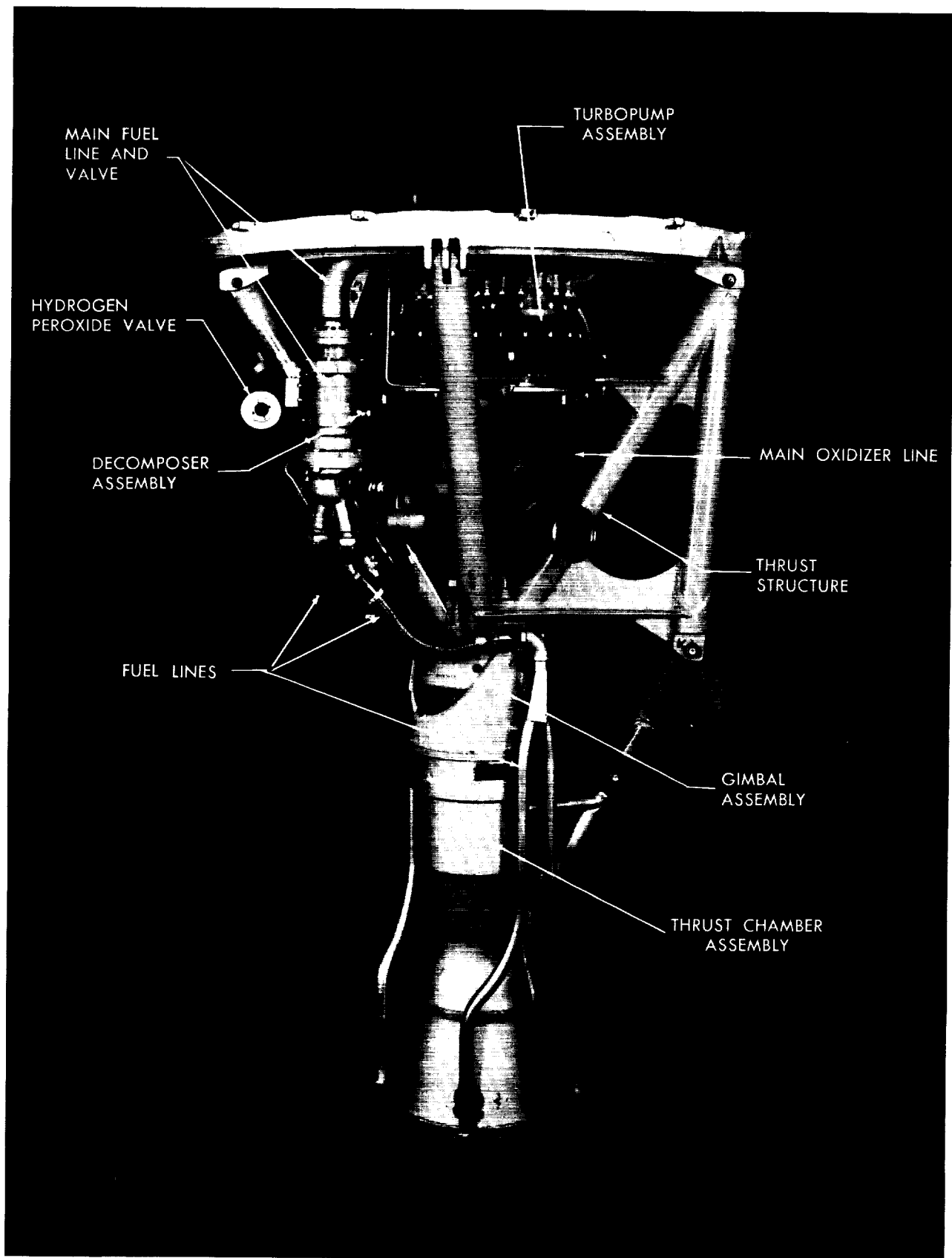
	OXIDIZER (LOX)
	FUEL (KEROSENE)
	HELIUM
	HYDROGEN PEROXIDE
	ETHANE
	NITROGEN

Fig. 16 First-Stage Propulsion System Schematic



**Fig. 17 First-Stage Engine Package**

ring by two additional gimbal bearings. The yoke was bolted to the thrust chamber prior to attachment to the gimbal ring. The gimbal ring and yoke assemblies allowed maximum thrust chamber movements of  $\pm 5$  degrees in the pitch and yaw planes, or combinations of these movements, to permit thrust vector control.

The thrust chamber assembly consisted of a reactant head and a motor body. The stainless steel reactant head injected the propellants into the combustion chamber in an atomized condition, achieved by a like-on-like style injector (Fig. 18b) with two similar streams impinging at an angle of 90 degrees. The sixteen alternate oxidizer and fuel rings contained a total of 554 pairs of self-impinging orifices of varying diameters, drilled in conical recesses on the ring surfaces. Ring No. 1 (in the center) was an oxidizer ring, while Ring No. 16 was a fuel ring. The outermost propellant ring also contained one hundred twenty 0.0225-inch-diameter, axially directed, non-impinging "fuel curtain" holes for combustion chamber wall cooling. The propellant rings were copper-brazed to the injector head plate and the injector was bolted to the motor body.

Figure 18a shows a cross-sectional view of the injector. A 100-mesh stainless steel filter basket and check valve were located in the opening at the top of the injector, through which liquid oxygen passed to reach the injector manifold. Kerosene entered from the motor body through radially drilled passages in the injector. A 100-mesh stainless steel wire filter was wrapped around the injector head to filter the fuel.

The motor body was comprised of inner and outer shells, separated by a helical baffle, thereby forming a cooling jacket with helical passages through which the fuel was passed on its way to the injector. The inner and outer shells were made of steel (AMS 6350) of varying thicknesses which averaged about 0.125 inch. The steel helices were welded to the inner shell. Helical copper fins were positioned between the steel helices around the combustion chamber and throat by brazing to the inner shell. Two brackets were integrally welded to the outer shell to provide connectors for the gimbal actuators. A fuel manifold ring, containing four fuel line bosses and the fuel system drain tap, was located at the aft end of the motor body. All surfaces of the motor body except the hot gas side of the inner shell were nickel phosphide coated. The hot gas side was chrome plated.

Four rigid fuel feed lines affixed to the aft manifold were connected through two flexible hoses to the fuel valve—a normally closed, spring-loaded, pneumatically actuated, sliding sleeve type, with a calibrated orifice in the valve inlet. A flexible bellows connected the injector to the liquid oxygen valve—a normally closed, spring-loaded, pneumatically actuated, pintle type, containing a calibrated spacer for orificing the flow. These

flexible connections permitted thrust chamber gimbaling without propellant flow interruption.

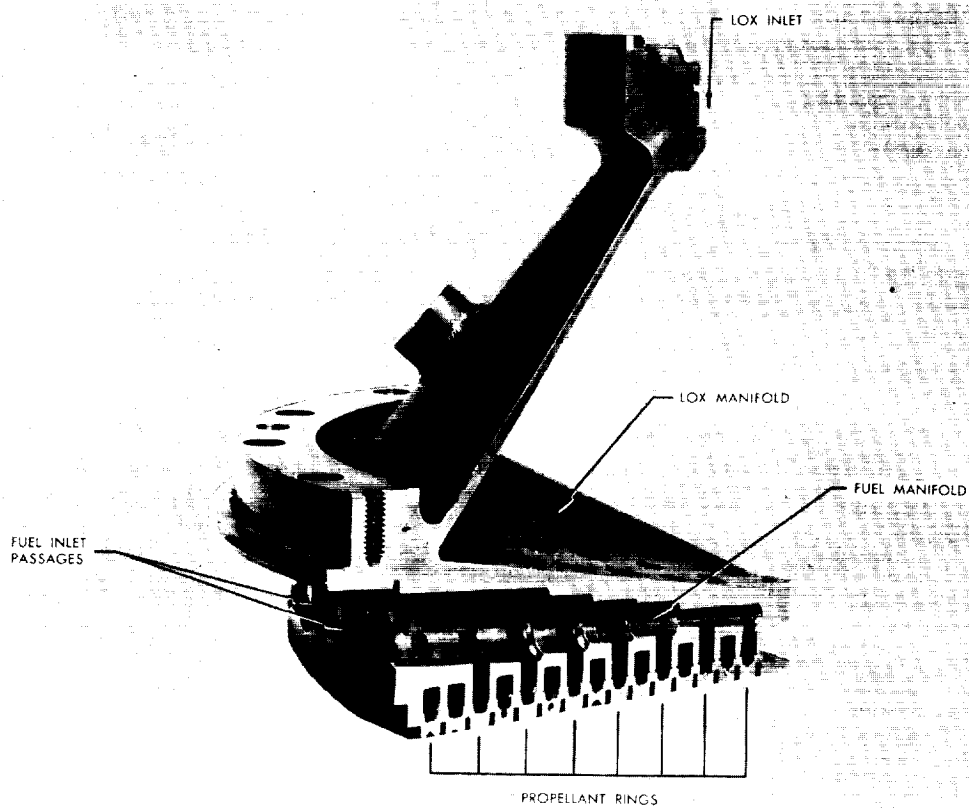
The turbopump was mounted on the thrust structure above the liquid oxygen valve. It contained the turbine wheel, two centrifugal pumps, a gear box, a heat reflector shield, a nozzle box with an attached peroxide catalyst chamber and an exhaust hood with two exhaust stacks. The exhaust hood also had two AN fittings for helium augmentation line attachments. The insulated reflector plate was located between the nozzle box and the gear case assembly to protect the propellants from the heat. All hot external surfaces of the turbopump assembly were covered with insulation.

The liquid oxygen and kerosene pumps contained six fully shrouded vanes and were 6.0 and 5.75 inches in diameter, respectively. The oxidizer pump was equipped with an electrical band-type heater to prevent thrust bearing freezeup when the pump contained liquid oxygen but was not operating. The LOX pump, the pump outlet line and the main valve were insulated to minimize boiloff. The oxidizer pump outlet line was also connected to the LOX fill, drain and disconnect valve at the first-stage tail ring.

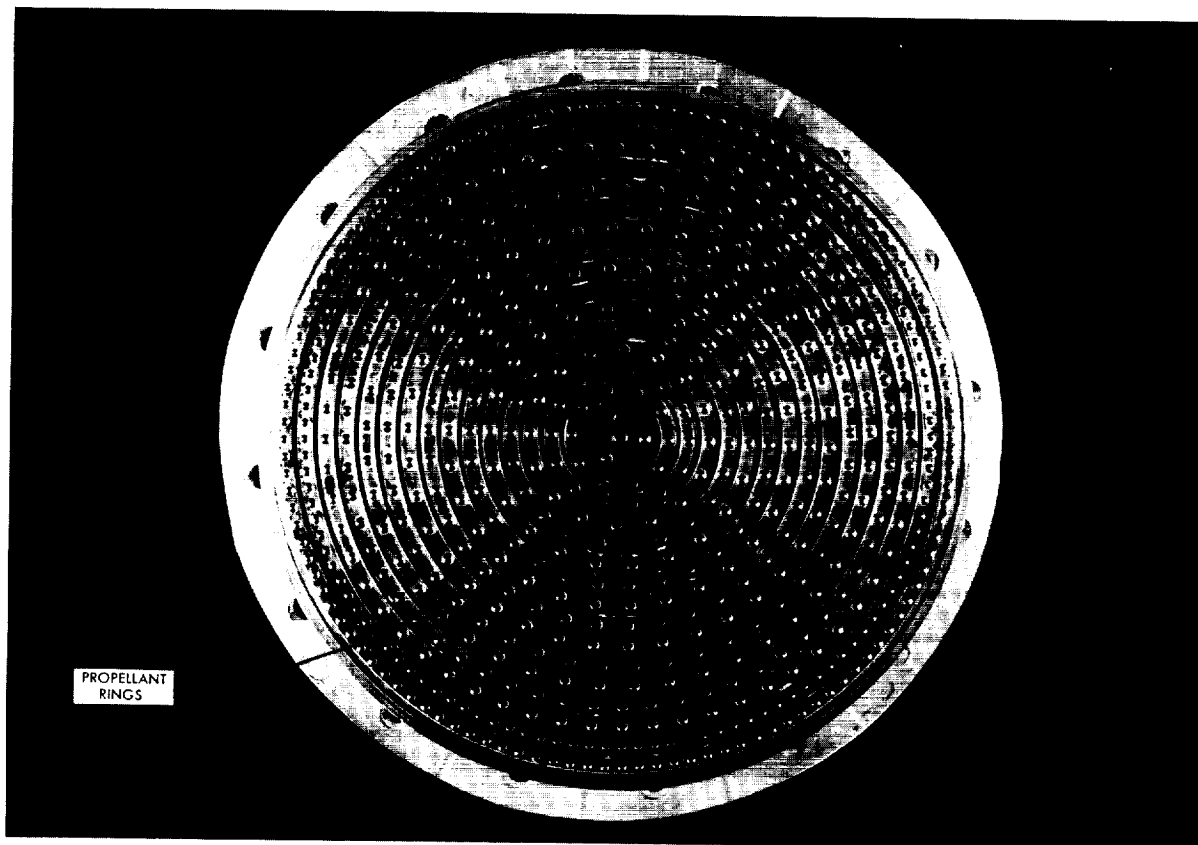
The hydrogen peroxide decomposer, consisting of a silver screen catalyst bed in a stainless steel chamber, was bolted to a flange on the turbine nozzle box. The peroxide valve attached to the inlet side of the decomposer, and included a fill and drain port with a hand valve attached.

Opening and closing of the engine package propellant valves was controlled by regulated helium pressure, supplied through four solenoid-operated pilot valves which were attached to one of the thrust struts and linked electrically to an engine control unit mounted on the same strut. The engine control unit contained all the airborne electrical control elements required for engine start, operation and shutdown.

**Pressurization system operation**—The helium spheres were pressurized through a tail ring disconnect. The peroxide system pressurization valve was closed, and the main pressure regulator was energized. This permitted high pressure helium gas to flow through an open hand valve to the regulator where pressure was reduced to  $650 \pm 20$  psia. Then, the kerosene tank was pressurized, after closing the vent valve and opening its flow control valve, until fuel pump inlet pressure was  $28.5 \pm 1.5$  psia. Next, the peroxide tank was pressurized to  $650 \pm 20$  psia by closing its vent valve and opening the system pressurization valve. The LOX vent pilot valve was energized, closing the two tank vents. Then, the LOX tank flow control valve was opened and the tank pressurized until LOX pump inlet pressure was  $59 \pm 2$  psia. After the fire signal, proper inlet conditions were maintained by the pump inlet pressure switches, electrically linked to open or



A. CROSS-SECTIONAL VIEW



B. PLAN VIEW

Fig. 18 X-405 Type A Precision Injector

close their respective flow control valves to adjust tank pressures on demand.

**Hydrogen peroxide system operation**—Hydrogen peroxide flowed from its tank under positive regulated pressure, through its feed line and a cavitating venturi orifice, to the normally closed, spring-loaded, pneumatically operated main peroxide valve. A signal from the engine sequencer energized the peroxide pilot valve solenoid and allowed pressurization gas to open the peroxide valve against spring tension. Peroxide flowed through the valve and an orifice to the catalyst chamber, where it was decomposed to a gaseous mixture of oxygen and superheated steam, which then entered the nozzle box and drove the turbine. Nozzle box temperature and pressure were 1300°F and 540 psia, respectively. Nominal turbine speed was 31,000 rpm. Power was transmitted from the turbine to the gearbox, which drove the LOX, fuel and hydraulic pumps. The peroxide decomposition gases collected in the exhaust hood and traveled out two exhaust outlets to the roll jets. Exhaust temperature and pressure were nominally 870°F and 30 psia, respectively.

**Oxidizer system operation**—Liquid oxygen flowed from the tank through an insulated four-inch feed line which passed through the fuel tank to the LOX pump inlet. The feed line contained two flexible bellows to compensate for contraction, and a Potter flowmeter and temperature probe for determining oxidizer flow rate. LOX was supplied to the pump at a pressure of  $49 \pm 1.5$  psia under flow conditions. A signal from the engine sequencer energized a solenoid pilot valve to allow pressurization gas to crack the main valve open. LOX flowed to the injector by gravity and tank pressure until the pump started. When the pump discharge pressure approached normal (about 912 psia), the valve pintle was forced open against the springs, and full LOX flow (about 75.4 pounds per second) entered the injector. At engine cutoff, pneumatic pressure from the LOX close solenoid pilot valve and the springs forced the valve closed.

**Fuel system operation**—Kerosene flowed from the tank through a 3.5-inch feed line to the fuel pump inlet. The feed line contained a flexible bellows to compensate for line movement and side loads, and a Potter flowmeter and temperature probe for determining fuel flow rate. Kerosene was supplied to the pump at a pressure of  $25 \pm 1.5$  psia under flow conditions. The pump increased the pressure to approximately 956 psia and supplied fuel to the injector at a flow rate of about 34.5 pounds per second. A signal from the engine sequencer energized the fuel valve solenoid pilot valve and allowed pressurization gas to open the fuel valve against spring tension. At engine shutdown, the gas was vented through an orifice in the control gas line,

which delayed the valve closing time to  $3 \pm 0.5$  seconds.

**Engine ignition sequence**—First-stage ignition was initiated by the fire switch, which supplied 28 volts dc to the igniter filament of a pyrotechnic device. The igniter was positioned in the combustion chamber below the injector by a wooden dowel, which was supported by a metal combustion indicator placed across the exit end of the motor body. Once the igniter power had been applied, all operations in the starting sequence were automatic and were controlled by a ground-based engine sequencer unit. Heat from the burning igniter melted a fusible link, which tripped the igniter indicator relay in the engine sequencer. This opened the LOX valve to preliminary position and actuated the ground-based ethane gas supply valve. Ethane gas entered the combustion chamber through the fuel injector pressure tap at a regulated pressure of 205 to 225 psig. The ethane combined with the vaporous LOX and burned in the presence of the igniter until kerosene entered the chamber. The fuel valve open relay in the engine sequencer was energized 1.5 seconds after the LOX valve left the closed position. The fuel valve opened, and approximately two seconds later, kerosene entered the combustion chamber. When chamber pressure increased to 23 to 28 psia, the combustion indicator and igniter were ejected from the motor body exit, which tripped an attached microswitch. The resulting combustion indication signal closed the ethane supply valve and energized the peroxide valve open relay in the engine sequencer. When the peroxide valve opened, the turbine and the propellant pumps started. When oxidizer pump outlet pressure approached normal, the LOX valve moved to full open to develop full engine thrust.

**Engine shutdown sequence**—First-stage engine shutdown was initiated by exhaustion of either liquid oxygen or kerosene. When the pressure at either pump outlet had decreased to  $500 \pm 50$  psia, the respective pump discharge pressure sensor switch energized the cutoff relay. The cutoff relay then de-energized the engine control unit, closing the hydrogen peroxide, fuel and oxidizer valves. Figures 51 and 52 illustrate typical first-stage chamber pressure decays at shutdown. The pressure sensors were armed by the program timer at 127 seconds after liftoff in order to preclude premature shutdowns due to erratic sensor operation or minor interruptions in propellant flow.

### 3. COMPONENT DEVELOPMENT

Immediately after award of the subcontract, the General Electric Company began modification of their existing engine to meet the Vanguard requirements. The requirement for a gimbaled engine dictated

changes in the design of the thrust structure, development of a gimbal mechanism and relocation of the propellant valves and feed lines. The selection of a higher performance propellant combination and the requirement to increase burning time from 60 to 150 seconds necessitated modifications to the existing injector and motor body. The existing turbopump had to be modified to operate for 150 seconds, to provide a power takeoff for the control system hydraulic pump, and to supply exhaust gases for the roll jets.

**Thrust structure**—The major problems associated with the thrust structure and gimbal ring assembly were attainment of the desired natural frequency and the prevention of gimbal bearing brinelling and permanent set. The natural frequency of the engine package assembly was increased to an acceptable limit (35 cps) by relocating the actuator brackets from the yoke to the thrust chamber outer shell. The brackets were supported on the motor body by a flange which stiffened the outer shell and minimized the possibility of "oilcanning." The yoke was lightened until its deflection approximated that of the gimbal ring under load. Spherical gimbal bearings were installed in lieu of the original needle-type roller bearings to compensate for deflection differences and eliminate brinelling of the bearing shafts.

**Turbopump**—The outer diameter of the fuel pump impeller was reduced and the fuel line metering orifice enlarged to decrease the turbine shaft horsepower output, in order to prevent turbopump operation from limiting engine thrust. This permitted nominal turbine speeds at nozzle box pressures below 550 psig, and also reduced the hydrogen peroxide flow rate by at least 0.1 pound per second.

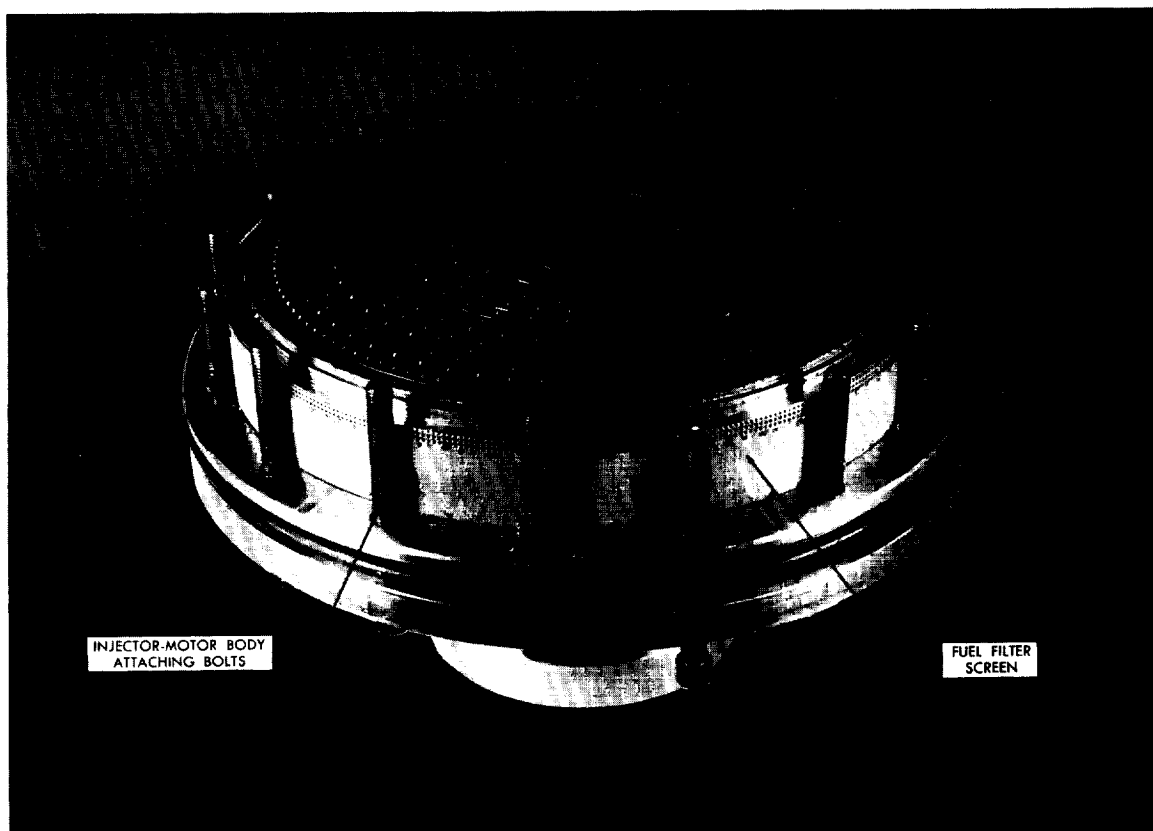
**Hydrogen peroxide system**—The initially designed hydrogen peroxide catalyst bed, the main hydrogen peroxide valve, and the peroxide valve inlet orifice were changed in the prototype engine package to avert nozzle box bulging and decomposer casing ruptures. These failures occurred during development testing because of excessive pressure surges during initial peroxide flow. The surges resulted, in part, from the high pressure drop across the decomposer, which permitted spontaneous initial decomposition of the peroxide. This condition was remedied by replacing the roll-up catalyst screen bed with one composed of 70 laminated flat silver screens separated by 10 stainless steel screens, and by replacing the original sharp-edged orifice at the peroxide valve inlet with a cavitating venturi in order to suppress initial lockup pressure flow. The reduction in peroxide flow due to decreased turbine shaft horsepower output also helped. The original peroxide valve experienced trouble with closing time, and was replaced by another design.

**Injector**—Injector development testing began in December 1955. The X-405 prototype injector was a modified version of that used in the Hermes A-3B, a like-on-like, self-impinging, multihole, stainless steel injector. The modification consisted of enlarging the injector holes to reduce the pressure drop and provide the best heat transfer conditions, and also to obtain an optimum reactant ratio of 2.2. Initial tests of the prototype injector resulted in hard starts, repeated injector explosions due to combustion instability and motor body burnthroughs. A variety of design modifications were tested in an attempt to eliminate these problems.

In May 1956, a prototype injector (BA8-255-5A) was developed which completed 700 seconds of firing and displayed smooth starting characteristics and good combustion stability. This was a high drop, matched propellant velocity, stainless steel injector containing like-on-like 90-degree self-impinging orifices with 120 nonimpinging orifices (0.022-inch diameter) in the outer fuel ring. It was combined with three prototype motor bodies and tested for a total of 3,300 seconds, while determining the effects of  $\pm 5\%$  mixture ratio variation, oxidizer exhaustion, fuel temperature of 120°F, variation in fuel and LOX valve operating times, engine gimbaling and 120°F engine compartment temperature. At the completion of these tests, the prototype injector design was released for production.

From September to December 1956, four production engine packages containing injectors of the BA8-255-5A type were assembled and tested in the production test stand. The first unit experienced a non-damaging hard start. It also demonstrated low overall specific impulse and mixture ratio, due to fuel leaking into the combustion chamber past the injector and motor body sealing joint. A copper lip-seal gasket was inserted between the motor body and the injector bearing surfaces on subsequent engine packages to eliminate this problem. The thrust chamber of the second engine package was scored twice in two tests. Prior to testing the third production engine package, the injector fuel curtain holes were enlarged to 0.028-inch diameter. This engine package experienced a hard start which destroyed the injector, motor body and thrust structure. The fourth engine package experienced two thrust chamber burnthroughs during testing. Figure 19a is a typical example of the type of injector failure that occurred during development testing.

Due to these failures, all assembly and testing of production thrust chambers was discontinued, and a thrust chamber improvement program was implemented to obtain a precision injector and a reliable motor body. Fifteen injectors with six variations in design were tested during the period January to April 1957. Of all the injectors tested, only one did not score a



**Fig. 19a. First-Stage Injector Showing Typical Failure**



**Fig. 19b. Motor Body Showing Inner Shell Burnthrough**

motor body. This injector, designated M-17, had a total run time of 1410 seconds. Injector M-17 was of the same design as BA8-255-5A except that it had 0.025-inch diameter fuel curtain holes in the outer fuel ring, and each hole of the impinging pairs of fuel and LOX orifices in the outer four rings was counter-sunk on the upstream side to better balance the propellant flow. A second injector which had a good history was UNMA-76A, which scored a motor body during its first test, then operated successfully for a total of 904 seconds. Injector UNMA-76A was similar to BA8-255-5A, except that it had 0.025-inch diameter radial cooling holes around the periphery of the outer fuel ring.

Attempts to duplicate injector M-17 failed, due to inadequate quality control of subcontracted injector components. Many of the injectors received by General Electric were rejected prior to testing, due to erratic spray patterns, off-center or burred propellant orifices, or misalignment of impinging orifices.

A reliable injector finally evolved during April 1957, as a result of intensified quality control. A prototype injector (M-29A1), designated "Type A," successfully completed 14 consecutive 150-second firings without motor body damage, for a total accrued time of 2100 seconds. This injector was similar to type BA8-255-5A, with the same propellant distribution and number of orifices, but different orifice diameters. It had countersinks in the outer four propellant rings. It also contained 120 nonimpinging curtain cooling holes (0.0225-inch diameter) in the outer fuel ring. The performance with injector M-29A1 was excellent—average thrust was 28,000 pounds and overall specific impulse was 253 seconds. The Type A design was released for production.

The use of precision tooling for fabricating injector rings, close quality control, and a flow test device for quantitatively measuring ring performance prior to assembly in an injector permitted repeated duplication of the precision injector for production engine packages.

**Motor body**—The original motor body was also a modification of the Hermes A-3B design. It consisted of two steel shells separated by helical passages through which fuel flowed for regenerative cooling. The coolant passage surfaces and the exterior of the motor body were cadmium plated to prevent corrosion.

Motor body testing began in December 1955, concurrent with injector testing. The wall thickness at the exit end of the inner shell had to be increased from 1/8 to 3/16 inch to prevent the bulging that occurred during development tests. As previously described, numerous burnthroughs and scorings of the inner shell occurred in the convergent section of the thrust chamber and at the throat. Figure 19b is an example of the type of inner shell destruction that was experienced.

After failure of the three production engine packages in December 1956, a series of thrust chamber tests were performed with motor bodies containing thermocouples. The major deficiencies found in the original motor body design were that it contributed to injector failures by impeding fuel flow, that combustion chamber cooling was marginal and that quality control of the manufacture was poor.

Flakes of cadmium broke loose from the liquid side of the inner shell and deposited on the fuel filter screen, thus reducing fuel flow to the injector. This resulted in high reactant ratios and generally produced either burnthroughs due to LOX impinging on the combustion chamber wall, or loss of injector rings due to instability within the injector. Flaking occurred at combustion chamber hot spots which exceeded the melting point of the cadmium coating (610°F). This problem was eliminated by plating the coolant passage with a high-melting-point corrosion-preventing material, nickel phosphide, instead of cadmium.

The problem of marginal combustion chamber cooling was eliminated by inserting three equally-spaced 1/16-inch thick copper fins in each of the helical flow passages around the throat and combustion chamber. Adding the fins increased both the effective area of fluid film contact and the fluid velocity, thereby increasing the rate of heat transfer and reducing the inner wall temperature of the coolant passage by about 100°F.

Improved quality control eliminated improper welds, motor bodies being out of round, wall thickness being out of tolerance, and improperly drilled bolt holes in the castellated ring used for attaching the injector to the motor body.

A 100-mesh stainless steel filter screen was wrapped around the injector fuel inlets to catch any metal chips that might be trapped in the motor body. The hot gas side of the inner shell was chrome plated to prevent corrosion and to minimize carbon formation. The external surfaces of the motor body were coated with nickel phosphide to prevent corrosion.

During April 1957, a prototype X-405 motor body containing the above improvements was combined with the Type A precision injector for the successful 14-firing, 2100-second operation previously described. This prototype thrust chamber was released for production. The first flyable X-405 production engine package was shipped on 27 April 1957.

**Starting technique**—Service use of the X-405 engine brought forth just one additional major problem that should properly be classed as development. This was the destruction of TV-3 at launch, which was attributed to the engine starting technique originally used, and resulted in the development of a radically different system. Details are given in Chapter VIII, Section B.

**Propellant feed and pressurization system**—The major problems encountered during development testing of the propellant feed and pressurization system were with the main helium regulator and the liquid oxygen vent valve. (See Ref. 28.)

Repeated failures of the main helium regulator occurred during early testing of the pressurization mock-up. The types of failure experienced were: leakage past the seal in the dome loader, which resulted in poor regulation; and failure of the seal at the outlet port, which allowed leakage when the regulator was in a de-energized or closed position. Failure of the dome loader seal occurred due to adjusting the regulator with pressure at the inlet. This difficulty was eliminated by placing a hand valve upstream of the regulator, which stopped gas flow to the regulator while it was being adjusted. The hand valve had to be opened to check regulator adjustment under flow conditions. Failure of the outlet port seal was attributed to damage sustained by the impact of high velocity foreign particles which entered through the regulator inlet. The addition of a filter screen at the inlet eliminated this problem.

Another regulator failed in full-open position and allowed unregulated gas to enter and rupture the hydrogen peroxide tank. Recurrence of this type of failure was prevented by the addition of a 750-psi relief valve on the dome loader and the insertion of a stainless steel porous filter in the dome inlet gas line.

The main problem associated with the LOX vent valve was improper operation due to excessive helium leakage. Excessive dome bleed port leakage was prevalent throughout development testing of the pressurization mockup. The cause was traced to seal damage from the ramming effect of high pressure gas at the pressurizing port. A small check valve was inserted at the pressurization port, which decreased the incoming gas velocity and minimized seal damage.

## C. SECOND-STAGE PROPULSION

### 1. BASIC DESIGN DECISIONS

Specific impulse, burning time and thrust chamber gimbaling were the primary factors influencing the selection of a liquid-propellant rocket for the Vanguard second stage. Reliability of operation, particularly engine starting, was considered of paramount importance, since the second stage did not have the option available to the first stage of shutting down in the event of a malfunction during the starting transient.

In order to achieve maximum reliability for starting at altitude, a hypergolic propellant combination was selected. A pressure-fed system was considered more desirable than a turbopump system because its relative simplicity offered potentially more reliable starting and operation. Both of these features were available in a modified version of Aerobee-Hi, which was used

as a basis for early design studies, in keeping with the program philosophy of using available hardware.

**System concept**—To assure a reasonable acceleration at the separation of the second stage from the first, a nominal thrust of at least 7500 pounds was required. The most optimistic foreseeable uprating of the Aerobee-Hi predicted the attainment of a vacuum thrust of less than 6000 pounds. Another deficiency of the Aerobee-Hi design was its 15-inch tankage diameter. Since the Vanguard configuration required approximately twice this diameter for the second stage, new tooling and possibly new manufacturing techniques would be required. Thus, it became increasingly evident that the existing Aerobee-Hi design would not meet Vanguard requirements without considerable modification.

The system design was therefore reconsidered from the standpoint of weight optimization. Three versions were studied: a turbopump system; a pressurized system utilizing cold helium and a heat exchanger; and a pressurized system utilizing helium gas heated by a solid propellant gas generator within the helium storage container. The turbopump system was the lightest because it afforded the use of light gage tankage. This system was rejected, however, because of reliability considerations and the likelihood of development problems. The heated helium system was the lighter of the two pressure-fed systems and was ultimately selected.

**Propellants**—The Aerobee-Hi propellants (red fuming nitric acid and 65:35 aniline-furfuryl alcohol) produced a characteristic exhaust velocity of only 4700 fps, compared to 5100 fps that could be attained with red fuming nitric acid (RFNA) and unsymmetrical dimethylhydrazine (UDMH), which also are hypergolic. UDMH was selected instead of hydrazine because of its more favorable storage and handling characteristics. The oxidizer (RFNA) was chosen as the coolant for the regeneratively cooled thrust chamber because of its superior heat capacity. Later studies indicated that white fuming nitric acid (WFNA) should be used instead of RFNA because WFNA has a higher boiling point and would therefore provide greater cooling capacity. Later in the program, it was decided to use an inhibitor, hydrofluoric acid (HF) in the acid in order to reduce its corrosive properties. Therefore, white inhibited fuming nitric acid (WIFNA) was used in all flight firings.

**Subcontract award**—A purchase order was issued to Aerojet-General Corporation on 14 November 1955 for the design, development and manufacture of the Vanguard second stage in accordance with a Martin Development Specification (Ref. 18). The contract covered the complete propulsion system because it was felt that a pressurized system required very close integration of all components in order to achieve an opti-

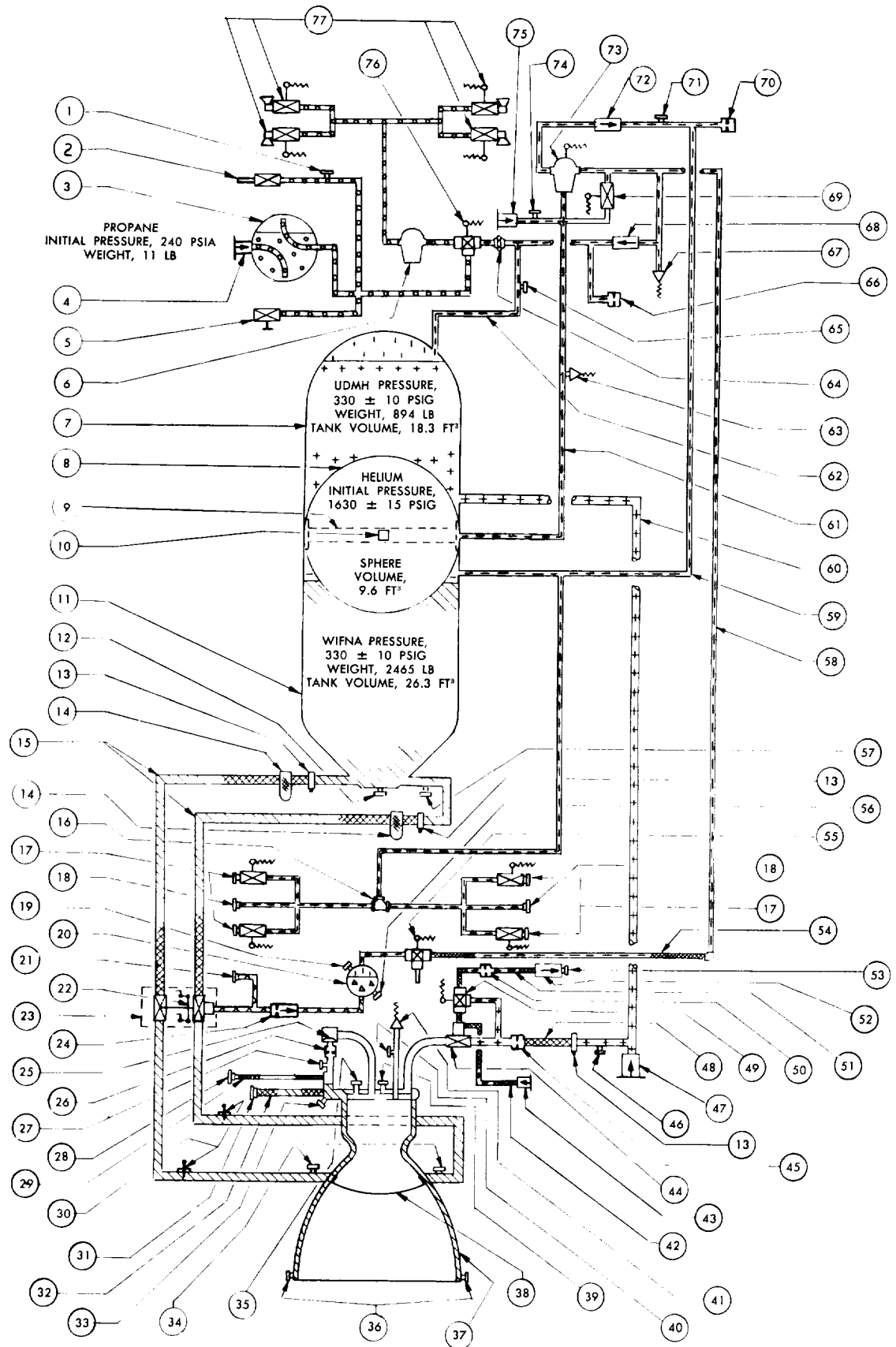

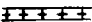

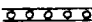



Fig. 20 Second-Stage Propulsion System Schematic

## PARTS LIST

1. PROPANE SYSTEM PRESSURE TAP
2. PROPANE SYSTEM VENT VALVE
3. PROPANE TANK
4. PROPANE TANK FILL DISCONNECT
5. PROPANE HAND BLEED VALVE
6. HELIUM-PROPANE PRESSURE REGULATOR
7. FUEL TANK (UDMH)
8. HELIUM SPHERE
9. HEAT GENERATOR ASSEMBLY (HGA)
10. IGNITER SQUIB (IGN)
11. OXIDIZER TANK (WIFNA)
12. OXIDIZER TANK DRAIN FITTING
13. FLOWMETER
14. FILTER
15. OXIDIZER FLEXIBLE FEED LINE
16. PRESSURIZATION SYSTEM CONNECTION TO PITCH AND YAW CONTROL SYSTEM
17. PITCH AND YAW SOLENOID VALVES
18. OXIDIZER OVERFLOW DRAIN FITTING
19. PRESSURE TRANSMITTER SERVICING CONNECTION
20. PRESSURE TRANSMITTER
21. CONTROL SYSTEM FILL CONNECTION
22. OXIDIZER THRUST CHAMBER VALVE POSITION SWITCHES (TVS<sub>1</sub> AND TVS<sub>2</sub>)
23. OXIDIZER THRUST CHAMBER VALVE (OTCV)
24. RESTRICTOR CHECK VALVE
25. BURST DIAPHRAGM
26. OXIDIZER BALANCING ORIFICE
27. OXIDIZER TEMPERATURE TAP
28. OXIDIZER ULLAGE BLEED FITTING
29. OXIDIZER ULLAGE BLEED FLEX LINE
30. OXIDIZER PROBE
31. OXIDIZER FILL RECEPTACLE
32. OXIDIZER FILL FLEX LINE
33. OXIDIZER COOLING JACKET OUTLET PRESSURE TAP
34. OXIDIZER COOLING JACKET INLET PRESSURE OR TEMPERATURE TAP
35. OXIDIZER INJECTOR PRESSURE TAP
36. THRUST CHAMBER DRAIN FITTING
37. THRUST CHAMBER ASSEMBLY
38. NOZZLE CLOSURE DIAPHRAGM
39. FUEL INJECTOR PRESSURE TAP
40. THRUST CHAMBER PRESSURE TAP
41. THRUST CHAMBER PRESSURE SWITCH (TPS)
42. FUEL VALVE BLEED FLEX LINE
43. FUEL VALVE BLEED (DISCONNECT)
44. FUEL THRUST CHAMBER VALVE (FTCV)
45. FUEL BALANCING ORIFICE
46. FUEL LINE TEMPERATURE TAP
47. FUEL FILL AND DRAIN CHECK VALVE (FFCV) (DISCONNECT)
48. FUEL FLEX FEED LINE
49. FUEL THRUST CHAMBER PILOT VALVE (FTCPV)
50. CONTROL ORIFICE
51. FTCPV VENT FLEX LINE
52. FTCPV VENT CHECK VALVE
53. FTCPV VENT FITTING
54. OTCPV FLEX LINE
55. OXIDIZER THRUST CHAMBER PILOT VALVE (OTCPV)
56. PRESSURE TRANSMITTER BLEED
57. OXIDIZER LINE TEMPERATURE TAP
58. OTCPV PRESSURE LINE
59. OXIDIZER TANK PRESSURIZATION LINE
60. FUEL FEED LINE
61. HELIUM PRESSURIZATION LINE
62. FUEL TANK PRESSURIZATION LINE
63. HELIUM SPHERE PRESSURE SWITCH (HPS<sub>1</sub>)
64. PRESSURIZATION SYSTEM CONNECTION TO ROLL CONTROL SYSTEM
65. FUEL TANK PRESSURE TAP
66. FUEL TANK VENT AND POROUS BLEED PLUG
67. PROPELLANT TANK PRESSURE SWITCH (HPS<sub>2</sub>)
68. FUEL TANK PRESSURIZATION CHECK VALVE (FCV)
69. BYPASS HELIUM SHUTOFF VALVE (BHSV)
70. OXIDIZER TANK VENT AND POROUS BLEED PLUG
71. OXIDIZER TANK PRESSURE TAP
72. OXIDIZER TANK PRESSURIZATION CHECK VALVE (OCV)
73. REGULATOR VALVE (RV)
74. HELIUM SPHERE PRESSURE TAP
75. HELIUM FILL CHECK VALVE (HFCV) (DISCONNECT)
76. 3-WAY HELIUM-PROPANE SOLENOID VALVE
77. ROLL JET SOLENOID VALVES (2 CLOCKWISE, 2 COUNTERCLOCKWISE)

## LEGEND

	OXIDIZER (WIFNA)
	FUEL (UDMH)
	HELIUM
	PROPANE
	HYDRAULIC OIL

**Fig. 20 Second-Stage Propulsion System Schematic**

imum design from the standpoint of weight, propellant utilization, reliability and performance. Since delivery of the first unit was due in one year, plans called for the use of as many existing components as possible, although it was already apparent that a new thrust chamber and tankage would have to be developed. The schedule was not considered unrealistic, as the design approach was conservative and did not involve much improvement in the state of the art. Aerojet's broad experience, particularly with Aerobee-Hi, was expected to permit rapid completion of the development program.

## 2. SYSTEM DESCRIPTION

The general arrangement of the second stage is shown in Fig. 12, and a schematic diagram is shown in Fig. 20. The Aerojet-General Model AJ10-37 liquid-propellant system is described by the manufacturer's Model Specification (Ref. 19). It used white inhibited fuming nitric acid (WIFNA) as oxidizer and unsymmetrical dimethylhydrazine (UDMH) as fuel, at a nominal mixture ratio (O/F) of 2.8. The engine operated for approximately 120 seconds at a minimum rated thrust of 7500 pounds in a vacuum. Other pertinent design parameters are listed in Table 8.

The tankage was comprised of three type AISI 410 stainless steel sections, welded into an integral assembly providing compartments for fuel, helium and oxidizer. Central location of the helium sphere permitted a relatively light unit because the differential pressure acting on the helium sphere was less than for any other

arrangement. This configuration also provided additional separation of the hypergolic propellants.

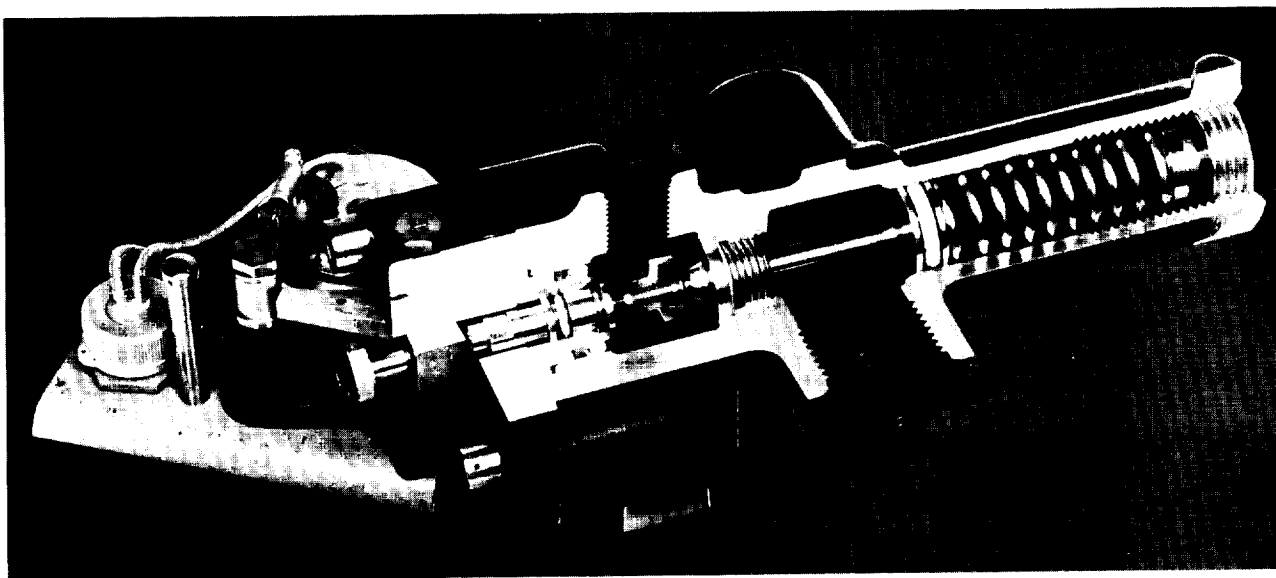
**Pressurization system**—The helium sphere was pressurized to  $1630 \pm 15$  psig through an umbilical disconnect just prior to launch. The solid-propellant heat generator (see Chapter IV, Section F) was installed in the helium sphere by means of a boss on the outside surface. As originally designed, decay of helium sphere pressure to  $1400 \pm 50$  psig, several seconds after ignition, actuated a pressure switch (HPS<sub>1</sub>) which ignited the heat generator. In the final configuration, the heat generator was ignited at first-stage separation. Sufficient energy was added to the helium during the burning time of the heat generator (approximately 100 seconds) to maintain the propellant tank pressures throughout flight.

Pressurizing gas flowed from the helium sphere to a single-stage spring-loaded regulator (Fig. 21) which controlled propellant tank pressures to  $330 \pm 10$  psig. In order to provide positive lockup, the regulator (RV) was manually closed prior to system operation and was electrically opened by a rotary-solenoid-actuated trip mechanism during the engine starting sequence. Pressurization of the propellant tanks before launching was accomplished by opening a solenoid-operated bypass valve (BHSV), which was controlled by a pressure switch (HPS<sub>2</sub>) sensing propellant tank pressure.

The gas downstream of the regulator and bypass valve divided and flowed through propellant tank check

**Table 8. Second-Stage Propulsion System Design Parameters**

	Minimum	Nominal	Maximum
Total impulse in vacuum—lb-sec	894,000		
Thrust in vacuum—lb	7500		
Characteristic exhaust velocity ( $c^*$ )—fps	5000		
Oxidizer flow rate—lb/sec		21.0	
Fuel flow rate—lb/sec		7.5	
Mixture ratio (steady-state, static test)—O/F	2.744	2.80	2.856
Thrust chamber pressure—psia	200	206	212
Thrust chamber throat area—sq in.		21.66	
Design thrust coefficient in vacuum ( $C_T$ )		1.75	
Thrust chamber nozzle area ratio		20	
Gimbal deflection in pitch or yaw planes—deg		$\pm 3$	
Thrust vector alignment tolerance (maximum deviation of nozzle centerline from tankage centerline when thrust line of action is parallel to tankage longitudinal axis)—in.			1/8
Thrust chamber support frequency—cps	30		
Propulsion system weight (excluding Martin components):			
Dry—lb			386
Loaded—lb			3760
At burnout—lb			448
Propulsion system envelope:			
Diameter—in.			32.092
Length—in.			191.0
Propellant tank ullage volume (below fill boss)—percent	1		
Design propellant outage and residuals—lb	45		
Tank volumes, capacities and pressures—see Fig. 20			
Oxidizer—Inhibited white fuming nitric acid (WIFNA), MIL-N-7524B (USAF)			
Fuel—Unsymmetrical dimethylhydrazine (UDMH), MIL-F-25604			



**Fig. 21 Second-Stage Helium Pressure Regulator Valve**

valves to the individual propellant tanks. The primary function of the check valves was to prevent propellant vapors from mixing, but the oxidizer check valve also served to prevent the acid vapor from attacking the nylon poppet of the regulator. Downstream of each check valve was a porous tank vent plug which allowed slow bleeding of propellant tank pressure, thus preventing pressure buildup due to thermal expansion of the propellants. Another function of the porous plugs was to bleed the propellant tank pressure from about 345 psia at liftoff to 330 psia at second-stage ignition, in order to maintain design differential pressures.

**Oxidizer system**—WIFNA flowed from two tank outlets through 1¼-inch flexible hoses to the oxidizer thrust chamber valve (OTCV), which was mounted on the thrust chamber. Each feed line contained a Potter flowmeter and an in-line, finger-type, 30-mesh screen. The oxidizer valve was a dual-pintle valve actuated by a self-contained hydraulic system (which provides more positive action than a gas system). The hydraulic accumulator was pressurized by regulated helium pressure when the oxidizer thrust chamber pilot valve (OTCPV) was energized. Hydraulic fluid then flowed through a restrictor check valve, which provided the pressure required to open the main valve and controlled the opening and closing times. Closing was accomplished by relieving the helium pressure through OTCPV. Two position switches were mounted on the oxidizer valve, at 27% (TVS<sub>1</sub>) and 78% (TVS<sub>2</sub>) of full valve travel.

Rigid dual feed lines continued downstream of the oxidizer valve until the flow was manifolded in the

thrust chamber cooling jacket. Oxidizer flowed through alternate tubes to the end of the divergent cone, where the flow was again manifolded and returned through the remaining tubes. The flow was again manifolded before entering the tubes which comprised the combustion chamber. After leaving the cooling jacket, the flow was collected and continued to the burst diaphragm housing. Opening the oxidizer valve at ignition caused the acid in the thrust chamber cooling jacket to become pressurized (from tank pressure) until the oxidizer burst diaphragm ruptured at  $110 \pm 20$  psig, allowing oxidizer flow into the injector and then into the thrust chamber. The purpose of using a burst diaphragm at the cooling jacket outlet was to permit rapid engine starting by eliminating the time lag for acid to fill the cooling jacket tubes.

Oxidizer fill and ullage bleed lines were connected to the thrust chamber just upstream of the burst diaphragm. Filling was accomplished by flowing oxidizer back through the thrust chamber cooling jacket and propellant feed lines into the tank. The oxidizer burst diaphragm housing also contained a flow-balancing orifice used to establish proper oxidizer flow rate.

Oxidizer probes were installed in both oxidizer feed lines just downstream of the oxidizer valve. Each probe consisted of a platinum wire prong extending into the acid flow and insulated from the probe body by teflon. An electrical current flowed from the probe through the acid to ground; a decrease in this current, caused by helium gas bubbles upon oxidizer exhaustion, initiated the engine cutoff signal.

**Fuel system**—UDMH flowed from the fuel tank through a 1¼-inch rigid line running down through a conduit on the outside of the tankage until it entered the engine compartment. The UDMH fill disconnect fed into this line. Inside the engine compartment, the rigid line connected to a Potter flowmeter. Downstream of the flowmeter, a flexible line led to the fuel thrust chamber valve (FTCV) which was mounted on the thrust chamber. A flow-balancing orifice was installed in the valve inlet.

The fuel valve was actuated by UDMH pressure, which was controlled through the solenoid-operated UDMH pilot valve (FTCPV). Fuel valve opening was accomplished by venting the actuating piston cavity through FTCPV, thereby providing an unbalanced UDMH pressure to open the valve. The valve was closed by de-energizing FTCPV, thereby providing equal UDMH pressure to both sides of the actuating piston and allowing a spring inside the piston to close the valve. A vent check valve was added to prevent liquid UDMH in the actuation circuit from boiling off during flight. Opening and closing time of the UDMH valve was controlled by an orifice in the pilot valve vent.

**Thrust chamber**—The thrust chamber was of welded aluminum tube bundle construction, with 162 tubes (3/16-inch outside diameter) in the combustion chamber and 258 tubes (1/4-inch outside diameter) in the divergent cone. The combustion chamber was wrapped with 0.031-inch square stainless steel wire to provide hoop tension strength (Fig. 22). The 20:1 area ratio divergent cone, which had relatively low pressures, was strengthened by intermittent aluminum bands, tack-welded to the exterior of the cone. Design operating chamber pressure was  $206 \pm 6$  psia. The throat area was 21.7 square inches. The thrust chamber was gimbal mounted to the aft end of the oxidizer tank through a "monoball" spherical bearing, which permitted universal engine deflections.

The injector (Fig. 23) was a one-on-one impinging type, having 72 pairs of orifices arranged in circular rows of 36 each, with the oxidizer rings being outermost. The orifice diameters were 0.120 inch for oxidizer and 0.055 inch for fuel. Twenty-four additional 0.031-inch diameter, axially directed, nonimpinging fuel orifices comprised the innermost ring.

A frangible aluminum disc was cemented in the divergent cone to maintain sea level pressure in the combustion chamber for altitude starting. This "nozzle closure diaphragm" was 0.010 inch thick, chem-milled to 0.0062 inch near the edges so that it would fail at a chamber pressure of 22 psig, if the bond did not fail first. The remaining ring was ejected in one piece as the chamber pressure increased.

Thrust chamber pressure at the injector face was sensed by a pressure switch (TPS), which provided a

signal when chamber pressure initially rose to 140 psia, and another when chamber pressure decayed below about 130 psia.

**Engine ignition sequence**—Ignition of the second-stage engine was initiated by a signal from the first-stage chamber pressure sensor, or its backup timer. This signal energized the oxidizer pilot valve (OTCPV), which started opening the main oxidizer valve (OTCV). Tank pressure caused rupture of the oxidizer burst diaphragm, and acid began to flow into the chamber. When the oxidizer valve reached 27% open, a valve position switch (TVS<sub>1</sub>) provided a signal to trip the helium regulator (RV) and to actuate the fuel pilot valve (FTCPV) which, in turn, opened the main fuel valve (FTCV). Fuel and oxidizer ignited hypergolically in the thrust chamber and, as chamber pressure increased, the nozzle closure diaphragm was blown out. Physical separation of the first stage (initiated by TVS<sub>1</sub>) broke a ground connection through the interstage disconnects, which caused the helium heating charge to ignite. Within 0.5 seconds after ignition signal, 90% of rated chamber pressure was attained. This ignition sequence was involved in the first-stage separation sequence, as described in Sections E and G of this Chapter.

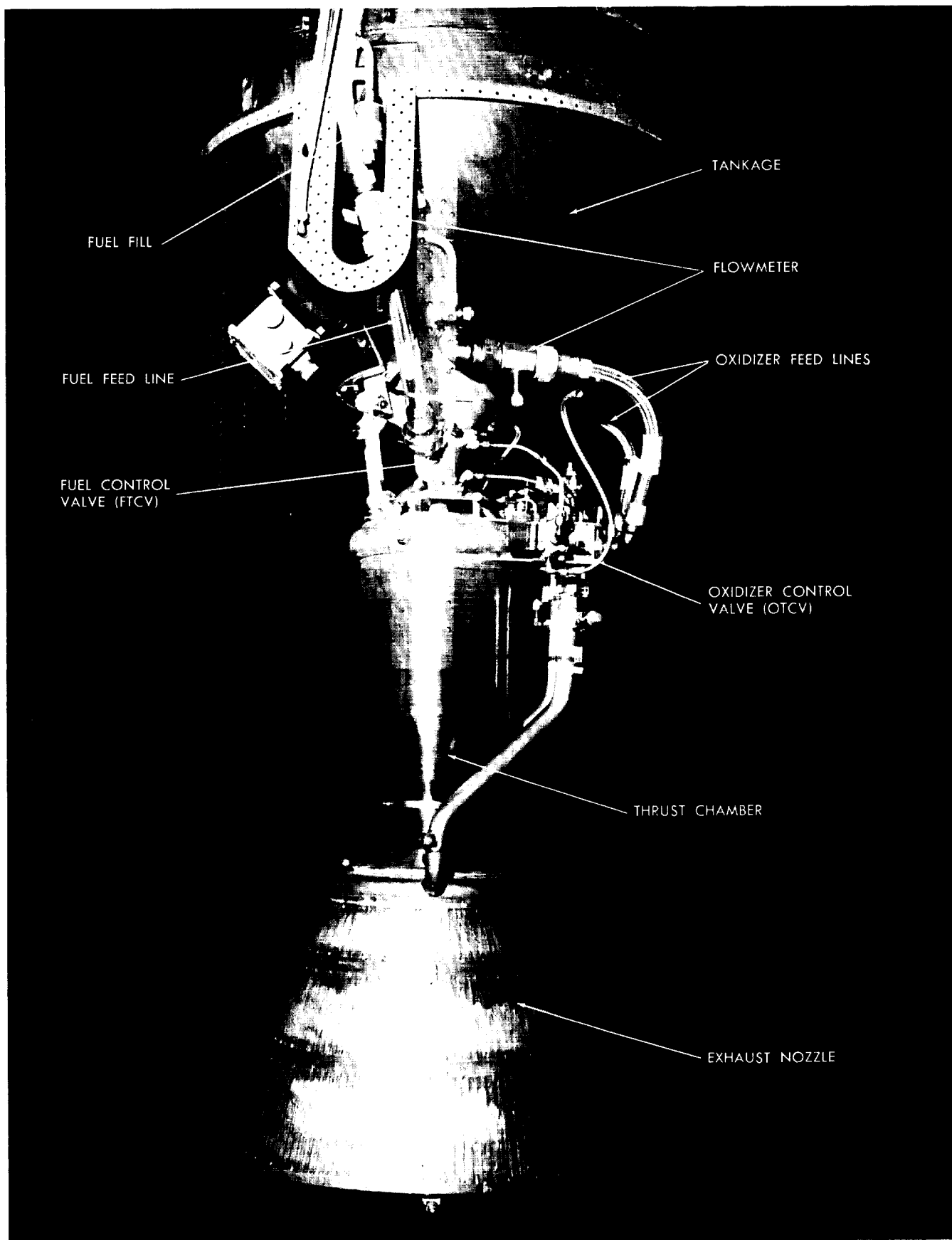
**Engine shutdown sequence**—Second-stage shutdown was initiated by exhaustion of either propellant. In the case of fuel exhaustion, the cutoff signal was generated by the thrust chamber pressure switch (TPS) when chamber pressure decayed to about 130 psia. In the case of oxidizer exhaustion, the resistance change in either oxidizer probe, as helium entered its feed line, would generate the cutoff signal. In either case, the cutoff relay de-energized the pilot valves, causing the main propellant valves to close. The second-stage shutdown signal also performed other vehicle functions, as described in Section G of this Chapter.

**Attitude control systems**—The second-stage propulsion system was intimately involved with the Martin-supplied second-stage attitude control jet systems, which are described in Chapter IV, Section A. The attitude control jets were also used as vents for the entire helium system when depressurization of the tanks was required.

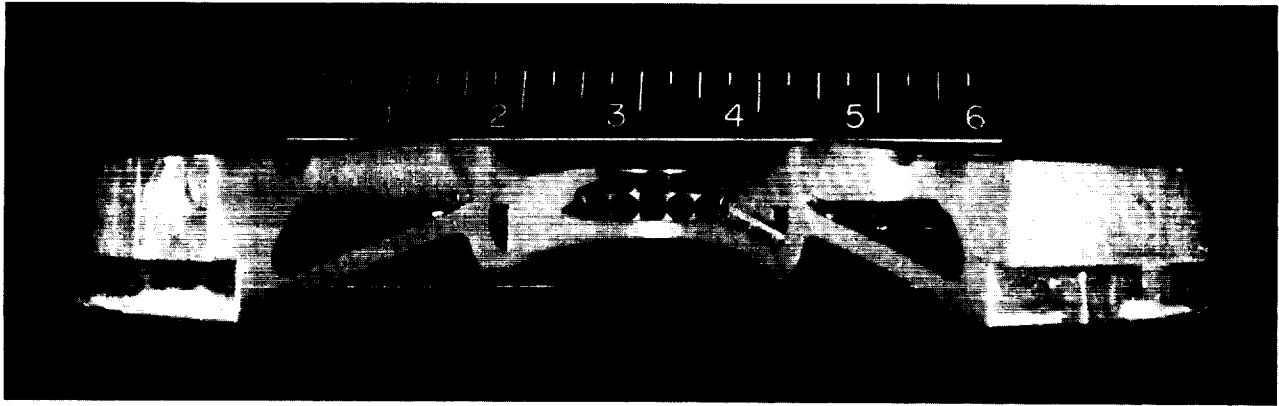
### 3. COMPONENT DEVELOPMENT

The configuration was established and basic component design was conducted for several months before testing could be started. Major development programs were undertaken for the injector, thrust chamber and tankage.

Development of minor components, such as propellant valves, heat generator, nozzle closure and engine controls, proceeded more or less according to plan and did not present any major difficulties. In the case



**Fig. 22 Second-Stage Engine Package**



**Fig. 23 Second-Stage Injector Assembly**

of the helium regulator, a backup development of a different type valve was pursued for a time, but was dropped when the original Aerojet design appeared to be satisfactory.

**Injector**—Injector development began in December 1955, with plans for a square-grid showerhead as the primary design and a one-on-one impinging type as a backup. Early tests to determine the effect of mixture ratio variation over a wide range were conducted with 6.5- and 5-inch diameter showerhead injectors. Performance was generally good, with characteristic exhaust velocities greater than 5000 fps usually achieved.

Testing of prototype showerhead injectors started in May 1956. Characteristic exhaust velocity was about 9% below theoretical. In addition, hard starts were experienced on injectors having low pressure drops. Continued difficulties with hard starts, combustion instability and low performance led to an intensified test program on the showerhead injector. Further development of the basic showerhead injector was terminated in August 1956, when the accelerated program did not produce the desired improvement. A total of 83 firings was conducted on 33 modifications of the basic design, using both aluminum and steel injectors. Several other configurations were rejected without being fired, on the basis of water flow pattern tests.

Because of the problems encountered with prototype showerhead development, it was decided to investigate the possibility of scaling up the 6.5-inch diameter-type YLR-63 showerhead injector that had provided good results in early testing. Problems encountered with this injector and its modifications were high oxidizer pressure drop and high rates of heat transfer. A total of 40 firings was made on 14 modifications of this injector. Addition of fuel film cooling produced some promising results, but in October 1956, a decision was made to use the one-on-one impinging-type injector.

This one-on-one impinging injector displayed smooth starting and excellent combustion stability throughout its development. At first, its performance was slightly lower than that of the showerhead, but continued development increased the characteristic exhaust velocity to values consistently above 5000 fps. One of the main problems associated with this injector was that the high velocity fuel streams tended to pierce the oxidizer streams, producing an oxidizer-rich mixture at the center of the combustion chamber and a fuel-rich condition near the wall. This condition was finally rectified in December 1956 by adding a ring of axially directed, nonimpinging fuel orifices in the center of the injector. During the development program, 48 modifications of the basic one-on-one impinging design were tested in 196 firings, using uncooled, water-cooled, and regeneratively cooled thrust chambers. An apparent increase in  $c^*$  of 1 to 2% was noted in firings using regeneratively cooled thrust chambers, because the uncooled and water-cooled nozzles experienced greater throat area increase due to thermal expansion.

**Thrust chamber**—The primary thrust chamber design used tubes of 5052 aluminum, hand-welded and wrapped with stainless steel wire. Mar-brazing instead of hand welding, 6061 tubes and fiberglass wrapping all were investigated but did not prove feasible. A steel thrust chamber was designed, fabricated and tested as a backup in case the aluminum chamber could not be adequately cooled.

Testing of experimental (nozzle area ratio of 5) aluminum regeneratively cooled thrust chambers began in July 1956. By the end of September, 45 tests of durations up to 149 seconds had been conducted on five thrust chambers. One chamber using an impinging-type injector had accumulated a total of 498 seconds without any signs of erosion or burnthrough. Further development of the stainless steel chamber was terminated. Development of the prototype aluminum

thrust chamber was continued with tests at various mixture ratios and chamber pressures, and was considered to be complete in January 1957.

Reasonable success in prequalification tests led to initiation of the formal thrust chamber qualification test program in May 1957. In June, a series of failures of thrust chamber coolant tubes was experienced. Four chambers developed internal leaks after 327, 240, 364 and 278 seconds of accumulated firing time. The failure at 240 seconds was attributed to local loss of cooling due to failure of a thrust chamber drain fitting. The others were diagnosed as tube erosion failures.

Thrust chamber tube erosion failures apparently were caused by a combination of conditions. Most occurred with high performance injectors; early in the program, when injector performance was low, no failures occurred. The tube wall temperature remained well below the melting point, but undoubtedly was high enough to cause some softening. One likely explanation was the UDMH streams piercing through the oxidizer streams and impinging on the walls. Most of the erosion occurred in the regions where UDMH might have impinged on the walls; in fact, Fig. 24 shows that the failures are generally in line with the inside pairs of orifices. The phenomenon is still not well understood, but fuel impingement on the walls may have caused erosion by the wearing action of the fluid or hot gas, by causing local hot spots, or by a combination of both. It was also suggested that the HF inhibitor in the oxidizer may have had some erosive effect. Gaps between tubes apparently contributed to the erosion process, causing a characteristic thinning of the sides of the tubes instead of the crest, as shown in Fig. 25.

Since a chamber lifetime of something less than 278 seconds was considered inadequate, an improvement program was immediately instituted. Various coatings were tested, including zirconium oxide, Devcon, electrolyzed chromium, anodized aluminum hard coat and tungsten carbide. The most promising results were exhibited by the tungsten carbide coating applied to the thrust chamber walls by the Linde Company. This chamber lasted for more than 400 seconds. Results of other coatings varied from actual acceleration of the erosion process (Devcon) to unsatisfactory adhesion (zirconium oxide). The steel thrust chamber, which had accumulated over 600 seconds of firing time without any evidence of erosion, represented a possible final recourse but would have involved weight and schedule penalties. Injector modifications, at that late date, were even less desirable.

Finally, in October 1957, the aluminum chamber with tungsten carbide coating was selected, and all flight thrust chambers beginning with TV-5 were so coated. A patching technique was devised to permit

sealing of incipient erosion failures—this was used in qualification testing, but never on a flight chamber.

**Tankage**—AISI 410 stainless steel was selected as the primary tankage material because of Aerojet's previous experience in forming and welding this material. Type 17-7PH stainless steel also was investigated because its higher strength offered the prospect of a substantial weight saving. This investigation was discontinued in August 1956, in order to concentrate all effort on the type 410 tankage.

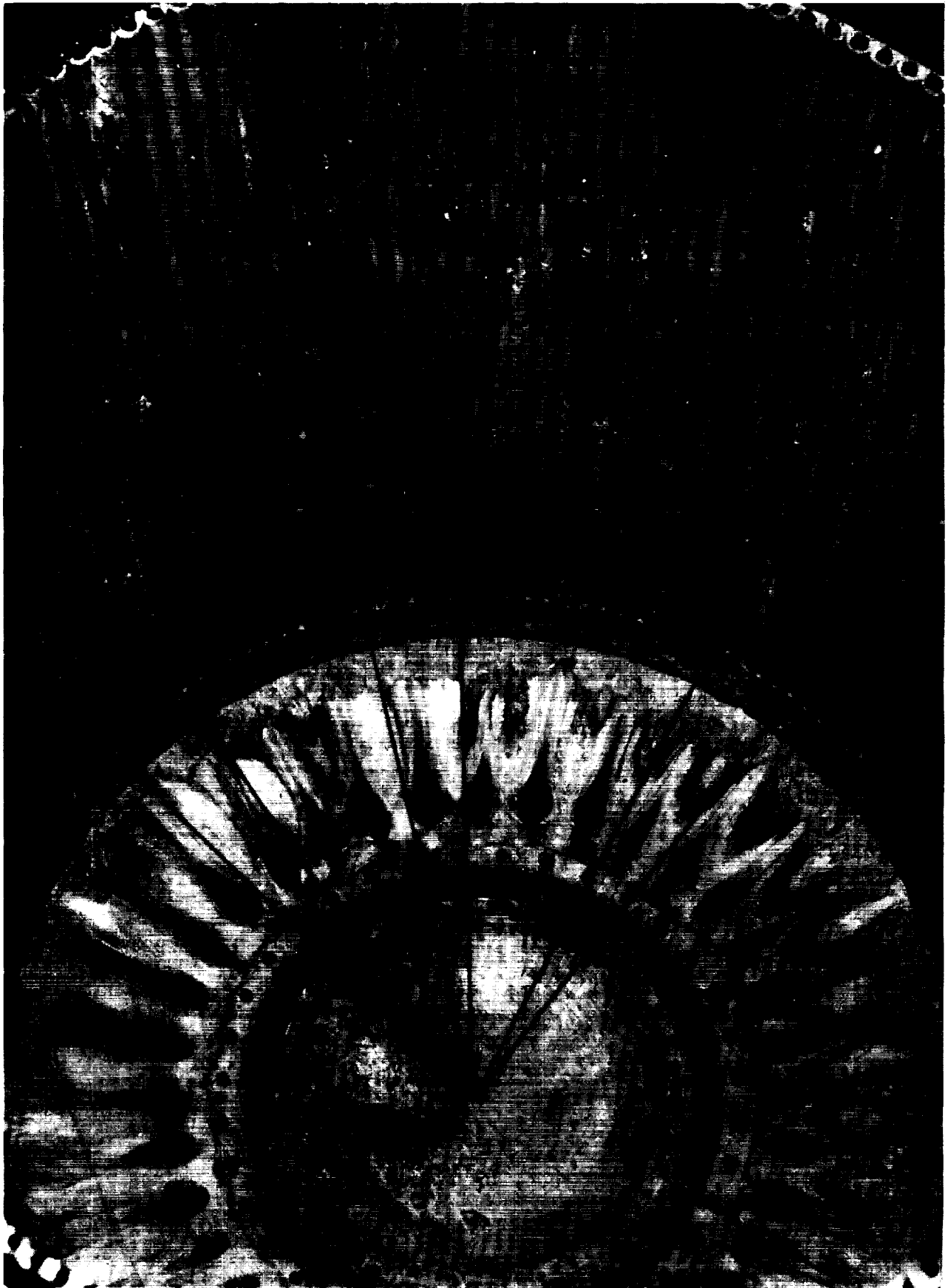
Considerable difficulty was experienced during early tankage fabrication. Approximately 50% of the helium sphere and propellant tank domes were scrapped during the drawing process. Some of the causes of failure were thin sheet stock, local thinning during drawing, difficulties with cleaning and annealing, and scratches because of galling in the die.

Changes in drawing dies and manufacturing procedures improved fabrication to the point where several complete prototype tankages were manufactured. The first two prototypes failed during proof testing, and some minor design changes were made. In November 1956, three more tankage failures occurred. All five failures were in tankages fabricated by one particular subcontractor to Aerojet. The causes of these failures were excessive brittleness due to carbonization during annealing, and poor welding. As a result of the failures, the entire heat treating process was reviewed. The cleaning procedures were improved, and a new heat treat procedure was instituted, involving a double temper at 825°F in an air atmosphere with argon inside the tanks. Stress corrosion investigations led to the use of HF as an inhibitor in the oxidizer.

Another result of these difficulties was that an alternate tankage design proposed by the A. O. Smith Company was implemented as a backup for the original design. The A. O. Smith approach involved the use of a separate forged ring instead of weldments to form the juncture between the helium sphere and the propellant tanks. Similar construction was used at the tank wall junctures of the fuel tank forward dome and the oxidizer tank aft dome. A. O. Smith tankage was flown on the SLV-4 and SLV-6 vehicles.

Successful completion of the structural loads, cycling and burst tests led to the conclusion that tankages were acceptable for flight use. Four production propulsion units were delivered between April and August 1957, following successful completion of acceptance tests.

On 6 May 1957, a leak developed between the helium and oxidizer tanks of the prequalification unit. Investigation disclosed a stress corrosion failure and a laboratory program was undertaken to evaluate the problem. On 6 July 1957, the helium sphere of the qualification test tankage ruptured due to stress corrosion. The tankage had been exposed to liquid WIFNA for a total of 40 hours, of which 45 minutes were at



**Fig. 24 Cutaway of Second-Stage Thrust Chamber Showing Tube Erosion Failure**



CROSS-SECTION OF COOLANT TUBES, SHOWING CONCENTRIC INNER DIAMETER OF TUBING 0.116-INCH I.D., DIFFERENCES IN GAP DISTANCES, AND EXTENT EXTERIOR SURFACE EROSION AND THINNING OF TUBE WALLS. ETCHANT: 2% HF. MAGNIFICATION: 8 DIAMETERS.

**Figure 25. Microphotographs Showing Typical Thrust Chamber Erosion Failures.**

full working pressure. Additional testing indicated that stress corrosion failures were caused by exposure of the sphere to liquid acid while fully pressurized, and that stress corrosion lifetime was short and unpredictable.

An intensive analytical and experimental investigation developed a new heat treat process, using a tempering temperature of 600°F instead of 825°F, which guaranteed 8 hours lifetime in the stress corrosion environment. It was also demonstrated that a reduction of 20 to 30% in the stress level would achieve the same result with the original heat treat.

All undelivered tankages were retempered at 600°F. Three of the already-delivered units were subsequently flown (TV-3, TV-3BU and TV-4), using an initial helium sphere pressure of 1365 psig instead of 1630 psig, at the price of a small performance tail-off during the latter portion of the burning time. No further difficulties were experienced with stress corrosion of the second-stage tankage during the program.

**Thrust coefficient**—Sea level firings of an altitude thrust chamber do not provide representative thrust data. In order to calculate the vacuum thrust of this system, therefore, it was necessary to multiply the product of throat area and chamber pressure by a "thrust coefficient" ( $C_T$ ) which would account for nozzle expansion effects and all losses due to nonparallel flow, friction, cooling, etc. Early design calculations, based on an average ratio of specific heats of 1.2, indicated that a corrected vacuum thrust coefficient of 1.741 could be attained. Substantiation of this value was to be accomplished by static test firings into a supersonic diffuser, in order to eliminate nozzle flow

separation; but repeated attempts to achieve satisfactory operation of this arrangement were unsuccessful. Failure of the test program led to another analytical approach which used Nike data for a nozzle area ratio of 16, adjusted to give a thrust coefficient for a nozzle area ratio of 20. Based on these studies, a thrust coefficient of 1.75 was considered reasonable for the Vanguard second stage, and was approved by all concerned in the Model Specification (Ref. 19).

**Flight Development**—A considerable amount of further development of this system was found to be necessary and was accomplished during the Vanguard flight program. These activities are documented in Chapter VIII, Section C.

## D. THIRD-STAGE PROPULSION

A solid-propellant rocket motor was a natural choice for the Vanguard third stage, primarily because of the decision for spin stabilization rather than conventional guidance, but also because of its relatively small size and simplicity. The performance requirements generated by the early design studies and the stage optimization were expanded into a Martin Development Specification (Ref. 20). The two best proposals produced in an industry-wide competition were those of the Grand Central Rocket Company and the Allegany Ballistics Laboratory. Since the requirements represented an advance in the state of the art, and the two best proposals were based on radically different approaches to the problem, it was decided to authorize parallel development programs by these two agencies.

**Table 9. Third-Stage Motor Design Requirements**

REQUIREMENT	GRAND CENTRAL 33-KS-2800 MOTOR	ALLEGANY BALLISTICS X248 MOTOR
Motor weight, not to exceed:	433 lb	507 lb
Velocity increment imparted to 22.1-lb payload (horizontal, drag-free, in vacuum), not less than:	14,182 fps	17,100 fps
Maximum acceleration imparted to 22.1-lb payload, not to exceed:	35 g	50 g
Thrust and spin axes each aligned with principal axis (axis of dynamic balance), within:	0.0003 rad (0.017 deg)	
Storage and firing temperature range:	+30°F to +130°F	+40°F to +100°F
Vibration input:	2 g for 2 hr at resonant frequencies	Rough road test (250 miles over secondary roads) in lieu of vibration tests
Accelerations:	Longitudinal axis, 7 g; Transverse axis, 2 g; Rotational, 20 rad/sec/sec	
Rain:	Two hours, in accordance with specification MIL-E-5272A	
Salt Spray:	Exposure in accordance with specification MIL-E-5272A	
Relative Humidity:	100% for 10 days, as per specification MIL-E-5272A, Procedure II.	
Ignition:	Reliable ignition under vacuum conditions	

## 1. GRAND CENTRAL ROCKET COMPANY MOTOR

The Grand Central approach used a steel motor case, with a GCR polysulfide-perchlorate case-bonded propellant grain. The major design requirements and special environmental criteria are listed in Table 9.

**Description**—The Grand Central 33-KS-2800 rocket motor configuration is described in detail in the manufacturer's Model Specification, Ref. 21, and is depicted in Fig. 26. It was a case-bonded, solid-propellant motor with an integral igniter. The chamber was 410 stainless steel with a nominal thickness of 0.030 inch. The chamber was lined with 91LD Re-frasil and rubber lining material, with glass cloth laminate used as additional insulation at the locations of the grain star points. The nozzle was SAE 1020 steel with an insulating lining of "Rokide A" aluminum oxide in the expansion cone and a graphite insert at the throat.

A polysulfide and ammonium perchlorate composite propellant, designated GCR-201C, was used. The grain was cast-in-case, with an internal-burning, star-shaped port. Polyvinyl acetate cement was placed at the star points to inhibit grain cracking under thermal stress.

The ignition system consisted of a slow-burning gas-

generating igniter, activated by two electrically fired Hercules SD2A7 15-second delay squibs, and a styro-foam erodable nozzle closure with a center plug designed to blow out at a chamber pressure of 20 to 27 psia. The remaining portion of the erodable closure maintained chamber pressure produced by the gas-generating igniter until the propellant grain was fully ignited.

**Development**—The GCR motor development proceeded in five steps, each step producing motors approaching the desired delivery configuration as the required lead time of the manufacturing techniques permitted.

Type I motors were heavy-walled, 15-inch diameter scale models used to determine interior ballistics and ignition requirements. Seven of these motors were fired. None failed, but pressure irregularities would have caused failure of light-walled motors in several instances.

Type II motors were heavy-walled, full-size models and were also used to determine ballistics and ignition characteristics, but now in full scale. Twelve motors were fired, of which seven suffered component failures or irregularities which would have caused failures in lightweight motor cases. Fuel liners separated from

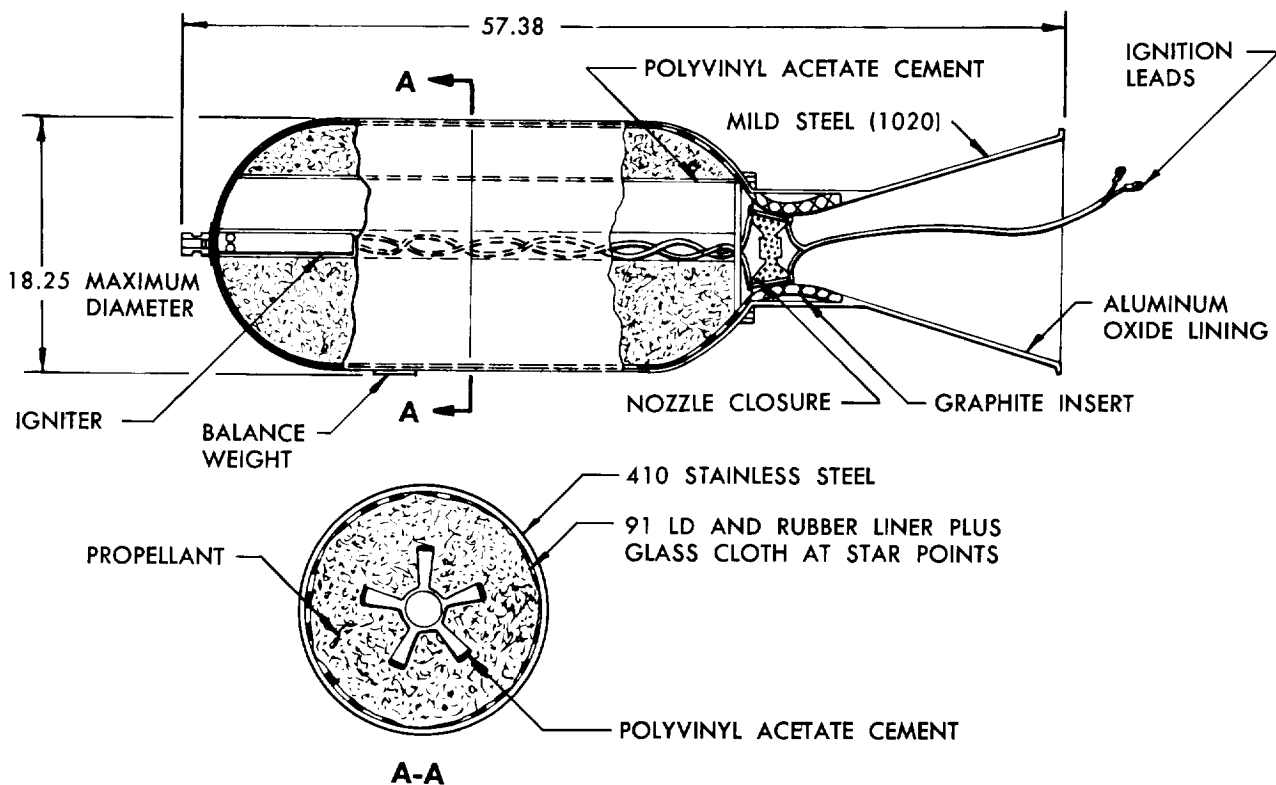


Fig. 26 Third-Stage Motor (33KS-2800) — Grand Central Rocket Company

four of the cases, and three nozzles burned through. The ignition characteristics were successfully determined with these motors, resulting in satisfactory development of the igniter and erodable nozzle closure.

Type III motors simulated those which were to enter qualification testing as closely as the short lead time permitted. Ten Type III motors were fired to obtain data on internal ballistics, overall performance, predicted performance and choice of case bonds. Three failures occurred—the chamber burned through in one motor and the nozzles burned through on two others.

Type IV motors were intended for delivery, but prequalification test results indicated that the mass ratio was too low to produce the required velocity increment. Weight saving studies were instituted to correct this. Thirty-five static firings were made, and six failures occurred when four reused and two new nozzles burned through.

Type V motors resulted from the weight saving studies. These motors entered prequalification tests, where eleven of them were fired. Three failures occurred due to insufficient insulation of the nozzle graphite throat, so the insulation was redesigned. Cracking from thermal stress was found at the propellant grain star points, so the star points were coated with polyvinyl acetate cement to inhibit cracking. These motors then entered qualification testing (see Chapter V, Section C).

## 2. ALLEGANY BALLISTICS LABORATORY MOTORS

The ABL approach to the Vanguard third-stage design was a "plastic" (resin-impregnated, glass-filament-wound fiberglass) motor case, with a high-energy double-base ABL propellant. However, technical development problems were encountered which made it evident that this unit, the JATO X241 A1 (39-DS-2400), would not be operational in time to meet the Vanguard schedule.

In June 1957, the Navy, recognizing the importance to solid rocketry of the fiberglass rocket case, authorized ABL to suspend work on the Vanguard motor as such, in order to concentrate on solution of the basic problems which had been uncovered. These problems were eventually resolved, and in February 1958, ABL was authorized to develop and qualify a dimensionally similar but higher performance motor, for use as an advanced Vanguard third stage and in other space vehicle applications.

This motor, originally designated JATO X248 (40-DS-3000), was designed to an NRL specification, Ref. 22, which was similar to the original Vanguard specification except for increases in weight, velocity increment, and maximum acceleration, and some modifications to the environmental criteria, as shown in Table 9. The nomenclature of the Vanguard version was later changed to JATO X248 A2 (38-DS-3100), see Ref. 23.

**Description**—The final configuration of the ABL X248 A2 rocket motor is shown in Fig. 27. This propulsion system was a case-bonded, solid-propellant motor with an integral igniter. The chamber was constructed of epoxy resin-impregnated, filament-wound fiberglass with a nominal thickness of 0.055 inch. A layer of cellulose-acetate cloth was bonded to the inner surface of the fiberglass case, acting as a bonding surface and as an insulator. A contoured rubber insulator covered the aft half of the chamber. Glass cloth was used for additional insulation in certain areas, notably the forward dome.

The propellant grain was a cast-in-case internal-burning type using an ABL double-base propellant, designated BUU. The grain was a single-perforated, four-slot design with hemispherical head and aft ends. Four additional smaller slots were added to obtain the proper burning surface. Case bonding was accomplished by the use of cellulose-acetate cloth and a case bonding lacquer. The forward end of the grain was pierced by a cellulose-acetate tube to accommodate the resonance suppressor shaft. A phenolic asbestos resonance suppressor paddle was attached to the head end of the motor, through the cellulose-acetate tube, and extended into the propellant grain port.

The igniter assembly consisted of high impulse propellant strips, an ignition charge of boron and potassium nitrate pellets ( $\text{BKNO}_3$ ), two 7 x 7-inch stainless steel mesh cages to hold the ignition charge, and two electrically actuated Hercules SD2A7 15-second delay squibs. The high impulse propellant strips were bonded to the forward end of the resonance suppressor paddle in two pieces, one on each side. The cages with the  $\text{BKNO}_3$  charges were mounted, one on each side of the paddle, aft of the propellant strips. The 15-second delay squibs extended into each ignition charge. Each squib also had a small ignition charge of crushed  $\text{BKNO}_3$  covering the active end of the squib. Additional propellant, having the same composition as the propellant grain, was bonded to the paddle aft of the  $\text{BKNO}_3$  cages in eight strips, four on each side.

The igniter leads extended through a nozzle closure made of styrofoam coated with an aqueous rubber latex solution. The closure was then bonded to the nozzle throat insert to hermetically seal the chamber.

The nozzle consisted of a glass-filament-wound expansion cone, with a liner of asbestos-impregnated phenolic and a graphite cantilevered throat. The entire throat section was contained within the motor chamber.

The motor attachment fittings were of aluminum and consisted of a spin shaft forward, a ring adapter for attaching the nozzle to the case, and a torque ring at the nozzle exit for attaching the motor to the vehicle spin table.

**Development**—Development of the ABL X248

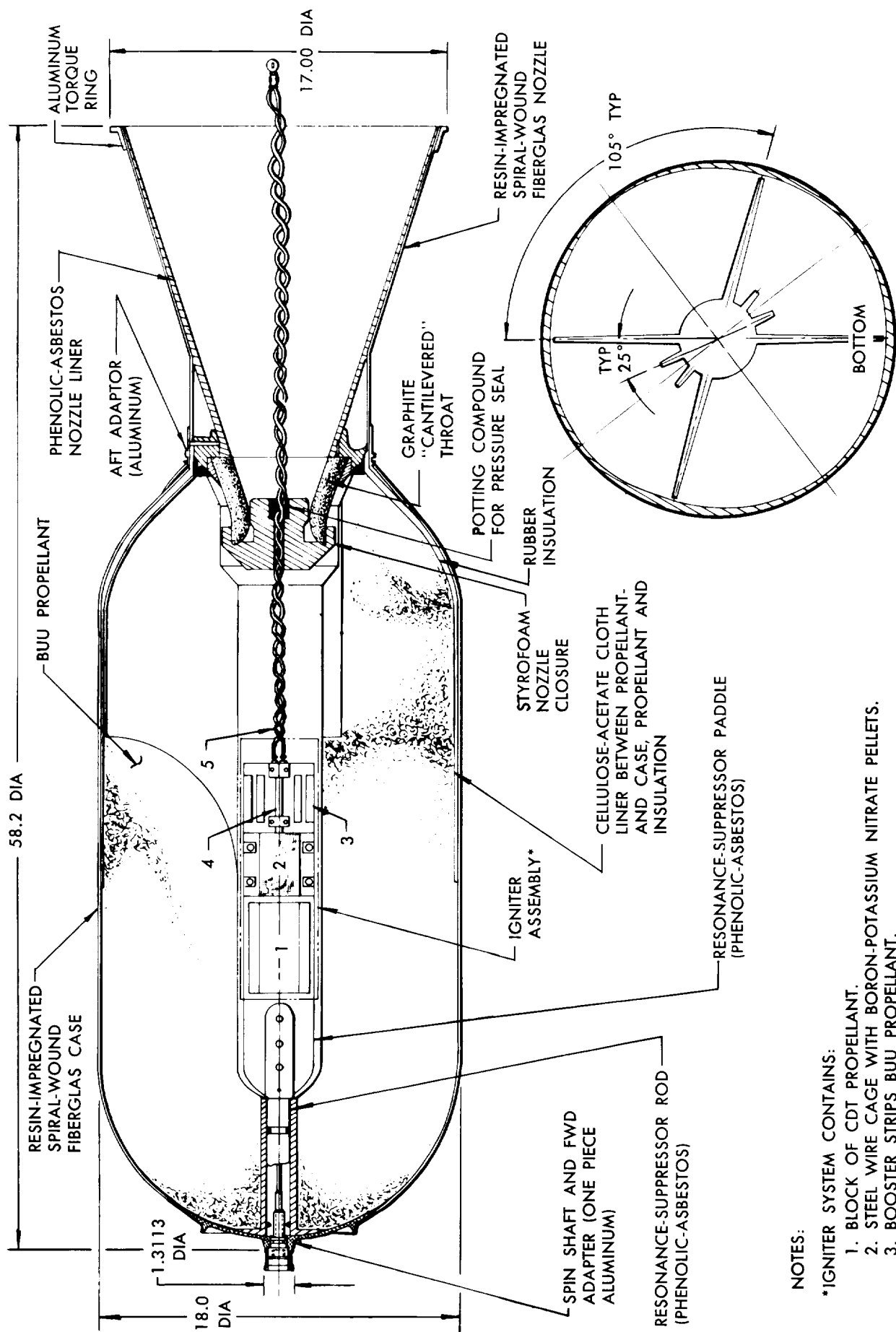


Fig. 27 Third-Stage Motor (38-DS-3100) — Allegany Ballistics Laboratory

# NOTES:

\*IGNITER SYSTEM CONTAINS:

1. BLOCK OF CDT PROPELLANT.
2. STEEL WIRE CAGE WITH BORON-POTASSIUM NITRATE PELLETS.
3. BOOSTER STRIPS BUU PROPELLANT.
4. 15-SECOND PYROTECHNIC DELAY SQUIBS.
5. ELECTRICAL FIRING LEADS.

utilized the technology learned from the original Vanguard competition. One of the major developments toward attaining a successful motor was the choice of proper insulation. Success was obtained by using a silica-loaded rubber insulator in the aft part of the motor and designing the propellant grain so that a portion of the insulator was consumed during the burning phase. Originally, a rubber insulator of uniform thickness was employed, but later a machined insulator was incorporated, where the thickness was greater in the areas of the propellant slots and less elsewhere, thereby reducing the weight of the insulator and improving the mass ratio. Burn-throughs of the cases occurred in a number of development firings and the insulator thicknesses were adjusted until this condition was corrected.

A second development of importance was the use of a cantilevered nozzle, with the entire nozzle throat contained inside the motor case. The nozzle configuration was tested by many development firings to demonstrate its ability to withstand damage.

A reliable ignition system was the object of an extensive test program, including configurations with the igniter as part of the nozzle closure and as part of the resonance suppressor paddle. The final configuration, with the igniter as part of the resonance suppressor, fulfilled the ignition requirements best and was incorporated in the motor.

Thirteen ABL X248 motors were tested at simulated altitude in a vacuum wind tunnel facility at the Arnold Engineering Development Center, Tullahoma, Tenn. Four firings were made to study ignition problems, and indicated reliable performance of the final igniter configuration. Three motors were fired to evaluate the insulator and resulted in development of the contoured insulator discussed above. Three firings were made as part of the X248 qualification program, to demonstrate reproducible performance in motors which had been subjected to environmental testing. Three motors were subsequently fired in a study of residual thrust after burnout.

## E. SEPARATION

### 1. LAUNCH

**System selection**—Operational missiles are required to fly under almost any environmental condition. The Vanguard was considered to be a research tool, which permitted reductions in launch environment capabilities in favor of increased vehicle performance. The original launch stand for the first half of the program permitted the first-stage engine thrust chamber to extend down into the stand. This eliminated the need for an extended vehicle skirt structure but incurred a launch wind limitation of about 17 mph. An additional saving of weight and a simplified operation was realized by locating most of the vehicle disconnects

on the tail frame of the vehicle. To avoid possible delays in the launching operation, an improved launch stand was designed midway in the program, to permit launching in ground winds up to 35 mph by providing retractable support arms. Both launch stands are described in detail in Chapter VI, Section A.

**Launch clearance studies**—Vehicle tolerances that could adversely affect the Vanguard launch were made up of three basic parameters: (1) vehicle vertical alignment with respect to the launch stand, (2) lateral shift of the center of gravity with respect to the vehicle centerline, (3) angular misalignment of the first-stage engine thrust vector. These tolerances were originally estimated and later modified to reflect operational experience and changes in the engine manufacturer's specification of thrust vector misalignment. Bending of the vehicle due to wind forces caused a lateral cg shift and, by inducing a gyro error, produced an engine deflection which acted as a thrust misalignment. Empirical formulas were determined for these conditions by measuring the vehicle deflection when exposed to ground winds. Bending of the vehicle and resultant lateral cg shift due to temperature differential between opposite sides did not contribute to thrust misalignment because the differential changed slowly and the gyro and motor position were nulled just prior to launch.

Early studies of the launch phase considered that first vehicle motion took place at liftoff. The allowable launch wind velocities for test vehicles were calculated based upon this assumption. Further analysis, however, indicated that a critical force was present prior to liftoff, in the form of vehicle pitch motion due to wind loads, misalignments, engine gimbaling, and disconnect forces. Moreover, when springs were used to restrain the swingaway arms of the stationary launch stand, the spring forces and spring unbalance moment contributed to the initial toppling motion of the vehicle.

The equations of motion for the latest study were those of a rigid body moving in a vertical plane. A specified point on the rigid body (the hinge point) was constrained to move in a specified path (a vertical straight line the height of the pins) until a certain altitude was reached, above which the vehicle acted as a free body. Because the equations of motion used by the computer did not employ coefficients of drag and lift, the aerodynamic side force was independently determined for these coefficients as a function of wind velocity. The first-stage engine thrust was a function of time. Investigations of various thrust buildup curves experienced in test vehicles showed that clearance was insensitive to small variations of thrust buildup. The liftoff weight was conservatively assumed larger than the predicted liftoff weight.

The studies indicated that the allowable ground wind of 17 mph for launch from the fixed stand was

limited by the clearance between the engine nozzle and either the pipe structure of the launch stand which supported the swingaway arms or the LOX disconnect fitting. The relationship of these protuberances to the centerline of the stationary launch stand is shown in Fig. 28. For the retracting launch stand, the trajectory of the vehicle with a 35-mph wind fell within the design curve. However, it was possible to collide with the umbilical tower if certain tolerance conditions occurred. Launch was therefore restricted to wind conditions of less than 28.5 mph, when the wind was toward the quadrant containing the tower.

## 2. FIRST-STAGE SEPARATION

For a remote start at altitude, as was the case with the second stage, it was considered important to have a simple and rapid starting technique, a separation system that produced environmental conditions conducive to reliable starting, and a physical separation which caused no damage or disturbance to the second stage.

**Engine starting requirements**—One of the primary objectives of the second-stage propulsion system

design was a fundamentally simple starting system. Past experience in the industry led to the selection of a hypergolic propellant combination and a pressure-feed system. In addition, a specification limit was established which required that the second-stage thrust buildup time from ignition to 90% of rated value would not exceed 0.5 second, and from 10 to 90% would not exceed 0.2 second.

**Environmental conditions**—It was decided early in the program that two of the environmental conditions which would contribute to successful ignition were the retention of sea level ambient pressure in the chamber and the maintenance of positive acceleration on the propulsion fluids throughout the prior flight and during the critical ignition period. Pressure was maintained in the combustion chamber by a nozzle closure installed before launch. The separation sequence adopted for Vanguard assured continuous positive acceleration of the fluids by programming second-stage ignition prior to separation, during a period when thrust was still being produced by the first-stage engine. The thrust shutdown characteristics of the first-stage

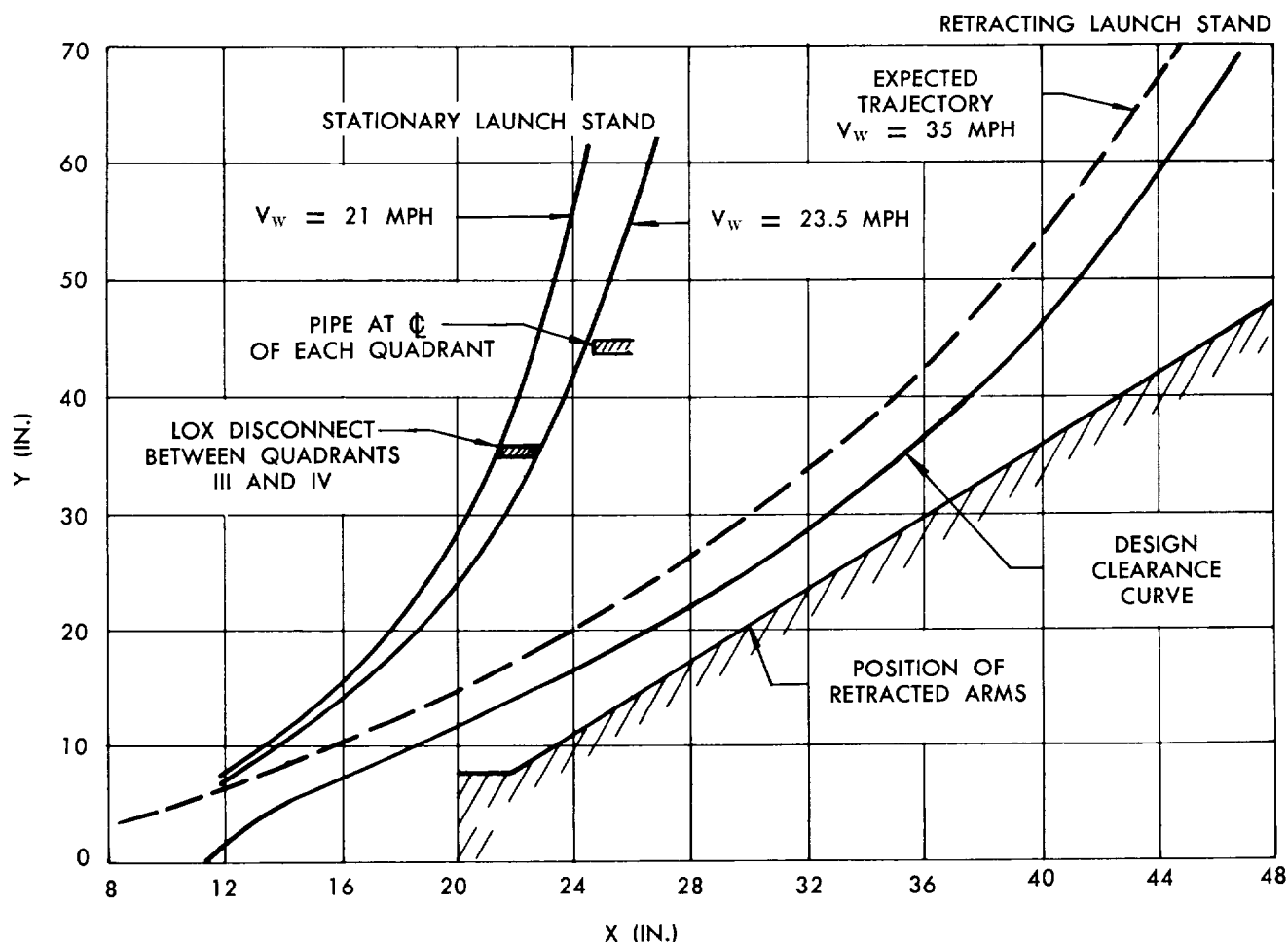


Fig. 28 Clearance Curves for Stationary and Retracting Launch Stands

engine were favorable for this type of sequence, and no additional complication in the form of thrust augmentation and/or controls was needed.

During the period between second-stage ignition and separation, a large volume of high temperature gas was produced in the interstage compartment. These gases required venting through blast doors to prevent damage to local hardware and to keep compartment pressure at an acceptable level. An insulating blanket on top of the first-stage LOX tank dome was also required as protection against the second-stage engine flame impingement, which could have caused LOX tank rupture.

**Sequence**—Shutdown of the first-stage engine was initiated by one of the two pump discharge pressure sensors, which detected exhaustion of LOX or kerosene and energized the cutoff relay, which then performed the engine shutdown by removing power from the propellant valves. In addition, the cutoff relay ignited explosive latches in the interstage compartment to allow the spring-loaded hinged blast doors to open. A third function of the cutoff relay was to energize the helium thrust augmentation valve, which permitted residual first-stage helium to flow into the roll control system at shutdown of the peroxide steam-generating system. This augmentation was necessary to maintain roll control during the separation, mainly to counteract the moment produced by the turbine deceleration.

A sensor in the first-stage engine sensed when chamber pressure dropped to 60 psia (3000 pounds of thrust), and then initiated the second-stage ignition signal. A backup timer initiated this signal 1.0 second after first-stage cutoff if the primary system failed to operate.

A sensor in the second-stage engine initiated the stage separation signal when chamber pressure reached 140 psig (5500 pounds of thrust), 0.35 to 0.50 second after second-stage ignition signal. A backup system operated by the oxidizer valve (78% open) initiated separation approximately 0.3 second later, if the primary system failed. For the SLV-6 and TV-4BU vehicles, the primary separation signal was given earlier by the oxidizer valve (27% open), and backup signals were initiated by the chamber pressure sensor and the oxidizer valve (78% open).

The separation signal energized two relays to detonate the six double-ended explosive bolts which held the first and second stages together. For increased reliability, each bolt had two independently wired detonators, either of which was capable of breaking the bolt. Physical separation of the two stages then resulted from the combined effects of pressure in the interstage compartment, second-stage thrust and impingement of second-stage exhaust on the first stage.

**Fragmentation protection**—The vehicle was protected from damage (caused by fragments from the

explosive bolts) in several ways. The top half of the explosive bolt was retained by a steel bolt extending through the legs of the channel surrounding the explosive bolt head; smaller fragments were stopped by an aluminum shield riveted to the separation plane stiffener frame. The bottom half of the bolt was retained by the flame shield installed over each explosive bolt to protect the explosive bolt assemblies from impingement of second-stage exhaust prior to separation.

The fragmentation problem caused rejection of the original concept of separating the first and second stages by means of primacord. Tests demonstrated that the heavy charges of primacord necessary to sever structural members resulted in high velocity metal fragments, which would have perforated the aluminum second-stage thrust chamber. An adequate shield would have been excessively heavy; therefore, the explosive bolt system was far superior in this respect.

**Analysis and tests**—The separation of the two stages was analyzed on the analog computer and demonstrated by mockup tests. The analog study showed that the reactive force on the first stage due to the exhaust of the second-stage engine was an important factor in successful separation. This force caused a significant deceleration, which increased the relative separation rate. In addition, the results of the study showed that there would not be any interference (collision) between stages, even under the most adverse conditions. The mockup tests demonstrated that the operation of various components (such as blast doors, explosive bolts, etc.) was satisfactory.

A series of short-duration firing tests was conducted at the Aerojet-General Corporation with a test engine and a mockup of the separation compartment. The tests verified that the engine compartment temperatures and pressures were within safe limits. The tests also qualified the adequacy of the LOX dome insulation blanket to protect the LOX tank during the ignition-to-separation time sequence (Ref. 29).

**Delayed second-stage ignition study**—Engineering was completed on an alternate separation system which was to be used in the event that the flight system proved inadequate (see Ref. 14). In this system, the explosive bolts separated the stages and then retrorockets on the first stage and booster rockets on the second stage provided about three feet of clearance between the stages before the second-stage engine was ignited.

An analog study was made to determine the number of retrorockets needed, whether the first-stage control system could maintain proper vehicle attitude until separation, and whether the second stage would experience an excessive angle of attack after separation. The final design employed three large retrorockets

with 410 pounds of thrust and two booster rockets with 45 pounds of thrust, and resulted in 32.5 inches of clearance. The study also indicated the adequacy of the control systems to perform their functions during this period.

Electrical tests were conducted to verify the time sequence of events between the first-stage engine shut-down signal and the second-stage ignition signal for the delayed sequence. Qualification testing of the retro-rocket was conducted by the Atlantic Research Corporation, and a series of tests conducted at The Martin Company demonstrated successful separation of the aerodynamic shields covering the nozzles of the retro-rockets. It was never found necessary to install the delayed-ignition separation system in a vehicle.

### 3. NOSE CONE JETTISON

The nose cone was attached to the second stage by two diametrically opposed canopy-type hinges. Each hinge was locked in place with a hinge pin and an L-shaped toe. The cone separation plane divided the nose cone longitudinally through Quadrants I and III. An explosive-actuated bolt latch pin locked the tip of the cone, and an explosive bolt surrounded by a compression spring locked the body of the cone. The latch pin and explosive bolt were actuated simultaneously by an electric signal to unlock the nose cone and free the compression spring. The spring imparted an impulse to the separated sections of the nose cone, rotating them outward about the hinges to jettison the cone from the vehicle. This impulse was sufficient to ensure that the longitudinal acceleration would not cause the cone halves to snap back into the closed position. Protection from fragment damage was provided by a cylindrical shield fitted around the explosive bolt.

**Analysis**—Beyond the angle at which the accelerations of the nose cone cg normal to the vehicle axis go to zero, a tension force was required at the hinge to hold the cone half to the vehicle. Since the hinge was not designed to apply to this kind of force for more than 55 degrees of motion, the disengagement angle occurred as soon after 55 degrees as the normal accelerations changed sign. This was determined to be 61 degrees. Further calculations revealed that the nose cone halves would not present any problems of collision with the second stage following their disengagement.

### 4. THIRD-STAGE SEPARATION

The third stage of the Vanguard rocket had no guidance system, but was spin-stabilized. The third-stage motor was contained in the forward shell of the second stage (see Fig. 12). The aft end was mounted on a spin table and the forward end was restrained from transverse motion by four jettisonable "spider" arms. The third-stage nozzle was clamped to the spin table by two sets of shear pins and collars. The spin

table, which was mounted on a spherical self-aligning bearing, was prevented from rotating prior to spinup by a shear arm and shear pin engaging a drive pin in the table.

**Separation sequence**—A signal from the ground or the airborne coasting time computer initiated the spin-up and separation sequence. This signal ignited the two spin rockets mounted on the periphery of the table, started a 1.5-second delay timer to ignite the retrorockets and shut off the second-stage control jet systems, and started a 15-second powder train to ignite the third stage. The initial thrust of the spin rockets sheared the pin restraining spin table rotation. Continued burning of these rockets spun the table and motor to a speed of approximately 185 rpm. During this time, the satellite was prevented from rotating by the spider arms, which engaged the forward bearing housing and rode in longitudinal tracks on the second stage.

After the first 45 degrees of table rotation, the third-stage powder train ignition wires were severed by a wire cutter mounted on the table. After one revolution of the spin table, two triggers mounted on the second-stage bulkhead were positioned. At two revolutions of the table, these triggers engaged two levers on the spin table which sheared the pins retaining the motor, leaving the third stage free within the second stage. This sequence required about 1.2 seconds. At 1.5 seconds after spin rocket ignition, two retrorockets mounted on the exterior of the second stage were fired, decelerating the second stage and achieving separation. At the same time, the pitch/yaw and roll jets were cut off to ensure minimum second-stage movement during the separation sequence. The release of the spider arms at separation allowed the satellite to rotate on the bearing.

**Separation clearance analysis**—To ensure successful third-stage separation, the second-stage shell which surrounded the third-stage motor had to retract approximately five feet longitudinally without contact. The disturbing factors of interest were those which induced relative motion between the second and third stages when the third stage became unrestrained. These included manufacturing tolerances in the motor cg and principal axis location, retrorocket alignment errors, retrorocket thrust and burning time variations, disturbances from non-simultaneous ejection of the spider arms, and residual second-stage vehicle motions from the control system.

A large number of computations was necessary to solve the equations of motion of the third-stage separation for a given set of initial conditions. Since the study was made for several vehicles and several different sets of initial conditions for each vehicle, it was decided to program most of the problems on the IBM-701 computer then available. Approximate hand

methods were used to compute the effects of several additional disturbances tending to produce third-stage wobble and translation.

Testing (see Chapter IV, Section H) and analysis of an early configuration, which tapered to a 26-inch external diameter at the forward end of the second stage, disclosed that only a small margin of clearance was likely, if any of the variables considered should assume a maximum tolerance. The configuration was modified to maintain a constant 32-inch diameter all the way to the nose cone separation plane. This latter configuration was the only one flown (except in TV-2, where no third-stage separation was planned).

## 5. RETROROCKET COVER CLEARANCE

The retrorockets were fired 13.5 seconds before the firing of the third stage, and imparted a velocity of approximately 80 fps, directed forward at a minimum of 11 degrees from the vehicle centerline, to the aerodynamic shields that protected these components during flight through the atmosphere. After the third stage was ignited, it passed the jettisoned rocket shields. It was therefore necessary to investigate the possibility of collision. Since only the relative motion between the rocket shields and the third stage needed to be considered, the effects of gravity and the actual

velocity of the vehicle at the time of retrorocket ignition were not included in the equations of motion. The solution of the equations and the resulting locus of rocket shields with respect to the third stage showed that there would be at least 100 feet clearance between the shields and the third stage.

## F. ORDNANCE

Ordnance components were used in the Vanguard separation sequences, in the second-stage helium heating system, and provided the explosive force for the destruct system.

**Explosive bolts**—The six explosive bolts used to connect, and later to separate, the first and second stages were ordinary 4130 steel bolts, center-bored to receive electrically initiated explosive detonators. For increased reliability, two independently-wired Dupont E-77 detonators, either of which could sever it, were sealed into each bolt.

The explosive bolt used in jettisoning the nose cone was similarly designed, and incorporated the same dual actuation feature, but was made of aluminum and used two Dupont X210 detonators.

**Explosive latches**—The first-stage blast doors and the nose cone halves were held in place, and later

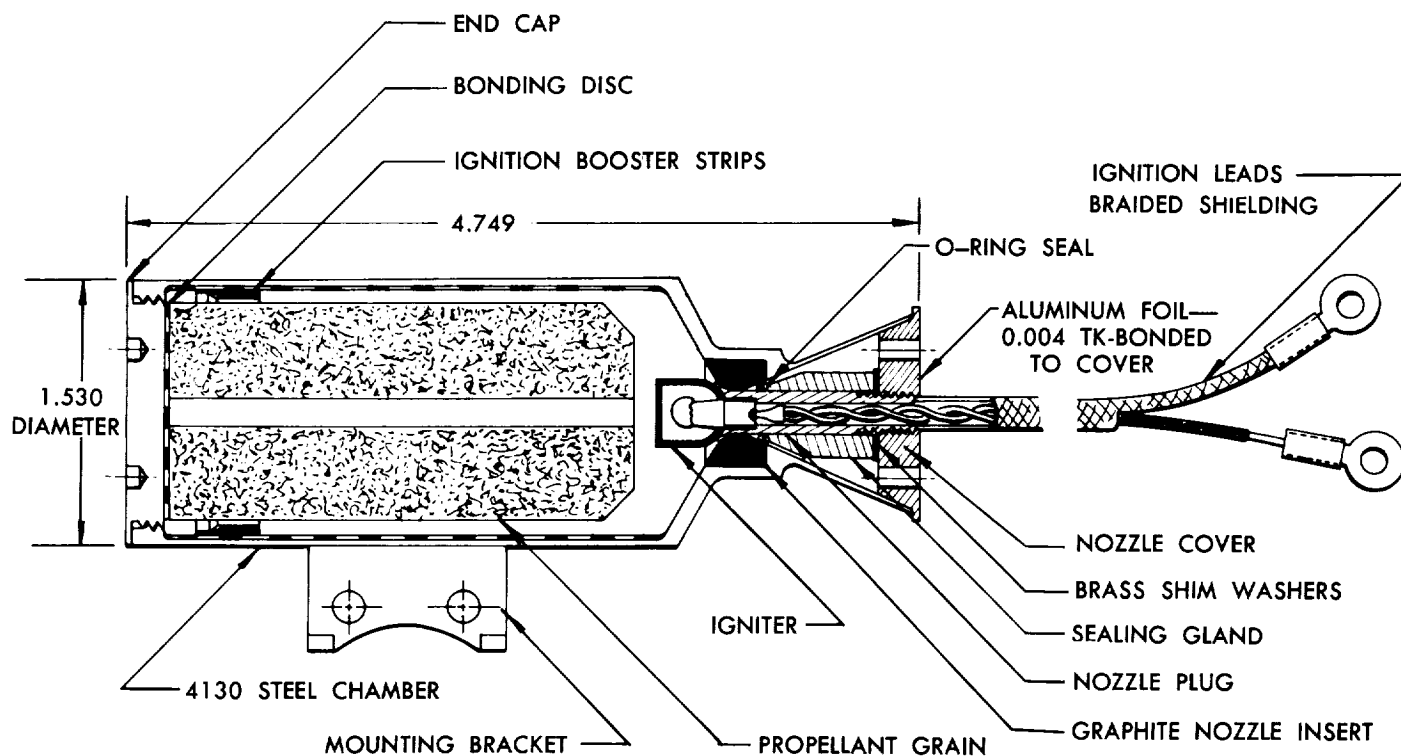


Fig. 29 Cutaway of 1XS-50 Spin and Retro Motor

released, by Conax explosive latches. Components used for the two applications were identical except for a reflective chrome finish applied to the nose cone latches to inhibit the absorption of thermal radiation. The latch pin was driven to the open position by pressure on an attached piston from the explosion of an electrically initiated squib. For increased reliability, each latch contained two squibs, wired in parallel, either of which was capable of actuating the latch pin.

**Spin and retrorockets**—Spinup of the third stage and deceleration of the second during the separation sequence of these two stages was accomplished by small solid-propellant rocket motors designed and manufactured by the Atlantic Research Corporation, in accordance with a Martin Development Specification, (Ref. 24). These motors, designated 1-XS-50, are described in the manufacturer's Model Specification, (Ref. 25) and are shown in Fig. 29. They nominally produced 50 pounds of thrust for one second, and had a maximum length of 4.85 inches, a diameter of  $1.510 \pm 0.032$  inches, and a maximum weight of only 0.70 pound. The rocket chamber and nozzle were 4130 steel, and the solid-propellant grain was a separately machined type, bonded to the forward end cap of the chamber. The propellant consisted of ammonium perchlorate, resin, plasticizer and other

additives in small amounts. The igniter contained powdered magnesium, potassium perchlorate and polyisobutylene, actuated by an Atlas electric match.

The spin motors had a reflective chrome finish to reflect radiant heat in order to prevent operating temperature of the rockets from being exceeded. The retro motors were protected from aerodynamic loads and heating by a protective insulating fairing of Haveg asbestos-impregnated phenolic (Fig. 30). The forward portion of the fairing was a removable nose cone which was blown off by the retro motor exhaust gases upon ignition. The cone was designed so that it was ejected at an angle of approximately 11.5 degrees to the vehicle centerline and away from the vehicle skin. Since the fairing also insulated the retro motors, a reflective finish was not required, and a zinc-chromate finish was used.

The development of the spin and retro motors was based upon existing propellants and hardware manufacturing techniques. Large numbers of static test firings were made to establish the reproducibility of performance over the operating temperature range of  $+20^{\circ}\text{F}$  to  $+130^{\circ}\text{F}$ , as well as for vacuum ignition characteristics.

**Helium heat generator**—Part of the second-stage propulsion system furnished by Aerojet-General was

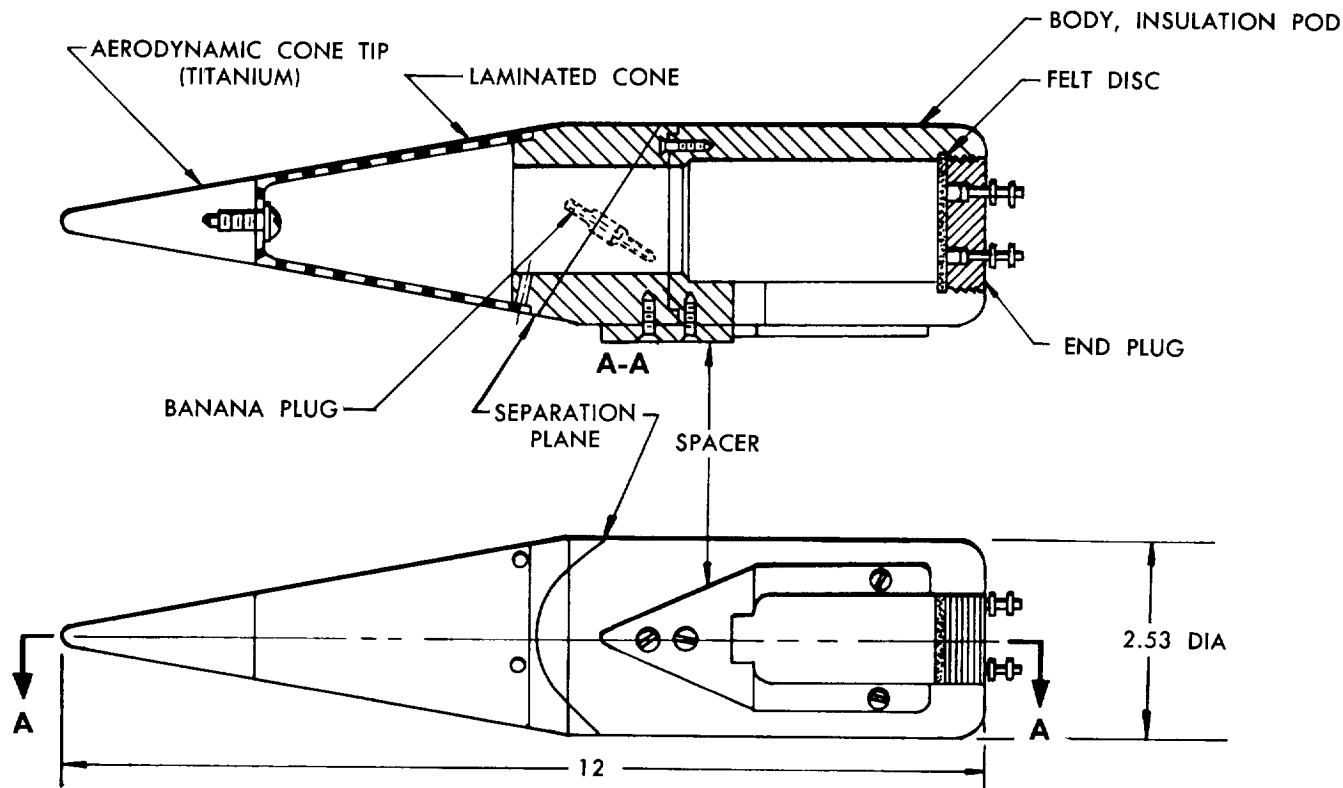


Fig. 30 Retrorocket Aerodynamic Cone and Insulation Assembly

the heat generator unit. The function of this unit was to provide additional energy to the helium pressurizing gas in the form of heat from the in-flight burning of a solid-propellant charge. This was essentially a weight-saving device, in that the initial helium sphere pressure could thereby be kept to a lower value, reducing the structural weight requirements.

This device, cylindrical in shape, contained two cast-molded solid-propellant grains actuated by an ignited assembly of two electrically fired squibs embedded in a black powder charge. Hot gas flow into the helium sphere was controlled by four gas ports in the heat generator. The propellant grains were a cylindrical, end-burning type, of polyurethane and ammonium nitrate composition. Functionally, the unit had a nominal burning rate of 0.115 inch per second and a chamber pressure of 1000 psia. Dimensionally, the unit had a nominal diameter of 2.5 inches and an overall length of 31.0 inches, with a nominal wall thickness of 0.090 inch. The unit was made of corrosion-resistant steel.

**Destruct system**—The destruct system consisted of multiple strands of explosive primacord, installed in the external conduits along the fuel and oxidizer tanks of the first and second stages. About 140 feet of primacord (five strands pyramided) were used on the first stage, and about 50 feet (four strands side-by-side) on the second stage.

The primacord consisted of a 100-grain-per-foot explosive core of Pentaerythritetetranitrate (PETN), contained within a moisture-proof Hycar rubber jacket. Initiation of each primacord circuit was provided by either of two electric detonators, connected to independent electrical circuits. Dupont E-81 instantaneous detonators were used for both oxidizer tank destruct systems, while Dupont D-1B-3 two-second-delay detonators were used for both fuel tank systems. The detonator assemblies were equipped with shorting plugs, which remained attached until plugged into the vehicle destruct panel. The lead wires were just 6 inches long to minimize possible interception of stray RF current.

There was relatively no danger in the handling or installation of primacord, since it cannot be set off by friction, sparks, stray electric currents or any ordinary shock. It can be exposed to temperatures of 200°F for an indefinite period without danger or damage. Loose PETN dislodged from the cord, however, is a high explosive sensitive to friction, and should be avoided at all times.

## G. ELECTRICAL

The electrical circuits provided operational control of the following: power generation and distribution; propellant servicing and pressurization; first-stage

engine start, cutoff and separation; second-stage ignition, hydraulic system operation and cutoff; nose cone jettison; third-stage spin, separation and ignition; and vehicle destruct.

Primary power was supplied from two 20 ampere-hour silver-zinc batteries, one in the first stage and one in the second stage in order to keep the second-stage battery weight to a practical minimum level. The flight batteries supplied power to an aircraft-type rotary inverter which, in turn, powered the transformer-rectifier B+ power supply. Two additional batteries were provided for the first- and second-stage telemetering systems. The first-stage telemetry battery also supplied power to the first-stage command system, while the second-stage telemetry battery supplied power to the radar beacon. The electrical system parameters are given in Table 10.

### 1. PRIMARY 28-VOLT D-C POWER SUPPLY

The two sources considered for 28-volt d-c power were batteries or a generator driven by a monopropellant such as hydrogen peroxide. Batteries were selected, since they had a definite weight advantage for the short use period required. The specific outputs of thermal, lead-acid, nickel-cadmium-alkaline, zinc-mercuric oxide, and silver peroxide-zinc-alkaline batteries were examined. A comparison of operating characteristics of the two types having highest outputs, i.e., the zinc-mercuric oxide (30 watt-hours per pound) and the silver peroxide-zinc alkaline (40 watt-hours per pound), showed the first to have a lower operating efficiency at high rates of discharge.

The most practical main power supply for the Vanguard vehicle therefore appeared to be the silver peroxide-zinc-alkaline-type battery. The batteries chosen were manufactured by the Yardney Electric Corporation. Each battery had a 20-ampere-hour capacity and was composed of 20 HR-20 silver cells, each having a nominal voltage under load of 1.4 volts. These batteries were light, weighing approximately one-fifth as much as a lead-acid battery of equal capacity. They had low internal impedance, which provided good voltage regulation with varying loads; a flat discharge curve, keeping the voltage relatively constant with flight time; and a small amount of free electrolyte, minimizing spillage problems. They were rechargeable, permitting usage during ground checkout and static firings to determine actual battery performance prior to flight firing, and had proven reliability in actual usage on other vehicles.

### 2. A-C INVERTER

Static inverters were procured and tested early in the program. Results indicated that cost and time would not permit satisfactory development. Therefore,

**Table 10. Electrical System Parameters**

	<i>First Stage</i>	<i>Second Stage</i>
Flight Battery:		
Volts	28	28
Capacity, amp-hr	20	20
Telemetry Battery:		
Volts	28	28
Capacity, amp-hr	5	5
Instrument Reference Battery, volts		5
Inverter (3-phase):		
Volts		115
Frequency, cps		400
Capacity, volt-amps		250
Maximum Allowable Voltage Modulation		0.5%
Transformer-Rectifier (B+ Supply):		
Volts		150
Capacity, watts		15
Telemetry Systems:		
Modulation System	PPM/AM	PWM/FM
Carrier Frequency, mc	238.5	231.5
Power, watts	35	15
Channels	15	43
Radar Beacon (C-Band)		AN/DPN-48(c)
Interrogation Frequency, mc		5490
Transmitting Frequency, mc		5555
Command Control:		
Receivers	AN/FRW-59	AN/FRW-59
Recorder	NRL E4680	NRL E4680
FM Radio Frequency, mc	410	410
Sensitivity, $\mu$ v	5	5
Minitrack (Satellite):		
Frequency, mc		108
Power, mw		10

a conventional aircraft-type rotary inverter was selected. The Leland SE-10-3 inverter was chosen over others because tests indicated that its voltage modulation (less than 0.5%) met the requirements of the control system. This inverter was capable of supplying 250 va at a power factor of 0.8 when connected for 115-volt, three-phase delta operation, with a voltage regulation of 109 to 121 volts and a frequency regulation of 380 to 420 cps.

The unit was a rotary motor-generator with a laminated yoke assembly, having a common shaft for the armature and motor. The prime mover was a compensated compound-wound d-c motor having a pole face winding for stabilizing the operation. Noise filters were included in both the d-c input and a-c output lines. Two built-in carbon pile amplifiers furnished automatic voltage and frequency regulation by controlling the current in the a-c motor winding for voltage control and in the shunt field of the motor for frequency control. The frequency could be adjusted by means of an internal rheostat. An external adjustable rheostat was also provided to permit manual setting of the a-c voltage.

This inverter satisfied the environmental requirements of standard drawing MS25093-1 and specification MIL-I-7032D. One inverter was checked for performance characteristics at extremely high altitudes,

especially commutator performance and temperature rise. The results of these tests showed satisfactory commutation and the ability of the inverter to operate for approximately 15 minutes before overheating. The decision to pressurize the inverter container was made in order to ensure inverter operation for the entire flight period of Vanguard, since 15 minutes of operation were considered marginal.

### 3. COMPONENTS

**Relays and timers**—There were 32 relays and timers used in the vehicle electrical system. All were hermetically sealed from the effects of moisture and altitude. Each relay or timer demonstrated satisfactory performance under the temperature, shock and vibration conditions imposed by the Vanguard vehicle. In addition, the electrical operating characteristics and capacity were proven adequate in a functional mockup of the electrical system. The types used were:

16—Hart four-pole double-throw. Contacts rated for 10 amperes resistive at 28 volts.

5—Union Switch and Signal six-pole double-throw. Contacts rated for 5 amperes resistive at 29 volts.

2—Filtors four-pole double-throw magnetic latch. Contacts rated 2 amperes resistive at 26.5 volts.

2—Filtors two-pole double-throw. Contacts rated 2 amperes resistive at 26.5 volts.

3—Cutler-Hammer 1-pole single-throw. Contacts rated 50 amperes, 27.5 volts (MS24140-1).

4—Wheaton Timers, two 5 to 195 second adjustable timers, one 1-second timer, one 1.5-second timer.

**Switches**—Seven switches were used in the electrical system, of which three operated during flight. The others were used during ground testing only. The three flight switches were all MS24331 first motion (ice breaker type) switches. These met the requirements of military specification MIL-S-6744 and in addition were sealed to meet the immersion test of Procedure I of MIL-E-5272. The contacts were rated at 4 amperes resistive. The test switches were all military standard toggle switches; three were AN3027-3 switches and the other was an MS25068-3. All test switches had contacts rated for 20 amperes resistive.

**Connectors**—There were approximately 100 electrical connectors used in the electrical system and associated interconnecting wiring within the vehicle. More than 80% of these were required to connect with various electrically operated components such as valves, motors, solenoids, etc. For example:

23 were required to connect with components of the first-stage propulsion system;

14 with components of the second-stage propulsion system;

21 with components of the controls system; and

22 with range safety and destruct system components.

The different types of connectors used were:

50 Military Standard type or MS modified for potting;

26 Titeflex connectors;

\*21 Bendix miniaturized connectors;

2 Cannon type K connectors;

\*11 Winchester type M connectors;

\*6 Amphenol type 165 connectors;

1 Cannon type GMA 140-pin, solenoid-disconnect type connector.

All connectors had 20-ampere contacts except those marked with an asterisk, which were miniaturized connectors with 7.5-ampere contacts. All connectors were potted to relieve strain on the soldered connections and to resist moisture, except the Titeflex connectors, which used individual wire collets around each wire to achieve the same results. The interstage and first-stage disconnects were all Titeflex plugs, where the use of teflon insert material gave a degree of resistance to nitric acid and to the relatively high temperatures encountered.

**Wiring**—The wiring used for interconnecting electrically operated components was selected and in-

stalled to meet the requirements of MIL-W-8160, except for high temperature applications (200°C) where teflon wire in accordance with MIL-W-16878A was used. The ambient temperature wiring (up to 105°C) was a nylon-jacketed thermoplastic-insulated copper wire, identified as MCI 58740. This wire met the requirements of MIL-W-5086. The high temperature wire was identified as MCI 58756, and was teflon-insulated copper wire which met the requirements of MIL-W-16878 type E or EE. The smallest size wire used was 22 gage and the largest 4 gage.

#### 4. SYSTEM OPERATION

The propulsion fire panel, the ground servicing panel and the electrical monitoring panel located in the blockhouse were used in conjunction with remote junction racks in the equipment house to service and fire the vehicle. A block diagram of system operation is shown in Fig. 31. A resume of all electrical sequencing is given below for completeness. Sequences are repeated elsewhere in the report insofar as they affect the operation of the various systems.

**Prelaunch**—Up to five minutes before launch, the vehicle was supplied with 28 volts d-c from a ground power source. The control system, and consequently the inverter, was energized when power was applied to the second-stage bus when the control switch was closed in the second stage. During WIFNA servicing, the oxidizer probe resistance was periodically monitored to ensure the physical and electrical integrity of the probes.

At approximately T-6 minutes, the second-stage hydraulic pump motor was energized from ground power to check out the second-stage control system and to arm the second-stage pressurization system. At T-5 minutes, the rotary selector switch on the propulsion fire panel was placed in the first arm position. This operation put the first-stage battery on the first- and second-stage busses and also armed the first-stage firing circuits. The fire signal could not be initiated unless the batteries were connected to the vehicle busses.

First-stage pressurization began at T-2 minutes, at which time the hydraulic pump motor switched to the second-stage battery. The peroxide and fuel tanks were pressurized automatically, with the fuel tank having the capability of being manually overpressurized. At T-60 seconds, the first- and second-stage batteries were paralleled. The helium and cooling air umbilicals dropped at T-45 and T-30 seconds, respectively. The LOX tank vents, which had been periodically cycled to ensure proper operation, were then closed and the LOX tank was manually pressurized at T-20 seconds. Once the fire signal was initiated, the LOX tank maintained pressure automatically. If the need arose, the

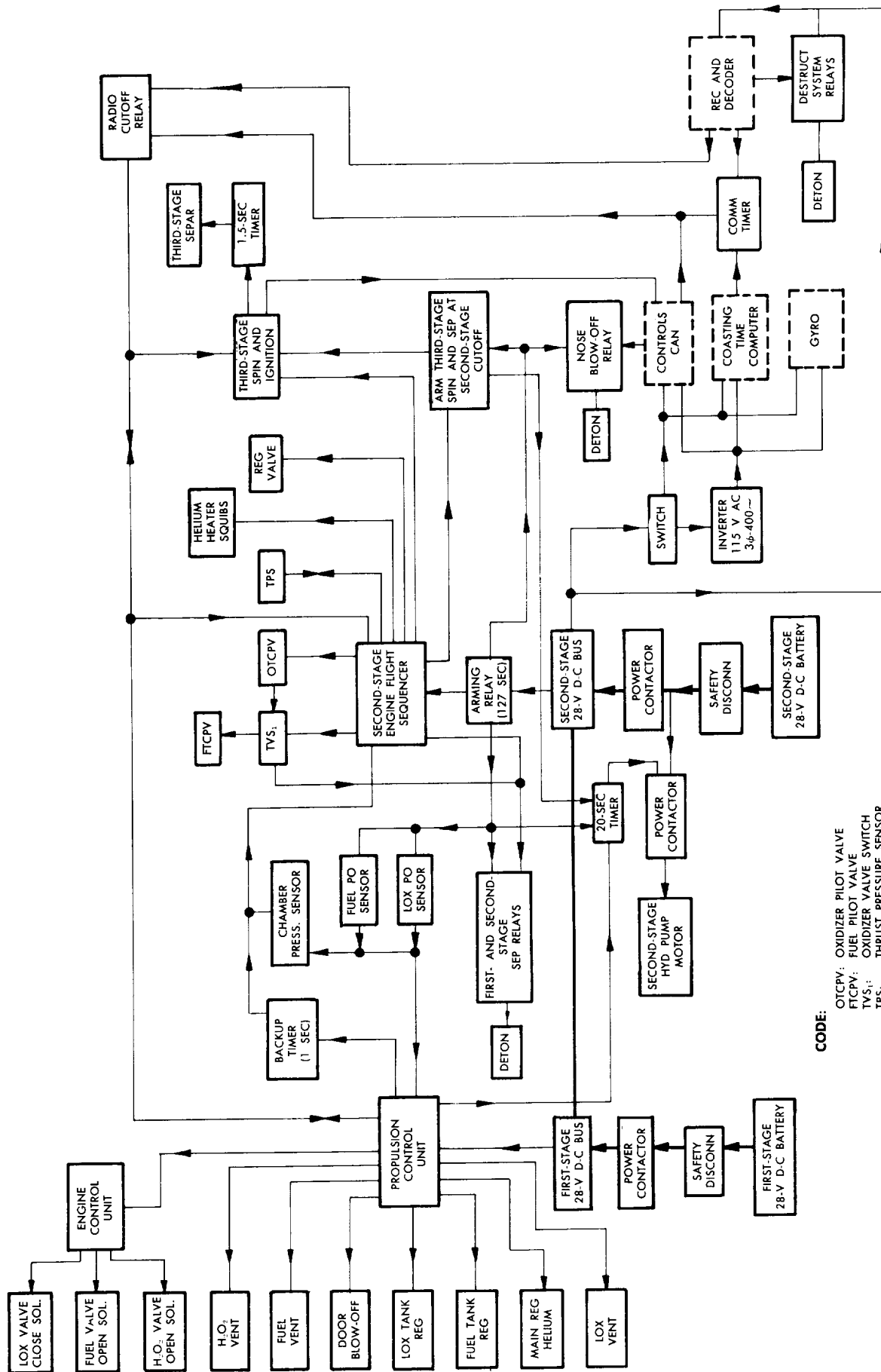


Fig. 31 Electrical and Engine Control Diagram

helium pressure of all tanks and spheres could be dumped. Ground cutoff opened all tank vents.

**Launch**—When the first-stage fire switch was operated at T-0, the electrical umbilical dropped and the firing sequence began. If all the propellant valves were closed, and if the combustion and ignition indicators were properly installed, the firing sequence continued, resulting in operation of the ignition relay in the ground sequencer. The igniter contactor then closed and applied 28 volts dc to the pyrotechnic igniter. The resulting flame burned through the fusible ignition indicator link, signalling the main oxidizer valve and ethane valve to open. Approximately 1.5 seconds after the oxidizer valve started to open, the fuel main valve opened. When combustion chamber pressure reached approximately 23 psia, the combustion indicator opened, which shut off ethane flow and signalled the peroxide valve to open, starting the turbopump. Certain functions, such as ignition, valve openings and combustion indication, had to occur within a specified time, as controlled by timers in the ground sequencer, otherwise cutoff would have been given automatically. Liftoff occurred when thrust exceeded vehicle weight, actuating first motion switches which started the program timer and the coasting time computer.

**First-stage flight**—The program timer activated the first four pitch rates consecutively at 10, 24, 45, and 112 seconds after liftoff. At 127 seconds, the program timer energized two relays in the second stage to arm first-stage cutoff, second-stage ignition and nose cone jettison. Normal first-stage burning time was approximately 140 seconds. When the fuel or LOX pump outlet pressure switches sensed exhaustion of either propellant, first-stage cutoff occurred through closing of the propellant valves. Residual helium in the spheres and peroxide tank was vented through the roll jets to provide roll control during the period from first-stage cutoff to second-stage separation. The blast doors in the interstage area unlatched to relieve the compartment pressure during the second-stage start sequence. The first-stage chamber pressure sensor or its backup (a one-second timer which started at first-stage cutoff) gave the second-stage ignition signal and armed second-stage roll control.

**First-stage separation**—Once the second-stage sequencer received the ignition signal, the second-stage oxidizer pilot valve opened the main oxidizer valve. When the main oxidizer valve opened 27%, stage separation was initiated by the detonation of six double-ended explosive bolts. The fuel pilot valve was also energized by this signal, causing the fuel main valve to open. At the same time, the main helium regulator was tripped electrically, so that second-stage propellant tank pressures were maintained under flow conditions.

Also, the helium heater squibs were ignited. When chamber pressure reached 70% of full thrust, a backup separation signal was sent. Another backup separation signal was given when the main oxidizer valve opened 78% of full open.

**Second-stage flight**—At approximately 172 seconds after liftoff, the program timer energized a relay which detonated the explosive bolt and latch to jettison the nose cone. Second-stage cutoff, which could be initiated by the exhaustion of either propellant, was armed at 240 seconds by the program timer. If fuel exhaustion occurred, the resultant decrease in chamber pressure was sensed by the thrust pressure switch. This energized the cutoff relay, which de-energized the pilot valves and caused the main propellant valves to close. If oxidizer exhaustion occurred, it was sensed by an electrical resistance probe in either oxidizer feed line, which gave the cutoff signal through a transistorized circuit. The second-stage cutoff signal also armed the pitch and yaw attitude control system for coasting flight, armed the third-stage firing circuits, and started a 20-second timer to de-energize the hydraulic pump motor. The fifth pitch rate was activated at 400 seconds by the program timer.

**Third-stage separation**—Upon receiving a spinup and ignition signal from the coasting time computer, the command timer, or the program timer, the third-stage spin and ignition relay closed, energizing the spin motors, the 15-second powder train to ignite the third-stage motor, and the 1.5-second separation timer. The separation relay energized the retro motors to separate the second and third stages 1.5 seconds after the spinup signal was initiated. At this time also, the pitch, yaw and roll attitude control systems were de-energized.

**Payload separation**—Payload separation from the third stage after burnout was initiated on several flights by a mechanical timer that was armed by the high accelerations (about 30 g) during third-stage burning. The range of timer settings used was from 0.5 to 5 minutes.

## 5. DEVELOPMENT TESTS

**Mockup tests**—The electrical system mockup which utilized actual vehicle wiring and components, was operated to simulate a vehicle flight from first-stage ignition to third-stage ignition, including actual interstage connector separation. Test results indicated that battery capacity and wiring were adequate even under the worst conditions.

**Interstage connector tests**—A test was run on the interstage connectors to explore the effects of separating connectors in a vacuum with power supplies on both sides of the connectors and with loads simulating those on TV-3. The test was successful in that no apparent arcing was visible during separation, and

examination of both sections indicated that none had occurred.

**Flame impingement tests**—The LOX dome impingement test at Aerojet determined the effects of the separation process on the electrical connectors, wiring and components located in the interstage area. Results indicated that the wiring and electrical components should be protected with several wraps of teflon-impregnated fiberglass tape, which were incorporated.

## 6. DEVELOPMENT PROBLEMS

**Moisture and condensation**—Moisture and condensation adversely affected the vehicle high impedance circuits at terminal strips and connectors, since the potting compound did not adhere to teflon wire. The terminal strips and some of the connectors in these circuits were eliminated and the splices were encapsulated in Scotchcast. All connectors (except Titeflex) that had teflon wires were scotchcasted and the Titeflex connectors were protected with fluorolube grease. In the final vehicle, all compartments were continuously purged with dry nitrogen until the gantry was retired. In addition, all terminal strips were treated with glyptol to minimize effects of moisture and condensation.

**Relay sequence**—As originally designed, the relay sequence in the Aerojet propulsion sequencer unit could prevent giving the cutoff signal to the second-stage engine. The basic problem was that, within established relay tolerances, the pull-in transfer time of the cutoff relay (the time from opening of the normally closed contact to closing of the normally open contact) could be greater than the drop-out time of another relay which armed the cutoff relay coil. This was eliminated by making cutoff relay operation independent of the drop-out time of the arming relay.

**Thrust pressure sensor switch**—The thrust pressure sensor (TPS) switch in the second-stage propulsion system sensed and reacted to the pressure of the second-stage engine thrust chamber. It was used to initiate a back up separation signal for first and second stages on rising pressure and to shut down the second-stage engine (sensing fuel exhaustion) on decreasing pressure. During engineering evaluation of the TPS and the propellant tank pressure switch (HPS<sub>2</sub>, same as TPS except for pressure setting) a number of switches performed erratically and did not operate within specified tolerances, especially after being subjected to a vibration environment. Further investigation revealed dirt and chips of metal within the switch's working mechanism, maladjusted stops and incorrect mounting. Later tests showed that properly cleaned and adjusted switches performed within specification. Each TPS and HPS<sub>2</sub> switch was thereafter inspected before, during, and after exposure to a vibration environment specified for the Vanguard.

**Oxidizer exhaustion cutoff**—An oxidizer probe-

differential relay shutdown system was designed and developed to give a cutoff signal to the second-stage engine as soon as the probe shutdown system sensed oxidizer exhaustion. The system consisted of an oxidizer probe in each oxidizer line and a differential relay circuit which would become unbalanced and give engine cutoff when both probes had sensed oxidizer exhaustion. The system depended upon an increase in resistance of the oxidizer probe (probe tip to the wall of the oxidizer line), once liquid oxidizer flow no longer existed. When the resistance of both probes started to increase, the current in the sensing winding of the differential relay decreased, which in turn gave the cutoff signal.

Further development testing with the second-stage engine showed that there could be a relatively large time difference between the exhaustions of the two oxidizer lines. This new input required the probe-differential relay system to be capable of giving the cutoff signal when either probe sensed oxidizer exhaustion. Careful evaluation of this requirement indicated that the differential relay could give an inadvertent cutoff signal because of its low drop-out characteristic. In view of this deficiency, the differential relay was replaced with a transistor relay circuit.

The final shutdown system (probe-transistor system) was capable of giving the cutoff signal when either probe sensed oxidizer exhaustion. The probes were employed as before, except that they were wired so that either probe could give the high resistance signal to the transistor circuit which gave the cutoff signal. The transistor circuit consisted of two transistors and a fast-acting relay; the transistors were employed as on-off amplifiers which drove the relay. In addition, arc suppression circuits were added to reduce induced voltages to a level that would not adversely affect the relay contacts and the transistors in the Aerojet sequencer.

**Inverter frequency drift**—Inverter frequency drift was a problem during ground checkout on the earlier vehicles. This problem was attributed to failure of regulating tubes and to carbon dusting. The tubes were replaced by silicon diodes, while all components in the inverter frequency and voltage control circuitry were treated with glyptol to preclude effects of carbon dusting.

## H. MECHANICAL

There were two significant mechanical systems utilized on Vanguard, the first-stage roll jets and the third-stage spin mechanism.

### 1. FIRST-STAGE ROLL JETS

**System selection**—Movable fin stabilization of the first stage in the roll axis was considered but abandoned in favor of individually controlled jet reactors because

of the weight saving advantages, simplicity of vehicle design, and requirement for roll control in regions where dynamic pressure was low or nonexistent. Originally, the first-stage roll control stabilization system was to have consisted of peripherally mounted jets fed by a separate gas supply. However, a large amount of fuel and storage space would have been required to supply the substantial correcting moment required during launch and at maximum dynamic pressure. Steam from the hydrogen peroxide turbine was expelled with considerable force during the entire first-stage flight. It was decided to harness this developed thrust for roll control moment.

**System description**—The turbine exhaust was ducted through flexible bellows to two rotatable spherical-shaped roll jet nozzles, placed 180 degrees apart on the periphery of the tail can (see Figs. 12 and 32). These were actuated in unison so that the individual thrusts combined to form a rolling couple. The nozzles had three positions: neutral, where the exhaust was pointed aft, and  $\pm 45$  degrees (see Fig. 32). There was no valving on the exhaust system; the nozzles operated from start until shutdown of the peroxide system. When the nozzles were not required for roll correction, they were pointed aft, augmenting the thrust of the first-stage thrust chamber. Since the available correcting moment was substantially larger than the maximum predicted disturbing moment, system stability was improved by deflecting the nozzles through only 45 degrees instead of the maximum 90 degrees. In this manner, the most advantageous combination of system damping and overshoot was realized, and the relatively long delay between hard-over in one direction and hard-over in the other direction was substantially reduced.

Movement of the roll jets was accomplished by a pair of on-off actuators, powered by helium pressure and controlled by pneumatic four-way, three-position valves which responded to signals from the roll gyro. Each of the actuators contained two single-acting pistons, a solenoid-operated three-position valve, a centering spring, and linkage to convert linear piston motion to rotary motion of the nozzles. A disconnect and two check valves were used so that the actuators could be operated without energizing the propulsion system. The design of the first-stage roll jet actuator was governed by the available 640-psi helium source and by maximum response requirements that the jet actuate from neutral to 45 degrees within 80 milliseconds and return to neutral within 110 milliseconds. The jet was also required to pass steam at 800°F without binding during the 140 seconds of first-stage flight. Since the pistons of the actuator were bottomed in the neutral position, it was not necessary to compress residual helium to start the actuator, which resulted in quicker starting and required less pneumatic power.

The centering mechanism was designed to put the centering spring in compression for any roll jet position, resulting in a positive, quick-action return to center and good damping.

**System tests and development**—The initial roll jet design employed a ball bearing joint on which the jet can rotated. Tests revealed that extreme friction and binding in the roll jet bearing and seal prevented the mechanism from meeting the response requirement because of differential expansion of the parts when subjected to the 800°F turbine exhaust. A redesign incorporated a floating labyrinth seal of aluminum bronze composition, and a three-bearing, track-roller design. The rollers were designed to center the jet by riding on the exterior surface, and were, therefore, removed from the 800°F environment. The friction problem was essentially eliminated and the response requirement was met, as substantiated by subsequent test and flight data.

Systems testing of the roll control system was accomplished by use of the first-stage roll mockup. Items such as thrust, response and nozzle position were monitored during the tests. Test results generally substantiated design predictions. Many helium control valves were rejected during ground tests because of leakage. This leakage was caused by small bits of line wall scale and the level of contaminant in the helium as purchased. These very fine contaminants would have had no effect on most valves but were sufficiently coarse to scratch the optically flat sealing surfaces in these valves. The condition was remedied by installing paper micronic filters at the valve inlets.

## 2. THIRD-STAGE SPIN MECHANISM

**System selection**—Several methods of spinning the third stage to a minimum of 150 rpm were considered during the Vanguard design phase. The spin could be imparted before launch, during flight, or just prior to separation, but the effect of spinup on other vehicle functions had to be considered. In addition, a maximum allowable spin of 1000 rpm was established by third-stage structural considerations.

The third stage would have to be rotated to about 1250 rpm on the ground to ensure 150 rpm at third-stage separation. This was above the allowable spin rate of the third stage, and would have introduced a large gyroscopic effect during first and second-stage flight. A helix screw was considered, wherein the third stage would be initially locked in place, then spin down the helix during some high acceleration portion of the flight, and rotate freely at the end of the helix thread. Weight and space considerations, however, ruled out this method. Weight also ruled out the use of a turbine driven by helium, ram air, or solid propellant gas generators.

The potential energy of a leaf spring wound on a

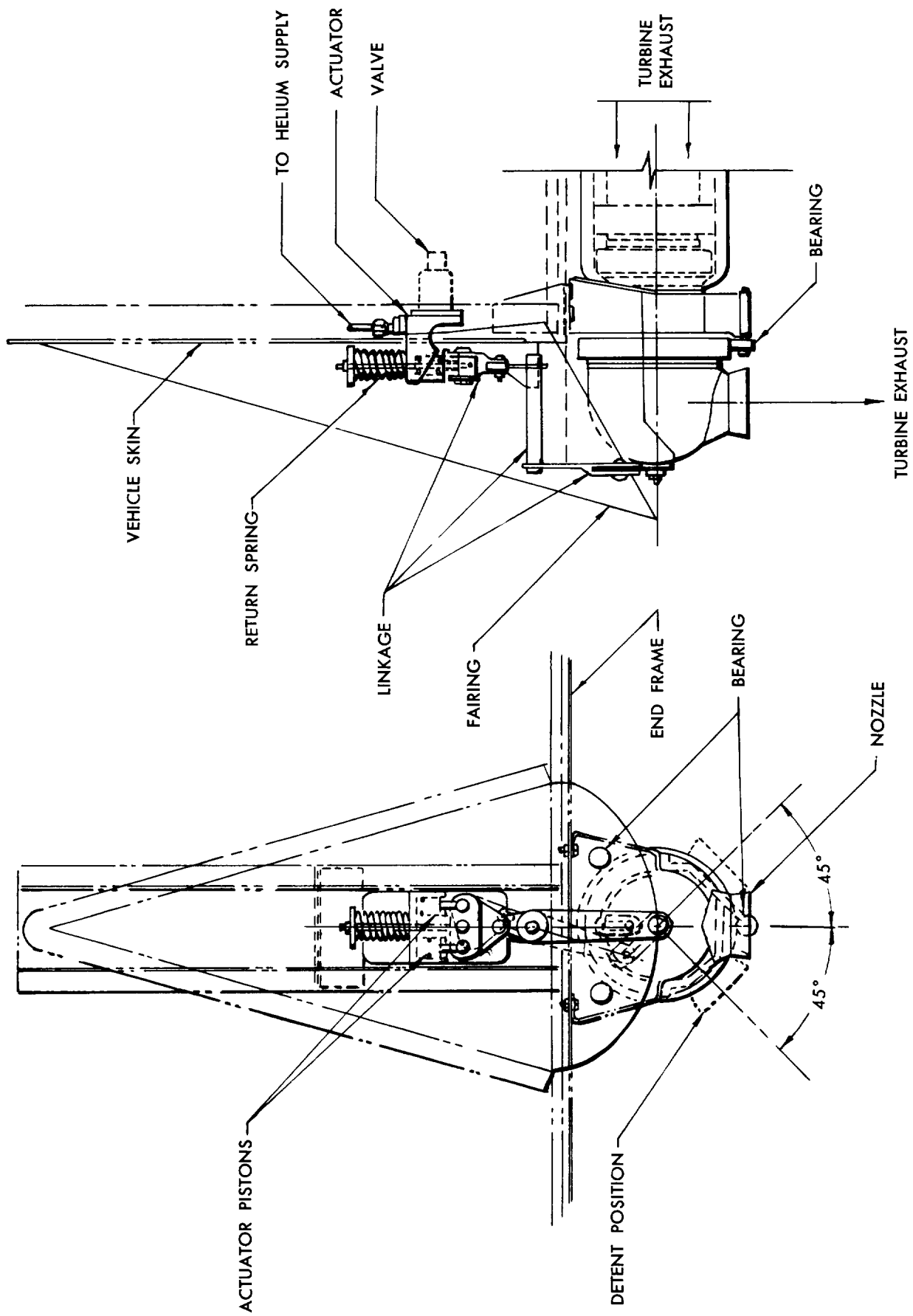


Fig. 32 First-Stage Roll Jet Actuation Mechanism

drum was also considered as a source of the rotational energy needed. Premature rotation would be prevented by a cam, held in place by a fuse link which could be melted by an appropriate electrical signal. Sufficient spin could also be imparted to the third stage by the ignition of two small solid propellant spin rockets mounted tangentially on a revolving spin table. The spring actuation method weighed about 2.5 pounds as compared to about 1.5 pounds for the spin rocket design. Since the reliabilities of both systems were considered excellent, the lighter spin rocket design was chosen.

**System description**—A description of the hardware and its operation may be found in Chapter IV, Section E.

**System tests and development**—A mockup was constructed to test the third-stage spin and separation system. The mockup consisted of the following: a tapered second-stage shell (top diameter, 26 inches), including retrorocket installations and weights to simulate second-stage mass and moments of inertia at burnout; a simulated third stage suspended in a manner to allow spin; and the third-stage spin and separation mechanism mounted in the second-stage shell. In addition, a stroker motor was utilized to give a low-frequency, low-amplitude pitch/yaw oscillation to the second stage to simulate motions during separation. The tests indicated that spin and separation could be accomplished with this configuration. Collisions did occur between the stages on the last three runs. However, this was alleviated by increasing the top diameter of the second-stage shell and locating the retrorockets at the center of percussion of the empty second stage.

The bearing housing on which the satellite was mounted permitted the satellite to attain a rotation of about 150 rpm prior to satellite separation from the motor. On several of the vehicles, it was desired to limit the satellite spin rate to 60 rpm. Since the initial spin rate of the third stage was 180 rpm and that of the satellite was zero, it seemed feasible to obtain the desired spin rate by merely separating the satellite from the third stage at the proper time. Precision bearings were evaluated and sets were chosen that had low enough friction characteristics to keep the satellite spin rate below 50 rpm until after burnout of the third stage. These bearings were cleaned and assembled into housings designed as one piece to ensure the close concentricity of the bearings themselves. A spacer was added between the bearings to distribute the thrust loading during third-stage burning (maximum of 650 pounds) equally between the bearings rather than allowing one bearing to support all the load. After assembling the housing, it was necessary to determine, through testing, the friction level of the assembly under loads that would be imposed during flight. From

these tests, the satellite separation time and expected final spin rate of the satellite were determined.

## I. HYDRAULIC

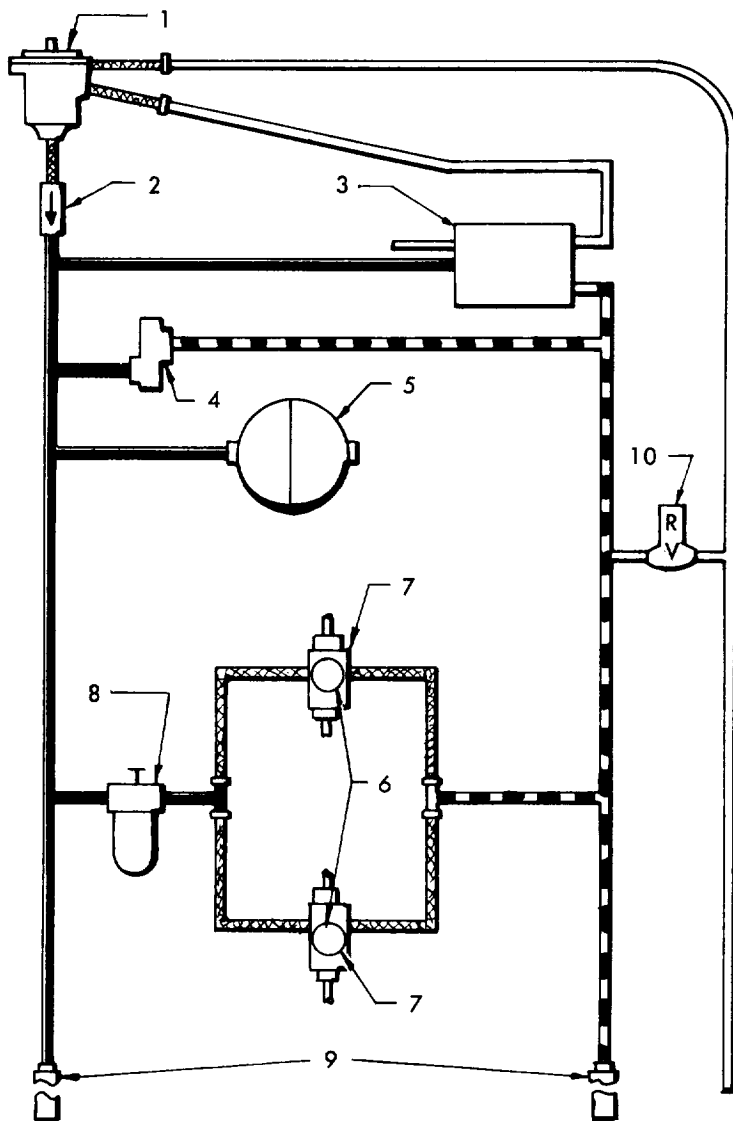
The gimbaled first- and second-stage Vanguard engines were positioned by electrohydraulic transfer valves and actuators in response to gyro commands. The transfer valves used on Vanguard were similar to, but had higher performance characteristics than those used on Viking rockets. They were chosen largely because of their good reliability and performance on Viking. Relief valves and constant displacement pumps were chosen to maintain system pressures in the first and second stages, since they were simpler and lighter than the available alternative of variable volume pumps.

### 1. SYSTEM DESCRIPTION

**First stage**—Design system parameters and a schematic of the final first-stage hydraulic system configuration are given in Fig. 33. The major components of the system were the pump, a pneumatically pressurized accumulator, a system pressurized reservoir, a high pressure relief valve which maintained system pressure between 1600 and 1700 psi during normal operation, a low pressure relief valve for thermal pressure relief, a filter, and the engine pitch and yaw hydraulic actuator assemblies.

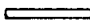



The first-stage pump was driven by the hydrogen peroxide turbine through a gear linkage, thus utilizing an available power source which eliminated the need for an electric motor. The first-stage pump was a seven-piston constant-displacement pump rated for 1 gpm flow at 1500 rpm. It was operated at 3900 rpm and delivered about 2.9 gpm flow to the system. When this flow was not required by the actuators, it was ported directly back to the return line by a high pressure relief valve. The fluid supply for the first-stage pump was contained in a reservoir which was pressurized by system pressure. This "boot-strap" type of reservoir was chosen because the pump required a relatively constant back-pressure of about 37.5 psi for proper operation. The position of the actuators was controlled by the electrohydraulic transfer valves (series 900 Moog Valves) which responded to attitude error signals from the gyros. As a gyro sensed a pitch or yaw vehicle error, it initiated a signal to the corresponding transfer valve, which ported high pressure oil to the correct side of the double acting actuator piston. The wiper rod of a linear follow-up potentiometer was connected to the moving end of the actuator, and fed back an indication of engine position to the control system summing point.

The first-stage hydraulic system was operated by a ground hydraulic source up to liftoff to provide a means for adjusting engine position prior to launching.



# **LEGEND:**

1. HYDRAULIC PUMP
2. CHECK VALVE
3. RESERVOIR
4. RELIEF VALVE
5. ACCUMULATOR
6. TRANSFER VALVE
7. PITCH AND YAW SERVO ACTUATOR
8. FILTER
9. DISCONNECT
10. LOW-PRESSURE RELIEF VALVE

-  SUPPLY AND DRAIN
-  PRESSURE
-  RETURN
-  FLEXIBLE HOSE

## **HYDRAULIC SYSTEM DESIGN PARAMETERS**

MAXIMUM ENGINE BIAS LOAD	600 FT-LB
MAXIMUM ENGINE DEFLECTION RATE	30 DEG/SEC
MAXIMUM ENGINE DEFLECTION ACCELERATION	4.8 DEG/SEC <sup>2</sup>
ENGINE MOMENT OF INERTIA	26.8 SLUG-FT <sup>2</sup>
PUMP CAPACITY	2.9 GPM
ACCUMULATOR VOLUME	0.26 GAL
RESERVOIR CAPACITY	0.82 GAL
PRESSURE	1750 PSIA

**Fig. 33. First-Stage Hydraulic System Schematic**

The ground hydraulic source was connected to the vehicle through two disconnects which separated at liftoff. A more detailed description of the first-stage hydraulic system is given in Ref. 13.

**Second stage**—A schematic of the final second-stage hydraulic system configuration is given in Fig. 34. The major components of the system were the pump, a pneumatically pressurized accumulator, a spring-loaded reservoir, a high pressure relief valve which maintained system pressure between 1000 and 1100 psi during normal operation, a filter, check valves, and the engine pitch and yaw hydraulic actuator assemblies.

A highly reliable electric-motor-driven, nine-piston, constant displacement pump was chosen to drive the second-stage hydraulic system. With 28 volts dc applied, the motor pump drew 35 amperes and delivered 0.875 gpm flow to the system. When this flow was not required by the actuators, it was ported to the return line by a high pressure relief valve. The fluid supply for this pump was contained in a spring-loaded reservoir, which compensated for thermal expansion of the oil and maintained a back pressure on the order of 37.5 psi. This reservoir was chosen over the "bootstrap" type because the pump was relatively insensitive to back pressure. The position of the actuators was controlled by electrohydraulic transfer valves (series 900 Moog Valves) in response to gyro initiated signals, as in the first-stage system.

The second-stage hydraulic pump was turned on six minutes prior to liftoff, to prevent in-flight starting transients. This caused the second-stage engine to "follow" the gyro signals throughout first-stage flight. Disconnects were provided in the system for use during testing when a ground hydraulic source was employed. A more detailed description of the second-stage hydraulic system is given in Ref. 13.

## 2. SYSTEM DEVELOPMENT

Breadboard testing of both the first- and second-stage hydraulic systems indicated successful component operation. Performance tests were run on the first-stage pump to determine the flow characteristics for various pump speeds and outlet pressures. Performance tests were run on the second-stage pump to determine the speed, flow, voltage, current and discharge pressure relationships. Tests were performed on both first- and second-stage transfer valves to determine the flow versus differential current relationships. Detailed information on hydraulic system development testing may be found in Ref. 14.

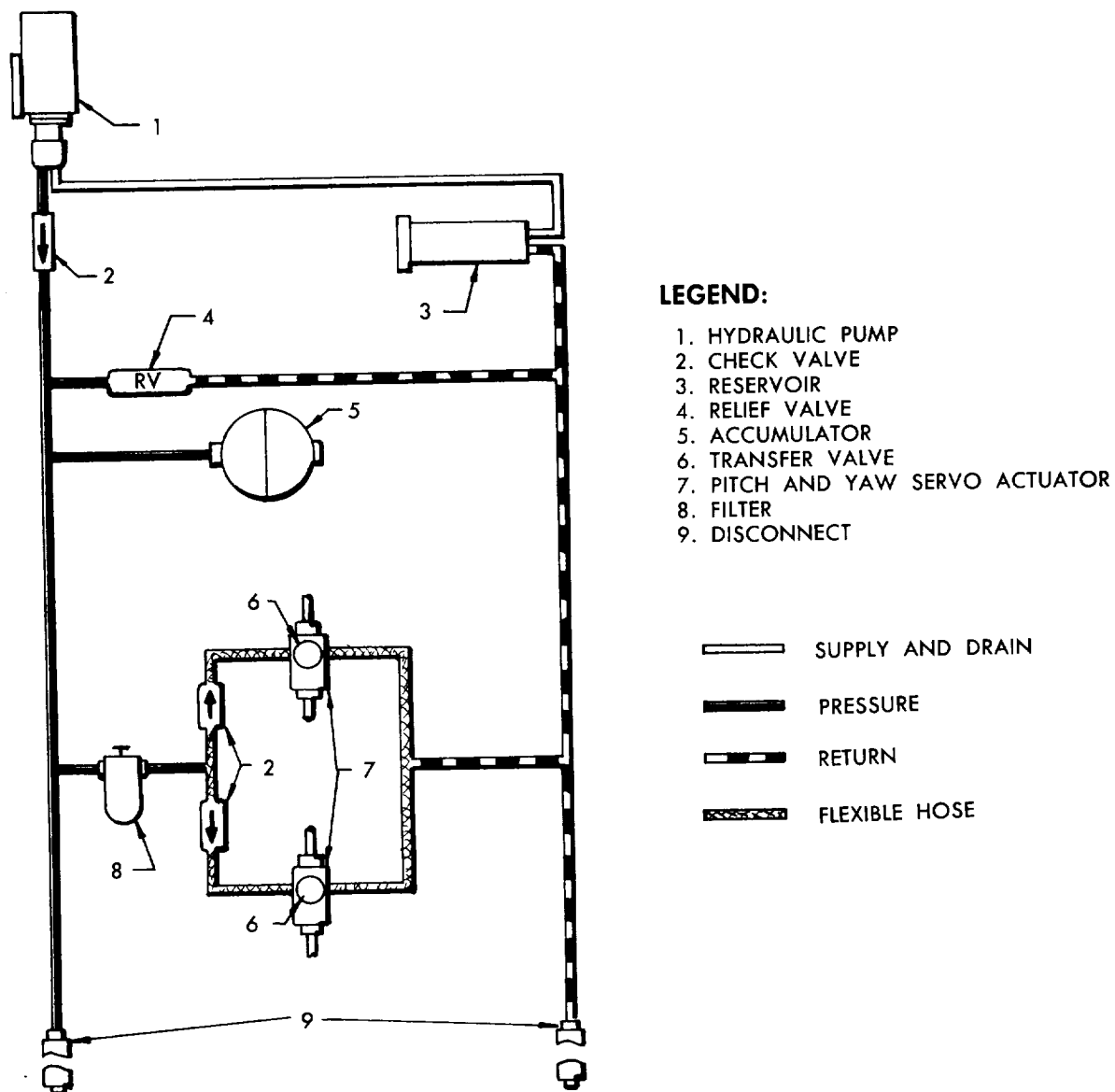
**Bias load tests**—Bias load tests were conducted, using the first-stage dynamic engine mockup, to investigate the frequency and transient responses of the first-stage pitch and yaw control systems with simulated actuator loads. These loads represented moments

caused by rocket engine thrust misalignments and gimbal bearing friction. A secondary purpose of the test was to determine the effect of "cold" (85°F) and "hot" (160°F) hydraulic fluid on the frequency response of the control system. Frequency response results indicated that bearing friction loading increased the phase lag of the system and caused the response to peak at a lower frequency than the unloaded system. The tests run with "cold" oil resulted in slightly noisy frequency response data, while the system response using "hot" oil was considerably quieter. The application of maximum expected bias loads of 550 foot-pounds resulted in a null shift of 0.2 degrees in the hydraulic servo. Transient response tests indicated that with the inclusion of bias loading and bearing friction effects, the vehicle was able to recover from one-degree gyro error steps.

**Battery paralleling**—In early vehicles, large electrical transients caused by battery paralleling occurred slightly prior to the critical first-stage burnout transient. These electrical transients resulted in fairly large engine and vehicle motions, and hence structural loading. A combined bias load, 28-volt electrical transient test was undertaken, utilizing the dynamic engine mockup and two analog computers to simulate aerodynamic and structural flight conditions. Test results indicated that the effects of the combined predicted maximum electrical transient and bias load effects were within the capabilities of the structure.

**Hydraulic oil contamination control**—A hydraulic oil contamination control program (reported at length in Ref. 26) was instituted early in the Vanguard program because the electrohydraulic transfer valve was known to be vulnerable to contaminant in the hydraulic oil. A test program was initiated to determine what level of contamination the transfer valves could safely tolerate for the effective life of the rocket (testing plus firing), and to determine how this level could be maintained. Tests were also performed on various filters to determine their effectiveness. While these tests were in progress, an interim contamination control program was instituted to protect rockets about to go into production. The acceptable contamination level of fluid in the vehicle systems and test carts was defined as "B" grade of the Allison contamination method, which was used as a standard.

The test program indicated the amount of contaminant tolerable to the system and that the most effective means of measuring fluid contaminant was by particle counting. Contamination control facilities were set up, based upon the test findings, both in the factory and at Cape Canaveral. The incorporation of Rigimesh woven metal screen-type filters into the hydraulic systems was a result of test findings which disclosed that the previously used paper filters were not only inadequately



#### HYDRAULIC SYSTEM DESIGN PARAMETERS

MAXIMUM ENGINE BIAS LOAD	283 FT-LB
MAXIMUM ENGINE DEFLECTION RATE	20 DEG/SEC
MAXIMUM ENGINE DEFLECTION ACCELERATION	1.6 DEG/SEC <sup>2</sup>
ENGINE MOMENT OF INERTIA	9 SLUG-FT <sup>2</sup>
PUMP CAPACITY	0.875 GPM
ACCUMULATOR VOLUME	0.26 GAL
RESERVOIR CAPACITY	0.39 GAL
PRESSURE	1050 PSIA

**Fig. 34. Second-Stage Hydraulic System Schematic**

filtering the oil, but were actually contributing fibrous contaminant to the system.

## J. RANGE SAFETY

The Vanguard range safety system provided engine cutoff and vehicle destruct capabilities to permit immediate termination of a flight if range safety criteria were exceeded during any period from first-stage engine ignition to the end of second-stage powered flight. No destruct system was provided for the third stage since re-entry temperatures would destroy the stage in any case.

Two separate and independent UHF command systems, capable of terminating flight from the ground and compatible with the standard Atlantic Missile Range (AMR) flight termination system, were flown in Vanguard: one set in the first stage and one set in the second. The only components common to the two systems were the antenna, the destruct package and their direct connections. The airborne systems were designed to provide a reliable destruct system with a minimum possibility of inadvertent flight termination.

### 1. AIRBORNE SYSTEMS

**Electronic equipment**—All electronic equipment was supplied by the Government. The airborne portion of the range safety system was composed of two AN/ARW-59 command receivers, two of NRL's transistorized decoders, an AN/DPN-48(c) C-band beacon, command cutoff and destruct circuitry, and beacon and command antenna systems.

The AN/ARW-59 is a UHF radio receiver that contains circuits which accept the frequency-modulated, 410-megacycle, radio control signals (if these signals are at a level of 5 microvolts or greater), demodulate these signals, and pass the resulting audio content to the E4680 decoder. The decoder contains audio filters for separating the audio output of the receiver into the proper control channel, and provides an "on-off" switching function for each channel. The command receivers and decoders constituted the airborne command systems. Command system No. 1 was in the second stage and could provide flight path trimming commands as well as range safety commands. It was powered by the second-stage, 28-volt d-c bus. Command system No. 2 was in the first stage and was used only for range safety commands. It was powered by the first-stage telemetering battery.

The AN/DPN-48(c) C-band beacon was included in the vehicle for range safety purposes to provide, at all times during powered flight, position information which was compatible with the tracking system utilized at AMR. It was a pulse-type receiver-transmitter that responded to single-pulse interrogation (at 5490 mega-

cycles) from either one or two radars, and retransmitted pulses (at 5555 megacycles) for radar detection.

**Antenna systems**—The command system and tracking system antennas were designed to provide adequate coverage to ensure that the UHF radio command signals and radar tracking signals would be received at any point along the powered flight trajectory, with the vehicle in any flight attitude. The command antenna system was composed of two arrays; one in the first stage and one in the second stage. Each array consisted of two antennas connected together with coaxial cable, such that one antenna was 180 degrees out of phase with the other. The antennas were used in pairs in order to obtain greater coverage than would be possible with one antenna alone. Each individual command antenna was a 50-ohm external-notch type having elliptical polarization.

The Martin C-band antenna system developed for Vanguard was composed of one cross-slotted flush-mounted wave guide antenna located in the second stage. The antenna was a 5-inch long section of non-standard size wave guide, whose axis was mounted parallel to the axis of the vehicle. The antenna was fed from a coaxial to wave guide junction. A quarter-wave length step transformer in the wave guide matched the slot impedance to the impedance of the coaxial junction. The C-band antenna system originally consisted of a four-antenna array, spaced at 90 degrees around the periphery of the vehicle. At the request of NASA, radiation pattern measurements were made on dual and single C-band antenna arrays, and results indicated a better gain coverage in the region of interest with the single antenna. In addition, the severe variation in gain experienced with the four-antenna array did not exist. The single antenna was successfully flown on SLV-4, -5 and TV-4BU. Four antennas were used on SLV-6 because of the more northerly flight azimuth. This antenna system was adopted intact for usage on the Thor-Able vehicle.

**Destruct system**—The destruct system consisted of multiple strands of primacord placed inside the external conduits of the fuel and oxidizer tanks of both the first and second stages. The exploding primacord would rupture the tanks to accomplish propellant dispersion. The firing voltage would be applied to all detonators simultaneously. The detonators that ignited the primacord along the fuel tanks had a two-second pyrotechnic time delay in order to rupture the fuel tanks a short time later. This delay feature was incorporated to preclude rapid mixing of the oxidizer and fuel and thus minimize a potential high order explosion. Two detonators were used in each primacord package to increase reliability. Further details of the ordnance components of this system are given in Chapter IV, Section F.

## 2. GROUND SYSTEMS

Radar tracking data, a prime source of information for range safety decisions, were obtained from the two AN/FPS-16 radars which tracked the AN/DPN-48(c) beacon in the vehicle. The AN/FPS-16 (XN-1) is located at Patrick Air Force Base (PAFB) and the AN/FPS-16 (XN-2) is located at Grand Bahama Island (GBI). Output information from both of these radars was fed to the IBM-704 computer at Cape Canaveral. Data from either could be used for computation of predicted impact points. These inputs, plus the data from the telemetry-ELSSE system, the optical trackers and the vertical wire skyscreens were used by the range safety officer in making his decisions.

The AN/FRW-2 radio command transmitters were equipped to send cutoff and/or destruct signals if the range safety officer's situation analysis indicated that the vehicle was exceeding a range safety limit. The specific command desired would be transmitted on one of ten separate channels by frequency modulating the transmitter with selected audio tones. The ground-transmitted signal would be received and demodulated by the airborne AN/ARW-59 receiver and applied to the input of the decoder, where audio filters would separate the signals and each tone would actuate a relay corresponding to the command to be initiated.

Channels 1, 2 and 5 were controlled solely by the range safety officer. Signals received on the range safety channels took precedence over any other control signals. The ground signals had to be transmitted in sequence: channels 1 and 5 (arm and cutoff) first, then channels 1 and 2 (destruct). When the decoder in either stage detected an "arm" signal, it provided an output which closed the arm relay, applying power to the cutoff or destruct relays in the decoder. The "cutoff" signal (given simultaneously with the arm signal) closed the cutoff relay in the decoder and operated the destruct power relay, which armed destruct relays if the liftoff switch was in flight position. The cutoff relay in the decoder also supplied voltage to the first- and second-stage radio cutoff relays. The radio cutoff relay opened the third-stage firing circuit and applied voltage to the Aerojet flight sequencer in the second-stage firing circuit. The cutoff relays for either engine were electrically latched-in, and therefore needed only a short-duration signal which could be immediately followed by the "destruct" signal. When the ground-transmitted destruct signal was given, the decoder destruct relay was energized. This applied voltage to the destruct relays, closing them and firing the destruct detonators.

Engine cutoff could be accomplished while the vehicle was on the launch pad by a manual cutoff signal from the fire switch on the propulsion firing panel, by a cutoff signal from the General Electric ground sequence

unit, by manual operation of the ground service panel cutoff switch or by momentarily holding the master switch on the propulsion fire panel in the emergency position.

## 3. ADDITIONAL DEVELOPMENT TESTS AND PROBLEMS

**Command antenna**—The conical radiation pattern measurements of the command array were taken to check the design and to determine the coverage and gain of the antenna in any direction. Radiation patterns of various combinations of the number, phasing and location of the antennas were recorded in order to determine the configuration giving the optimum angular coverage. The best combination was found to be an array of two antennas located at Quadrants II and IV, and fed from a coaxial tee through unequal lengths of cable, one cable being one-half of a wave length longer than the other.

**C-band antenna**—Initially, it was difficult to tune the C-band antenna to meet VSWR limits. Capacitance was added to the antenna in the form of teflon spacer washers in the feed connector to make impedance more resistive.

## K. INSTRUMENTATION

Instrumentation in the vehicle and on the ground provided information required for prelaunch testing and for establishing flight performance, as well as a basis for analysis of any malfunctions which occurred.

### 1. TELEMETRY SYSTEMS

Three telemetry systems were used to supply a maximum of instrumentation for the test vehicle program. A PPM/AM (Pulse Position Modulation) system, developed by NRL and successfully flown on the Viking program, was used for first-stage propulsion and controls measurements. A PWM/FM (Pulse Width Modulation) system was used for gathering data on the second stage. An FM/FM (Frequency Modulation) system was utilized in the second stage for gathering high frequency data from both the first and second stages. A second PWM/FM system was used in the TV-1 vehicle to obtain data from an instrumented nose cone. The satellite launch vehicle instrumentation was somewhat reduced from that for the test vehicles. A PPM/AM system was used for first-stage performance data and a PWM/FM system for second-stage data.

RF radiated power for the FM carriers was between 12 and 15 watts, which afforded excellent reception, in some cases up to 1200 miles line of sight. The AM carrier radiated approximately 35 watts during pulse transmissions. Quadraloop antennas were employed, which gave a fairly omnidirectional pattern. The an-

tennas were machined to a wedge or fin shape from a block of stainless steel, and then stress relieved to better withstand aerodynamic heating.

Sensing devices, in most cases, provided outputs compatible with the telemetry systems, (i.e., 0 to 5 volts input). Very little signal conditioning equipment was used, except for demodulators for the gyro signals and frequency converters or counters for use with the flowmeters. The airborne power source for the instrumentation and telemetry system was separated from the primary vehicle power source. The instrumentation power supply consisted of silver cell battery packs which furnished 28 volts dc.

Radiation patterns of various combinations of the number, phasing and location of telemetering external notch antennas were recorded in order to determine the configuration giving the optimum angular coverage.

## 2. TEST AND CALIBRATION PHILOSOPHY

All end instruments received their primary calibration in the Quality Control receiving and inspection laboratory. After installation in the vehicle, instrument calibrations were spot-checked. The instruments were again spot-checked against the original calibration at the launch site. All instruments out of tolerance were rejected and replaced.

## 3. SPECIAL PROBLEMS

**High pressure measurements**—A special line of pressure transducers, developed by Rahm Instruments and the U. S. Gage Company, solved the high pressure measuring problem in extremely corrosive media such as WIFNA and UDMH. These transducers consisted of specially welded stainless steel bourdon tubes with the media present inside the bourdon tube. The case was designed to withstand the media and pressure without damage to any other component in the event of bourdon tube failure. These transducers featured good performance for average pressure measurements under all expected environmental conditions, but were not of much benefit in studying transient responses.

**High temperature measurements**—Nose cone skin temperature measurements were obtained with small "postage stamp" resistance wire gages developed by Aero Research, Incorporated. The gage consisted of a small platinum wire gage bonded to a very thin strip of steel (about the thickness of a sheet of paper) which was then fastened to the surface of the nose cone. Temperatures in the region of 2000°F could be recorded.

**Propellant temperatures**—Propellant temperature measurements during flight in different types of media and different temperature ranges presented another problem. A series of temperature probes were developed by Aero Research and Bendix-Friez, utilizing thermistors as the sensing elements. In cases where

temperatures of corrosive media were to be sensed, the sensing thermistor was placed in a thin aluminum casing. Noncorrosive media were sensed by the uncovered thermistor to minimize temperature lag. The probes developed by Bendix were found to have extremely long response times because the thermistor was enveloped in a plastic covering. Consequently, the probes developed by Aero Research, which featured much faster response times, were utilized. These probes have since found acceptance in the rocket field for the measurement of propellant temperatures adaptable for use with telemetry.

**Pressure transducer calibrations**—Difficulty was experienced in repeating pressure transducer calibrations in the field similar to those obtained during factory checkout. This problem became more acute as time progressed. Investigation disclosed that the basic source of error was a discrepancy in the various pieces of calibration equipment. At the same time, it was also found that the transducers shifted calibration slightly over a period of time. By instituting more rigid control over expired time between calibrations and a more effective method of keeping the test equipment in calibration, the number of rejections for these reasons was drastically reduced.

**Phase-sensitive demodulators**—Considerable trouble was experienced throughout the program with the phase-sensitive demodulators used for conditioning the gyro signals for adaptation to telemetry. The initial units developed were extremely sensitive to a temperature environment above 120°F, and high rejection and failure rates resulted. A new and improved unit was capable of operating in temperatures up to 185°F. However, a few critical components in these units caused more than a normal number of failures. The critical areas of the demodulator were redesigned, replacing critical components with those of higher temperature rating and paralleling some diodes to reduce the current flow in critical areas. These changes considerably reduced the number of failures, and a reliable unit was the end result.

**Antenna ionization**—Ionization breakdown of the PWM/FM antenna was experienced in the earlier vehicles. The antennas were relocated away from the second-stage roll jets to reduce propane gas exhaust effect. The teflon insert was also redesigned to increase breakdown distance.

## L. SYSTEM AND PAYLOAD INTEGRATION

Physical integration of the various systems into the complete Vanguard vehicles (space provisions, elimination of interferences, etc.) was the specific responsibility of an Integration Group within The Martin Company. Functional integration of the individual systems

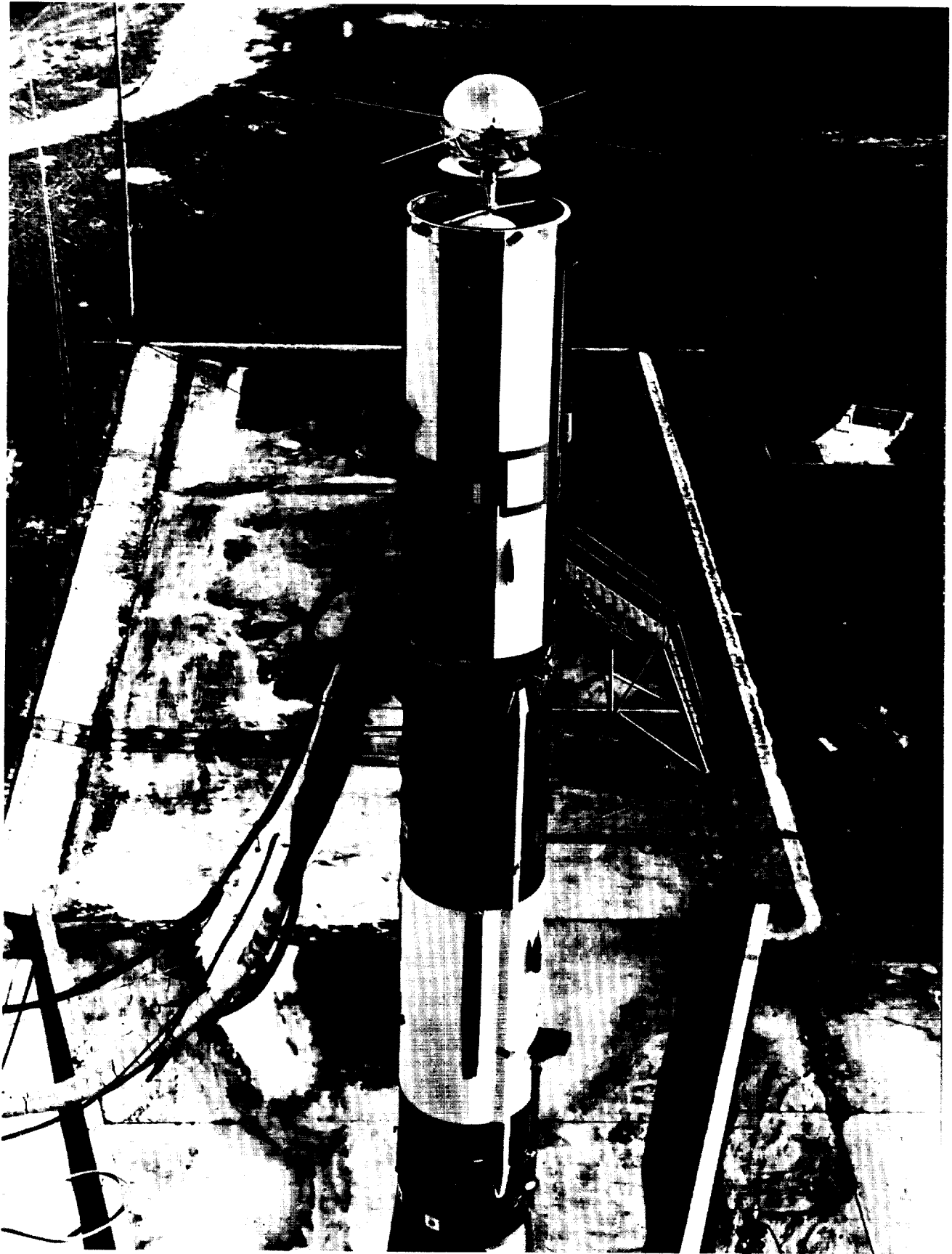


Fig. 35 SLV-4 Satellite

was accomplished by the closely knit nature of the Vanguard Project organization, whereby each group was responsible for the correct functioning of its hardware in the integrated vehicle. This overlapping of responsibility provided double checks of integration problems in the important areas, and contributed greatly to the success of the Vanguard.

Design of the satellite payloads was accomplished by the Naval Research Laboratory (and, later, by NASA), with the single exception of the early vehicle performance inputs by The Martin Company which established the sphere diameter. A shaft was provided at the nose of the third-stage motor, upon which was mounted a low-friction bearing for attaching the centering spider arms (see Chapter IV, Section H). The Government-furnished satellites (including the

mechanism for separation from the third stage after burnout) were mounted atop this bearing. Some of the satellites were provided with a dish-shaped heat shield (shown in Fig. 35) to protect the payload from heat radiated by the hot third-stage motor case at or near the time of burnout, and from the exhaust products of the spin motors during separation.

Space provisions were made within the nose cone for the retracted satellite antennas. A ground-supplied cooling air system was provided for the payload compartment, to ensure that satellite outer shell temperature would never exceed 30°C prior to launch. Liaison was maintained with the satellite designers at NRL and NASA, to ensure the resolution of mutual problems (e.g., satellite spin rates after separation).

## V. RELIABILITY

### A. REQUIREMENT

Budgetary and schedule restrictions dictated the scope of the Vanguard reliability program. The philosophy is best described in the wording of the Design Specification (Ref. 3, paragraph 3.1.10):

**“Reliability**—The vehicle shall be designed and components selected on the basis of available reliability data to ensure reliability consistent with the state of the art. Reliability studies and statistical testing to establish such data shall not be required.”

### B. ENVIRONMENTAL CRITERIA

An environmental study was undertaken during the early stages of the system design to define the anticipated environmental climate for the Vanguard vehicles. The primary sources for this study were data from Viking and Redstone missile flights and Specification MIL-E-5272A. Information on the spectrum of the engine forcing functions was gathered from the engine manufacturers, based on preliminary test firings. The initial results of the study were used as a basis for component and system selection. Modifications were continually made to these criteria as the program progressed and as additional information became available from analytical, experimental or flight data. Figure 36 presents a summary of the end result of this refining process.

### C. COMPONENT AND SYSTEM QUALIFICATION

Qualification tests were performed on all new components and systems of the vehicle to demonstrate their compliance with applicable specifications. Where off-the-shelf hardware was used, previous qualification data were accepted insofar as they were compatible with Vanguard requirements and criteria.

**First-stage engine package**—Extensive qualification tests were made by the manufacturer on individual components of the X-405 engine. Among the more important results were:

- (1) A prototype thrust chamber, injector and motor body successfully completed 14 consecutive firings using a pressure-fed system. Total accrued burning time on this particular thrust chamber was 2100 seconds.
- (2) A prototype turbopump successfully completed 15 hot runs for a total accumulated time of 2250 seconds.

- (3) A prototype hydrogen peroxide decomposer completed 50 runs for a total operating time of 7500 seconds.

The engine was qualified as a system in accordance with an approved General Electric specification, Ref. 27, by successfully completing eight consecutive static firings for a total accrued burning time of 900 seconds. One firing was preceded by a three-hour “cold hold” with all propellants loaded. Engine gimbaling was satisfactorily demonstrated during two of the firings. Two oxidizer and three fuel exhaustion shutdowns were accomplished in this series, and satisfactory performance was demonstrated with  $\pm 5\%$  variation of liquid oxygen flow. Performance and repeatability within specification limits were conclusively demonstrated by these tests. No hardware damage occurred, nor were there any component failures or replacements during the qualification program. The qualification engine later successfully completed a 200-second firing after 8 hours “cold hold” with all propellants loaded.

**First-stage propellant feed and pressurization system**—An operational mockup of the complete first-stage propulsion system, less the engine package, was subjected to qualification tests (Ref. 28). The planned program was not fully completed because the mockup was damaged due to a malfunctioning pressure regulator. However, adequate information was obtained to functionally check out the system and verify the production test specifications, the helium roll thrust augmentation system, the method for adjusting the main helium regulator, and the proper LOX filling technique.

Structural integrity of the individual tanks (LOX, fuel and hydrogen peroxide) was verified by proof and burst pressure tests on prototypes. The structural integrity of the vendor-supplied helium spheres was verified by pressure cycling, proof pressure testing, and burst testing prototype vessels. All fuel lines and high pressure plumbing were proof pressure tested. Verification that the LOX tank forward dome could withstand actual external temperatures and pressures during first-stage separation was demonstrated by LOX dome impingement tests at Aerojet (Ref. 29).

The scope of the qualification tests of all vendor components used in the propellant feed and pressurization system is presented as a part of Table 11.

**Second-stage propulsion system**—Although complete qualification testing was not performed on each component, functions were tested under anticipated critical environments (see Table 11). In addition,

**Table 11. Propulsion Component Environmental Test Program — Vendor Supplied**

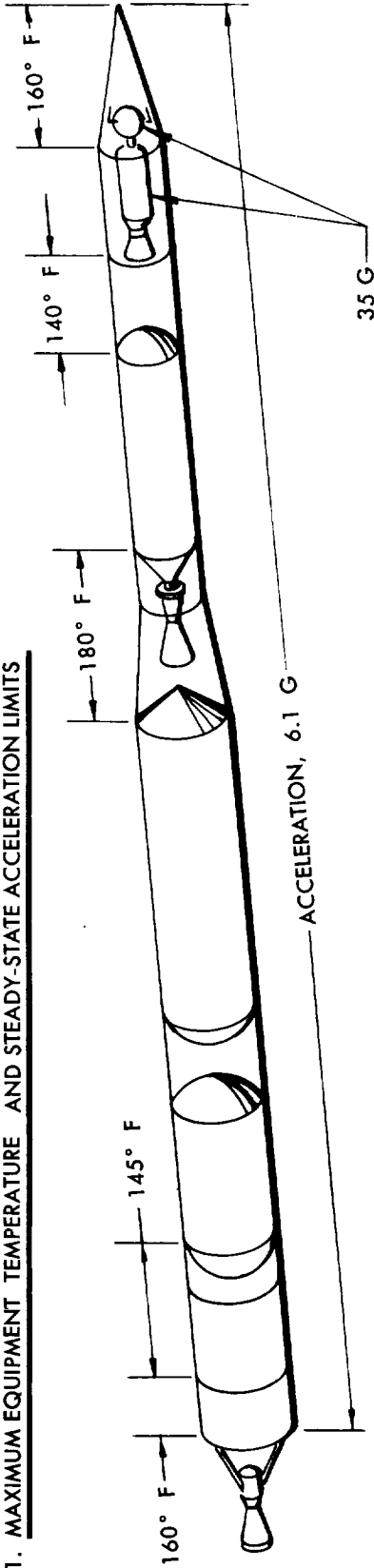
	High Temp	Low Temp	Humidity	Altitude	Vibration	Shock	Acceleration	Salt Spray	Sand and Dust
<i>A. First Stage</i>									
Solenoid Pilot Valve (LOX, fuel)	V	V	V	V	V	V	V	V	V
Helium Sphere	X	X	X	X	X	X	O	O	O
Vent Valve (fuel)	V	V	V	V	V	V	V	V	V
Plug Valve (H <sub>2</sub> O <sub>2</sub> ) Linden Tool	X	X	X	X	X	X	X	O	O
X-405 Rocket Engine	Qualified per GE Qualification Test Spec DR-E-586-d								
Exhaust Pipe Insulation Blanket	V	O	O	V	O	O	O	O	O
LOX Dome Insulation Blanket	O	V	V	O	V	V	V	V	O
Pressure Sensor	V	V	V	V	V	V	V	V	V
Pressure Sensor	V	V	V	V	V	V	V	V	V
Pressure Sensor	V	V	V	V	V	V	V	V	V
Helium Sphere Strap Assy	O	O	O	O	O	O	O	O	O
Coupling V-Band	O	O	O	O	O	O	O	O	O
Bellows (steam)	V	V	V	O	V	V	V	V	V
Bellows (fuel)	V	V	V	O	V	V	V	V	V
Bellows (LOX)	V	V	V	O	V	V	V	V	V
Disconnect (N <sub>2</sub> )	V	V	V	O	V	O	V	V	O
Disconnect (He)	V	V	V	O	V	O	V	V	O
Disconnect (fuel)	V	V	V	O	V	O	V	V	O
Valve—3-Way (He)	O	O	O	O	O	O	O	O	O
Valve—Check (He)	V	V	O	O	V	V	V	V	O
Valve—Check	V	V	O	O	V	V	V	V	O
Valve—Solenoid	V	V	V	V	V	V	V	V	V
Valve—Solenoid Progressive Research	X	X	X	X	X	X	X	X	X
Relief Valve (H <sub>2</sub> O <sub>2</sub> )	V	V	V	V	V	V	V	V	V
Pressure Regulator (He)	V	V	V	V	V	V	V	V	V
Solenoid Valve	V	V	V	V	V	V	V	V	V
Vent Valve (LOX)	V	V	V	V	V	V	V	V	V
<i>B. Second Stage</i>									
Propane Disconnect	V	V	V	O	V	O	V	V	O
Propane Bleed Valve	O	O	O	O	O	O	O	O	O
Roll Jet Solenoid Valve	V	V	V	V	V	V	V	V	V
Tumble Jet Solenoid Valve	V	V	V	V	V	V	V	V	V
3-Way Helium/Propane Solenoid Valve	V	V	V	V	V	V	V	V	V
Propane Relief Valve	V	V	V	V	V	V	V	V	V
Helium/Propane Regulator	V	V	V	V	V	V	V	V	V
Propane Heater Blanket	O	O	O	O	O	O	O	O	O
Helium Pressure Regulator (RV)	V	V	—	V	V	V	O	V	V
Heat Generator (HGA)	V	V	V	O	O	O	O	O	O
Position Switch (TVS <sub>1</sub> , TVS <sub>2</sub> )	V	V	O	V	V	O	V	V	V
Pressure Switch (TPS, HPS <sub>2</sub> )	V	V	O	V	V	—	O	V	O
Oxidizer Valve (OTCV)	V	V	O	O	O	O	O	V	V
Oxidizer Pilot Valve (OTCPV)	V	V	O	V	V	O	O	V	V
Fuel Valve (FTCV)	V	V	O	O	O	O	O	V	V
Fuel Pilot Valve (FTCPV)	V	V	O	V	V	O	O	V	V
Helium Bypass Valve (BHSV)	V	V	O	V	V	O	O	V	V
Electrical Sequence Unit	V	V	O	V	V	O	O	V	V
Helium Disconnect	V	V	V	O	V	O	O	V	O

V = Vendor tested.

O = Requirement satisfied by design criteria.

X = Not required.

# 1. MAXIMUM EQUIPMENT TEMPERATURE AND STEADY-STATE ACCELERATION LIMITS



## 2. RELATIVE HUMIDITY: 100 %

## 3. ALTITUDE (UNPRESSURIZED EQUIPMENT)

ELECTRICAL EQUIPMENT 30 IN. TO 0.040 IN. HG AT TEMPERATURE OF 120° F AND RELATIVE HUMIDITY OF 95 %

ALL EQUIPMENT EXCEPT ELECTRICAL 30 IN. TO 0.51 IN. HG

## 4. VIBRATION

### SINUSOIDAL:

TEST LEVEL	FREQUENCY RANGE (CPS)	VECTOR ACCELERATION *	TIME SPAN
1.5 $\sigma$	10 TO 2000	0.030 IN. DA TO 12 G	20 TO 30 MIN
2.5 $\sigma$	10 TO 2000	0.050 IN. DA TO 10 G	4.5 TO 6.7 MIN
3 $\sigma$	10 TO 2000	0.060 IN. DA TO 12 G	7.5 SEC TO 2 MIN

\* DA = DOUBLE AMPLITUDE

### RANDOM:

10 TO 2000 CPS, 0.2 G<sup>2</sup>/CPS FOR 3 MIN

## 5. SHOCK (BASED ON 2 SHOCKS)

SECOND-STAGE EQUIPMENT COMPARTMENT AND NOSE CONE (TV-3 AND UP)  
15 G FOR 1 M SEC

FIRST-STAGE ENGINE COMPARTMENT AND TAIL CAN  
20 G FOR 11 M SEC

ALL OTHER VEHICLE LOCATIONS  
15 G FOR 5 M SEC

NOTE: ENVIRONMENTAL PARAMETERS SUCH AS SAND AND DUST, FUNGUS, RAIN, IMMERSION, SALT SPRAY, ETC., WERE SATISFIED IN MOST CASES BY DESIGN CRITERIA; IN THOSE AREAS WHERE TESTING WAS REQUIRED, THE PROCEDURES DIRECTED BY MIL-E-5272A WERE UTILIZED.

Fig. 36 Summary of General Environmental Criteria

functional tests were conducted on mockups of various subsystems. Extensive structural testing and corrosion testing were accomplished on complete tankages and tankage sections (see Chapter III, Section F).

The thrust chamber was qualified as a component by accumulating a total of 738 seconds of firing time on a single thrust chamber, utilizing a tungsten-carbide coating on the inner wall. A total of 13 runs of various durations from 10 to 118 seconds was made under conditions of high and low mixture ratio, high and low chamber pressure, and high and low temperature soak prior to firing. The thrust chamber coolant jacket began to leak because of tube erosion failures after about 280 seconds of accumulated firing time, and patching was required before each of the subsequent runs.

Qualification of the complete propulsion system was required by an approved Aerojet specification, Ref. 30. Four attempts to qualify the system for 540 seconds, using prototype hardware, ended in failure after 352, 173, 305 and 271 seconds, due to three cases of thrust chamber erosion and one of tank failure due to stress corrosion (see Chapter IV, Section C). Use of the tungsten-carbide chamber coating and the associated patching technique, together with a new tankage tempering temperature, permitted satisfactory completion of the system qualification test. A total of 567 seconds was accumulated on a single thrust chamber and tankage during eight runs, including three for full duration. Thrust chamber patching was used after 549 seconds.

Although the system qualification test was considered acceptable, it was not entirely trouble-free. There were isolated instances of failure of the regulator to trip, clogging of the oxidizer filter screens, and leaky fuel and oxidizer tank check valves. In retrospect, it is apparent that some "scrubbed" field operations and

flight failures were foreshadowed during the second-stage qualification tests. These problems were not ignored—field procedures were developed and modified to guard against such malfunctions. Operational experience indicated, however, that complete reliability requires correction of observed deficiencies by design rather than by procedural changes.

**Third stage**—The qualification program for the Grand Central 33-KS-2800 included tests of 32 motors (see Table 12). Thirty motors were individually tested for certain environmental conditions and then fired successfully to observe the effects of the environment on motor performance. Two motors incurred nozzle damage as a result of sequential salt spray, humidity and rain tests, and were not fired. In order to preclude such failures on delivered motors, all nozzles were packed in hermetically sealed containers with desiccant for shipment and storage.

The qualification test program of the Allegany Ballistics Laboratory X248 consisted of the firing of 14 motors which had been subjected to sequential environmental tests in such a manner as to ensure that several motors would be tested at each condition (Table 13).

Aging tests were also conducted on both GCR and ABL motors. As of this writing, a storage life has been demonstrated for the GCR motor of at least 24 months, and for the ABL motor of at least 8 months.

**Spin and retro motors**—The spin and retro motors (Atlantic Research 1-XS-50 rockets) successfully passed qualification tests (Table 14) including reproducibility of performance, vacuum ignition, and environmental tests in accordance with Ref. 24. Retro motor aerodynamic fairing ejection tests were also made.

**Table 12. GCR 33-KS-2800 Qualification Test Program**

TEST	NUMBER OF MOTORS TESTED
Thrust Alignment	All motors with altitude nozzles
Statistical Performance	12
Temperature Cycling	6
Acceleration	2 + 4 motors from temperature cycle tests for total of 6
Altitude Ignition	6
Rough Handling and Drop	2
Truck Shipment	2
Rain, Humidity and Salt Spray	2

Total motors tested = 32

**NOTE:**

*One additional empty case was static tested to destruction.*

**Ordnance**—Ordnance components such as explosive latches, bolts and primacord were certified by the manufacturer as qualified to the manufacturer's specification. Certain ordnance components had to be subjected to additional tests to qualify for the Vanguard environment. Some components were ignited under vacuum conditions of about  $3 \times 10^{-4}$  millimeters of mercury; other samples were ignited after exposure to liquid nitrogen at about  $-300^{\circ}\text{F}$ .

**Guidance, control, hydraulic and mechanical systems**—The principal environmental qualification

tests performed on these systems and their components are shown in Table 15. Certain environmental requirements were satisfied by design criteria; for example, the controls can, a sealed pressurized container, did not require any formal humidity or altitude tests. Additional qualification tests, such as the controls cooling air test, and a complete description of the tests shown in Table 15, may be found in Ref. 14.

**Electrical system**—Standard electrical units that had already been qualified to Government procurement specifications were used throughout the Vanguard ve-

**Table 13. ABL X248A2 Qualification Test Program**

QUALIFICATION MOTOR NO.	1	2	3	4	5	6	7	8	9	10	11	12	13	14
1. Hydrotest	X	X	X	X	X	X	X	X	X	X	X	X	X	X
2. Pressure Test	X	X	X	X	X	X	X	X	X	X	X	X		
3. Dynamic Balance	X	X	X	X	X	X					X	X	X	X
4. Thrust Alignment	X	X	X	X	X	X					X	X	X	X
5. Rotational Acceleration	X	X	X	X	X	X					X	X	X	X
6. Humidity Test	X													
7. Rainfall Test		X												
8. Salt Spray Test			X											
9. Thermal Cycle	X	X	X	X										
10. Vacuum Fire	X		X	X										
11. Lateral Acceleration					X	X					X			
12. Rebalance and Alignment											X			
13. Longitudinal Acceleration and Centrifuge Fire					X	X								
14. Longitudinal Spin-Fire											X	X		
15. 250° F Soak Test									X					
16. Storage Evaluation													X	X

**Table 14. ARC 1-XS-50 Spin and Retro Motor Qualification Test Program**

Thrust Alignment	All
Statistical Firing	12
Statistical Firing with Sea Level Nozzles	13
Thermal Cycling (high to low)	3
Thermal Cycling (low to high)	3
Pressure Test and Altitude Ignition	7
Vibration and Shock	6
Drop Test (one each at 130°F, 70°F, 0°F)	3
Rain	2
Humidity	2
Salt Spray	2
Acceleration, 7g Longitudinal (one each at 130°F, 70°F, 0°F)	3
Acceleration, 2g Transverse (one each at 130°F, 70°F, 0°F)	3
Acceleration, 20 rad/sec <sup>2</sup> Rotational at 70°F	2
Nozzle Seal Modification	8
Static Fired at 130°F	23
Static Fired at 70°F	29
Static Fired at 20°F	10

Total Motors in Test Program

131

hicle, with the exception of timers and flight batteries. All standard units and the timer were subjected to additional tests (see Table 15) to satisfy Vanguard requirements. Extensive testing was performed on the flight battery, which was built specifically for Vanguard requirements.

**Instrumentation**—All new components developed for the Vanguard were thoroughly tested and qualified to the expected environmental conditions. All other instrumentation components were either tested or certified on a similarity basis before use in the program.

**Table 15. Guidance and Control Components — Environmental Test Program**

	Vibration		Shock	Acceleration	High Temperature	Low Temperature	Altitude	Humidity
	Sinusoidal	Random						
1. Guidance System								
Gyroscope Assembly	V		M	O	V	V	O	V
Coasting Time Computer	V		M	V	MV	MV	O	O
Program Timer	MV	M	MV	MV	MV	MV	O	O
2. Control System								
Pitch-Yaw Amplifier	M	M	M	M	M	M	O	O
Roll Amplifier	M	M	M	M	M	M	O	O
Slave Relay Chassis	M	M	M	M	M	M	O	O
Auxiliary Chassis	M	M	M	M	M	M	O	O
Regulated B+ Supply		M	M	M	M	M	O	O
3. First-Stage Hydraulic								
Servo Package	M		M	O	M	M	M	O
Pump	V		V	V	MV	MV	MV	V
Reservoir	M		M	O	M	M	M	O
Relief Valve	MV		MV	V	MV	MV	MV	V
Accumulator		M	O	O	MV	MV	M	O
Filter		M	O	O	V	V	O	O
4. Second-Stage Hydraulic								
Servo Package	M		M	O	M	M	M	O
Pump	V	M	V	V	MV	MV	MV	V
Reservoir	M	M	M	O	M	M	M	O
Relief Valve	MV	M	MV	O	MV	MV	MV	O
Accumulator		M	O	O	MV	MV	M	O
Filter		M	O	O	V	V	O	O
5. Mechanical								
Roll Jets		M	O	O	M	O	O	M
Roll Jet Pneumatic Valve	V		V	V	V	V	V	V
6. Electrical								
50-amp SPST Power Contactor	M		M	V	V	V	V	V
4PDT Latching Relay	M		V	V	V	V	V	V
2PDT Relay	V		V	V	V	V	V	V
4PDT Relay	M	M	M	M	M	M	V	V
5- to 195-sec Adjustable Timer	V		V	V	V	V	V	V
Time Delay Relay (1 sec and 1.5 sec)	V		V	V	V	V	V	V
6PDT Relay	V	M	V	V	V	V	V	V
20 A-H Flight Battery	M		M	M	M	M	M	M
250 VA Rotary Inverter	M		V	V	M	V	M	M
2PDT Liftoff Switches	M		V	M	V	V	V	M
7. Range Safety								
C-Band Beacon Antenna	M		M		M	O	O	O
Command Control Antenna	M		M		M	O	O	O
Telemetry Antenna	M		M		M	O	O	O

M—Martin tested

V—Vendor tested

O—Requirement satisfied by design criteria

## D. COMPONENT AND SYSTEM ACCEPTANCE TESTING

Acceptance tests were performed on the major Vanguard components and systems to ensure that flight hardware measured up to the standards of the qualification test articles.

**First-stage propulsion**—Each production engine package was acceptance tested in accordance with an approved General Electric specification (Ref. 31). Acceptance was based upon successful completion of two consecutive 150-second static firings, without component malfunction or change. Repeatability of performance within applicable specifications and accurate orientation of the thrust vector were also required.

The complete propulsion system was functionally checked after assembly of the engine package with its tankage, propellant feed and pressurization systems. These checks included leakage, electrical and pneumatic functional tests of each component. The first-stage static firing in the field (see Chapter VI, Section B) really constituted final acceptance of this system for flight.

**Second-stage propulsion**—All components were acceptance tested to Aerojet specifications prior to installation on a production unit. Each complete Aerojet system was subjected to a 60-second static firing to demonstrate proper functioning of all components and adequate system performance, in accordance with an approved Aerojet specification (Ref. 32). The system was decontaminated and inspected after the acceptance test firing.

Following assembly of this system with acceptance-tested Martin components into a vehicle second stage, the entire system was functionally checked for leakage, electrical continuity and component operation during a simulated flight sequence. Provisions were available for static firing of the second stage in the field, but were used only on TV-3, TV-3BU and SLV-3 (see Chapter VI, Section B).

**Third-stage propulsion and ordnance**—This type of component does not readily lend itself to a functional type of acceptance test. For small ordnance items such as detonators and squibs, which were delivered in relatively large lots and certified by the manufacturer, samples of each lot were fired under simulated vacuum conditions (approximately  $10^{-4}$  mm Hg) to determine acceptability of the lot.

Third-stage motor acceptance was based upon the documentation of rigid quality control during manufacture, firing of samples from each batch of propellant mixed, and visual inspection, weighing and measuring each motor after final assembly. The measurements made consisted of checking critical dimensions, geometric determination of the thrust axis alignment

and dynamic balancing of the motors about the spin axis in a specially designed fixture.

**Guidance and control, electrical and hydraulic**—Acceptance tests were performed on all guidance and control system components prior to installation in the vehicle. All important performance parameters of the gyroscope reference system, coasting time computer and program timer were checked by the vendor prior to shipment to Martin. The electronic autopilot units, such as the pitch amplifier, etc., were thoroughly bench tested after fabrication. Some of the more important performance characteristics checked on all units as a prerequisite to acceptance were:

- (1) Gyroscope reference system—drift under vibration, cross-coupling, reaction torques, mass unbalance, pitch program and transfer functions.
- (2) Coasting time computer—coasting time accuracy for various velocities and velocity potentiometer telemetering accuracy.
- (3) Program timer—timing accuracy checks, load tests and effects of vibration.\*
- (4) Pitch/yaw and roll amplifiers—frequency response, linearity, gain, jet deadspot and jet hysteresis.
- (5) Controls can—frequency response, gains, linearity, jet deadspot, jet hysteresis, remote centering, pitch program rate resistance and effects of vibration on the complete assembly.
- (6) Inverters (Leland 250-VA)—voltage modulation.
- (7) Hydraulic actuators—leakage, piston stroke, evidence of binding or chattering and frequency response.

\* A special reliability program was started in July 1958, to increase program timer reliability and decrease the number of failures in ground checkouts, due mainly to relay malfunctions. The reliability program consisted of performing the following additional tests during the program timer acceptance test: relay load test; vibration of 15 minutes in each plane at qualification specification levels; time check; and five additional relay load tests.

## E. VEHICLE ACCEPTANCE TESTING

The primary goal throughout fabrication and assembly was the delivery of a vehicle that was ready for flight. Voluminous test specifications were prepared to formalize the procedures. Testing was designed to confirm integrity with a minimum of aging. Sub-components were tested prior to assembly wherever practical, to maximize the possibility of a successful system checkout. Backup and alternate systems were also checked, but not necessarily in the simulated flight sequence.

Acceptance testing of the completed vehicles was accomplished in both horizontal (stages physically separated) and vertical (vehicle erected) positions. The factory and field test equipment and procedures were identical, insofar as possible, to maintain personnel familiarity (many on the field crew had helped fabricate and test the initial vehicles at the factory), to help correct procedure inconsistencies and to pinpoint troublesome areas. Much of the extensive checkout equipment was supplied by the Polarad Electronic Corporation.

**Horizontal tests**—The horizontal phase of factory acceptance testing began with checks on each individual system in each stage. The stages were then electrically mated and further tested as a unit. These “marriage” tests included checks of the power adjustment and polarity, gyro linearity, drift and noise, jet deadspot, time delay and phase angle, control system frequency response, program timer, coasting time computer and command control system.

**Vertical tests**—Upon satisfactory completion of all horizontal tests, the vehicle was erected and aligned in the vertical test fixture (Fig. 37), which was specially built to accomplish these tests. Individual system acceptance tests were made, and operation of the spin table and satellite bearing were checked, using a dummy third-stage motor. The final Vertical Interference Test checked out the integrity of the entire rocket system, including sequencing functions and the electrical, guidance, control and range safety systems. The rocket was then disassembled, final propulsion-pneumatic and general checks and cleanups were made and a final wiring inspection was conducted. The vehicle was painted, weighed, packed and shipped on a special trailer to Cape Canaveral.

**Second-stage rejuvenation**—The second stages of the SLV-4, SLV-5, SLV-6 and TV-4BU vehicles were not sent directly to the field, but were air-lifted to Aerojet-General for rejuvenation to ensure clean, flight-ready systems. Rejuvenation consisted of forward and back-flushing the thrust chamber, water-flow testing the thrust chamber using laboratory instrumentation, disassembly, cleaning, replacement of seals, reassembly and acceptance testing of all components.

After rejuvenation, SLV-4 and SLV-5 were static fired, and SLV-6 and TV-4BU were expulsion tested, using WIFNA in the oxidizer system and water in the fuel system. The primary purpose of these static firings or expulsion tests was to demonstrate satisfactory operation of the oxidizer probe shutdown system. The tests also served as functional checks of the pressurization and propellant feed systems, although the subsequent disassembly for decontamination more or less invalidated the systems check here as well as after

static firing in the field. The static firing contributed system pressure and flow data, but the expulsion test data were not applicable because special engine orificing was used to simulate combustion chamber pressure.

## F. RELIABILITY FOLLOW-UP

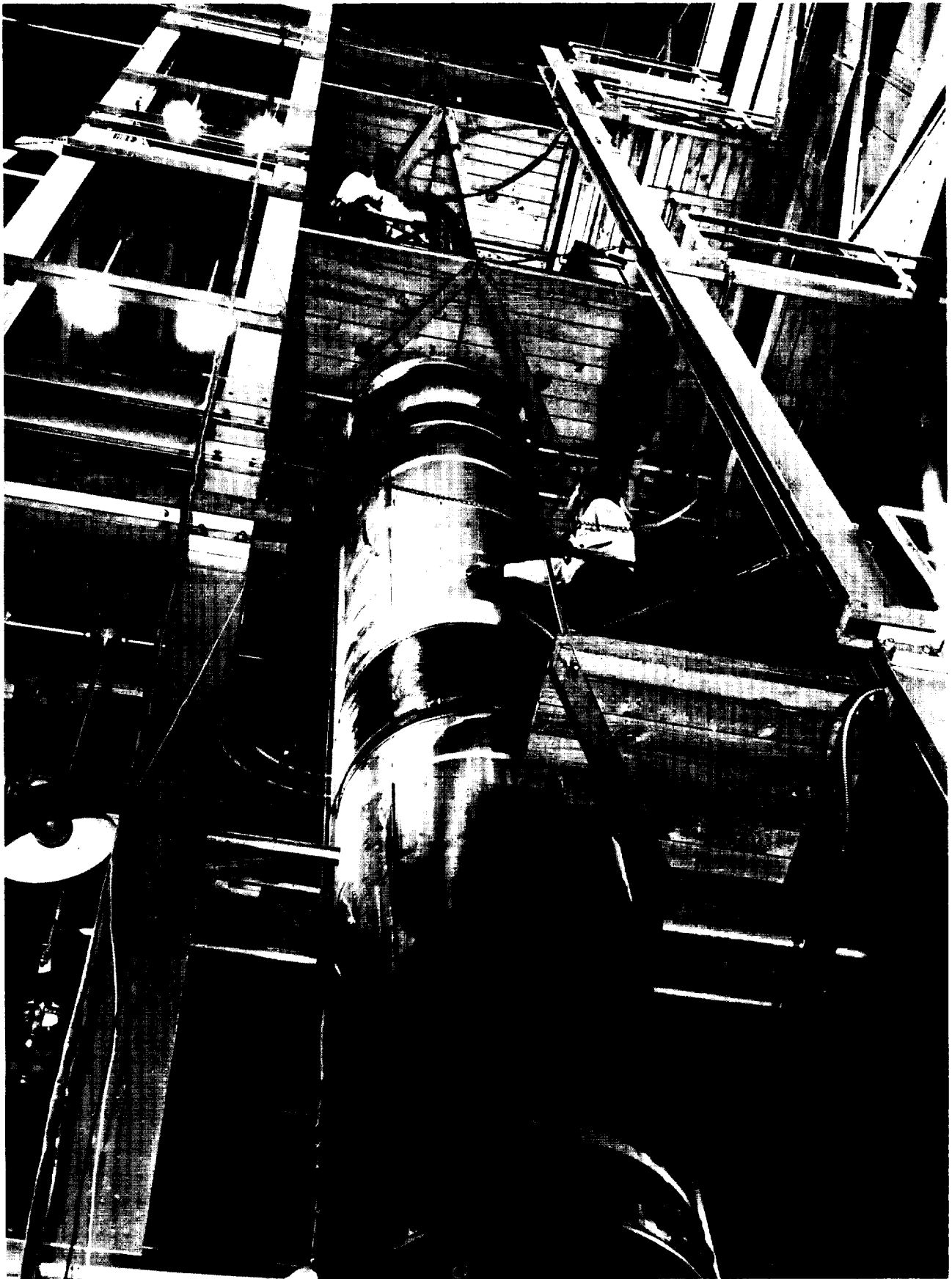
Close liaison was maintained for correcting hardware discrepancies. Each design group responsible for a Vanguard subsystem was in daily communication with its field counterpart by telephone and via direct teletype (TWX). Problem areas and corrective measures taken were documented by the latter means.

The more formal channel for liaison and reliability follow-up was the “Discrepancy and Trouble Report” system, which was used to record discrepancies, malfunctions and potential problem areas. Copies of these forms were screened for problems requiring immediate action. A Corrective Action Team, consisting of members from engineering, manufacturing, quality and procurement, met periodically to review each discrepancy report and initiate or verify corrective action. (In the majority of cases, the less formal channels described above had already resolved the problem, but the team action constituted a final follow-up.)

There were three instances during the Vanguard program of extraordinary effort in the area of reliability follow-up; these are described below.

**TV-3BU**—Following the flight failure of TV-3BU (February 1958), which was attributed to a spurious electrical signal in the control system, an intensive effort was made to strengthen quality control of the remaining vehicles, with emphasis on electrical wiring. Additional personnel were assigned to quality control supervision and to the origination and follow-up of Service Trouble Reports (forerunners of the Discrepancy and Trouble Report mentioned above). Access to vehicles and vehicle compartments in the factory and hangar areas was restricted. Tool procedures and process handbooks were emphasized. The system of solder certification was revised to more rigid skill requirements and personnel were recertified. Special checks were instituted for problem areas. An independent Martin inspection team, including engineering personnel, reviewed the wiring integrity of each subsequent vehicle prior to acceptance. The next vehicle, TV-4, produced the first Vanguard satellite orbit in March 1958.

**Goett committee**—Late in 1958, the National Aeronautics and Space Administration assumed responsibility for the Vanguard program. Although the next vehicle (SLV-4) was ready on the launching stand, operations were suspended while a comprehensive review of the entire program was conducted. An



**Fig. 37 Vertical Test Tower**

eleven-man committee of independent rocket experts, headed by Mr. Harry Goett, of NASA, found that there were no major deficiencies in the rocket design, but made valuable suggestions for improvements in vehicle reliability. SLV-4 produced the second Vanguard satellite orbit in February 1959.

**SLV-6**—Following the malfunction of the second-stage helium regulator in SLV-6 (June 1959), a new operational approach was taken, involving total quality assurance control of the rocket areas and access to the rocket, as well as more rigid control over testing of flight components and spares. This system was instituted with receiving inspection of the rocket in the hangar area. Vertical testing, change work and access into and about the complex were subject to the same safeguards, plus inspector surveillance of the work done in each accessible area of the rocket. Although a certain amount of operational difficulty was introduced, the results associated with this concept of "100% inspection" were considered worthwhile, in that higher confidence existed in the rocket's readiness for flight than on any previous operation. The next vehicle, TV-4BU, produced the third Vanguard satellite orbit in September 1959.

The extent to which the three completely successful Vanguard satellite launchings were influenced or made possible by the extra reliability follow-up activity described above is a matter of opinion. It is evident, however, that intensive reliability follow-up is a factor that cannot be ignored in a program of this kind.

## **G. OBSERVATIONS ON RELIABILITY**

The reliability program laid down for Vanguard was the maximum effort compatible with the overriding considerations of cost and schedule, and included the following essential elements of today's more formal reliability programs.

- (1) Application of realistic engineering criteria in the selection of components and systems.
- (2) Establishment of an environmental description early in the design phase of the program.
- (3) Revision of the environmental description to reflect test and flight experience.
- (4) Qualification of hardware consistent with the environmental criteria.
- (5) Repeated testing to demonstrate hardware capability.
- (6) Corrective action and follow-up control to resolve hardware discrepancies uncovered by equipment usage.

The principles were sound, though their application was limited. This program was adhered to, not without human errors, but to the fullest extent consistent with the project's environment. It is a matter of record that the original Vanguard overall reliability goal of at least one orbit in six attempts was more than achieved. The final tally was three orbits in eleven attempts, including one for seven in the originally specified time span of the IGY. Following the two-month suspension of launching activities late in 1958, the remaining four vehicles produced two satellite orbits.

## VI. FIELD OPERATIONS

### A. LAUNCH COMPLEX

Vanguard vehicles were launched from Complex 18A at the Atlantic Missile Range (AMR), Cape Canaveral, Florida. The basic site (Figs. 38 and 39) consisted of a concrete main equipment house, a movable gantry, a working platform with launch stand and an umbilical tower. The working platform incorporated a 90-degree flame deflector tube that was cooled during a firing by a water flow of about 3,000 gallons per minute. An auxiliary equipment house, located about a hundred feet from the stand, was used to house the first-stage firing control and several cooling air units (i.e., compressor, heat exchanger, dehumidifier, etc.). Adjacent to the area was the concrete blockhouse, which protected personnel during firings and was the center of all remote control operations. The blockhouse was connected to the launch stand and the equipment houses by an underground trench which carried wiring and plumbing necessary to remotely test and launch the vehicle. A LOX storage facility, consisting of two large Dewar tanks, with a pressurized vehicle servicing system, was located behind the main equipment house. A photograph of the vehicle mounted on the launch stand is shown in Fig. 40.

#### 1. GROUND SERVICING SYSTEMS

Ground servicing systems were installed on the complex to supply and service the Vanguard with propellants, pressurization and purging, and to provide temperature conditioning and fire prevention or extinguishing capabilities. Remotely operated systems accomplished the filling, topping, draining and dumping of LOX and supplied ethane gas for first-stage engine starting. Hydrogen peroxide and kerosene were supplied from trucks. A helium system was connected to the vehicle for pressurizing the first- and second-stage helium spheres, and also provided pressure to operate various ground servicing LOX, kerosene and CO<sub>2</sub> control valves. A nitrogen system was installed for purging the first- and second-stage engine tanks, first-stage thrust chamber, tail can and peroxide compartments. Nitrogen was also used to actuate various ground servicing helium, LOX and ethane control valves, the LOX disconnect ground unit, and the second-stage helium umbilical disconnect. Other second-stage, gantry-mounted systems included a UDMH fill and drain, a WIFNA fill, drain and emergency dump and a tank flushing water system. Liquid propane filling was accomplished manually. A cooling air system was installed to provide dehumidified, tem-

perature-controlled air to the satellite and the guidance and controls units.

**Fire fighting systems**—The CO<sub>2</sub> system served two functions: first, as a fire prevention, by being expelled into the first-stage tailcan area immediately after shutdown of a static firing; and second, as an extinguisher in the same area if required during static or launch countdown. A water fire extinguisher system, with fixed position nozzles, was mounted on top of the working platform for extinguishing fires at the base of the vehicle in the platform area. The UNOX fire extinguishing system (NRL supplied) had rotating swivel nozzles mounted on poles at diagonal corners of the concrete pad for extinguishing fires anywhere in the pad area, including the working platform.

**LOX disconnect ground unit**—The entire operation of LOX filling, topping, draining and dumping was accomplished through a single disconnect, mounted to the launch stand, which mated with the vehicle fill unit. A microswitch attached to the ground half of the disconnect was in physical contact with the shut-off valve in the vehicle. Thus, a positive indication of the valve position was electrically signaled to the blockhouse to ensure that the vehicle LOX valve was closed before takeoff. A valve in the ground half of the disconnect permitted precooling and dumping.

#### 2. GROUND SUPPORT EQUIPMENT

Specialized ground support equipment was required at the Vanguard complex to support static and flight firings and to permit extensive vehicle testing. The more significant of these equipments are described below.

**Vehicle handling**—Dollies were provided for transporting vehicle stages. They were constructed to have minimum deflection, permitting the use of casted wheels for maximum maneuverability. Hoist slings employed for the erection of vehicle stages allowed the stages to be rotated between the horizontal and vertical positions. The third-stage motor sling was made of nonsparking webbing material to ensure maximum safety. Hoist doors (specially designed replacements for the large structural doors of the equipment compartment) were used with the second stage to maintain structural integrity during erection. Snubbers secured the vehicle to the gantry during high wind conditions. Gantry shielding was added to protect both vehicle and personnel from abnormal weather conditions. A Greer unit supplied hydraulic pressure for launch stand operations.

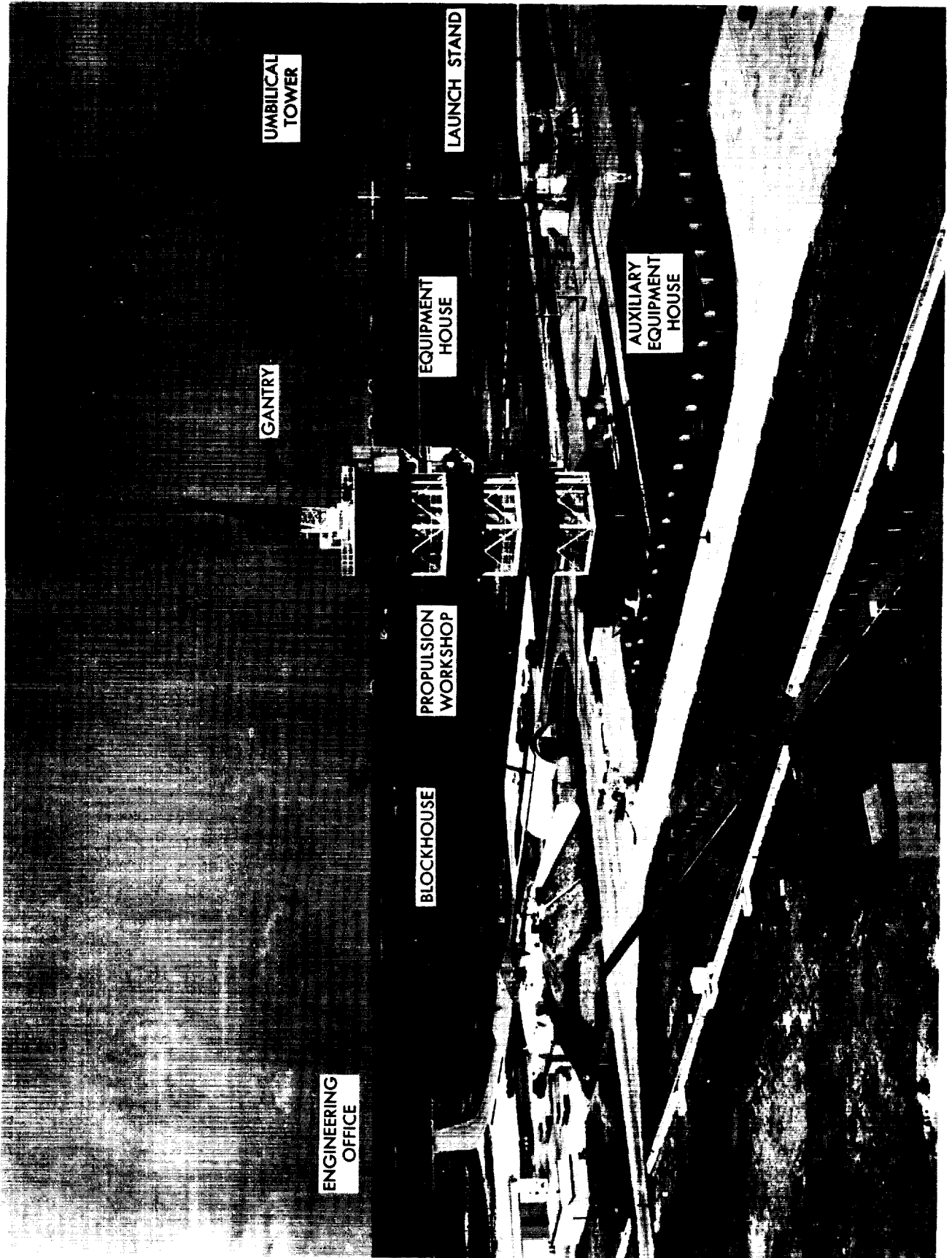


Fig. 38 Vanguard Launch Complex

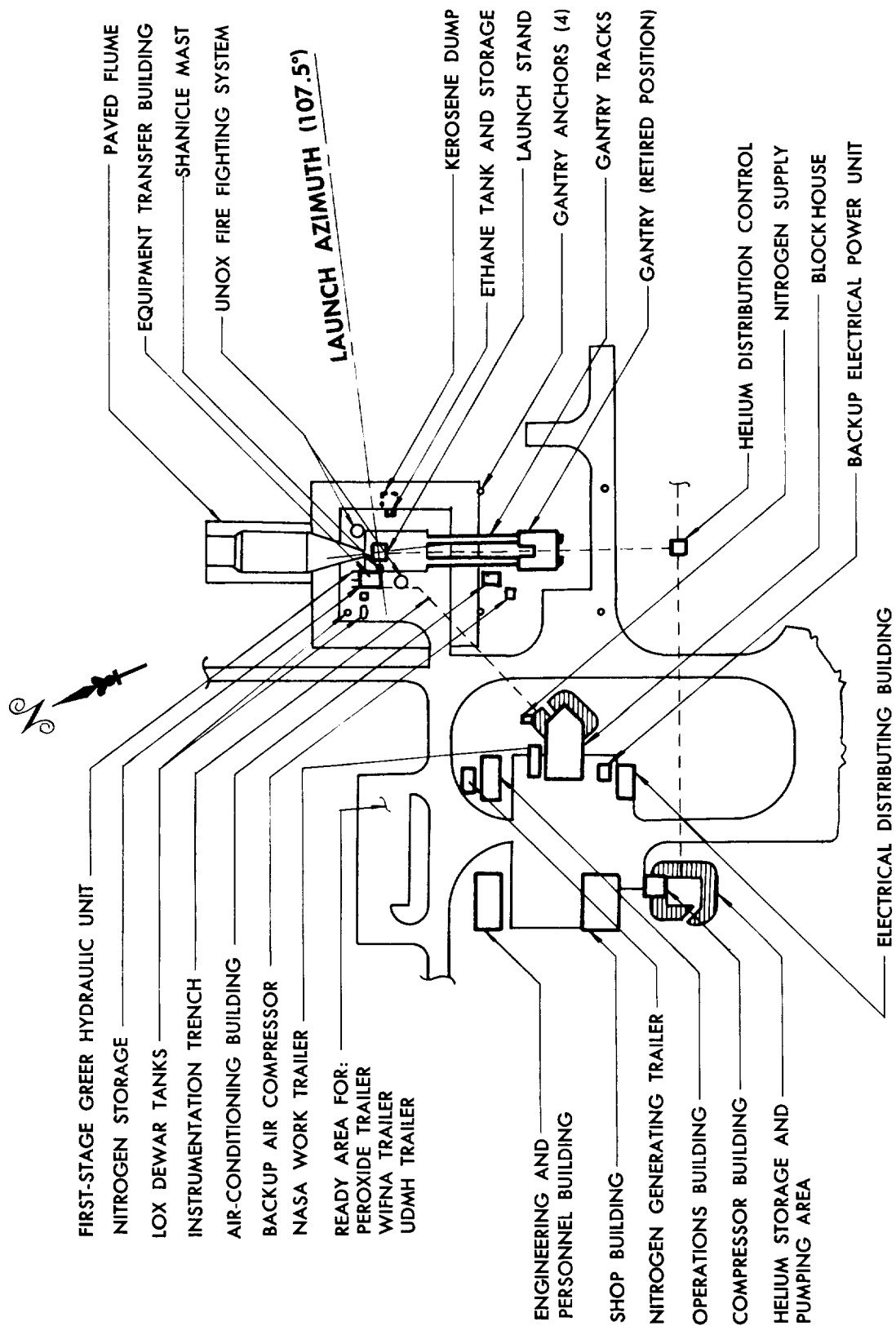


Fig. 39 Vanguard Launch Area Schematic (AMR Launch Complex No. 18A)

**Launch stands**—The original launch stand was made by the Loewy Hydropress Division of the Baldwin-Lima-Hamilton Corporation, and provided launch capability up to a ground wind speed of 17 miles per hour. This stationary launch stand was a structure built up with tubular steel members mounted on the working platform about 10 feet above the launch pad ground level. The base of the vehicle was supported on the launch stand by four "acorn" fittings mounted on "swingaway" arms. The first-stage thrust chamber extended 52 inches down into the structure of the stand.

As the vehicle started to move vertically out of the launch stand, the swingaway arms were rotated upward and outward by 75-pound counterweights acting on one-foot moment arms. Two 150-pound springs were mounted on each of the four swingaway arms to restrain the arms until the vehicle had risen one inch. The springs were restrained from further expansion by displacement limit devices. Steel pins, centrally located on each acorn fitting, prevented undesirable lateral motion of the vehicle base until the electrical, hydraulic, helium and propellant disconnect fittings had disengaged.

Midway in the flight program, it was decided to increase the allowable launch wind condition. A retractable launch stand was designed and built by The Martin Company to provide a launch capability up to ground wind speeds of about 35 miles per hour. Figure 41 illustrates the retractable launch stand in both the launch and retracted positions. The retracting launch stand was similar to the stationary launch stand up to the top of the base of the parallelpiped section. Four retracting arms, which were hinged at the top of this section, supported the vehicle base 6.64 feet above the working platform, or 4 inches higher than on the stationary stand. When the vehicle rose 1.75 inches, a switch triggered the retracting motion of the support arms. Hydraulic cylinders forced the retracting arms to rotate about their hinge points, providing outward and upward motion of the support points. The position of the vehicle-supporting acorn fittings was the same as on the stationary stand. Several of the disconnect fittings, however, were relocated onto the retracting arms.

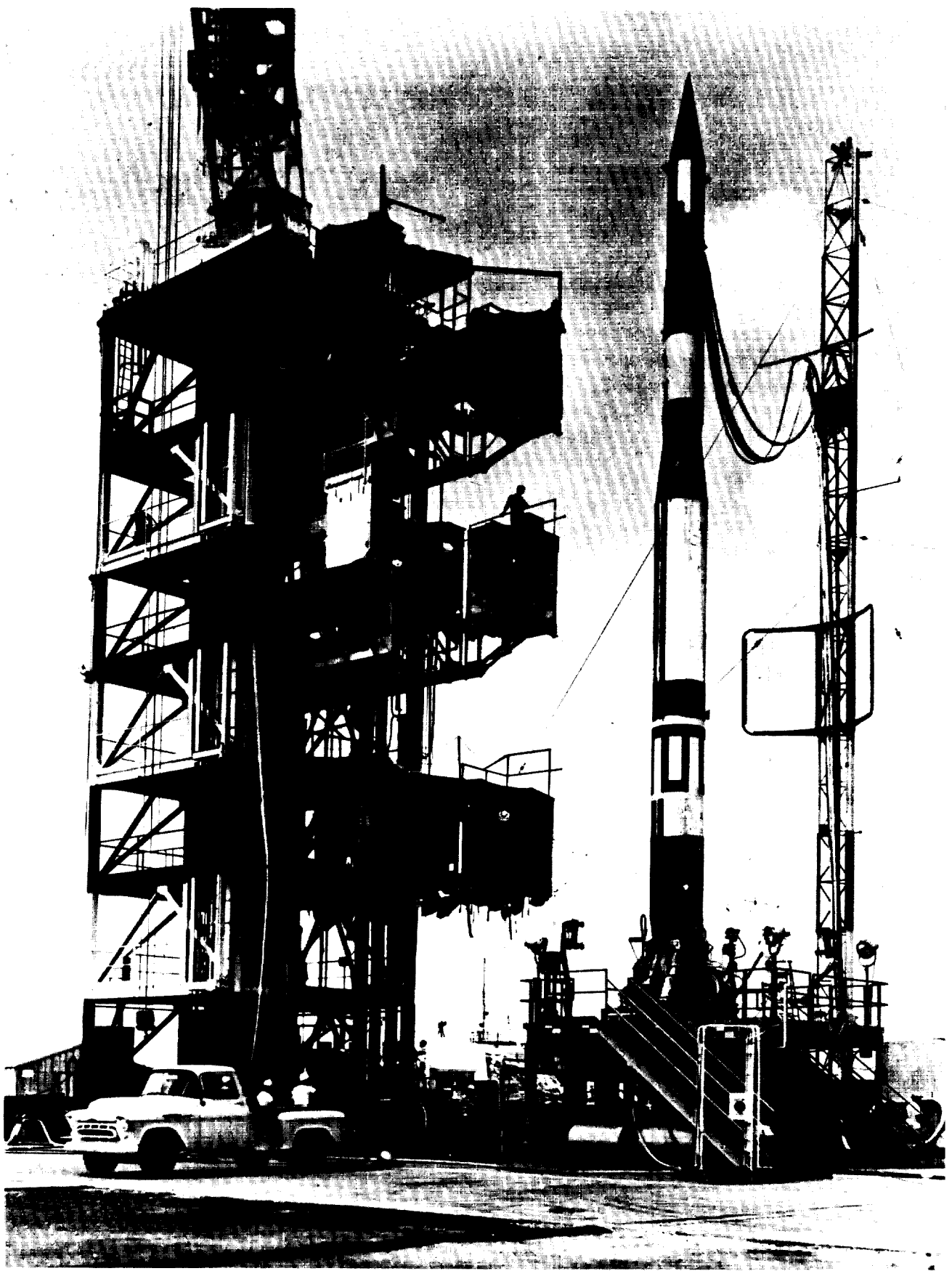
A feature of the retracting design was that the vehicle initiated retraction of the support arms by its own vertical motion, and the time of retraction was between 0.3 and 0.5 second. The arm retraction was based on a triangular linkage principle, rotating over dead center, thereby providing an absolute locking feature while the vehicle was at rest on the stand. Another important characteristic was the adjustable swivel design of the launch stand disconnects to ensure proper alignment to the vehicle disconnects. These

disconnects remained engaged until separated by the vehicle liftoff.

**Guidance and control equipment**—The basic guidance and control ground support equipment consisted of various monitoring, testing and power supply panels. A gyro panel was used to control gyro operation and to monitor signals and torque currents. A controls monitoring panel checked engine motions, hydraulic pressure and power supply voltage. This panel also monitored all jet operations, program timer reset and running, and coasting time computer reset. It controlled the operation to remotely center the engines, to start the second-stage hydraulic pump motor, and to operate the first-stage roll jets. A controls tester panel was provided for checking the coasting time computer and all channels of the program timer; it was also used to initiate command signals to the vehicle guidance system. A signal generator panel tested the frequency responses, jet hysteresis and jet time delays. Switching provisions were included in this panel for selecting the system and type of signal to be supplied. Power supply panels generated power necessary for the test equipment, including B+ voltage and 60 cps a-c voltage. A remote junction panel served as a junction for wiring between the vehicle and the blockhouse. Part of the metering circuit and relays required for testing and launching were also contained in this panel.

**Propulsion equipment**—Ground equipment directly associated with the propulsion systems included a considerable amount designed for specific purposes and used for "local" testing. A regulator adjustment panel was required to set the first-stage main helium regulator. A portable pressure sensor panel was used to check the vehicle gas pressure sensors to ensure that they were within proper operating ranges. Another portable functional test panel indicated gas pressure levels in the vehicle propellant tanks and gas storage spheres. A second-stage functional pressure panel applied appropriate gas pressures to functionally check components and sense pressures of the second-stage pressurization system. A hydrostatic flush panel controlled the filling, draining, and gas pressure during the water-flushing of second-stage tanks. An oxidizer probe tester monitored the oxidizer probe electrical resistance.

**Electrical**—The basic electrical ground support equipment consisted of a propulsion fire panel to control power to the vehicle, to initiate pressurization of the first stage, to drop umbilical connections and to start the first-stage firing sequence. The ground service panel was provided to remotely pressurize the first- and second-stage helium spheres, to service the vehicle with LOX, to manually increase the fuel and LOX tank pressures, to dump propellants and to con-



**Fig. 40 Vanguard Vehicle During Prelaunch Operations**

trol the propane heater. Two remote junction racks contained relays and timers used in conjunction with the propulsion fire panel and the ground servicing panel for remote control of vehicle firing, servicing and power transfer. An ordnance checkout panel containing flash-bulbs and associated circuitry simulated squibs and detonators for vehicle tests. A separation simulator, consisting of cabling and quick-disconnects, was used to electrically simulate separation of the vehicle stages during vertical tests. Other simulators of first- and second-stage propellant valves and pilot valves provided a check for automatic sequencing in various propulsion-electrical tests. An electrical monitoring panel was required to monitor the first- and second-stage battery running time and to check out the oxidizer probe resistance prior to liftoff.

**Cooling air system**—The cooling air system automatically controlled the mixing of proportionate amounts of dehumidified supply and refrigerated air to temperature condition the satellite and various guidance and control components. The flexibility of the design, using two refrigeration units in parallel, allowed the air to be temperature-controlled by either or both of the refrigeration units.

**Ground instrumentation**—Numerous land line measurements were necessary for operation and count-down procedures. Such measurements as tank pressures and temperatures, combustion chamber pressures, servicing temperatures and pressures were needed for fueling, static firing and flight readiness checks of the vehicle. These items were monitored in the blockhouse on visual panel meters or recorded on strip chart recorders. The weight recorders measured and recorded vehicle weights and provided thrust indications during static firings and before liftoff in flight operations.

No specialized automatic or semi-automatic checkout equipment was employed for the instrumentation and telemetry systems. Standard test and calibration equipment was used, except for a special pressure cart used for calibrating pressure transducers.

## B. FIELD TESTING

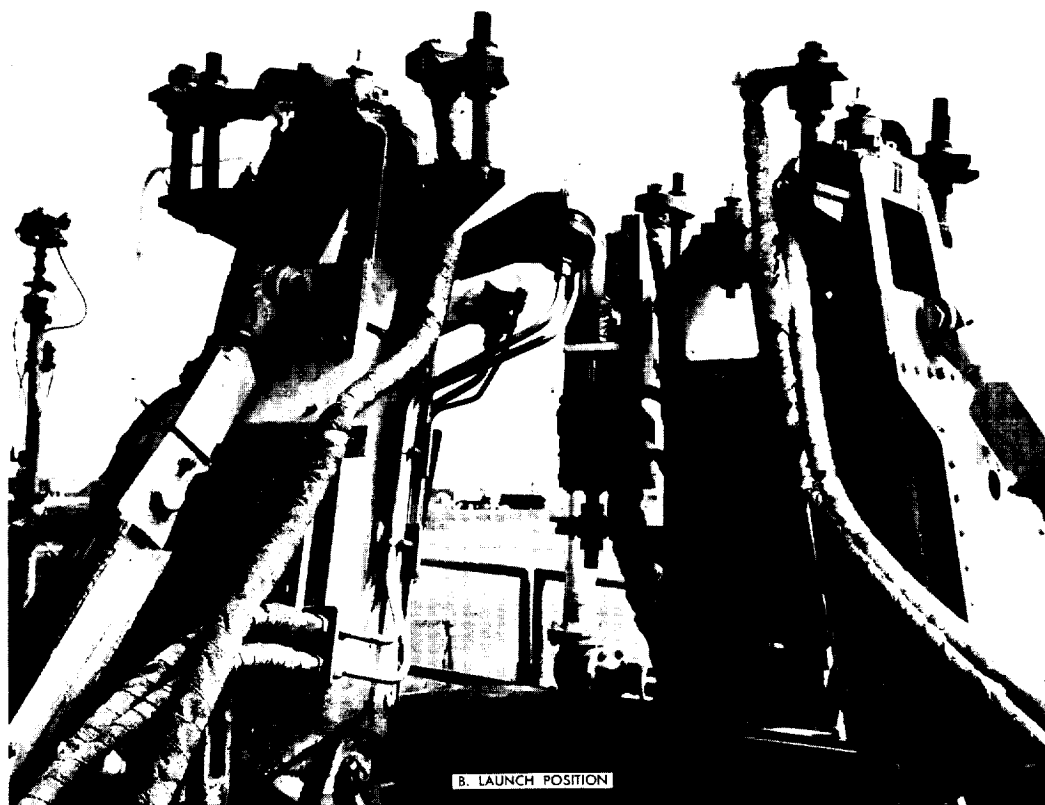
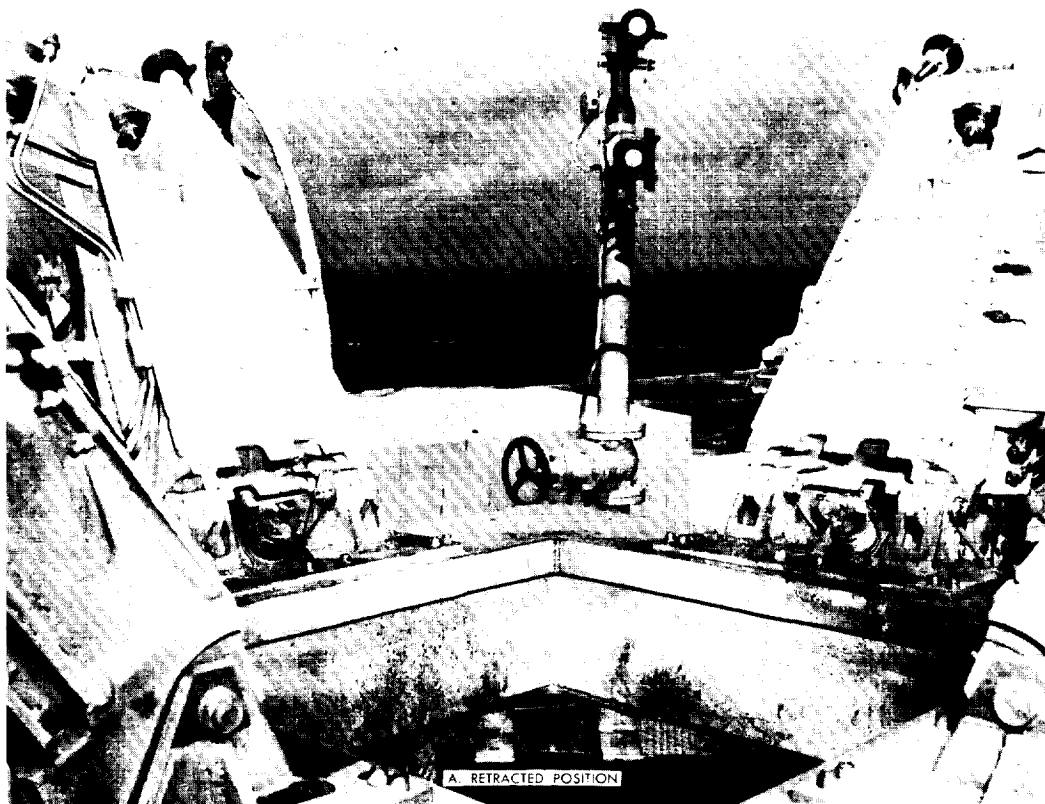
**Hangar tests**—Hangar operations at Cape Canaveral started with receiving inspection of the vehicle by Martin quality assurance personnel. The primary objective of the hangar tests was to ensure complete system integrity of the vehicle prior to erection at the complex area. These tests were performed in accordance with checkout procedures that were similar to those used in horizontal tests at Baltimore. The tests included functional and operational tests of all components: pressure; leakage; electromechanical; controls and guidance; instrumentation and range safety checks. Incorporation of minor changes and checking the fit

of the heat generator were accomplished as required. The final hangar test, prior to vehicle erection, was the Horizontal Functional Test (HFT), which was similar to the horizontal electrically mated tests performed in Baltimore. The destruct system primacord and the second-stage nozzle closure were installed after the HFT.

**Prestatic tests**—Prior to arrival of the vehicle at the launch pad, a complete ground service test of the complex was performed. This included such items as the LOX disconnect leakage test, launch stand conditioning tests and the azimuth alignment of the launch stand. The vehicle was then erected on the stand (using a dummy third stage) in preparation for the static firing. After alignment, a thorough check was made to verify the compatibility of the rocket to the launch stand, to ground service equipment, to blockhouse controls, and to instrumentation. The telemetry systems were also checked. Vertical tests were then performed to prove that all systems of the rocket were ready for a first-stage static firing. The first stage was passivated, the turbopump lubricated, instrumentation calibrated, and the first-stage igniter installed. A visual general inspection of the entire vehicle was then performed by quality control and engineering personnel.

**First-stage static firing**—The primary purpose of the static firing was to qualify the first stage for flight by verifying engine package compatibility with its propellant feed and pressurization systems, by demonstrating the propulsion system performance, reliability and repeatability and by demonstrating satisfactory operation of all subsystems and components. The static firing was conducted with range support and tested the propulsion, electrical and control systems in a simulated 50-second first-stage flight. All residual propellants were drained from the first stage after the static firing, the hydrogen peroxide tank was flushed and passivated, the thrust chamber was cleaned and decarbonized and the LOX injector was flushed and dried. There was also a post-static visual inspection of the vehicle and launch stand. After acceptance of the static firing data, all ground-based instrumentation was removed from the vehicle.

**Second-stage static firing**—A capability existed for static firing the second stage at Cape Canaveral, but this was done on only three Vanguard vehicles. The question of whether or not the second stage should be static fired in the field was controversial. A firing was desirable to verify satisfactory propulsion system start and operation, and to provide additional system pressure and flow measurements. However, the process added approximately ten days to the field operation because a separate erection of the second stage was involved, and the system verification was at least partially invalidated by the necessary post-static decon-



**Fig. 41 The Vanguard Break-Away Launch Stand**

tamination procedures. In addition, flow separation within the altitude nozzle during sea level firings precluded determination of thrust for performance evaluation, and associated side forces produced severe vibration and buffeting of the thrust chamber.

The first two units in the field (TV-3 and TV-3BU) were static fired, then the practice was discontinued. However, second-stage difficulties encountered in the TV-5, SLV-1 and SLV-2 flights caused reinstatement of the requirement for SLV-3. The SLV-3 static produced side forces of such severity that one of the thrust chamber actuator lugs was cracked. This resulted in the decision, for SLV-4 and up, to substitute a "rejuvenation" program at Aerojet for the field static firing (see Chapter V, Section E).

**Prelaunch preparations**—The preparations for flight consisted of thorough alignment checks, instrumentation calibrations and system functional tests, culminating in the Vertical Functional Test (VFT), which was patterned after the Vertical Interference Test at the factory. It was conducted with range support and was in effect a dry run of the entire countdown and flight. The Flight Readiness Test (FRT), conducted after a thorough visual inspection by quality and engineering personnel, was similar to the VFT, but was necessarily less comprehensive because the rocket was almost completely "buttoned up." A minimum of handling was permitted after the FRT in order to preserve the rocket's established integrity for flight. The vehicle then entered final servicing and launch operations.

## C. RANGE SAFETY CONSIDERATIONS

Information was required prior to flight to ensure proper interpretation of real time flight data received by the Range Safety Officer. Studies to obtain pertinent information were completed for each Vanguard vehicle.

**Performance predictions**—Range safety reports (Ref. 33 is typical of such reports) were prepared that presented time histories of speed, altitude, ground range, flight path angle, accelerations, thrust, propellant weights and gross weights for minimum, nominal and maximum performance of each vehicle. Trajectory variations included the maximum expected deviations in the ground plane from the intended flight azimuth, the variations in ground range versus altitude and speed versus time, and the maximum lateral angles through which the velocity vector could turn in the event of malfunction. Range and altitude versus time and range versus altitude were provided for all three stages. Estimates of the three-sigma impact contours for the first and second stages on a ground plane and the locus of impact points with a  $\pm 5$  degree flight

azimuth tolerance were given. Discussions of power-off conditions and the expected effects of a destruct explosion were included in Ref. 34.

Supplementary range safety reports (e.g., Ref. 10) included the effects of performance parameter variations on range, the behavior of the vehicle during the initial launch phase and the wind shear criteria for flight.

**Launch azimuth studies**—Studies were made to determine the extreme allowable values of the nominal launch azimuth such that the vehicles would remain within range of ground-based electronic stations, and would not require the use of the command control system. A three-sigma lateral deviation (assumed to be a  $\pm 5$  degree shift in launch azimuth) in the most unfavorable direction was permitted on each of the above requirements. On the basis of the above premises, and by inclusion of minimum, nominal and maximum variations in performance, the launch azimuth for a most southerly trajectory was determined to be 107.5 degrees. Similarly, 48 degrees was determined as the most northerly course.

**Command control charts**—Command control charts were furnished to be used as a guide in determining the need for pitch or yaw commands to the vehicle during flight. An IBM-704 digital computer, with C-band radar tracking data as input, was used to convert real time coordinates to impact points, which were then plotted in real time on the control charts. The command lines on the charts were constructed such that if a command (one degree per second rate for four seconds) arrived at the rocket four seconds after the plotting pens became parallel to any of these lines, the resulting change to the vehicle's motion would prevent the need for destruction of the vehicle by the Range Safety Officer. If at any time the plotted impact point exceeded the predetermined limits set by range safety, the flight would be terminated. Vehicle trim commands were to be used only for range safety purposes, as described, and never to "steer" a vehicle that was not in danger of command destruction.

## D. FLIGHT LOADING AND PERFORMANCE PREDICTIONS

### 1. FLIGHT LOADING

Maximum total impulse from the first- and second-stage propulsion systems was sought by minimizing outage (usable residual propellant at burnout). The absolute magnitude and sensitivity of all relevant parameters were studied to determine what was necessary to keep flight performance within acceptable tolerances. In general, the main factors which influenced outage were operating mixture ratio and quantities of loaded propellants.

**Mixture ratio**—Prediction of the flight mixture ratio began with accurate determination of the mixture ratios that were measured in acceptance tests and static firings. All data sources, including Potter flowmeters, loaded and residual propellant weights, propellant temperatures and system pressure drops, were evaluated; the static mixture ratio and its accuracy were determined. (Flight mixture ratios differ slightly from static mixture ratios because predictable acceleration and additional heating effects cause slight variations in propellant flow rates.) Variations occurred in these and other parameters such as tank pressures, propellant temperatures and specific gravities, starting and stopping losses, and system pressure drops, all of which contributed to the mixture ratio "tolerance" or uncertainty. The one-sigma deviation in mixture ratio was estimated to be 2% for the first stage and 1.5% for the second stage.

**Outage**—The operating mixture ratio may be high or low, with theoretically equal probability. It was therefore desirable to minimize the outage at both extremities of the mixture ratio tolerance. Figure 42 illustrates how loading for the expected mixture ratio would result in unequal outages at the mixture ratio tolerance limits. Figure 42 also shows how the outage could be equalized and the maximum amount actually reduced by intentionally loading for a slightly different mixture ratio. Thus, for the Vanguard first stage, an overload of 38 pounds of fuel decreased the maximum outage (within a one-sigma deviation) from 215 to 135 pounds. Similarly, second-stage maximum outage was reduced from 39 to 21 pounds by a 7-pound UDMH overload.

**Expected propellant loading**—The propellant loading of each Vanguard vehicle was calculated individually, based on measured tankage volumes, expected operating mixture ratio, offload or overload, expected propellant specific gravity, and predicted losses (starting, stopping, trapped and boiloff). Total available propellants were maximized by overflowing the limiting tank.

**Actual propellant loading**—A volumetric loading method was developed which permitted loading the vehicle within 0.7% (three-sigma) of the desired weights. This method consisted of filling the propellant tanks to overflow and then draining back a small quantity of ullage to establish the desired load. The required accuracy was achieved by careful calibration of the tank at the factory and by accurate determination of the specific gravity and temperature of the actual flight propellants in the field. This method was used to fill the WIFNA, UDMH and kerosene tanks. The LOX was loaded by weight as determined by the

vehicle weight recorder. Additional LOX was loaded aboard to compensate for that lost by boiloff between lock-up and the fire signal, and also for the weight of ice that formed on the outside of the tank during loading. Topping was continued as late in the countdown as possible to minimize boiloff losses. The specific gravity was controlled by venting the tank to one atmosphere and allowing the LOX to boil and reach equilibrium.

The hydrogen peroxide was weighed prior to loading. The loaded weight was checked by means of the vehicle weight recorder. The third-stage inert parts and the loaded motor were weighed by the manufacturer.

## 2. DRY WEIGHT

The assembled vehicle was weighed after manufacture in Baltimore. Subsequent additions and changes were carefully weighed. The total weight was checked by the weight recorder readings before and after vehicle erection.

## 3. PROPULSION SYSTEM PERFORMANCE PARAMETERS

The predicted performance and the possible variation in performance of the numerous components involved in the first- and second-stage propulsion systems were estimated from flight results, static and acceptance test results and engineering judgment. The complete system performance then was expressed by the nominal, minimum and maximum values of the flow rates, characteristic exhaust velocity, propellants consumed for power and propellant outage.

The nominal outage was at the tolerance limit of the mixture ratio. Outage for maximum vehicles occurred at the predicted mixture ratio. Minimum vehicles had oxidizer outage at twice the mixture ratio tolerance. The propellants consumed for power were the loaded propellants minus the starting losses, stopping losses, trapped propellants, boiloff and outage.

**Third-stage performance**—Performance of the third-stage rocket motor was based on the measured weight of the flight motor, the satellite payload weight and the specific impulse based on statistical performance data obtained from static firings conducted during the motor qualification test programs. The motor burnout weight was considered to be the inert parts weight. This assumption was adequate in the case of the GCR rocket motor; however, the ABL rocket motor was constructed such that approximately 7 pounds of rubber insulation would be consumed. This effectively decreased the specific impulse by approximately four seconds for performance predictions, and also decreased the burnout weight by 7 pounds.

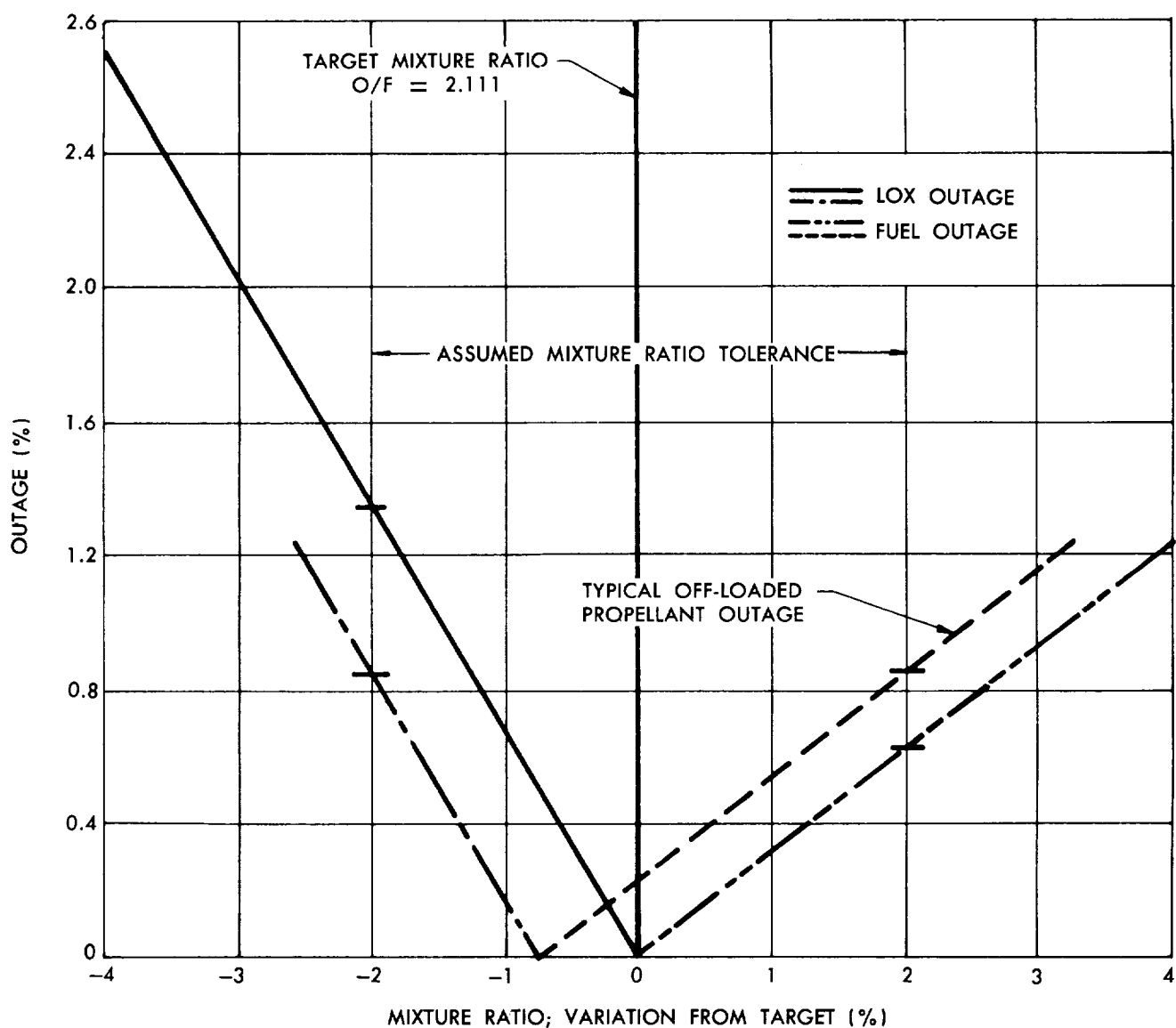


Fig. 42 Variation of Outage with First-Stage Mixture Ratio

#### 4. PERFORMANCE PREDICTION

Vehicle performance data for the Estimated Performance Reports (Refs. 35, Vols. I and II, and 36) and for the Range Safety Reports (e.g., Refs. 33 and 10) considerably predated the launch. Late changes and the results of the first-stage static firing were included in "post-static" maximum, nominal and minimum performance predictions which were delivered to

the field a day or two before launch. The difference between these results and the data from which range safety provisions had been made were generally considered negligible from the range safety standpoint and no modification was made.

**Expected performance**—The conservatism of the maximum, nominal and minimum performance approach was shown by a subsequent method of per-

formance prediction which considered the system performance from a probability standpoint (see the Appendix of this report). "Expected" second-stage apogee altitudes and velocities, as predicted by the probability method, are compared to actual flight results and to the maximum, nominal and minimum performance predictions in Fig. 43. This expected performance is seen to agree closely with the actual performance of all vehicles which achieved successful second-stage flight.

## E. LAUNCH OPERATIONS

Launch preparations were started after the Flight Readiness Test, generally two days before flight (F-2 day), and included turbopump lubrication, setting of ethane and nitrogen pressures, peroxide load preparation, Dewar tank servicing and cooling air system maintenance. The third-stage motor and other ordnance items were assembled and resistance-checked at the AMR solid propellant storage area and installed in the vehicle. The third stage and the retrorockets were aligned after installation.

The Vanguard flight firing countdown was split into two separate parts, occurring on successive days, to reduce the number of continuous working hours required of supporting personnel. Operations on the day preceding flight included checks on propulsion system pressures, satellite, launch stand water, UNOX fire fighting system and range hold fire circuit. The nose cone and helium heat generator were installed. Ordnance was armed and resistance-checked.

**Flight day preparations**—The final operation started approximately eighteen hours before launch, with checks to ensure that the various systems were in operating order and the vehicle was ready to be serviced with propellants. Prior to propellant servicing, the first-stage helium spheres were pressurized to 1500 psig to ensure that the main propellant valves were closed and to provide pressure for adjusting the main helium regulator and pilot pressure for component actuation. Kerosene was the first propellant to be serviced and was pumped directly from a truck. Then hydrogen peroxide, which had been batch-mixed on F-2 day, was serviced from a special drum by a pump. The loaded peroxide temperature was monitored as a safety measure to detect any reactivity.

Second-stage propellants were originally cooled prior to servicing, in order to maximize the propellant loads. The 60°F temperature limitation and the removal of the second-stage insulation or cooling blanket at the time of gantry retirement caused considerable operational difficulty, particularly in the event of long holds or flight postponement. For SLV-4 and up, the propellant temperature limitation was raised to 90°F, which eliminated precooling the propellants and use

of the cooling blanket. This change greatly improved the operation and allowed second-stage propellants to be loaded prior to the actual range time countdown.

Liquid propane, UDMH and WIFNA were serviced in that order. Propane was gravity-fed until the tank overflowed. UDMH and WIFNA were serviced from special trailers which incorporated their own pumps and a control panel as well as the refrigerating equipment used prior to SLV-4. The volumetric loading of each propellant was checked against launch stand weight recorder readings. The remaining preparations for the formal countdown included instrumentation preparations, electrical cleanups and controls cleanups.

**Flight countdown**—The formal range countdown was begun five hours before launch, and was a closely coordinated operation involving personnel of the Atlantic Missile Range, the NRL-NASA Vanguard Operations Group (VOG), Martin and various subcontractors. VOG personnel checked out the satellite and the electronic and range instrumentation, as well as maintaining overall coordination for the operation. The Martin Company was responsible for preparation and launch of the vehicle. A complete sequence of operation of both vehicle and ground functions is presented in Ref. 37. A summary of the more significant operations during the final countdown follows.

Time (minutes)	
T-255	Satellite turned on and checked
T-235	Radar beacon checked
T-225	Electronic instrumentation checked
T-210	Range sequencer checked
T-205	Hold fire circuit checked
T-180	Cutoff and destruct system checked
T-160	Destruct system detonators installed and armed
T-135	Igniter and combustion indicator assembly installed
T-120	LOX servicing preparations
T-95	LOX servicing
T-65	Gantry retired
T-45	One-hour built-in hold which was designed to allow completion of outstanding items
T-40	Launch stand area cleared
T-35	Igniter arming
T-30	IBM impact/apogee predictor ready (704 computer and associated equipment)
T-25	All personnel in blockhouse or retired to fall-back area
T-20	Instrumentation on internal power
T-15	First-stage helium sphere pressurized to 4000 psig.
T-10	Check wind condition at blockhouse, preload second-stage helium sphere to 400 psig.

T-6 Second stage pressurized, second-stage hydraulic pump on  
T-5 XN-1 radar aligned on vehicle  
T-4.5 Gyros freed and command control system checked

Time  
(seconds)

T-180 Telemetry, radar beacons, command receivers on internal power; tailcan nitrogen purge on  
T-175 Flame deflector cooling water on  
T-120 Kerosene tank pressurized

T-100 Peroxide tank pressurized  
T-60 First- and second-stage flight batteries paralleled  
T-45 Second-stage helium umbilical dropped  
T-30 Cooling air umbilical dropped, LOX vent valves closed  
T-20 LOX tank pressurized  
T-10 First-stage helium topping stopped  
T-0 Fire switch closed, electrical umbilical dropped  
Liftoff occurred about 6 seconds later and was designated T + 0.

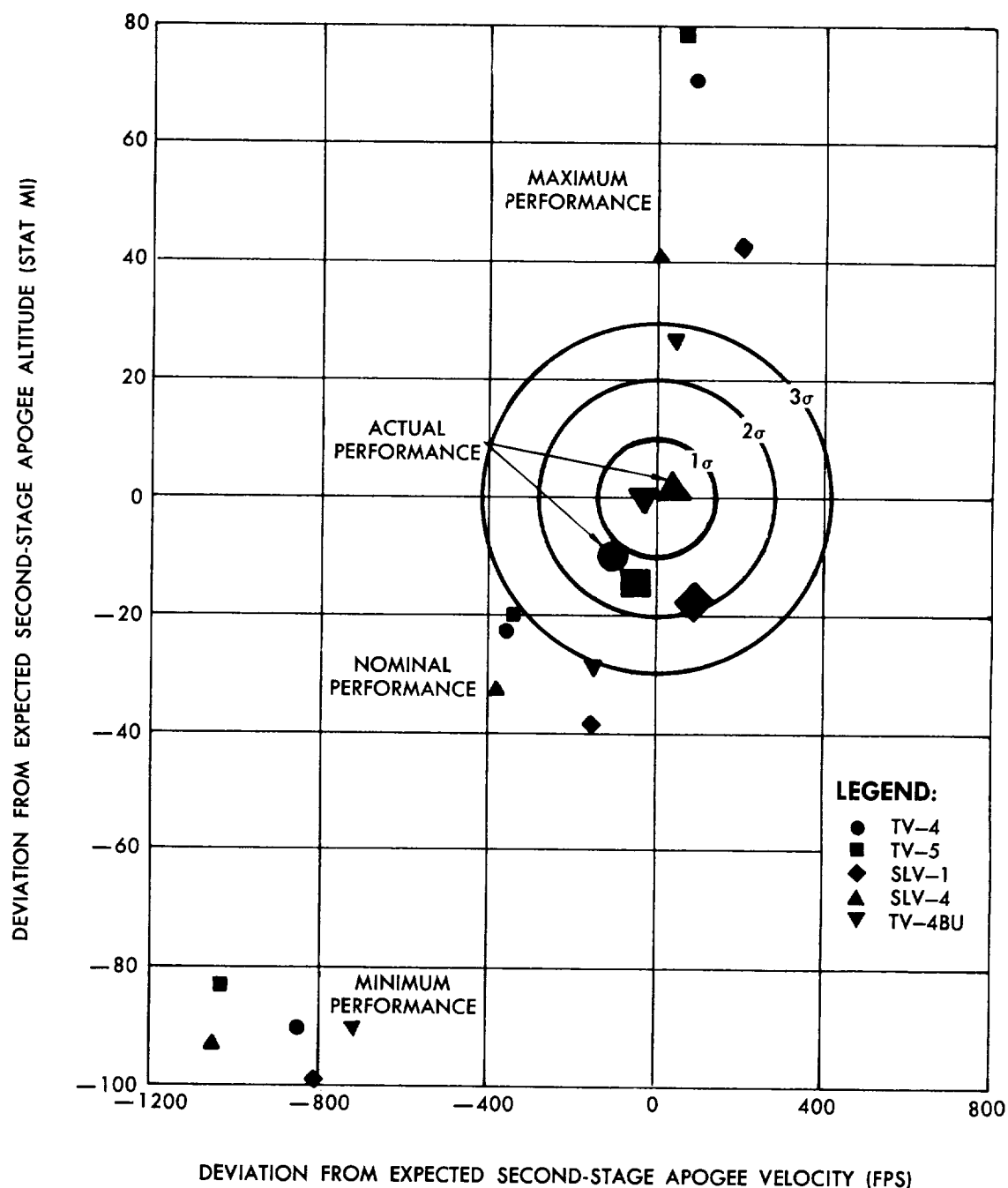


Fig. 43 Comparison of Predicted and Actual Second-Stage Apogee with Expected Vanguard Performance

## **VII. VEHICLE FLIGHT ANALYSIS**

A flight analysis of each vehicle is documented at length in the series of Vanguard flight analysis reports (Refs. 38 through 51). This Chapter presents a flight summary and vehicle trajectory, aerodynamic and structural performance.

## A. FLIGHT SUMMARY

Vehicle	Flight	
	Objectives	Results
<b>TV-0</b> <p>Launched 8 December 1956.  Martin Viking No. 13, a liquid-propellant single-stage rocket, was redesignated TV-0 and fired as the first Vanguard Test Vehicle.</p>	<p>Primary: to evaluate the performance of the internal telemetry system, to evaluate the launching complex, and to become familiar with the operations, range safety and tracking systems of the AFMTC rocket range.  Secondary: testing of the Vanguard Minitrack transmitter and evaluation of the coasting flight attitude control system.</p>	<p>All objectives were met except evaluation of coasting-flight attitude control. During powered flight, the performance of all components was either satisfactory or superior. The vehicle reached an altitude of 126.5 stat mi and range of 97.6 stat mi. Rocket-borne instrumentation and telemetry systems performed excellently; ground instrumentation coverage was adequate.</p>
<b>TV-1</b> <p>Launched 1 May 1957.  A two-stage test vehicle. The first stage was the Martin Viking No. 14 slightly modified for Vanguard objectives. The second stage was a prototype solid propellant Vanguard third stage, built by Grand Central. The second-stage payload was an instrumented nose cone.</p>	<p>Primary: to flight test the Vanguard third-stage prototype for spin-up, separation, ignition, and propulsion and trajectory performance.  Secondary: further evaluation of ground handling procedures, techniques and equipment, and in-flight vehicle instrumentation and equipment.</p>	<p>All test objectives were met. Flight operation and performance of all powerplant systems were very good. The vehicle was properly controlled throughout flight to an altitude of 121 stat mi and range of 451 stat mi.</p>
<b>TV-2</b> <p>Launched 23 October 1957.  A Vanguard prototype consisting of a live first stage (Martin tankage and the General Electric X-405 liquid propellant engine), a simulated (but inert) second stage and an inert third stage.</p>	<p>Primary: to evaluate the Vanguard launch system and the flight performance of the first-stage propulsion system, the second-stage retrorocket system and the third-stage spin-up system, and to obtain data on the first and second-stage structural characteristics.  Secondary: to evaluate equipment, test procedures, first-stage handling, and the SHF (C-band) beacon and radar equipment.</p>	<p>All test objectives were met. Performance of all components throughout flight was superior. This test confirmed that the first stage operated properly at altitude, conditions were favorable for successful separation of the first and second stages, launch stand clearance for the condition of low surface winds was no problem, there was structural integrity throughout flight. The test also demonstrated dynamic compatibility between the control system and the structure.</p>
<b>TV-3</b> <p>Launched 6 December 1957.  The first complete Vanguard test vehicle with three live stages. This was to have been the first flight firing of the second-stage propulsion system and the complete Vanguard guidance and control system.</p>	<p>Primary: to launch into orbit a minimal (6.4-in., 4-lb) satellite. This satellite was to determine atmospheric density and the shape of the earth, to evaluate satellite thermal design parameters and to check the life of solar cells in orbit.  Secondary: to test and evaluate all vehicle stages and systems.</p>	<p>Less than one second after liftoff, the first-stage engine lost thrust because of an improper engine start. The vehicle settled back on the launching stand and exploded.</p>
<b>TV-3BU</b> <p>Launched 5 February 1958.  A backup vehicle identical to TV-3.</p>	<p>Identical to those of TV-3.</p>	<p>After 57 seconds of normal flight, a control system malfunction caused loss of vehicle attitude control. Vehicle breakup occurred only after an angle of attack of at least 45 degrees had been exceeded.</p>

## FLIGHT SUMMARY (cont)

Engineering Achievements	Vehicle Improvement	
	Deficiency	Corrective Action
<p>Successful receipt of Minitrack signals throughout flight demonstrated the practicality of the design for satellite telemetry and tracking purposes.</p> <p>Excellent correlation between tracking, telemetry and predicted data indicated that the retrorocket separation technique and the use of spin stabilization for flight path control of the solid propellant stage were signal successes. Aerodynamic heating data demonstrated that the maximum design temperature limitations of antennas and the nose cone were conservative.</p> <p>The first flight attempt with the Vanguard external configuration carried a 4000-lb payload to an altitude of 109 stat mi and to a downrange distance of 335 stat mi, as planned. Excellent pitch/yaw control through the atmosphere demonstrated practicality of gimbaled engine control with no stabilizing fins at the base of the rocket. First-stage powered flight roll control demonstrated the adequacy of the twin roll jets using turbopump exhaust products.</p> <p>This flight provided unique information for evaluation of Vanguard structural design methods. An analog simulation of the TV-3BU breakup transient was made, using controls and servo hardware, and simulating elastic structure and aerodynamic loads. The calculated time and location of structural failure, as well as the vehicle response to the spurious engine deflection, were practically identical with these measured in flight. This correlation substantiated the validity of Vanguard structural design procedures and philosophy.</p>	<p>Attitude control was lost at burnout when the auxiliary peroxide jet control system (peculiar to Viking) did not function.</p> <p>The improper engine start was traced directly to a low fuel tank pressure which was responsible for a low fuel injector pressure prior to the start of turbopump operation. A low fuel injector pressure allowed some of the burning contents of the thrust chamber to enter the fuel system through the injector head. Fire started in the fuel injector before liftoff, resulting in destruction of the injector and complete loss of thrust immediately after liftoff.</p> <p>Spurious electrical signals caused first-stage engine motions in the pitch plane, starting 57 seconds after liftoff. These engine motions developed dynamic structural loads which, coupled with a rapid pitch-down that superimposed air loads of about the same magnitude, caused the vehicle to break up at the aft end of the second stage.</p>	<p>Extreme care was used on the next vehicle (the last Viking to be fired) to ensure successful operation of the control jet system. Measures were taken to prevent hardware corrosion. Countdown procedures for Viking and Vanguard vehicles were revised to include actual operation of the control jets.</p> <p>The minimum allowable fuel tank pressure head was increased about 30%. Provisions were made for manual override of the regulator to assure that this condition could be met. Fourteen static and flight firing starts, identical to the TV-3 start except for the increased minimum allowable pressure, were subsequently made without incident.</p> <p>Parallel wiring was installed for all critical control system wire runs between stages. The mounting panel for controls hardware was strengthened to reduce vibration. Close quality control was maintained, along with continued review and redesign of wiring and connections. There was no recurrence in flight of spurious signals to cause destructive engine motions.</p>

## FLIGHT SUMMARY (cont)

Vehicle	Flight	
	Objectives	Results
<b>TV-4</b> Launched 17 March 1958. The third complete Vanguard configuration test vehicle, identical to TV-3 and TV-3BU.	Identical to those of TV-3 and TV-3BU.	TV-4 placed 57 lb (a 4-lb payload and the 53-lb third-stage motor case) in an orbit estimated to last at least 1000 years. The initial orbit had a perigee of 406 stat mi, an apogee of 2465 stat mi and a period of 134 min. The guidance system produced an overall error of less than one degree in satellite injection angle. The Minitrack oscillator, operating on solar battery power, is still functioning after two years in orbit.
<b>TV-5</b> Launched 28 April 1958. The final test vehicle, which differed from a production satellite launching vehicle (SLV) only in the greater degree of instrumentation.	Primary: to launch into orbit a fully-instrumented, 20-in., 21.5-lb "X-ray and environmental" satellite. This satellite was to study maximum variations in the intensity of solar X-ray radiation in the 1 to 8 Å wave length bands, and to make certain space environment measurements. Secondary: to verify the complete vehicle performance.	Flight was normal through second-stage burnout, but the second-stage shutdown sequence was not completed electrically, which prevented arming of the coasting flight control system and separation and firing of the third stage. Second-stage performance was below nominal, but combined first- and second-stage performance was somewhat better than nominal.
<b>SLV-1</b> Launched 27 May 1958. First production satellite launching vehicle.	To launch into orbit a fully-instrumented, 20-in., 21.5-lb "Lyman-Alpha" satellite. This satellite was to study solar "Lyman-Alpha" radiation and to make certain space environment measurements, and was identical to the X-ray satellite of TV-5 except that it covered the 1100 to 1300 Å wave length bands.	Successful operation and performance were achieved throughout flight, except at second-stage burnout. At that time, a disturbance caused loss of attitude reference of the pitch gyro so that the remainder of the flight was controlled to a false reference. The third stage was launched at an angle of approximately 63° to the horizontal, thus precluding a satisfactory orbit.
<b>SLV-2</b> Launched 26 June 1958.	To launch into orbit a 20-in., 21.5-lb "X-ray and environmental" satellite identical to that of TV-5.	The second-stage propulsion system shut down after 8 sec of burning, so that the velocity was low and the third stage was never armed for firing. As a normal result of the premature shutdown, second-stage propellant tank pressures exceeded design values, proving the structural integrity of the tankage.
<b>SLV-3</b> Launched 26 September 1958.	To launch into orbit a 20-in., 23.3-lb "cloud cover" satellite. This satellite was to measure the global distribution and movement of cloud cover and to contribute to the basic knowledge of the earth's energy budget.	The flight was normal (or better) in all respects, except that second-stage performance was well below minimum predicted. The burned-out third stage and the satellite reached an altitude of about 265 stat mi, but the velocity was about 250 fps short of the 25,000 fps required to orbit. The satellite was presumably destroyed during atmospheric re-entry some 9200 stat mi downrange.

## FLIGHT SUMMARY (cont)

	Vehicle Improvement	
Engineering Achievements	Deficiency	Corrective Action
<p>The objective of launching an earth satellite during the IGY was accomplished 2½ years after inception of the program. It was accomplished by a vehicle originally intended for flight test purposes only, the first time the Vanguard second stage was ever separated and ignited in flight. The flight also demonstrated the practicality of the use of strapped-down HIG gyros for guidance and of the Vanguard technique for first-stage separation without auxiliary thrust.</p> <p>SLV-1 carried 75 lb (a 22-lb satellite and the 53-lb third-stage rocket case) to an altitude of about 2130 stat mi and to a downrange distance of about 5860 stat mi. The satellite flew for 20 min and was in the space environment long enough to be of significant scientific value. Micrometeorite impacts were measured over a large altitude range.</p>	<p>The second-stage shutdown sequence was not completed because a relay (K2) did not "latch in" electrically after being energized by the second-stage thrust chamber pressure switch. This was due either to a design deficiency in the relay sequencing (K1-K2) or to an in-flight component malfunction within the relays.</p> <p>Attitude reference was lost at second-stage burnout because of a disturbing moment, probably caused by structural failure of the second-stage thrust chamber as a result of high frequency combustion instability at shutdown. This phenomenon can apparently occur during oxidizer exhaustion shutdowns if the fuel valve is not closed rapidly enough.</p> <p>A restriction in the second-stage oxidizer feed system, and the resulting low oxidizer flow rate, was probably caused by heat-treat scale from the oxidizer tank walls collecting at and partially clogging the filter screen in the feed line. The low oxidizer flow rate kept the chamber pressure below the level necessary to continue engine operation after the cutoff system was armed.</p> <p>A restriction in the second-stage fuel feed system, and the resulting low fuel flow rate, was probably caused by contamination from the fuel tank partially clogging the fuel injector. The low fuel flow rate produced inefficient burning and a total impulse from the second stage that was about 20% below the nominal predicted. The contamination was believed to be Buna-N rubber particles inadvertently introduced during prelaunch testing.</p>	<p>The contact that could result in de-energizing the relay that arms the second-stage separation and third-stage firing circuits was removed. The purpose of this contact had been to open a bypass valve permitting greater flow of helium from the propellant tanks to the control jets during coasting flight. Flight analysis showed that this feature could be eliminated.</p> <p>In addition to the thrust chamber pressure switch (TPS) shutdown, an oxidizer probe shutdown capability was provided for subsequent vehicles. The oxidizer probe was designed to initiate an earlier shutdown than the TPS system in the case of oxidizer exhaustion, thus preventing the conditions that lead to combustion instability.</p> <p>"Pickling" procedures were implemented for removal of heat-treat scale from the interior of the second-stage oxidizer tanks. Arming of the TPS shutdown was delayed about 25 sec to preclude shutdown due to slow thrust build-up.</p> <p>The Buna-N helium fill hose was replaced by a flexible metal hose. All second-stage tanks were "pickled" to completely remove heat-treat scale. All second-stage thrust chamber assemblies were returned to Aerojet-General for complete reconditioning. Testing procedures were changed to minimize the necessity for breaking into the propulsion system and to prevent contamination of any kind.</p>

## FLIGHT SUMMARY (cont)

Vehicle	Flight	
	Objectives	Results
<b>SLV-4</b> Launched 17 February 1959.	To launch into orbit a 20-in., 23.7-lb "cloud cover" satellite identical to that of SLV-3.	SLV-4 placed 71.5 lb (23.7-lb payload and 47.08-lb third-stage motor case) in an orbit estimated to last at least 200 years. The initial orbit had a perigee of 346 stat mi, an apogee of 2063 stat mi and a period of 125.9 min. The guidance system produced a negligible overall error in injection angle of $0.02^\circ \pm 0.2^\circ$ .
<b>SLV-5</b> Launched 13 April 1959.	To launch into orbit a fully instrumented, 13-in. diameter "magnetometer" satellite and an expandable (30-in.) aluminum sphere. The satellite was to determine if the predicted Störmer-Chapman ring current exists and to improve our knowledge of the earth's magnetic field. The expandable sphere was to supply information on upper air density.	Second-stage pitch attitude control was lost during first-stage separation. The resulting tumbling motion in the pitch plane aborted the flight.
<b>SLV-6</b> Launched 22 June 1959.	To launch a 20-in. diameter, 23.8-lb "radiation balance" satellite into an orbit with a relatively high inclination angle (about 48 degrees) to the equator. This satellite was to measure the direct radiation of the sun, the radiation reflected from the earth and the long-wave radiation emitted by the earth and its atmosphere.	There was a rapid decay of tank pressures immediately after second-stage ignition. Abnormally low flow rates and chamber pressures resulted, accompanied by combustion instability. About 40 sec later, the helium sphere exploded due to unrelieved buildup of pressure by the heat generator. The trajectory was accurately modified from a launch azimuth of $100^\circ$ to a flight azimuth of about $48^\circ$ by the use of in-flight roll programming just after launch.
<b>TV-4BU</b> Launched 18 September 1959. This vehicle incorporated the Allegany Ballistics Laboratory X248 A2 solid propellant motor as the third stage in place of the Grand Central motor used in previous Vanguard vehicles.	To launch into orbit a fully-instrumented, 52-lb "magnetometer, X-ray and environmental" satellite. This payload combined the scientific objectives of the TV-5 and SLV-5 satellites.	TV-4BU placed 94.6 lb (52.25-lb payload and 42.3-lb third-stage motor case) in an orbit estimated to last at least 50 years. The initial orbit had a perigee of 317 stat mi, an apogee of 2326 stat mi and a period of 130 min. The guidance system produced a negligible overall error in injection angle of $0.05^\circ \pm 0.2^\circ$ .

## FLIGHT SUMMARY (cont)

Engineering Achievements	Vehicle Improvement	
	Deficiency	Corrective Action
<p>A full-sized satellite was successfully launched seven weeks after the official end of the IGY. Two weeks after launch, the separated third-stage motor case was found to be in a higher-energy orbit than the satellite, which was the first detected flight evidence of significant residual thrust in the third stage after burnout. Further evidence was discovered in the TV-4, SLV-1, and possibly the SLV-3 and TV-4BU flights.</p> <p>The successful use of in-flight roll programming to rotate the flight azimuth some 52 degrees from the launch azimuth demonstrated the practicality of this technique on the first attempt. Completely successful operation of the first stage occurred with better than nominal performance for the eighth consecutive time.</p> <p>The third orbit achieved by the Vanguard program was accomplished about nine months after the end of the IGY, four years from the inception of the program. A total of four out of the six scientific experiments originally planned for Vanguard were placed in orbit. This flight also demonstrated the remarkable accuracy of the Martin probability method of performance prediction. As a result, it can be shown that this vehicle would be expected to launch a 100-lb payload into a 180-mile perigee orbit.</p>	<p>An undesirable satellite tumble rate of approximately 15 rpm about an axis almost normal to the spin axis was superimposed on the existing spin rate of less than 1 rpm about the spin axis. This apparently occurred during separation of the satellite from the burned-out third-stage motor case. The major contribution to the observed tumble rate was attributed to interference between the spring and a sharp shoulder on the separation device.</p>	<p>A thin metal sleeve was placed in the separation hardware to prevent such binding for SLV-5 and SLV-6. The separation spring was restrained at the third-stage side, rather than being a free body between the stage and payload.</p>
	<p>Unusually large side forces acted on the second-stage engine nozzle during the first-stage separation sequence, presumably caused by nozzle flow separation as back pressure built up in the interstage compartment. This condition lasted longer than normal because of a nearly 0.3-sec delay in stage separation. The actuators were overpowered and the engine driven hard into the limit stops, causing the pitch actuator lug to fail in tension.</p>	<p>The primary first-stage separation signal was changed so that separation would be initiated 0.1 to 0.3 sec earlier. A check valve was added in the hydraulic system to reduce the rate of engine deflection due to any overpowering force on the actuator. Precautions were taken to prevent excessive or nonuniform accumulation of nozzle closure adhesive on the thrust chamber wall.</p>
	<p>The second-stage main helium pressure regulator that controlled the flow of pressurizing gas to the propellant tanks apparently opened only partially when energized during the ignition sequence.</p>	<p>The regulator was modified to prevent mechanical binding, provided with a protective cover and subjected to special flow checks prior to flight. A back-up energizing signal for regulator operation was installed.</p>

The Vanguard vehicle is considered "operational" inasmuch as a thorough analysis of the TV-4BU flight was the first such effort on Vanguard that resulted in no significant vehicle change recommendations. It is considered a major engineering achievement to have developed an "operational" multistage space vehicle after a program of 14 flight firings.

## B. VEHICLE TRAJECTORIES

The ability of the Vanguard flight plan and trajectory to achieve the necessary orbit injection conditions was demonstrated three times (TV-4, SLV-4 and TV-4BU). Command control capability was maintained throughout the critical portions of all Vanguard flights, and range safety requirements in general were fulfilled. Impacts of the various stages were always in safe areas, and impacts of all nonmalfunctioning stages were within predicted areas. Measured trajectory parameters at significant trajectory events are presented for the Vanguard flights in Table 16.

***Azimuth control***—All vehicles deviated slightly to the south of the launch azimuth, primarily because of the earth's rotation (coriolis effect). Most of the remaining deviations, which could not be predicted in advance, were accounted for by the effects of measured winds and thrust misalignments. The small remnant was attributed to gyro heading misalignment. Flight values at second-stage burnout that may be considered typical are given for SLV-3. The vehicle was 1.1 degrees south of the 107.5-degree launch azimuth at second-stage burnout, of which 0.6 degree was expected from the Coriolis effect. The combined effects of measured winds and thrust misalignments accounted for 0.1 degree, and 0.3 degree was caused by a roll jet malfunction which rotated the pitch plane three degrees between 105 seconds and first-stage burnout. The remaining 0.1-degree deviation was attributed to gyro heading misalignment.

***Pitch control***—The attitude pitch programs were inserted as planned. All pitch programs successfully produced near zero-lift trajectories. The injection angles of the successful flights were well within the  $\pm 1.2$ -degree (three-sigma) tolerance, indicating the adequacy of the spin-stabilized attitude control of the third stage and the overall guidance system performance.

## C. AERODYNAMICS

Ten successful Vanguard firings, through the regime where aerodynamic forces were significant, have proven the validity of the aerodynamic design procedures.

***Angle of attack***—Calculated angles of attack, based on best estimates of flight performance and the measured wind profile, were in good agreement with the angles measured on the TV-4 and TV-5 flights, lending confidence to the values calculated for later vehicles. The angle of attack for all vehicles at maximum dynamic pressure was always within a safe limit. The largest calculated value of 5 degrees occurred during the SLV-1 and SLV-5 flights. This compared to the maximum allowable angle of 5.5 degrees (which was later changed to 7 degrees as more information became available). The 5-degree angles of attack

were a result of unusually high wind shears encountered at these times. In fact, the wind profile measured preceding the SLV-1 launch was considered marginal, as evaluated by the current wind shear criteria. Maximum dynamic pressures averaged about 600 psf and occurred about 78 seconds after liftoff, generally near the 39,000-foot altitude (see Table 16). This value exceeded the early design maximum dynamic pressure of 590 psf because final first-stage engine performance exceeded that which was expected to be the maximum during the early design phase.

***Aerodynamic heating***—Skin temperature measurements on the nose cone and along the length of TV-2, and motor compartment and internal equipment measurements on the test vehicles verified the conservatism of the design temperatures. The peak measured temperature at a station 47 inches aft of the theoretical cone tip was 234°F compared to a design value of 750°. Moving aft, the margin between design and actual temperature decreased approximately as follows: nose cone, 500°F; truncated cone, 100°F; tail can, 90°F. Compartment and internal equipment temperatures measured on the test vehicles were also much less severe than those for which the equipment was designed.

***Wind shear criteria***—The wind profile was measured before all Vanguard flights and evaluated with the existing wind shear criteria to determine whether the vehicle could fly without exceeding design limits. There were no excessive wind shears during flight countdowns, although conditions were considered marginal before the SLV-1 flight, when a wind shear of 12.7 fps per 1000 feet of altitude was measured between 24,000 and 32,000 feet four hours before launch. The maximum limit between these altitudes was 13 fps per 1000 feet, according to the criteria then in use. Wind shears aloft preceding the SLV-5 flight were even more severe, but they were considered satisfactory in terms of revised wind shear criteria.

***Wind-induced oscillation spoilers***—The rubber spoilers mounted on the second stages of all Vanguard vehicles appeared to perform their function, as there were no periodic oscillations of significant amplitude noted prior to any flight or static firing. The times of spoiler peel-off for the TV-4 and SLV-3 flights were later than desirable to keep aerodynamic drag and roll disturbances to a minimum. Considerable additional effort was expended to develop an installation procedure that would ensure early peel-off times. Motion pictures of the early portions of the SLV-4 flight showed that all twelve spoilers peeled off as intended.

***Launch wind criteria***—The winds during the TV-3 launch came closest to maximum allowable condition, being only 3 miles per hour less than the limit of 17 miles per hour with the original fixed launch

**Table 16. Measured Trajectory Parameters**

	TV-4	TV-5	SLV-1	SLV-2	SLV-3	SLV-4	SLV-5	SLV-6	TV-4BU
<b>MAXIMUM DYNAMIC PRESSURE</b>									
Velocity (fps)	1,300	1,365	1,360	1,480	1,452	1,305	1,313	1,400	1,386
Altitude (naut mi)	6.04	6.38	6.43	7.29	6.90	6.26	5.94	6.55	6.62
Range (naut mi)	1.25	1.15	1.33	1.68	1.52	1.40	1.35	1.51	1.49
Time (sec)	76	75	76	82	77	76	71	78	79
Dynamic pressure	601	620	606	600	610	594	583	625	603
<b>FIRST-STAGE SEPARATION</b>									
Velocity (fps)	5,820	5,970	6,155	5,910	6,050	6,182	6,281	6,200	6,030
Altitude (naut mi)	35.6	34.2	34.7	33.3	35.0	34.7	36.6	34.5	34.3
Range (naut mi)	20.4	21.9	23.8	22.0	21.6	23.9	24.4	23.6	23.9
Time (sec)	144	140.7	143.5	143.4	140.2	144.1	142	144.5	145.6
<b>SECOND-STAGE CUT-OFF</b>									
Velocity (fps)	12,600	13,690	14,030	6,085	11,057	13,680	5,000		13,500
Altitude (naut mi)	148	131	134	39.5	120	117	81.9		129
Range (naut mi)	142	166	169	28.2	130	139	91.5		161
Time (sec)	266	262	261.5	152.6	248.6	260.8	243.9		263.1
<b>THIRD-STAGE IGNITION</b>									
Velocity (fps)	10,946		13,110		10,663	12,772			12,857
Altitude (naut mi)	351		325★		223	300			276★
Range (naut mi)	655		721		410	652			673
Time (sec)	606		568		436	542			546.4
<b>SECOND-STAGE APOGEE</b>									
Velocity (fps)	10,946	12,870	13,030	5,516	10,558	12,743	4,998		12,851
Altitude (naut mi)	351	294	323★	89	228	306	82.0		275★
Range (naut mi)	657	713	773	127	475	716	91.9		691
Time (sec)	607	574	599	296	484	580	248		559.1
<b>THIRD-STAGE BURNOUT</b>									
Velocity (fps)	26,935		23,045		24,770	26,860			27,193
Altitude (naut mi)	355		360		227	300			276
Range (naut mi)			808		467	741			768
Time (sec)	640		601		469	575			582.3

★ Apparent discrepancy is the result of tolerances in different measuring systems (Radar & Minitrack)

stand. Surface winds for the SLV-3 and SLV-5 launch were as large, but were not considered significant, since the retractable launch stand had been incorporated with allowable surface winds of 35 miles per hour.

## D. STRUCTURE

The performance of the Vanguard structure, as indicated by telemetered flight data, demonstrated that the design criteria, except for the conservatism in aerodynamic heating, were reasonable and sufficiently accurate. There were no known structural failures in flight, except in cases of component or system malfunctions.

**Differential pressures across skins**—Calculations were made to determine the magnitude of air bleeding through joints and other small openings during ascent. Telemetered measurements (the first of this kind known to have been made) on TV-2 and TV-4 (Refs. 40 and 43) verified these theoretical calculations given in Ref. 12.

**Information gained from the failure of TV-3BU**—Experimental verification of many of the parameters entering into the structural analysis was obtained during the ground vibration survey of the complete Vanguard vehicle structure; however, no experimental verification had been obtained for the complete system analytical representation upon which the dynamic load calculations were based. The TV-3BU flight failure (see Chapter VIII, Section A) provided the opportunity for determining the validity of the system analytical representation. The telemetry data gained from the flight before breakup showed vehicle and engine motions similar to cases analyzed to predict the dynamic bending moment contributions to the design bending moment envelope.

A program correlating the flight data of TV-3BU with the theoretical analyses was undertaken to establish the accuracy of the analyses and to obtain failure predictions for comparison with the actual flight failure. Control, servo and engine hardware were used, while the elastic structure and aerodynamic loads were simulated by analog techniques (see Ref. 52). The engine pitch deflections were externally commanded to follow the TV-3BU flight transient motion that occurred from 57.35 to 57.51 seconds. The one-second oscillation that followed arose from the first elastic mode through structural feedback, since the external command to the engine during this time was zero. All subsequent spurious pitch engine motions were externally commanded to produce the remainder of the simulated flight. The correlation of the simulation with the flight motion is shown in Fig. 44. The actual engine deflection and the simulated engine deflection

differ during the first portion of the transient because no flight trim angle was included in the simulation study.

Stations 327 to 358 were the longitudinal stations at which the failure limit moment was exceeded. A bending moment time history that resulted from the simulation engine motions was obtained for this area (see Fig. 44). Failure was expected at about 61.7 seconds but could have occurred any time after 60.5 seconds because of the neglected static trim moments. The simulation study indicated failure within about 0.1 second of the time of actual failure and in the approximate region where it occurred. Failure was not predicted in any other region.

Such a correlation is particularly significant in that a new philosophy was developed during the Vanguard design. This design philosophy, as previously noted, is embodied in the use of the control system, through otherwise detrimental structural feedback, to control the loads and the bending moments which the vehicle would normally develop in flight. Experimental verification of this philosophy was extremely important if its application to future designs were to be effected.

**Controls bay panel**—Telemetered data indicated a high vibration environment at the controls bay panel in the second stage. However, the high indicated g levels 47 seconds before ignition on TV-3BU, coupled with 30 g's recorded prior to burnout on the successful TV-4 flight, must cause the recorded accelerations to be viewed with care. Improvements were incorporated in later vehicles that precluded the possibility of an adverse vibration environment. These included stiffening the structure to raise the natural frequency, spraying the inside of the controls can with insulating lacquer and changing the major wiring cable to the pitch servo amplifier.

**Proof of design, second-stage tankage**—Two aborted flights (SLV-2 and SLV-6) may be considered as exceptional structural tests of the second-stage tankage. On SLV-2, ignition of the heat generator in the second-stage helium sphere, coupled with premature cutoff of the engine, caused unusually high system pressures which were near (within 89 to 95%) the design burst pressures of the helium sphere and propellant tanks. However, there was no indication of structural failure prior to atmospheric re-entry. On SLV-6, rupture of the second-stage helium sphere, caused by a malfunction of the helium pressure regulator, occurred only after the differential pressure between the sphere and the tanks had built up to more than 115% of the minimum design burst pressure.

**Second-stage actuator support lugs**—The maximum tension load imposed on the second-stage engine actuators during the first-stage separation sequence of SLV-5 occurred when an overpowering force of about

11,000 pounds (computed from the engine motion rate of 146 deg per sec) drove the engine into the stops in the pitch-up direction. When the engine hit the stops (assuming that all components of the actuation system were still within the elastic range), the total load, including impact forces, was between 12,000 and 16,000 pounds, which was sufficient to fail either the actuator or the engine lugs. Records from the actuator follow-up potentiometer after the engine hit the stop, maintenance of hydraulic pressure and continued engine thrust indicate that only the end of the actuator or the connecting lugs on the engine could have failed. For tension loads, the engine lug was the weakest link and would be expected to fail first.

The engine lugs were made of 6061 aluminum alloy and, as originally designed, were to have a heat treat condition of T6 (maximum strength). Welding of the injector assembly to the thrust chamber, however, caused the lugs to become overaged and to have strength properties between 0 (soft) and T4 (intermediate). Lugs in this condition would be adequate for the limit design load of 2500 pounds but would be expected to yield (0.2% permanent set) at about 3000 pounds and fail at about 8000 pounds tension. Modifications to the first-stage separation sequence for SLV-6 and TV-4BU (see Chapter VIII, Section E) reduced the loads on the actuator lugs to acceptably safe values.

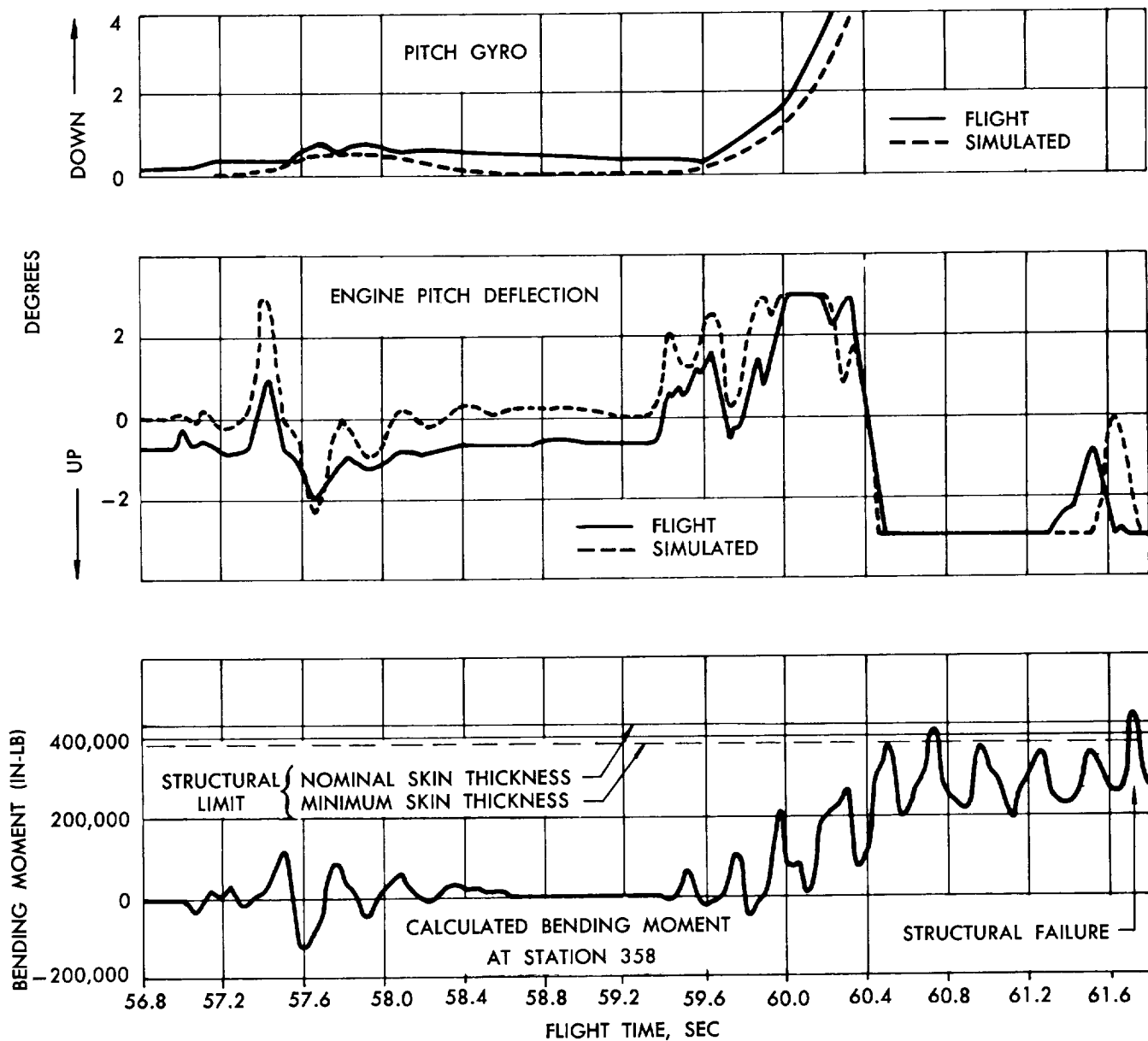


Fig. 44 Time Histories of Vehicle Bending Moment Resulting from Abnormal Engine Pitch Motions, TV-3BU



## VIII. SYSTEMS

### FLIGHT ANALYSIS

Important system flight analysis results are summarized below. More detailed studies may be made if desired by referring to the series of Vanguard flight analysis reports (Refs. 38 through 51).

#### A. GUIDANCE AND CONTROL

The adequacy, integrity and reliability of the Vanguard guidance and control system was demonstrated by the accuracy of vehicle trajectories on all flights and the small satellite injection angles achieved on the orbits. A graphical summary of flight performance of the major components and systems is given in Figs. 45 and 46 for TV-4 through TV-4BU.

##### 1. AIRBORNE GUIDANCE

**Gyroscope reference system**—There were no indications of any gyroscope reference system malfunctions throughout the program. Pitch rate information was telemetered as a function of pitch torquer voltages, from which the rates could be derived. Ripple in the torquer voltages prevented an exact determination of the pitch rates. However, the maximum and minimum rates, derived from the maximum and minimum torquer voltages, always bracketed the prescribed rate, thus indicating that pitch rates were nominal.

A further check on the accuracy of the pitch program rates and, indeed, of the entire guidance and control system, was obtained as a result of the trajectory match program (see Chapter IX, Section B). The fact that the match data so closely followed the predicted trajectories was another excellent indication of the accuracy of the gyro system as a control reference and as part of the vehicle guidance system.

**Program timer**—Performance of the program timer in flight is given in Fig. 47. The specification tolerance for pitch rate insertion times was  $\pm 0.10$  second. The maximum deviation occurred on TV-5, when the fourth pitch rate came through 0.07 second late. Deviations of 0.10 second for the second-stage arming signal occurred on SLV-1 and SLV-2 flights. The time tolerance for this function was  $\pm 2.0$  seconds. The average error for all functions on all flights was 0.03 second.

The only instance of a program timer failure in flight occurred on TV-4, for which the 10-second telemetry timing signal was lost after 460 seconds of flight. The signal returned at 650 seconds and continued normally

until 720 seconds, the termination time for program timer operation. The loss of information from this channel could have been the result of a sticking micro-switch. This signal loss complicated the data reduction process somewhat but was in no way detrimental to the flight of the vehicle.

**Airborne third-stage firing system**—The airborne third-stage firing system initiated the third-stage spinup and firing sequence on all three of the successful satellite launches and also on SLV-1. Telemetry records indicated proper coasting time computer operation on all flights. Flight firing operations, as well as pre-launch tests, all demonstrated that the airborne third-stage firing system was a reliable and accurate unit.

Coasting time errors, based on the difference between the actual coast time and the coast time calculated from the telemetered coasting time computer velocity, were all less than 2.5 seconds. Typical error values were 2.4 seconds on TV-4BU, 1.3 seconds on SLV-4 and 0.7 second on SLV-1. The coasting time mechanism was not started on TV-5 because a second-stage burnout signal was not received from the second-stage engine sequencer. The timing arm did not start on SLV-2, SLV-3 and SLV-6 because vehicle velocity was less than the minimum required to start the mechanism.

##### 2. GROUND-BASED THIRD-STAGE FIRING SYSTEM

The independent ground-based backup third-stage firing system was actuated on five Vanguard flights and appeared to function reliably. Third-stage ignition was successfully initiated by the ground-based system on SLV-3, with an indicated coasting time error from the ideal of 3.2 seconds, which was somewhat large, but still well within tolerances. The actuation signals were received by the SLV-4 and TV-4BU vehicles, but were merely exercises to check the hardware since the airborne system had already given third-stage ignition.

A ground-based attempt was made on SLV-1, but did not succeed because of a faulty command receiver (see Chapter VIII, Section J). However, unknown to ground personnel because of a temporary telemetry loss, the airborne system functioned properly. A ground signal was also sent on SLV-2, but was blocked because the second stage did not burn long enough to arm the third-stage firing system.

Slight modifications to the ground-based system were made during the Vanguard program. The smoothing

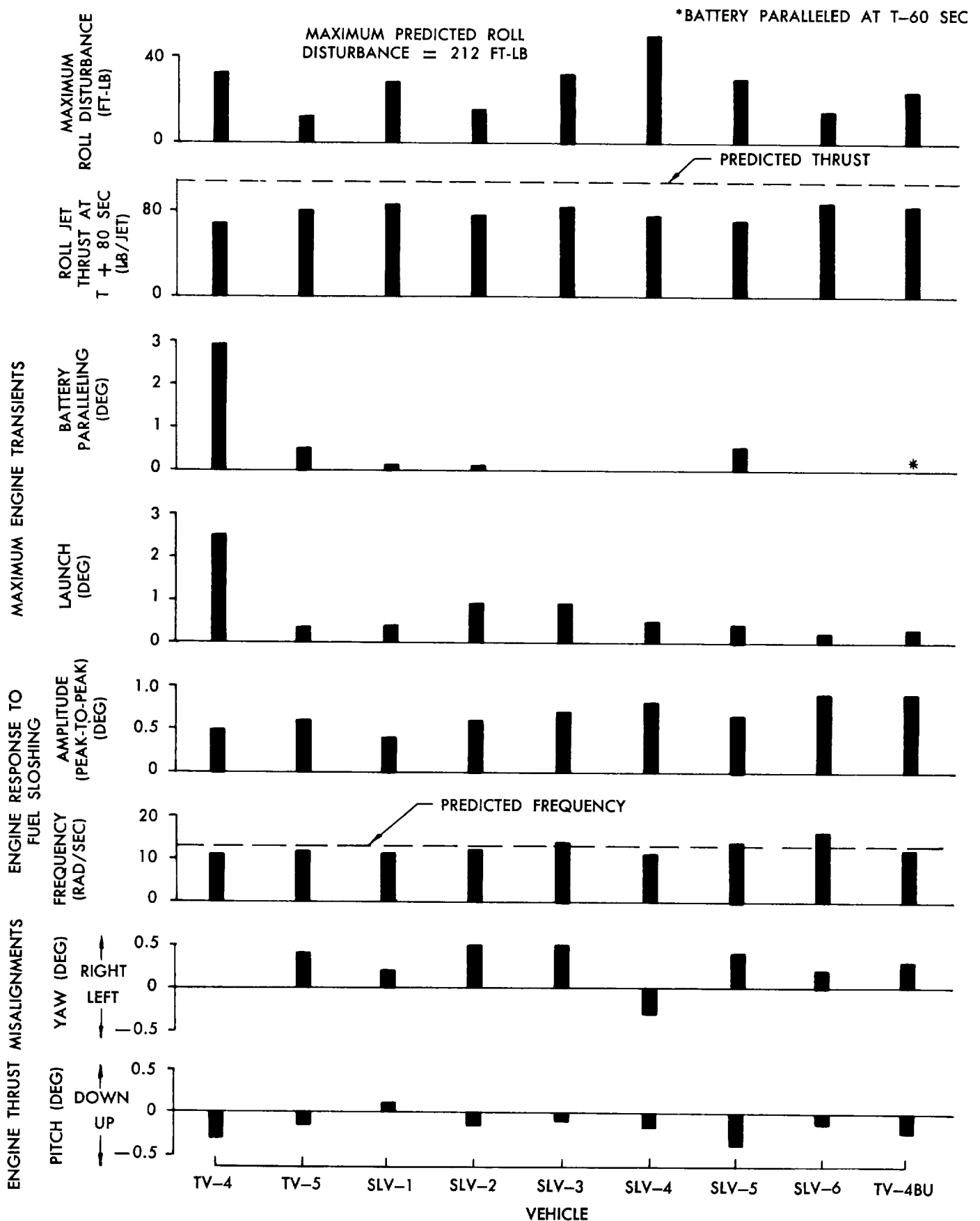


Fig. 45 First-Stage Controls Performance

NOTES:

- 1 NO TELEMETRY DATA DURING COASTING FLIGHT.
- 2 COASTING FLIGHT SYSTEM NOT ARMED.
- 3 NO DATA DUE TO POWERED FLIGHT MALFUNCTION.

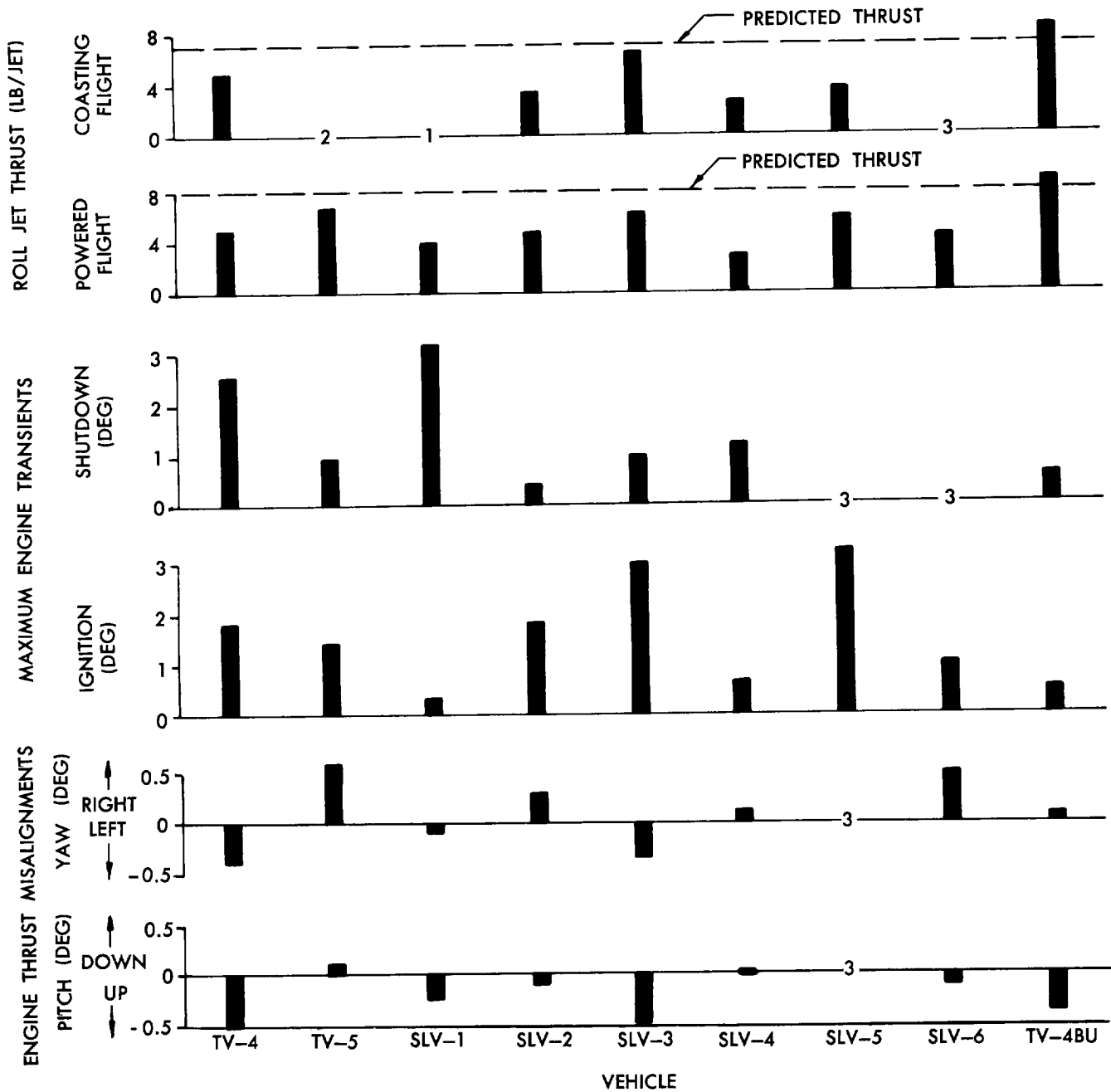


Fig. 46 Second-Stage Controls Performance

process of the radar data was improved. Capability was added for a backup direct firing command after spinup had been initiated by either system. In addition, a second-stage burnout signal was transmitted to the computer operator from a person watching several real-time telemetry channels, an improvement over the previous method of watching the impact point.

### 3. FIRST-STAGE PITCH AND YAW CONTROL

The operation of the first-stage pitch and yaw control system for TV-4 and all subsequent vehicles is summarized in Fig. 45. Typical vehicle motions and controls reactions are shown in Fig. 48.

**TV-3BU malfunction**—The only flight failure in the guidance and control system occurred on the TV-3BU flight. The pitch and yaw control system operated satisfactorily for the first 57 seconds of flight, as indicated by telemetered data. At that time, spurious first-stage engine motions in the pitch plane produced large dynamic structural loads on the vehicle. These loads, coupled with a rapid pitch down of the vehicle (which developed large air loads), caused a major structural failure at the aft end of the second stage (see Chapter VII, Section D). Each abnormal engine pitch movement that occurred was accomplished with maximum engine-down rate, indicating a hard-over hydraulic transfer valve. The second-stage engine did not follow the spurious motions. To produce such a condition would require a malfunction in the first-stage servo-amplifier or in interconnecting wiring associated with the first-stage pitch follow-up potentiometer, servo-amplifier, or hydraulic valve. A malfunction involving the follow-up potentiometer circuitry appeared most likely and was most probably caused by a broken or open circuit somewhere in the associated wiring. The corrective action consisted of increased quality control and the use of redundant interstage wiring, as discussed in Chapter V, Section F and in Ref. 42.

**Thrust misalignments**—Engine thrust misalignments were present to a degree on all flights, as indicated in Fig. 45. The thrust misalignments were almost invariably in the pitch-up and yaw-right directions, and were generally greater in yaw than in pitch. Maximum misalignments present on any flight were 0.5 degree yaw-right on SLV-2 and SLV-3. However, the average misalignment was only 0.3 degree in yaw and 0.15 degree in pitch. These relatively small misalignments were not considered detrimental to vehicle control.

**Propellant sloshing**—Propellant sloshing in the tankage, initiated by vehicle motions, caused engine oscillations as indicated in Fig. 45. The frequencies of the oscillations varied, vehicle to vehicle, from about 1.8 cps to 2.5 cps. The predicted slosh frequency was

2.1 cps. The amplitude of the oscillation varied from 0.5 to 0.9 degree peak-to-peak. This engine oscillation represented a limited instability in the autopilot loop, but never affected overall pitch and yaw control. The engine oscillations generally began in the interval between 100 and 120 seconds and continued until first-stage burnout.

**Launch transient**—Vehicle and engine motions associated with launching were relatively small, with the exception of TV-4, as shown in Fig. 45. An engine correction of 2.5 degrees right (in yaw) resulted from a 1.3-degree left vehicle error at liftoff on TV-4, when one swingaway arm of the launch stand did not release properly. This transient motion was sufficient to excite first bending mode oscillations (about 3 cps) which were damped out within 3 seconds, indicating effective control of structural feedback. Control during the launch transient was considered excellent in view of the adverse conditions.

**Maximum dynamic pressure**—Control through the maximum dynamic pressure region of first-stage flight, where the airloads could be high, was excellent in all cases. Engine deflections required to correct for vehicle attitude errors ranged from 0.5 degree to 1.5 degrees on most flights. Engine deflections of about 2 degrees were required for pitch and yaw control of SLV-1 because of the unusually high wind shears aloft. However, pitch and yaw control was adequately maintained during this transient.

### 4. FIRST-STAGE ROLL CONTROL

First-stage roll attitude control was adequately maintained on all flights by the two rotating jet nozzles. System performance is summarized in Fig. 45.

**SLV-3 roll jet malfunction**—The only instance of a partial first-stage roll control system malfunction occurred on SLV-3 flight where, after 106 seconds of flight, the up-left roll jet stuck in a 30-degree clockwise position. This caused the down-right jet to cycle at a rate of 2.5 cps in order to maintain vehicle roll control. The up-left jet deflection gradually decreased to an angle of about 7 degrees at first-stage burnout, with a concurrent decrease in the cycling rate of the down-right jet to about 1 cps. The maximum roll attitude error of 5.7 degrees during this malfunction was attained at 106 seconds. Thereafter, until first-stage burnout, roll attitude was maintained within 3.4 degrees by the rapid counterclockwise cycling of the down-right jet.

**Roll jet thrust**—First-stage roll jet thrust, calculated from vehicle inertias, jet-on times and roll gyro rates at 80 seconds flight time, was consistently lower than the predicted thrust level (Fig. 45). Although thrust was consistently low, it was always more than adequate to maintain roll control. For example, the

NOTE:

1. TIMES SUBJECT TO TELEMETERING ACCURACY OF  $\pm 0.00$  SEC.  
-0.05
2. ① NO REQUIREMENT FOR FUNCTION.
3. ② FUNCTION NOT TELEMETERED.

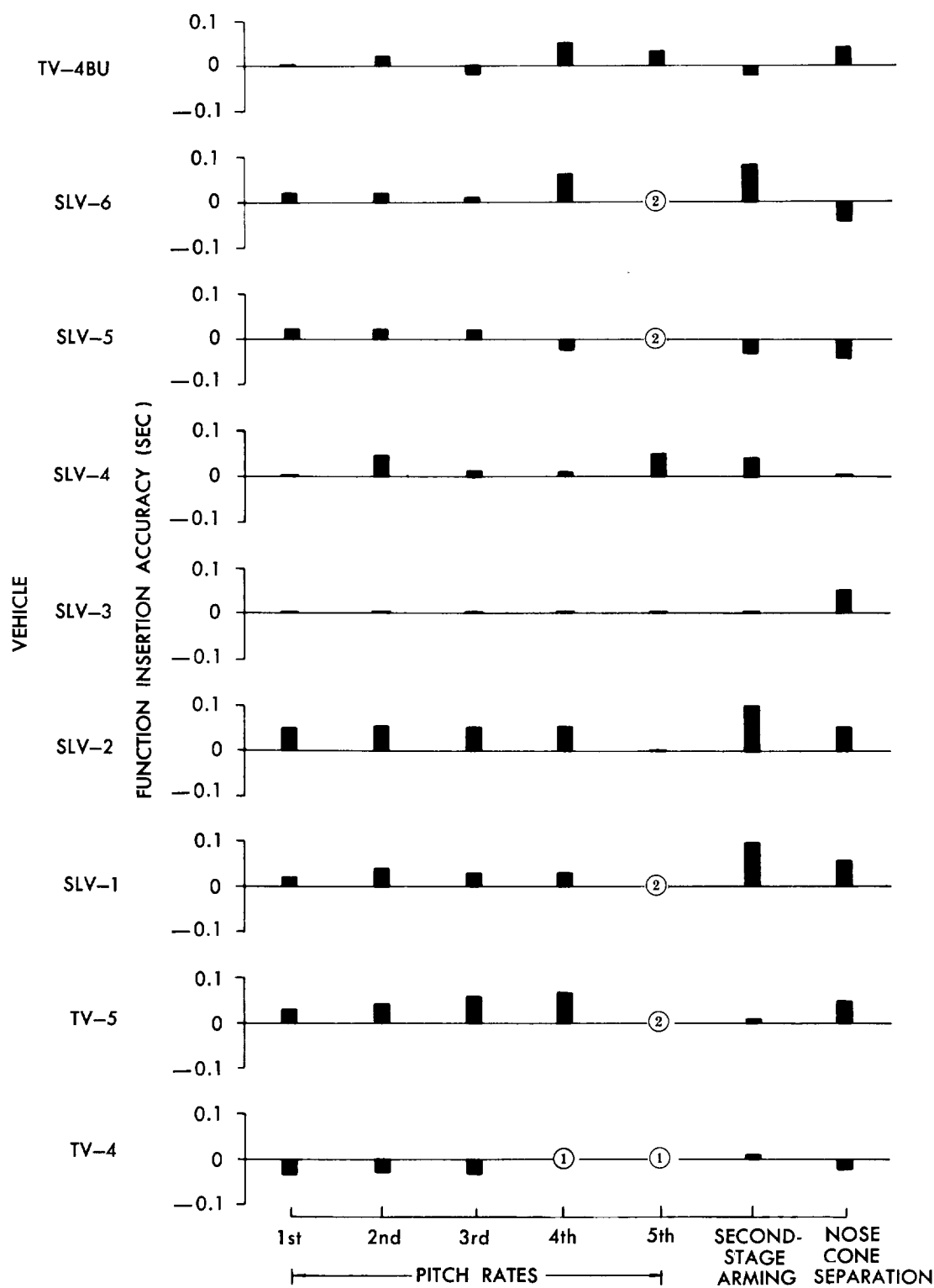


Fig. 47 Program Timer Operation

thrust at 80 seconds on TV-4 (the vehicle with the lowest roll jet thrust) was 68 pounds, which represented a 200-foot-pound correcting moment capability. The maximum roll disturbing moment encountered during this flight was only 33 foot-pounds, which was one-sixth of the magnitude of available correcting moment. Disturbances of similar magnitudes were experienced by other vehicles, with a maximum roll disturbance of 50 foot-pounds occurring on SLV-4 (Fig. 45).

The lower than predicted roll jet thrust levels can probably be attributed to leakage in the roll jets. The thrust levels were improved on the last two flights by using a new tool to form the flanges of the jets, which resulted in smoother flanges and tighter fits.

**Helium augmentation system**—The helium augmentation system provided additional roll control during the interim between first-stage cutoff and separation of the first and second stages, at which time roll disturbances could exceed the correcting capabilities of the second-stage roll jets alone. Thrust levels of the helium augmentation system were calculated on TV-5 and SLV-3 to be 117 pounds and 110 pounds, respectively. These thrusts were slightly below nominal, but were more than sufficient to ensure good roll control during separation. Thrusts could not be determined on other flights due to characteristic PPM/AM telemetry dropouts around first-stage burnout. However, from roll gyro records (PWM/FM telemetry) it appeared that helium augmentation thrust was always adequate.

**Roll program**—A roll program chassis was installed in the controls compartment of SLV-6 in order that an effective flight azimuth of 48 degrees could be achieved after an actual launch at 100 degrees. The chassis fed a signal to the roll torquer, which rotated the roll gyro reference axis at a rate of 3.07 degrees per second counter-clockwise from  $5 \pm 0.1$  seconds to  $22 \pm 0.1$  seconds. Roll torquer voltage was not telemetered, but the accuracy of the vehicle flight path indicated that the torquer rate was correct.

## 5. SECOND-STAGE POWERED FLIGHT PITCH/YAW CONTROL

The gimballed second-stage engine successfully maintained powered flight pitch and yaw control of the vehicle on all flights except on SLV-5, where data indicated that an engine pitch actuator lug broke during the second-stage ignition sequence.

**Ignition transients**—The magnitudes of engine motions occurring during the second-stage ignition sequence are shown in Fig. 46. Although engine transients were fairly large on several of the flights, pitch and yaw control was maintained except for SLV-5. For instance, the engine deflected 1.8 degrees at ignition of TV-4 and SLV-2, and may have hit the mechanical stop in yaw at ignition on SLV-3. These

engine motions and resultant vehicle motions, however, were rapidly damped out and adequate vehicle control was maintained.

The engine transients at second-stage ignition resulted from a combination of causes. At first-stage separation, loss of first-stage servo loads and changes in battery voltage (on vehicles TV-4 through SLV-5 where the dynamotor-filter combination supplied B+ to the autopilot) resulted in autopilot B+ transients, and hence in engine motions. The overpowering moments from the nozzle flow separation resulted in additional large engine deflections. Steady-state engine deflections following separation were caused by engine thrust misalignments.

**Shutdown transients**—Engine transients at second-stage shutdown were fairly small on all vehicles other than TV-4 and SLV-1, as shown in Fig. 46. The 2.6-degree engine yaw deflection on TV-4 was almost instantaneous and was rapidly damped out. The hard-over engine pitch-down deflection on SLV-1 at shutdown was called for by the control system in response to vehicle pitch-up motions due to a large external disturbing moment. The disturbance resulted from engine side forces such as would have been associated with a failure of the welds between the thrust chamber tubes caused by an unstable shutdown (Chapter VIII, Section C). This large disturbance produced a vehicle attitude error of about 75 degrees up. The gimballed engine was not capable of correcting for the large disturbance since thrust was decaying during this time (post-cutoff). The attitude jets regained control of the vehicle during coasting flight, but the 12.5-degree limit of the pitch gyro had been exceeded. Therefore, the control was about a new pitch reference, 63 degrees above the desired reference.

**Spurious gyro transients**—Spurious pitch gyro transients of about one degree were recorded during TV-4 flight, commencing at about 236 seconds. The engine response to the gyro signals was normal. The pitch accelerometers indicated vehicle accelerations were in phase with the initial engine deflections rather than the initial gyro errors. The large gyro error rate (7.6 degrees per second) would have required a 5000-foot-pound disturbance for 0.1 second. Such a disturbance would have caused a 0.5-g tail can acceleration, but there was none recorded. It was concluded that the pitch gyro transients were spurious, and were probably caused by an intermittent open circuit in the isolation amplifier of the gyro reference system. This type of malfunction, especially in the feedback loop, could have caused insertion of erroneous gyro signals. An occurrence of this type was not noted on any other flight. The TV-4 transient at 236 seconds was sufficient to induce pitch engine oscillations of about 2 cps, which agreed closely with the calculated propellant slosh fre-

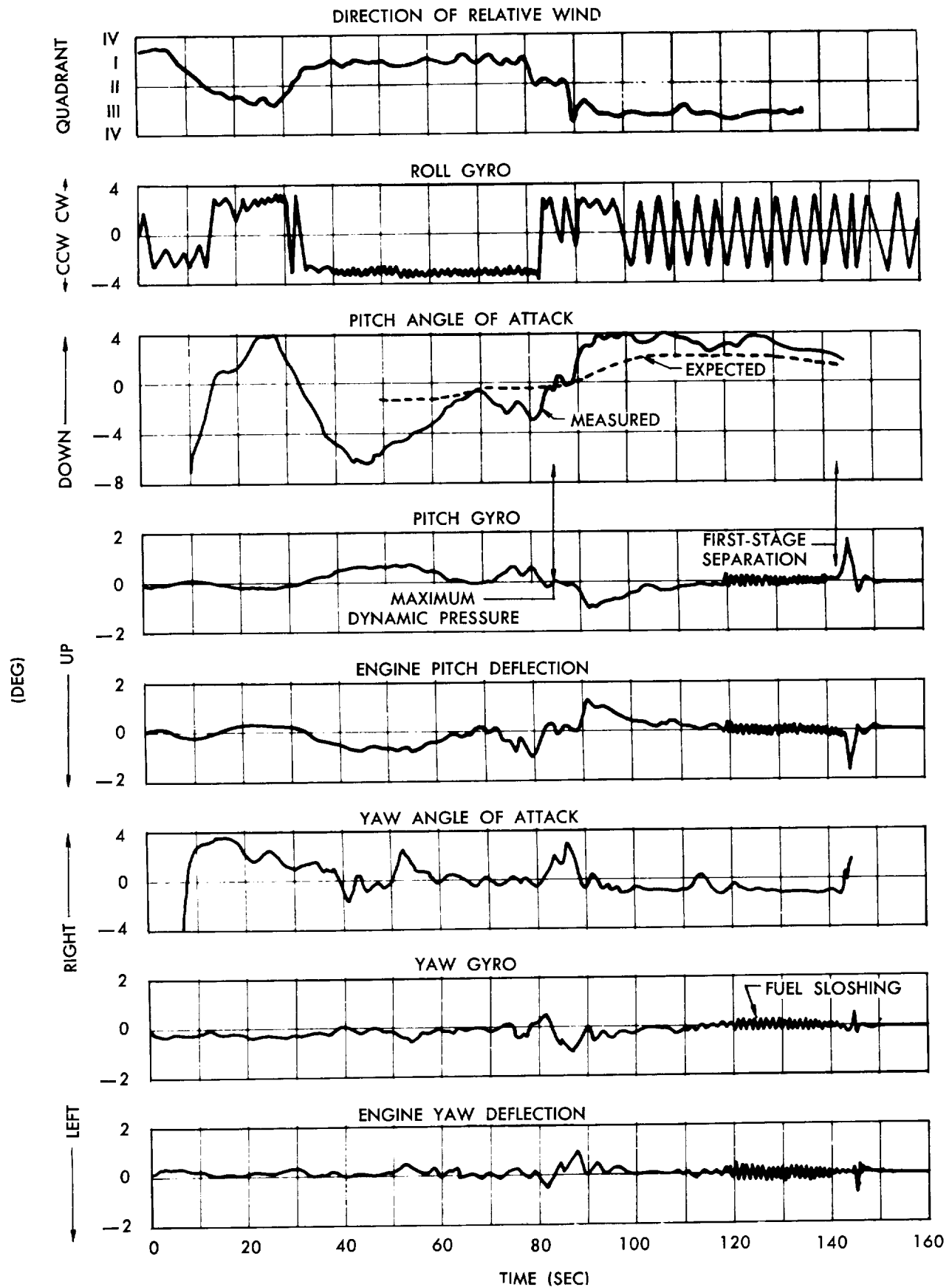


Fig. 48 Typical Angle of Attack, Vehicle Motions and Controls Reactions During First-Stage Powered Flight

quency. The oscillations were damped out within six seconds, and no detrimental effects on vehicle control were developed.

**SLV-5 actuator lug failure**—The second-stage engine of SLV-5 exhibited violent pitch and yaw motions, not commanded by the gyros, almost immediately after the start of chamber pressure rise, which were most probably caused by flow separation in the engine nozzle (see Chapter VII, Section D and Chapter VIII, Sections C and E). The engine bottomed on the 3.2-degree limit stops at least twice, once in the yaw-left direction at a rate of at least 55 degrees per second and again in pitch-up at about 146 degrees per second. This last pitch rate was high enough to fail the pitch actuator lug when the engine hit the stop.

After failure of the actuator lug, the normal hose loads in the flexible propellant feed lines probably moved the engine to a position 3 degrees down in pitch, while the actuator and follow-up potentiometer returned to zero deflection, as indicated on the telemetered engine records. The pitch thrust moment accelerated the vehicle down at about 35 degrees per second.<sup>2</sup> The resulting tumbling motion produced sufficient centrifugal force to throw the third stage and satellite free of the second stage 5 seconds after separation. About one second later, the vehicle began to roll, probably due to a roll moment from the hard-over engine in pitch. The vehicle rolled 25 to 30 degrees initially and was partially stabilized by the propane roll jets at a roll reference error between 20 and 25 degrees counterclockwise.

At about the same time that the vehicle began to roll, the yaw engine and gyro records, which had been normal, showed that the vehicle yawed right at an increasing rate. The engine moved hard over in yaw to effect a correction, but was unable to re-establish yaw attitude control during powered flight. It is believed that this motion was a result of the combined pitch tumbling and rolling motions being coupled into yaw, and possibly failure of either the thrust chamber torque link or the monoball, which would result in engine rotation as well as linear motion when the yaw actuator moved.

Propane was nearing exhaustion at 186 seconds flight time, whereupon roll control was completely lost and the vehicle began to spin up. Ten seconds later, the vehicle had become spin-stabilized along the longitudinal axis. The roll rate continued to increase until burnout, when it had reached 170 rpm.

**Thrust misalignments**—Engine thrust misalignments were present in varying magnitudes on all second-stage flights, as indicated in Fig. 46. The average magnitudes of the misalignments were 0.24 degree in pitch and 0.30 degree in yaw. The misalignment components indicated a tendency to lie along the up and right axes. Second-stage engine thrust misalignments were

more detrimental to control than first-stage engine thrust misalignments because of the gain relationship (2.67 degrees of gyro motion per degree of second-stage engine motion). Since the gyro error is in effect integrated throughout powered flight, the overall vehicle trajectory of the second and third stages after second-stage burnout could be adversely affected.

The procedures and specifications for second-stage engine alignment were reviewed and modified after the SLV-3 flight to correct for misalignments due to structural deflection and alignment of vehicle center of gravity off the gyro axis. Thrust vector misalignments on the next flight (SLV-4) were slight, as is indicated in Fig. 46. However, fairly large misalignments were in evidence again on SLV-6 and TV-4BU, indicating that still tighter control would be warranted on alignment procedures and specifications if there were more vehicles to be flown.

## 6. SECOND-STAGE POWERED FLIGHT ROLL CONTROL

Powered flight roll control was adequately maintained on all second-stage flights, except on SLV-5. In this instance, applied roll disturbing moments (see Subsection 5) were in excess of the design capabilities of roll jet correcting moment, and the partial loss of roll control was not attributed to the roll control system itself.

**Roll disturbance**—A small, fairly constant disturbing moment was present during second-stage powered flight on most vehicles. The disturbance varied in magnitude from 0.1 to 0.5 foot-pounds from vehicle to vehicle, sometimes clockwise and sometimes counterclockwise, but never changed direction on any given flight. The disturbance was attributed to moments initiated by propellant vortices forming in the emptying tankage and/or to small misalignments in the tubing that forms the inside surface of the exhaust nozzle. Other contributing factors might have been small aerodynamic disturbances and effects of engine thrust misalignments. Roll control was always adequate because of the small magnitude of the disturbance as compared to the available correcting movement.

**TV-5 roll control**—Roll control was maintained during powered flight of TV-5. An electrical malfunction prevented operation of the three-way roll valve at second-stage shutdown, so that the roll jet fuel supply was not switched to helium for coasting flight, as would have occurred in normal sequencing. The adequacy of the propane fuel reserve was demonstrated, since coasting flight roll control was maintained by the propane supply for more than 100 seconds of coasting flight recorded before telemetering signals were lost.

**SLV-6 roll disturbance**—The problem of low roll jet thrust never seriously affected vehicle control, since

even the low thrust on SLV-4 (Fig. 46) sufficed to ensure roll control during powered flight. A danger of low thrust, however, was pointed out by the large roll disturbance which occurred on SLV-6 at first-stage separation. This disturbance, apparently due to pivoting or tipping about the interstage disconnects (Chapter VIII, Section E), produced a high second-stage roll rate at the time of separation of the interstage disconnects. A telemetry dropout obscured the flight data for about 0.15 second after separation. When telemetry was regained, the vehicle was rolling clockwise at about 23 degrees per second. The counterclockwise second-stage roll jets were on, but the high rate caused the roll gyro to move beyond the telemetry demodulator saturation point (11.6 degrees); therefore, the maximum vehicle error could not be determined from the telemetry records alone. Phase plane analysis of this roll transient indicated that the maximum roll error attained before the rate was brought to zero was 12.2 degrees. Since the roll gyro gimbal capability, as determined by preflight bench tests, was 12.5 degrees, no loss of roll attitude reference was indicated. The roll jet thrust of 4.6 pounds per jet was about 40% below predicted. A nominal roll jet thrust of 8.5 pounds per jet would have contained the maximum roll excursion to less than 7 degrees. Within 2 seconds after separation, the roll jets were able to reduce the roll error below the telemetry demodulator limit and usable data were again obtained. Subsequent roll oscillations were eventually damped and a limit cycle was established within 10 seconds after separation. Adequate roll control was maintained throughout the remainder of powered flight.

**Roll jet thrust**—The roll jet thrust history is shown in Fig. 46. Adequate roll control was always maintained, but thrust values were generally below the nominal predicted level of 8.5 pounds per jet throughout the flight of vehicles up to and including SLV-6. The thrust ranged from 60% low on SLV-4 to 15% low on TV-5. The low SLV-4 thrust was attributed to low propane flow, due either to a low regulator setting or failure of one clockwise and one counterclockwise jet to operate properly.

A test program was conducted after the flight of SLV-6 to correct the low thrust level. The dynamic mockup that had been used in original system development tests (Chapter IV, Section A) was employed. It was discovered that leakage of an O-ring seal in the helium-propane regulator dome would cause a 25% reduction in regulated pressure and thrust at altitude. Other possible causes of low roll jet thrust were: failure of a jet solenoid valve to operate because of low pilot pressure; excessive system pressure drop; vena contracta effect at the sharp-edged nozzle throat; and/or liquid propane in the sensing port of the regulator. A

leakage test of the regulator dome was instituted, the regulator setting was increased, and nozzles having smooth throats were provided. The regulator was re-oriented to prevent liquid from entering the sensing port. The propane servicing procedure was also modified to purge liquid propane from the plumbing and to ensure attainment of the desired temperature. All of these modifications were incorporated on TV-4BU, and roll system performance in that flight was essentially as predicted.

## 7. SECOND-STAGE COASTING FLIGHT CONTROL

Adequate control was maintained on all flights other than TV-5, when the pitch/yaw jets were not energized due to an electrical malfunction, and SLV-6, which malfunctioned during second-stage powered flight.

**Pitch/yaw jet thrust**—Pitch/yaw jet thrust was relatively difficult to calculate using vehicle inertias, jet-on times and gyro rates, due to the small deadzone settings ( $\pm 0.4$  degree) of the control system, and to the resolution of the telemetered gyro data. Calculations on TV-4 yielded 6.0 pounds of thrust per jet (excluding the malfunctioning down jet which had 0.1 pound of thrust). The thrust on SLV-4 and TV-4BU was determined to be about 8.0 pounds per jet, or slightly above the nominal 7.2-pound value. Thrust levels on other flights were in the same general range, since coasting flight control was always maintained.

**Roll jet thrust**—Roll jet thrust history for the coasting flights of TV-4 and subsequent vehicles is presented in Fig. 46. The trend, as in powered flight, was for thrust to be lower than the predicted nominal value. The low thrust of 2.5 pounds per jet obtained on SLV-4 flight was due to the same items as the low thrust during powered flight; a low regulator setting, or the failure of one clockwise and one counterclockwise jet to operate properly. The low thrust of 3.5 pounds per jet obtained on SLV-2 was believed to be caused by liquid UDMH (considerable UDMH remained in the tank after the early cutoff) being expelled through the nozzles along with the helium. The thrust levels on SLV-2 and SLV-4, as on all other vehicles with low thrust, did not prevent the system from maintaining adequate vehicle roll attitude control. The action taken after SLV-6 flight (see Subsection 6) resulted in a thrust level about one pound higher than the 7.5 pounds per jet value predicted for TV-4BU.

**TV-4 pitch-down jet malfunction**—The pitch-down jet on TV-4 required 22 seconds of jet-on time to correct for a 2-degree up gyro error that existed at second-stage cutoff. Similar operation of about 18 seconds duration occurred about the time of third-stage separation. This indicated a thrust level of only 0.1 pound for the pitch-down jet, which was far below nominal. Apparently, the down-jet solenoid valve be-

came stuck in a partially open position during the initial actuation and remained in this position throughout coasting flight. This condition was supported by the frequent up-jet actuations to correct for the resulting down disturbance. Drops in battery voltage during the 22- and 18-second intervals also indicated a 10- to 15-amp load on the battery, which could have been caused by the pitch-down solenoid using about 12 amps while continuously attempting to open the jet valve. The holding solenoid, which normally operated after the valve was open, required only 0.4 amp.

Pitch/yaw attitude control was adequate despite the marginal TV-4 down-jet operation. The valve sticking may have been caused by the DC-11 silicone valve lubricant reacting with WIFNA fumes in the helium gas supplied to the jets. This reaction would form contaminating products (silicon dioxide) which would establish an environment where the valve would probably stick. GR-362 lubricant was used on TV-5 and up and the trouble did not recur.

**SLV-5 coasting flight**—The SLV-5 vehicle was spinning at 170 rpm about the roll axis at second-stage burnout. Helium was supplied to the roll jets and the pitch/yaw jets were energized when the cutoff signal was given. Approximately 70 seconds later, the vehicle was completely attitude-stabilized, but about some random reference, since all the gyros had exceeded their limits during the tumbling and spinning. Attitude control was maintained for an additional 70 seconds, at which time the aerodynamic moments caused by re-entry into the atmosphere overpowered the jet correcting moments.

## B. FIRST-STAGE PROPULSION

The first-stage propulsion system operated successfully through burnout, and performed as predicted, in ten of twelve flight attempts. Of the two incomplete flights, one (TV-3BU) was terminated by a malfunction in the control system after 57 seconds; until this malfunction occurred, propulsion operation was normal. The only flight failure attributed to first-stage propulsion was that of TV-3, where an improper start resulted in loss of thrust and destruction of the vehicle just after liftoff.

The reliability of the propulsion system was conclusively demonstrated when it successfully completed its last nine consecutive flights (TV-4 through TV-4BU). Performance for all flights was between nominal and maximum predicted. No problems were experienced during the shutdown transients as a result of running to propellant exhaustion. Thrust decay during shutdown was always rapid and stable, and the engine consistently provided low level thrust of sufficient duration to provide positive acceleration to the second stage during its ignition.

Success of the first stage was attributed to a sound basic design and to the detection and correction of troublesome items during static firings. Each flight was preceded by a successful 50-second static firing. Prior to flight firings, a thorough analysis was made to determine the system's readiness for flight. Only after verification of a successful static firing, by data and a thorough hardware inspection, was the system considered qualified for flight.

### 1. STARTING TRANSIENTS

All vehicles prior to SLV-3 used the original X-405 "purge-prime" starting sequence, wherein the thrust chamber was primed with kerosene vapor introduced by a flow of nitrogen "purge" gas. The nitrogen entered the system downstream of the fuel valve and flowed through the engine manifold and regenerative cooling passages into the injector. In passing through the manifold, the gas picked up vapors from a small quantity of liquid kerosene placed there for the purpose. This "purge-prime" provided the fuel for the initial stages of burning until the main flow of kerosene, released by the opening fuel valve, filled the cooling jacket and reached the injector.

The flight failure of TV-3 resulted from a previously unsuspected deficiency of this starting technique. After pressurization of the fuel tank, the lockup pressure at the engine fuel pump inlet was 23.7 psia, well above the minimum value of 19.9 psia specified for the X-405, but nevertheless at a slightly lower value than for any previous starting of this engine.

Flight analysis indicated the following sequence of events. The relatively low pressure head on the fuel resulted in slightly late arrival of the main kerosene flow at the injector, a condition verified by the overly long time (2.33 seconds) from fuel valve open to peroxide valve open, and by the excessive decay in fuel flow rate as indicated by the Potter flowmeter. This resulted in the fuel side of the injector being insufficiently protected by the mixture of prime-fuel and purge gas prior to arrival of the main fuel flow, so that combustion chamber products (hot igniter gases and vaporous LOX) entered the fuel side of the injector. Fire and detonation then occurred when the fuel did reach the injector. The damage thus incurred permitted further mixing and burning of the propellants within the injector. This created an unbalanced condition across the injector face, which caused a momentary surge in chamber pressure, structural vibrations and continued loss of the injector rings. During the time interval of injector failure, sufficient thrust developed to lift the vehicle off the launch stand. Chamber pressure rose until 0.4 second after liftoff, then dropped, which was indicative of complete loss of the injector rings and burnthrough of the combustion chamber. Approximately one second after liftoff, an extreme

structural vibration ruptured the fuel feed system at the fuel valve dispersion cap, which resulted in total loss of engine thrust. The vehicle rose about 50 inches, then dropped back on the launch stand and was completely destroyed. Time histories of chamber pressure and LOX and fuel flow rates, with valve opening times, are shown in Fig. 49. The extent of damage to the injector is shown in Fig. 50.

The immediate corrective action taken to prevent future engine failures during the starting transient was to increase the minimum value for fuel pump inlet lockup pressure from 19.9 to 25.5 psia and later to 28.5 psia, until a more reliable engine start system could be developed. An analysis of engine starts indicated that this increased lockup pressure was adequate to compensate for all engine package fuel system pressure drop variations, and would reduce the time from fuel valve open to peroxide valve open to less than two seconds. A minor modification of the ground electrical system provided a fuel pump inlet switch override, which allowed controlled over-pressurization of the fuel tank after lockup, to ensure meeting this requirement. The effectiveness of this corrective action was borne out by successful starts on the next fourteen consecutive static and flight firings, after which the new ethane system (Chapter IV, Section B) was introduced.

A new and improved engine starting procedure, which utilized ethane gas instead of the purge-prime vapor, was developed after the TV-3 failure. The ethane start was qualified by the engine manufacturer by successfully completing 41 starts using the qualification engine with Vanguard vehicle and ground system hardware. The ethane start demonstrated improved reliability and repeatability over the purge-prime start. It abolished the previous requirements for wetting the motor body cooling passages with fuel; priming the engine with one quart of kerosene; and purging the fuel side of the injector with nitrogen five seconds prior to starting the engine. It also prevented the possibility of random hard starts by maintaining a positive pressure on the fuel side of the injector until fuel arrived at the injector, and by eliminating the characteristic chamber pressure drop which occurred between "fuel valve open" and "peroxide valve open" with the purge-prime start. Vehicle modifications required for the ethane start were the addition of a tail-ring disconnect and a feed line containing a check valve. The ethane start system was installed and performed successfully on SLV-3 and all subsequent vehicles.

## 2. SHUTDOWN TRANSIENTS

For all flights except two, the first-stage shutdown signal was initiated by the LOX pump outlet pressure switch upon oxidizer exhaustion. Shutdown signals for the TV-5 and SLV-2 flights were initiated by the fuel

pump outlet pressure switch at fuel exhaustion. Figures 51 and 52 are examples of LOX and fuel exhaustions, showing valve closing times and typical pressure decays.

All shutdown transients were as predicted. There were no propellant valve malfunctions or indications of thrust chamber failures. Thrust decay was rapid and stable regardless of which propellant was exhausted and the engine consistently provided a low level of thrust, sufficient in duration to ensure second-stage ignition under positive acceleration.

All second-stage ignition signals were initiated by the first-stage chamber pressure switch which functioned when the chamber pressure decayed to  $60 \pm 15$  psia. Time for chamber pressure decay to this value was within the design limit of 0.5 second.

## 3. PRESSURIZATION AND PROPELLANT FEED SYSTEM OPERATION

**Helium regulator**—The main problems associated with the regulator were creepage (increase in initial setting during engine operation) and inability to precisely adjust the initial regulator settings. Both of these shortcomings resulted in higher thrust than predicted because of increased peroxide tank pressure. Regulator creepage occurred during the TV-2 flight, with a resulting sea level thrust of 29,800 pounds. Creepage was attributed to excess pressure buildup in the regulator dome. This problem was eliminated before the next flight by the addition of a constant bleed vent on the regulator dome. This modification provided thrust control within 1% of the calculated values for all subsequent flights except SLV-3 and SLV-5, which were about 2.5% higher than predicted, due to inaccurate regulator settings. Re-evaluation of the regulator adjustment panel curve and adjustment of the regulator dome pressure by increased pressure increments reduced the initial setting tolerances to acceptable values for the last two Vanguard flights.

**Peroxide feed system**—The peroxide feed system functioned well during all flights (Fig. 53). The feed system line diameter was increased from  $\frac{1}{2}$  to  $\frac{3}{4}$  inch prior to the TV-2 flight to eliminate the excessive system pressure drop observed during the TV-2 static firing. Vent valve closing problems experienced during static firings were eliminated by replacing the vent valve pressure probes with a normally open solenoid valve in the peroxide tank pressurization line; this permitted positive closure of the vent valve prior to peroxide tank pressurization. The peroxide system fill and drain quick-disconnect was replaced by a hand valve on SLV-1 and later vehicles in order to prevent minor leakage which had been observed prior to peroxide tank pressurization.

**LOX vent valves**—The venting capacity of the liquid oxygen tank was doubled after the TV-2 static firing by the addition of a second vent valve identical

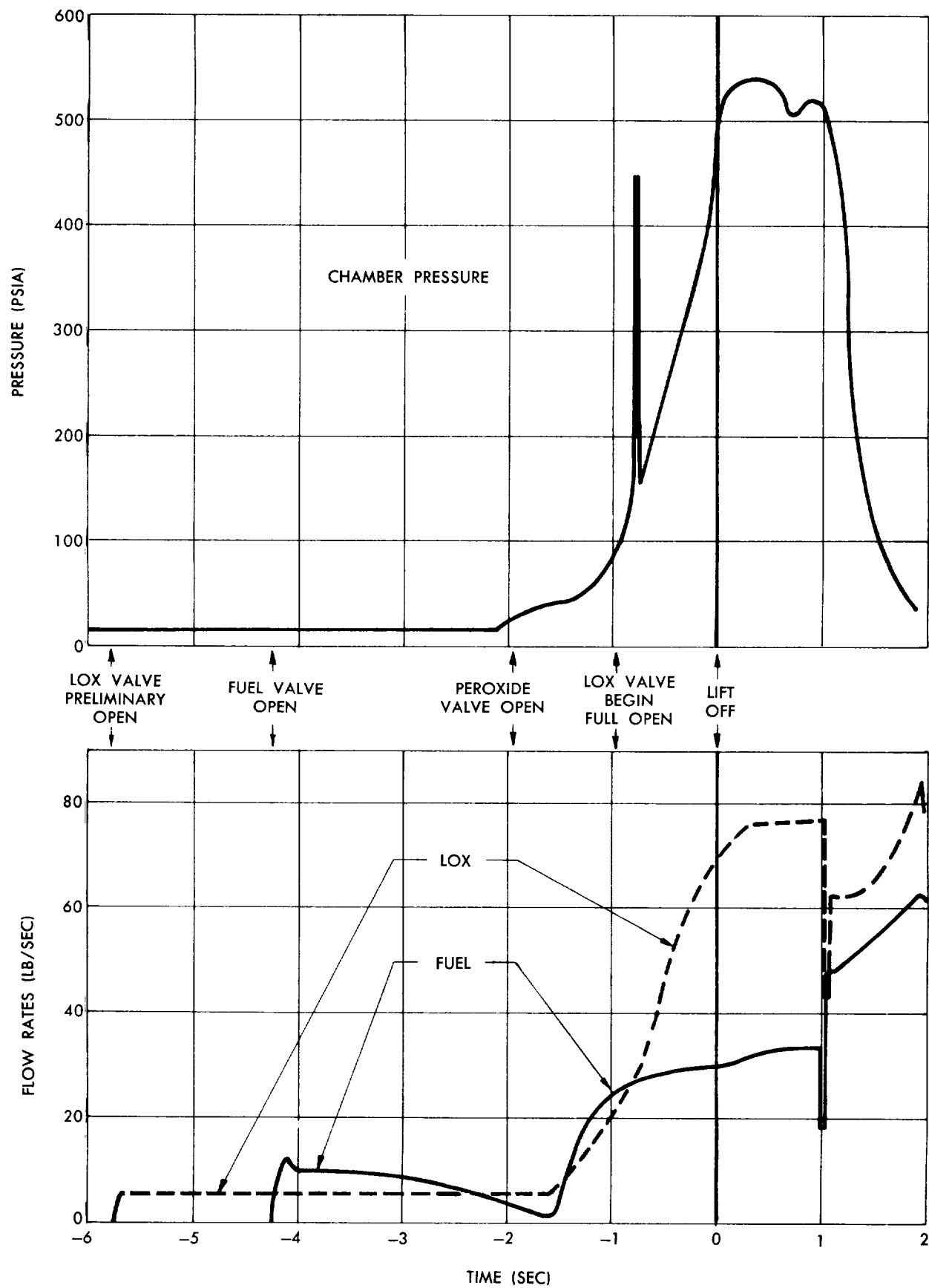
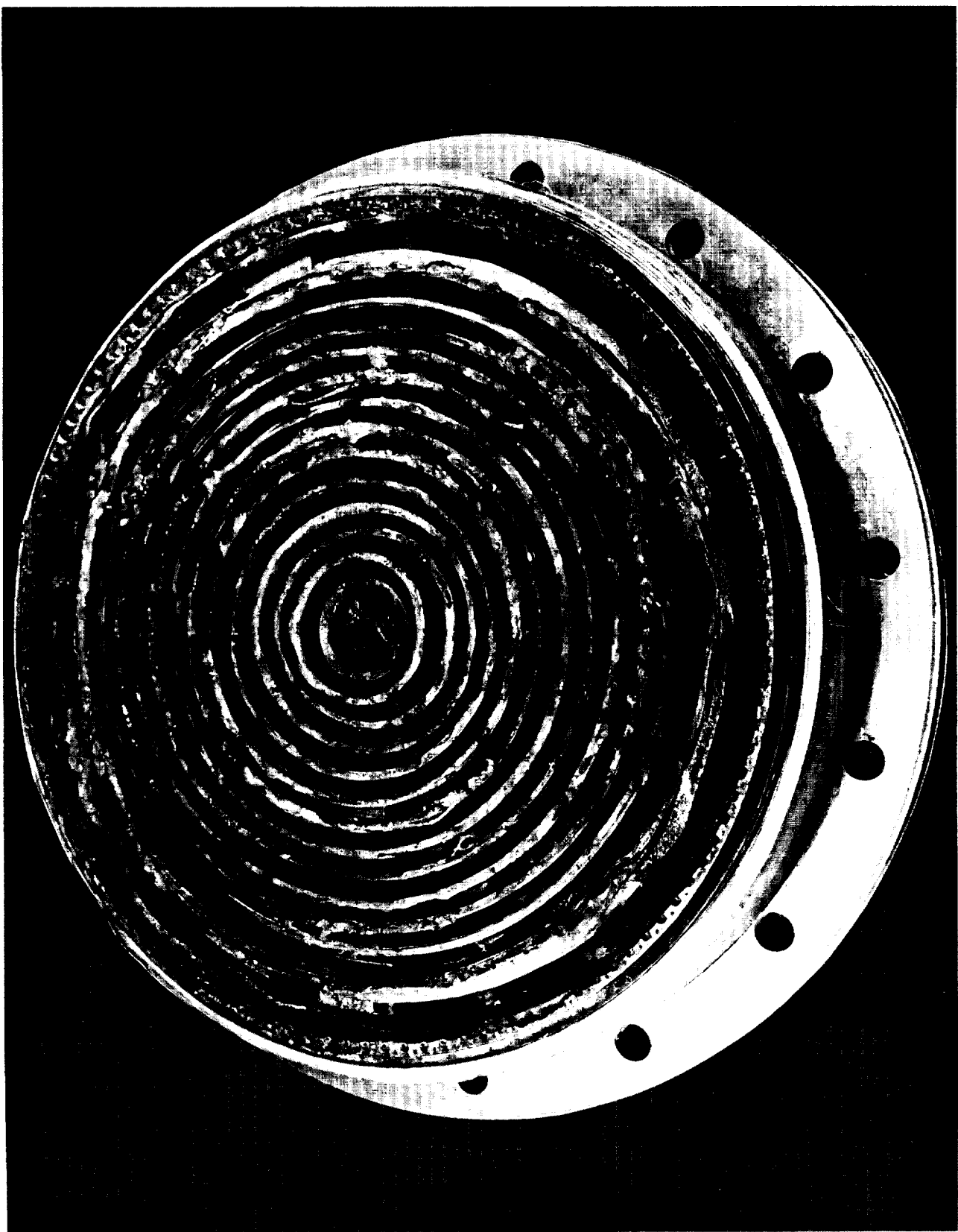


Fig. 49 Time History of Chamber Pressure and flow rates During TV-3 First-Stage Starting Transients



**Fig. 50 The First-Stage Injector After the Flight Firing of TV-3**

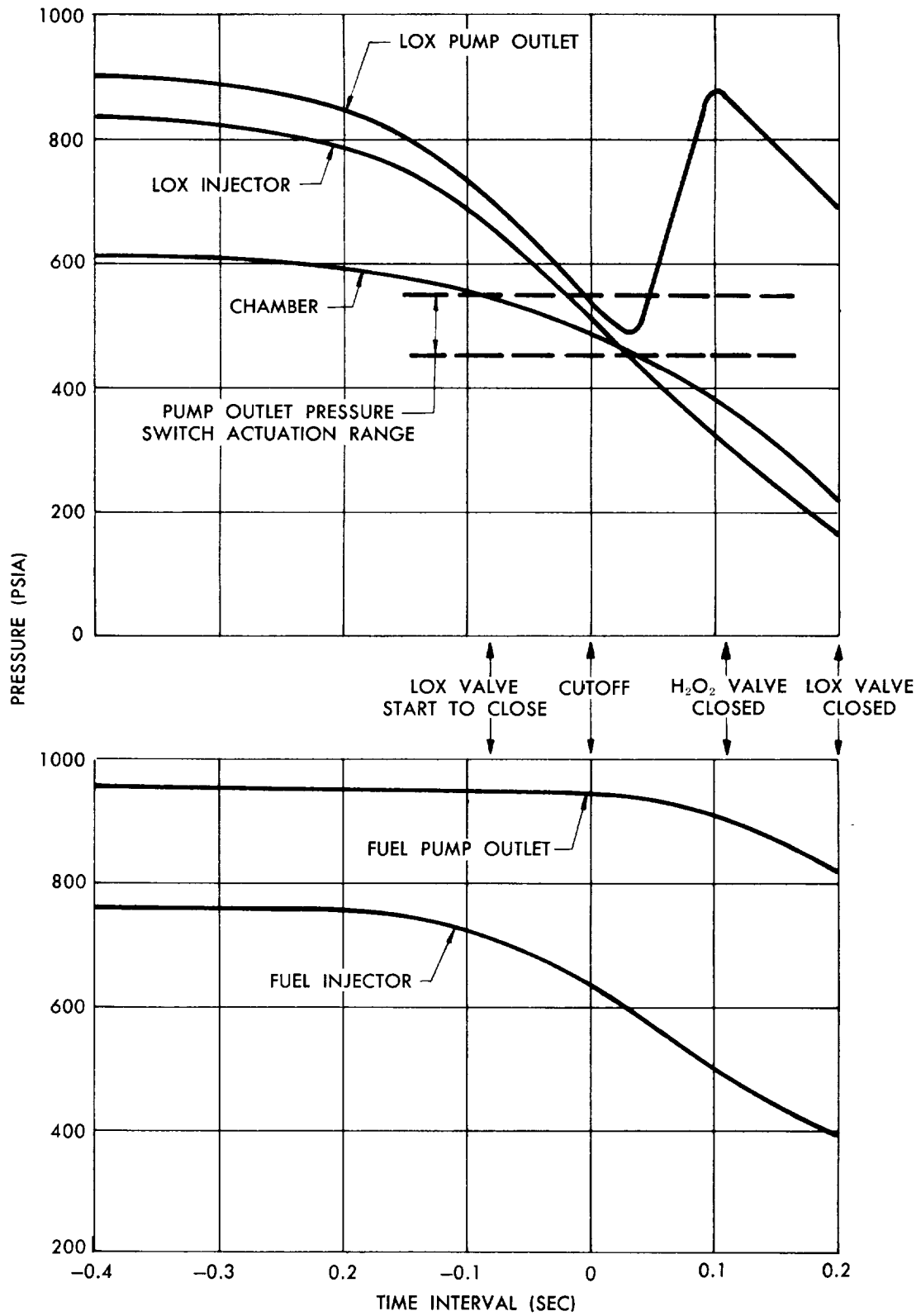


Fig. 51 Typical First-Stage LOX Exhaustion Shut-down Transient

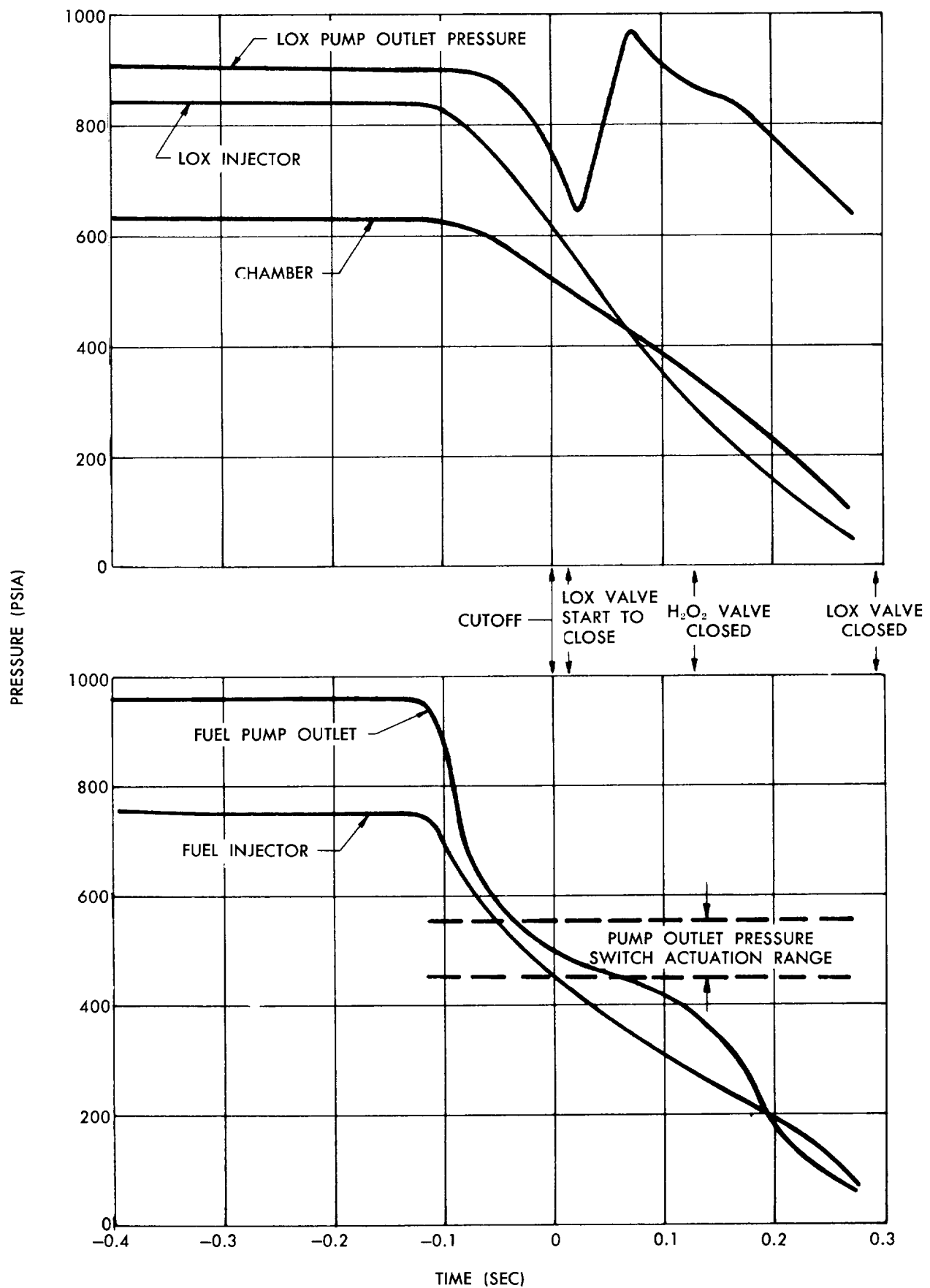


Fig. 52 Typical First-Stage Fuel Exhaustion Shut-down Transient

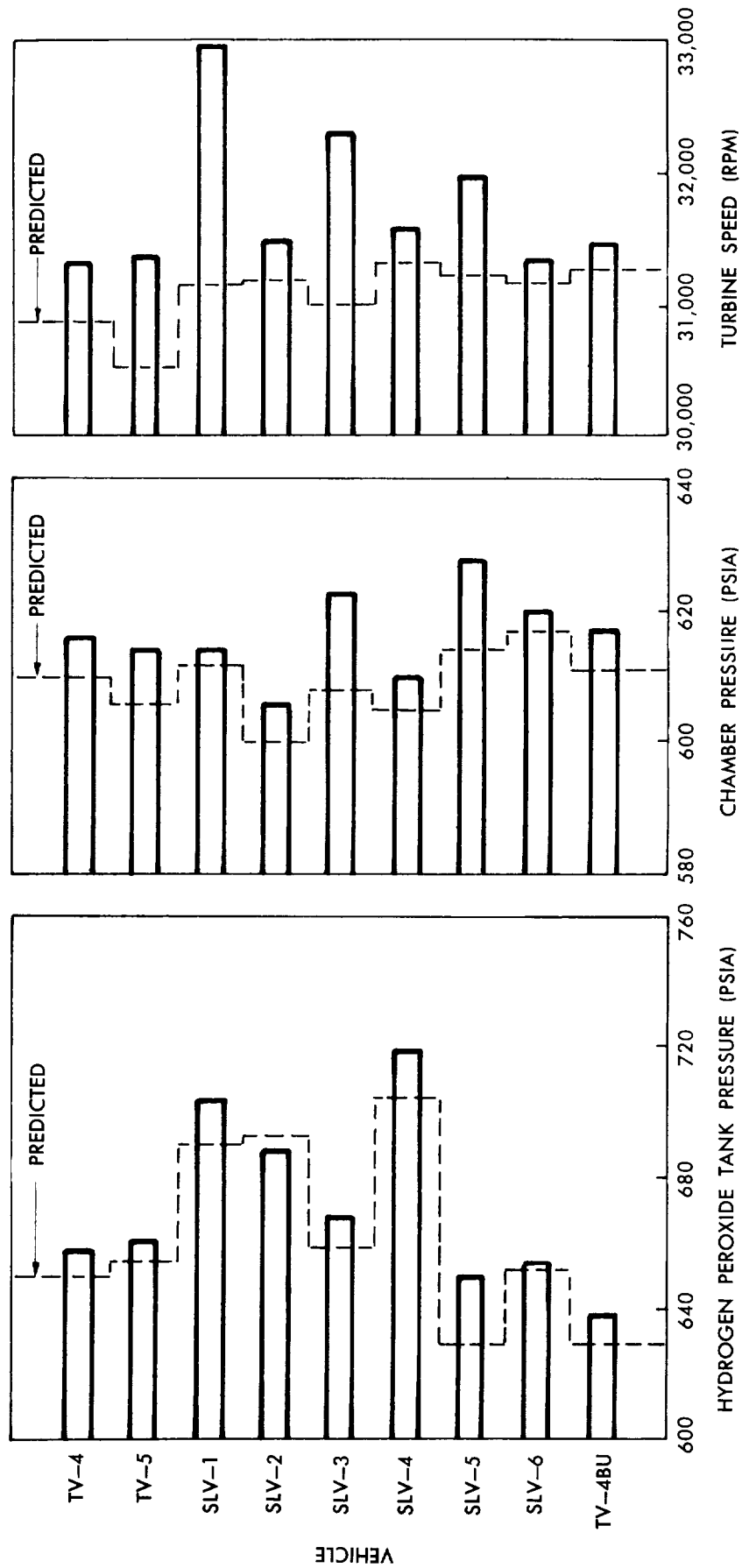


Fig. 53 First-Stage Hydrogen Peroxide System Parameters

to the original. Increased venting capacity was necessary in order to reduce the LOX tank pressure to less than 2 psi prior to pressurization, so that the nominal LOX temperature requirement ( $-294.7^{\circ}\text{F}$ ) could be met. Sluggish and improper vent valve operations observed during the TV-2 static firing were eliminated by relocating the vent solenoid pilot valve from its cold environment, by adding longer bleed extensions from the valve bodies, and by attaching desiccants to the bleed ports. Failure of the LOX vents to close on the TV-3BU and TV-5 static firings was attributed to trim wires installed in the valve inlet restrictor orifices. Differential contraction between the wires and orifices at LOX temperatures caused the effective orifice openings to shrink and reduce the pneumatic gas flow to the valves. Correct orificing without trim wires eliminated this problem. No vent valve failures occurred during flight.

**Propellant inlet lines**—The wall thickness of the oxidizer and fuel inlet lines was doubled after the TV-2 static firing to prevent damage due to pressure surges resulting from rapid engine valve closure during shut-down. The integrity of these inlet lines was verified when they were attached to the qualification engine package and successfully completed a series of 10 engine start tests at the engine manufacturer's production test pit. These tests were performed after the TV-3 flight failure.

#### 4. PROPELLANT UTILIZATION

Low propellant outages were achieved during all flights (see Fig. 54) through the practice of precise determination of mixture ratio and propellant loadings. Propellant outage was conservatively estimated during the early flights by assuming the most adverse accumulation of tolerances. As flight experience was gained, it was possible to reduce the spread of expected tolerances and thus make more realistic predictions. The original mixture ratio tolerance spread was reduced from  $\pm 5\%$  to  $\pm 2\%$ .

The highest outage experienced, as determined by post-flight analysis, was 70 pounds of fuel during the SLV-3 flight. On most vehicles, near-simultaneous LOX and fuel propellant exhaustions occurred. SLV-2 and SLV-5 were the only other flights with measurable outages, having 39 pounds of LOX outage and 31 pounds of fuel outage, respectively.

#### 5. ENGINE PERFORMANCE

The first-stage engine performance was always between the nominal and maximum predictions. Burnout

velocities were always above nominal. High performance was attributed to the attainment of maximum overall specific impulse and consistently low propellant outage.

**Thrust coefficient**—Thrust coefficient ( $C_t$ ) is a measure of nozzle efficiency. Sea level thrust coefficient was determined during engine package acceptance tests by calculation from the relationship:  $C_t = \frac{F}{P_c A_t}$

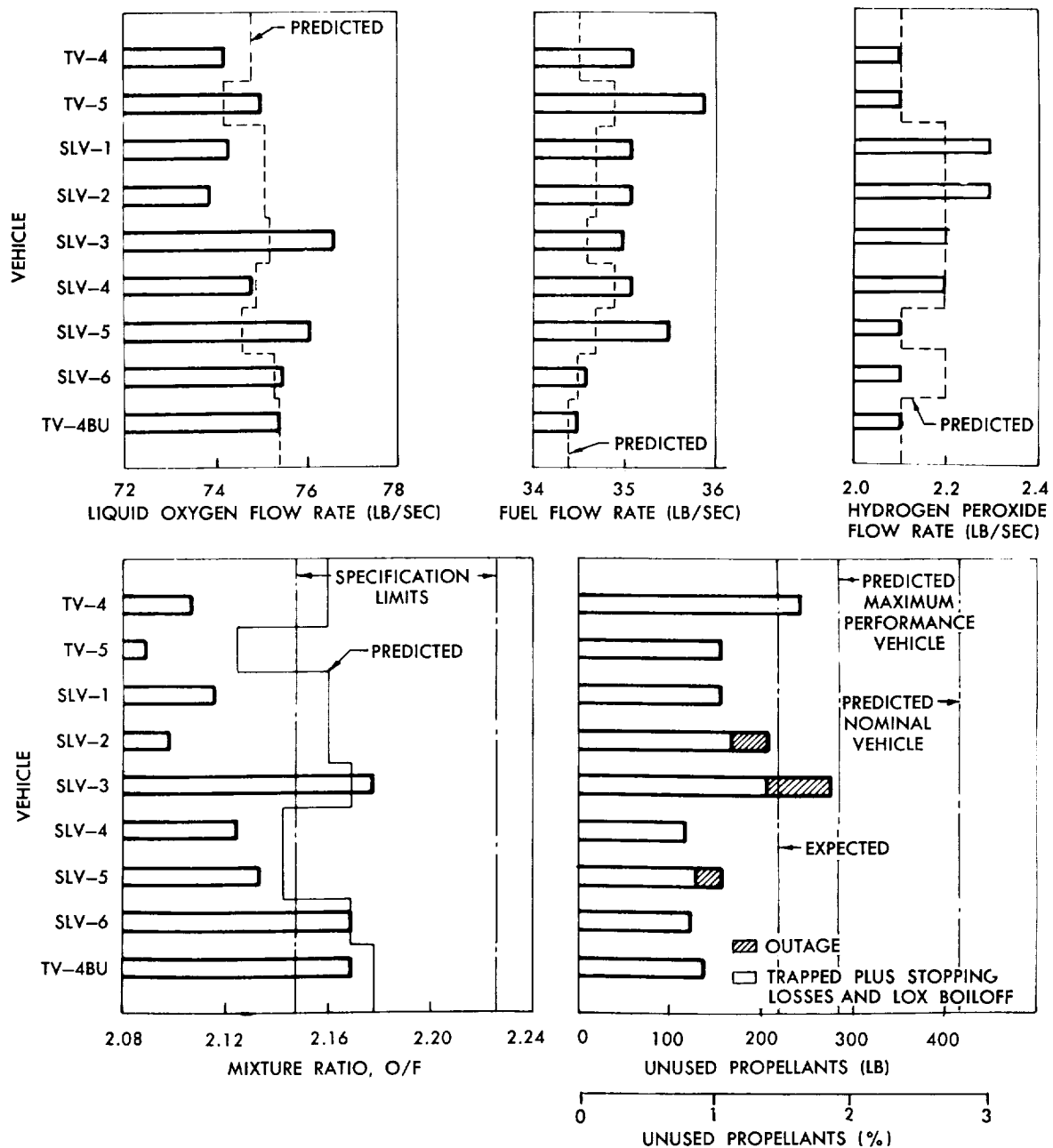
Thrust ( $F$ ) and chamber pressure ( $P_c$ ) were recorded during acceptance tests, while the throat area ( $A_t$ ) was physically measured before and after each firing. The altitude thrust coefficient was calculated from the accurately determined sea level coefficient by a correction for the change in ambient pressure. The mean value of sea level thrust coefficient thus obtained for the X-405 engine was 1.43. Thrust coefficients were also calculated from flight data, using "best estimate" flight thrust, telemetered chamber pressure and the previously measured throat area. The mean  $C_t$  from flight was 1.435.

**Characteristic exhaust velocity**—Characteristic exhaust velocity ( $c^*$ ) is a measure of combustion efficiency and injector performance. The characteristic exhaust velocity on all flights was slightly greater than that calculated during acceptance tests (Fig. 55). The mean values were 5760 fps for flight and 5708 fps for acceptance test.

**Overall specific impulse**—Specific impulse is the amount of impulse produced by an engine (in pound-seconds) per pound of consumed propellant. Overall specific impulse was calculated from the best estimates of engine thrust and propellant flow rates (including peroxide) obtained from a variety of data sources in the flight analyses. The average overall flight specific impulse (Fig. 55) varied from 250 to 253 seconds, which was two to three seconds greater than that obtained during acceptance tests and static firings.

### C. SECOND-STAGE PROPULSION

The second-stage propulsion system operated and performed as predicted only on the three flights which succeeded in placing satellites in orbit. The first two flights to carry the second stage, TV-3 and TV-3BU, were terminated by first-stage malfunctions. The second-stage system performed satisfactorily throughout



**Fig. 54 First-Stage Propellant Parameters**

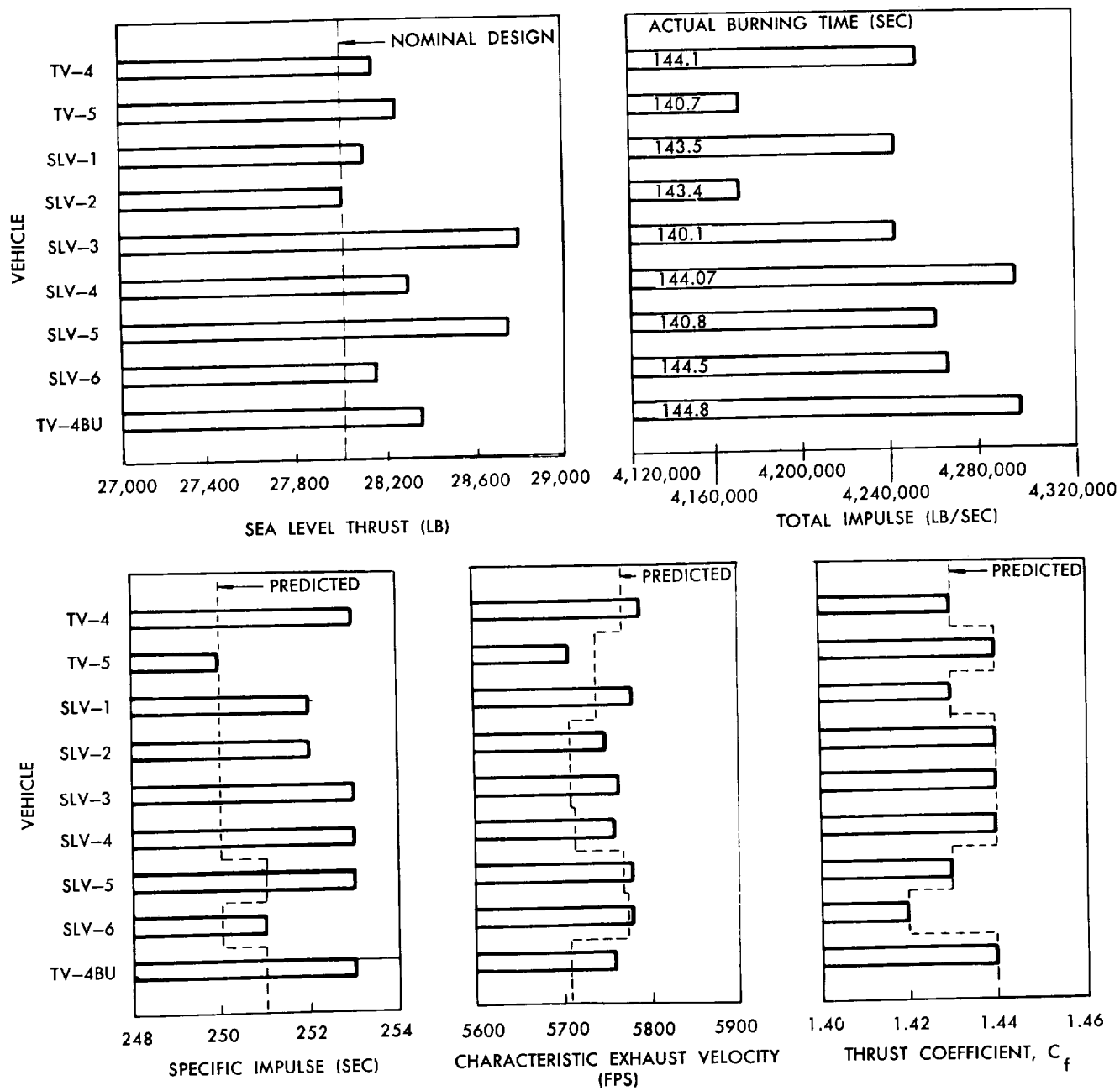


Fig. 55 First-Stage Performance Parameters

powered flight on two other occasions, TV-5 and SLV-1, but malfunction of the engine shutdown system prevented successful completion of the missions. In the remaining four flights, malfunctions occurred immediately after engine starting.

Although the second-stage propulsion system performed successfully on only three of nine opportunities, the design was demonstrated to be basically sound. Relatively minor changes were required to correct the deficiencies which led to flight failures. In some cases, only changes in procedures or ground equipment were required. There was no evidence of any flight malfunction attributable to thrust chamber erosion or stress corrosion of the tankage, which had been major development problems. No specific cause of flight failure was ever repeated. The success of modified Vanguard second stages in other space programs is further indication that the design was fundamentally sound.

## 1. STARTING TRANSIENTS

The validity of assuring reliable engine starting through the use of hypergolic propellants was demonstrated—successful ignition occurred on all nine flights.

**Nozzle flow separation**—Ignition of the second-stage engine caused a pressure buildup in the interstage compartment until stage separation occurred. The level of back pressure was a function of compartment volume, blast door area and the time from engine start to first-stage separation. A maximum back pressure of about 16 psia was possible if stage separation was delayed. The separation signal was normally given by the thrust chamber pressure sensor (TPS) when chamber pressure reached 140 psia (see Chapter VIII, Section G). During the short time interval from ignition to separation, the buildup of back pressure prevented the exhaust gases from completely filling the 20:1 area ratio divergent nozzle. This produced asymmetrical, random and oscillatory flow separation in the nozzle, which caused side loads that often were sufficient to overpower the engine servos. Both flow separation and overpowering of the servos were characteristic of sea level static firings of this engine.

On SLV-5, side loads were much more severe than any previously experienced in flight, and the engine was driven hard against the actuator stops, causing failure of the servo mounting lug (Chapter VII, Section D) and consequent loss of the vehicle. The reason for unusually severe side loads on SLV-5 could not be clearly established from the data available. They could have been caused by some unsymmetrical obstruction in the nozzle (such as uneven rupture of the nozzle closure), by high or uneven pressure distribution in the interstage compartment, or simply from the random nature of the flow separation phenomenon. The condition was alleviated on later flights

by providing an earlier separation signal (Chapter VIII, Section E) and by using check valves in the hydraulic system to reduce the rate at which the servos could be overpowered (Chapter VIII, Section I).

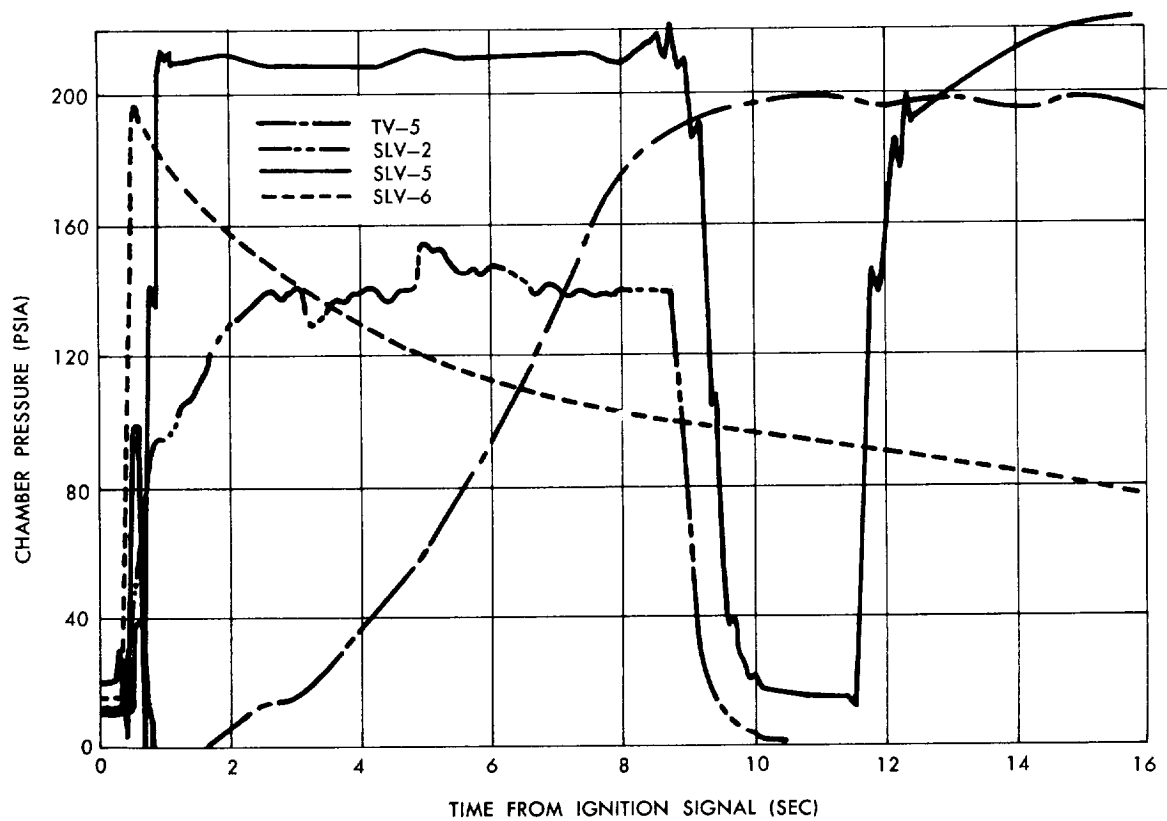
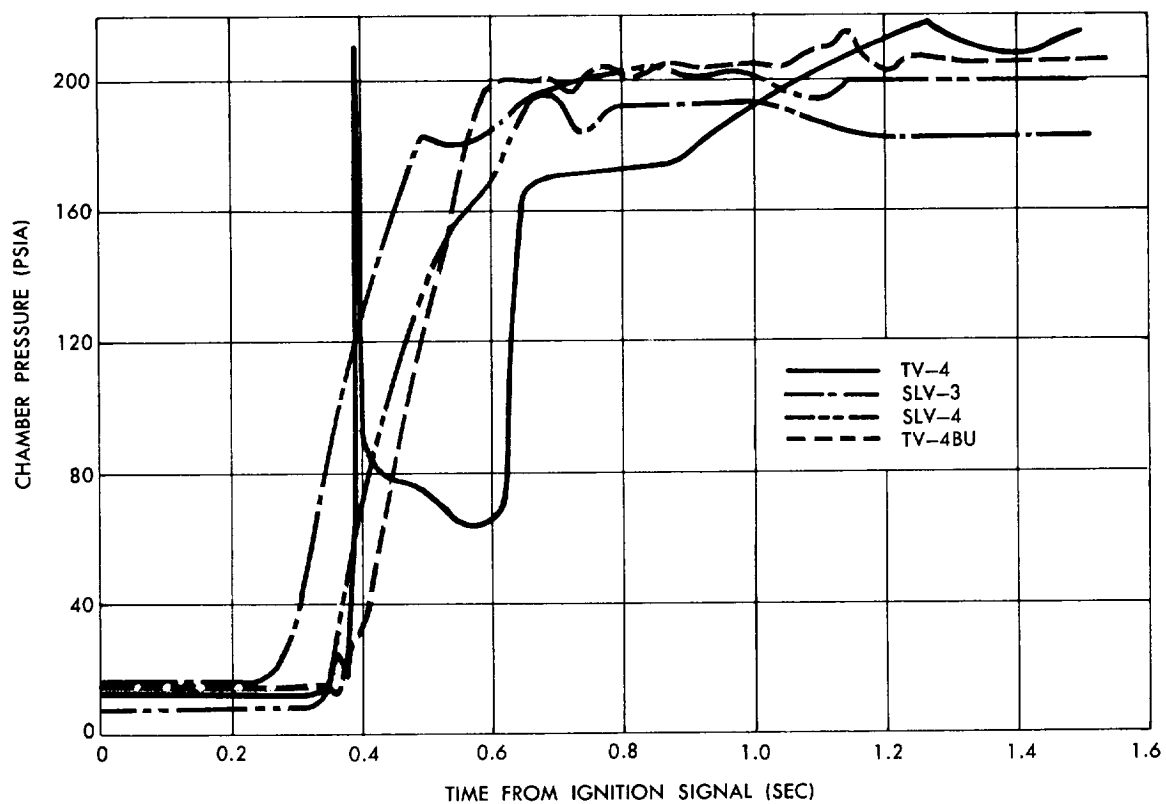
**Instrumentation**—Nozzle flow separation also caused extreme vibration, probably in excess of 100 g. The vibration did not appear to affect operation of the propulsion system, but did affect the pressure instrumentation during the starting transients. The injector and chamber pressure traces for many of the flights were erratic and generally lower than expected (Fig. 56). However, the earlier separation signal used on SLV-6 and TV-4BU seemed to provide a more acceptable environment, as the transient indications for these flights were quite smooth. A vibration test of a typical transducer demonstrated that the wiper would lift away from the potentiometer coil under conditions of severe vibration, thereby giving an indication of erratic pressure, always either equal to or lower than the true pressure.

## 2. SHUTDOWN TRANSIENTS

For all flights through SLV-1, the TPS provided the only shutdown signal. The oxidizer probe, originally planned as the primary system for oxidizer exhaustions, had been removed because a malfunctioning or broken probe could initiate premature shutdown. The TPS performed satisfactorily on TV-4 and SLV-2, but on TV-5, a relay sequencing problem prevented delivery of the shutdown signal to the propellant valves and the coasting flight arming functions (see Chapter VIII, Section G).

**Oxidizer probe**—On SLV-1, a high frequency combustion instability occurred, causing TPS to chatter for 1.5 seconds before the shutdown signal was consummated. During this time, the vehicle experienced a severe pitch-up movement (Fig. 57). Analysis indicated that this must have been caused by combustion gases escaping through the thrust chamber wall. The thrust chamber probably split in the welds between tubes, due to severe vibration and pressure fluctuations induced by the combustion instability; a failure of this type occurred on a thrust chamber during a development test. The probable cause of high frequency combustion instability was intermittent interruption of oxidizer flow into the combustion chamber by helium bubbles which became entrained in the flow upon oxidizer exhaustion.

As a result of this flight failure, it was concluded that oxidizer exhaustion must be sensed, and the system shut down, sooner than was possible with the existing TPS system. Accordingly, various modifications of the oxidizer probe system were used on all following flights. SLV-2 and SLV-3 used dual oxidizer probe systems which required both probes to sense oxidizer exhaus-



**Fig. 56 Time Histories of Second-Stage Chamber Pressure During Starting Transient**

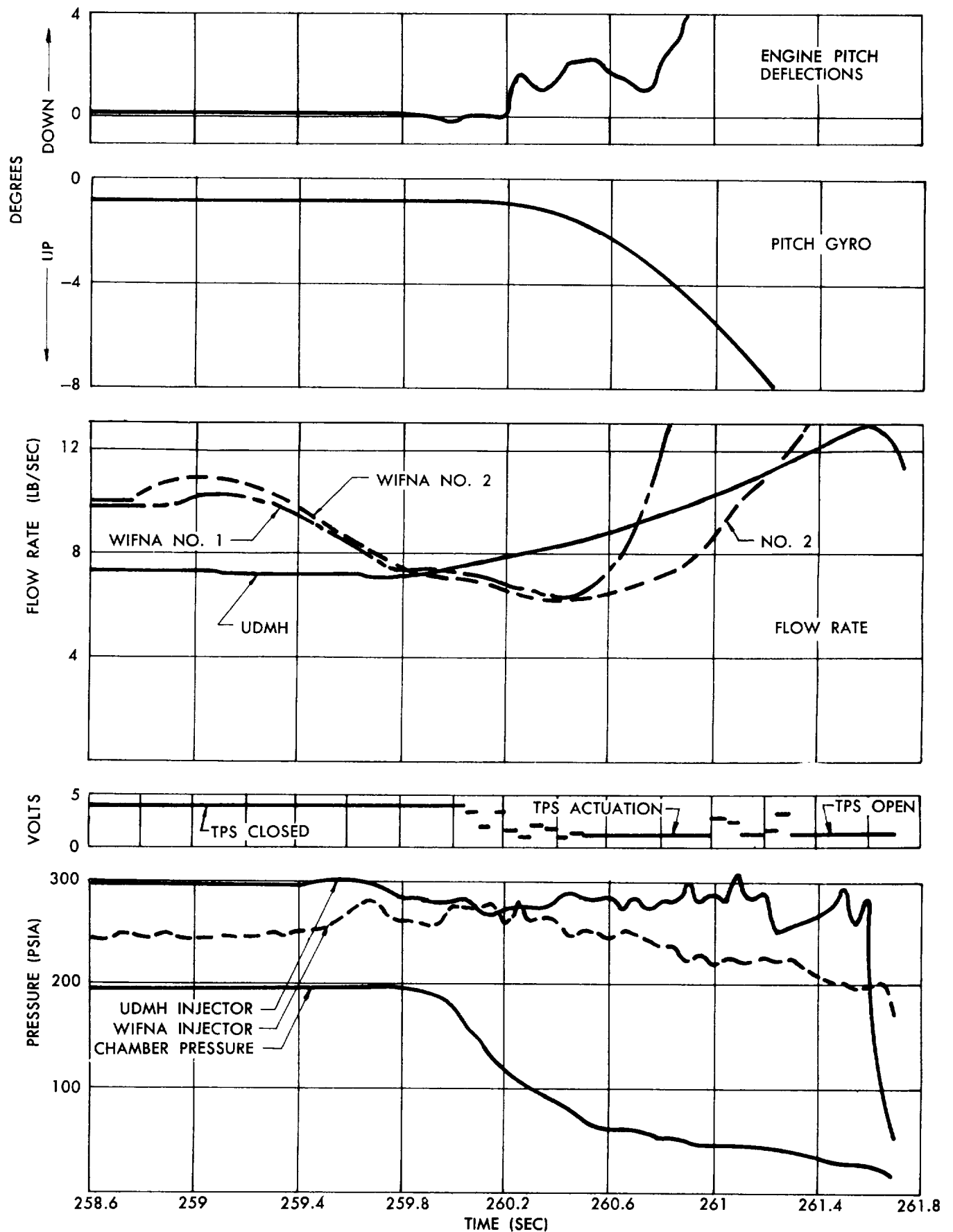
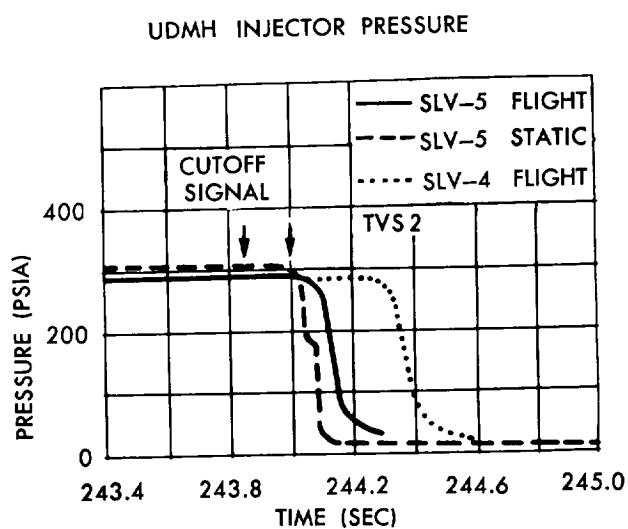


Fig. 57 Time History of SLV-1 Second-Stage Shut-down Transients

tion before the cutoff signal was given. This arrangement was used to prevent premature cutoff should either probe malfunction. Several successful test firings were made with this type of system, but, during the field static firing of SLV-3, some of the thrust chamber coolant tubes burned through at shutdown. It was determined that the dual oxidizer probe system sometimes delayed shutdown because considerable entrainment of helium had to be present for the probes to remain simultaneously uncovered long enough to energize the shutdown relay. The dual probe system was flown on SLV-3, but UDMH was off-loaded to ensure a fuel exhaustion which could be safely handled by the TPS shutdown system. As luck would have it, the fuel system became clogged, oxidizer exhaustion did occur, and the dual probe system operated perfectly.

In the meantime, an intensified development program was initiated to develop a fully reliable oxidizer probe shutdown system. The effects of probe location, geometry, acid constituents, acid temperature, arming time and vibration were determined. The final configuration consisted of two probes, one in each feed line downstream of the oxidizer valve, either of which could signal shutdown independent of the other. This arrangement provided for the possibility of one feed line exhausting before the other. The probe was modified to prevent internal breaks such as those which led to its earlier deletion. A transistor network was used in place of differential relays in order to provide a precise resistance setting for system operation. This system was used with success in SLV-4 and subsequent vehicles.



**Fuel valve**—A 0.25-second delay in fuel valve closing was observed during the shutdowns of TV-4, SLV-3 and SLV-4. It was deduced that UDMH in the valve actuation system boiled off because of the near-vacuum ambient pressure in flight. A vent check valve which opened at 10 psig was installed in the pilot valve vent line, beginning with SLV-5. This valve prevented UDMH boil-off, thus permitting more rapid closing of the fuel valve. The sketch shows a comparison of the fuel injector pressures on SLV-4 and SLV-5, indicating the more rapid valve closing on SLV-5.

### 3. PRESSURIZATION SYSTEM

**Heat generator**—The heat generator ignited and burned satisfactorily on all flights. However, in TV-5 and SLV-6, it ignited immediately after first-stage separation instead of at the expected time, several seconds later, after decay of the sphere pressure to 1400 psig. Tripping the helium regulator during the engine start transient initiated the flow of high-pressure helium, causing a pressure transient in the vicinity of HPS<sub>1</sub>. Sometimes the pressure dipped low enough to cause actuation of the switch, thus firing the heat generator. This "malfunction" was not detrimental to system operation; in fact, on TV-4 and TV-4BU, the heat generator was purposely ignited at first-stage separation.

**Helium regulator**—The performance of the helium regulator proved to be rather unpredictable. On five flights, the regulated pressure was above or below specified tolerances (see Fig. 58). Regulated pressures as much as 20 psi outside specification limits could be tolerated, however, as the effect on overall performance was determined to be small.

The regulator opened only slightly, if at all, on the flight of SLV-6. This caused all downstream system pressures to decay rapidly, after the starting transient, to less than half of their normal flight values (Fig. 56) with consequent low thrust and combustion instability. Since the heat generator ignited at first-stage separation, the helium sphere pressure continually increased until rupture occurred. Corrective action consisted of every conceivable precaution to ensure that the regulator was in operating condition at launch. Minor mechanical modifications were made to the rotary solenoid and tripping mechanism. A protective cover was provided for the regulator. Improved field procedures were instituted, including flow tests and, on the day of the flight, a check of the trip mechanism just before final torquing.

A more desirable regulator would have been one that did not require manual closing, but which would automatically lock up at the proper propellant tank pressures. This was recognized early in the program, and an attempt was made to develop such a regulator,

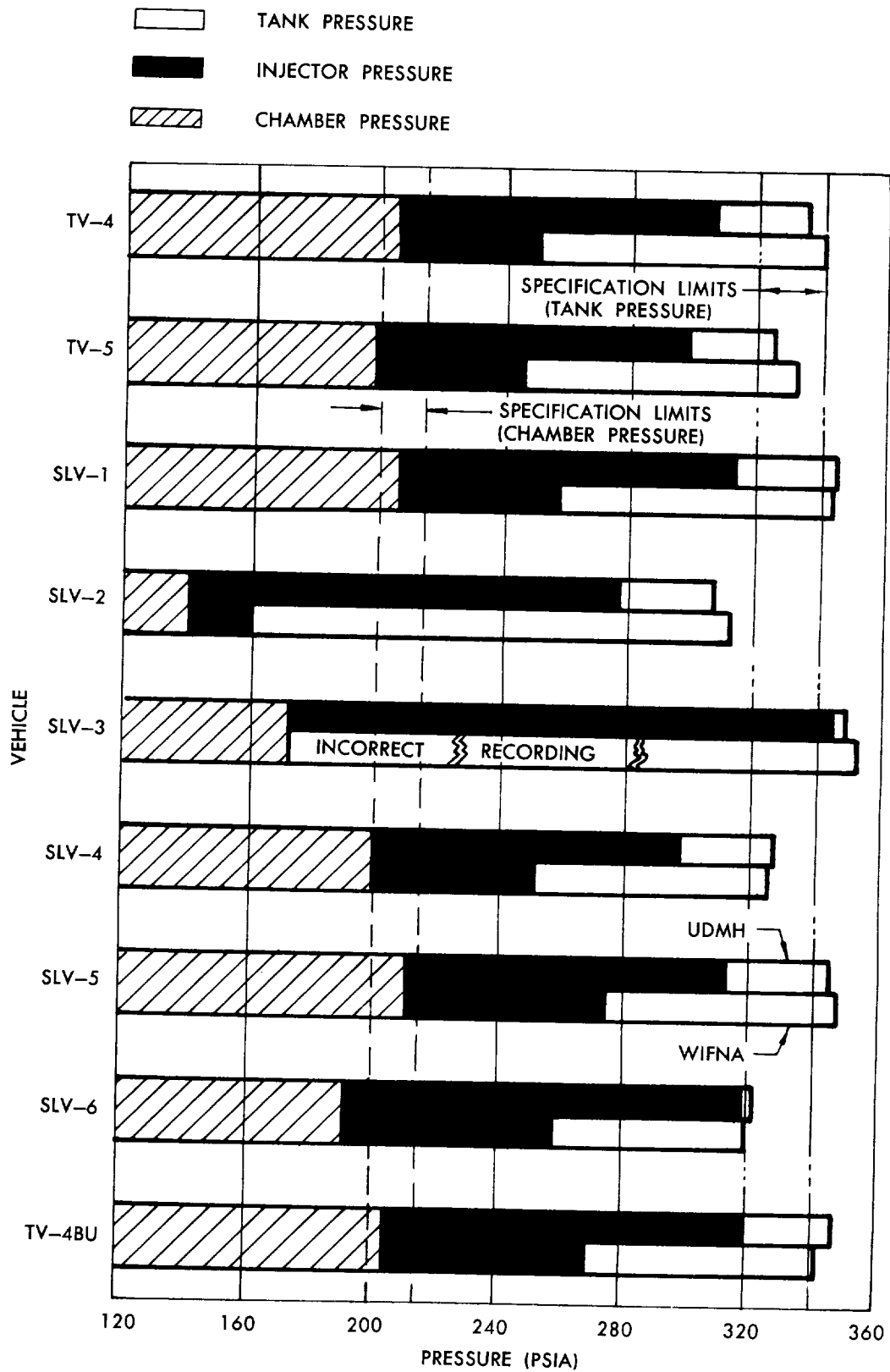


Fig. 58 Second-Stage System Pressures

but difficulty was experienced in achieving satisfactory regulation with heated helium, and the decision was made to use the existing regulator.

#### 4. PROPELLANT FEED SYSTEMS

The oxidizer and fuel propellant valves operated satisfactorily in all flights. On the flights of SLV-2 and SLV-3, however, foreign matter caused severe clogging in the propellant feed systems, causing failure of these flights.

**Heat treat scale**—On SLV-2, loose heat treat scale lying in the bottom of the WIFNA tank entered the propellant feed lines during the starting transient, and clogged the oxidizer filter screens. Clogging initially occurred in only one feed line; then, as scale entered the second line, the clogging in the first line was relieved somewhat, probably due to the particles breaking up and passing through the screen. The oxidizer flow rate was about 60% of the normal value, and the chamber pressure was slightly less than 70% of normal. Shutdown occurred after about 8 seconds of burning, when the TPS shutdown system was armed (Fig. 56).

Varying degrees of oxidizer screen clogging had been experienced during qualification testing. As a result, a field procedure had been instituted for water-flushing the oxidizer tank to remove loose heat treat scale. SLV-2 had a history of scale contamination, and required 16 flushing operations in the field before all the loose scale was apparently removed. The screens were inspected and cleaned. Following a scrubbed flight attempt, the propellant tanks were drained, and about two quarts of water were inadvertently introduced into the oxidizer tank during flushing of the pitch/yaw jets. This water was removed but not before it might have combined with acid adhering to the tank walls to form a dilute acid solution, which would further remove heat treat scale by a pickling action.

In order to prevent future malfunctions of this type, a pickling process was developed to remove the heat treat scale altogether. The oxidizer tank of SLV-3 was pickled in the field, using dilute nitric acid. An improved pickling process, using a sodium hydroxide-potassium permanganate solution followed by a dilute acid solution, was used to pickle the WIFNA, UDMH and helium tanks of SLV-4 and following vehicles.

**Buna-N rubber**—The clogging which occurred on SLV-3 was attributed to Buna-N rubber particles which lodged in the fuel injector, clogging about a third to half of the orifices. The fuel flow rate, after rising to a normal level, suddenly decreased after one second to about 85% of normal and then gradually dropped off to 70% of normal. Figure 56 shows the resulting effects of this on chamber pressure. The second stage operated for 108 seconds, shutdown occurring upon oxidizer exhaustion. Due to the low fuel flow rate,

almost 300 pounds of UDMH remained in the propellant tanks. The resulting low second-stage performance prevented the satellite from attaining orbital velocity.

The Buna-N rubber particles were inadvertently introduced into the second-stage tankage during vertical testing, after the second-stage static firing in the field. Silica gel particles from a broken drier in the ground helium system passed through a 4-micron filter and eroded the interior of the Buna-N rubber helium fill line. The rubber particles entered both propellant tanks and the helium sphere. After an unsuccessful attempt to remove these particles with water containing a detergent, the UDMH tank and helium sphere were flushed with toluene and the WIFNA tank with methylene chloride. It was physically impossible to visually inspect the interior of the propellant tanks, but the clean appearance of the helium sphere led to the conclusion that the other tanks were clean also. Unfortunately, some of the particles may have been trapped in the UDMH tank. After the flight, it was learned that Buna-N rubber swells in the presence of toluene and then becomes tacky and coheres upon later exposure to UDMH. It was theorized that the enlarged rubber particles, having a specific gravity near that of UDMH, were agitated from the tank bottom and swept into the feed line at the start of fuel flow. The timing of the initial clogging (Fig. 56) and the increasing restriction throughout powered flight correlate well with this theory.

Corrective action for this problem consisted of removal of the silica gel driers, using a metal helium fill hose instead of rubber and installing an additional 4-micron filter at the connection of the hose to the vehicle.

#### 5. PROPELLANT UTILIZATION

The feasibility of achieving low propellant outages through the practice of precise determination of mixture ratio and propellant loading was demonstrated (see Fig. 59) on four flights which experienced no feed system malfunctions (TV-4, TV-5, SLV-1 and TV-4BU). In the earlier flights, propellant outage was conservatively estimated by assuming the most adverse accumulation of tolerances. As flight experience accrued, it was possible to narrow the spread of expected deviations and thus to make more realistic predictions. A statistical approach to performance prediction was finally developed which produced quite accurate results. This probability study indicated that 68% of the vehicles should have a mixture ratio variation within 1.5% of the predicted value. Most of this uncertainty was attributable to inaccuracy in determining the original static firing mixture ratio.

There were high propellant outages on several flights due to malfunctions. The radical changes in flow rate and the short burning times caused by propellant feed system clogging on SLV-2 and SLV-3 produced large

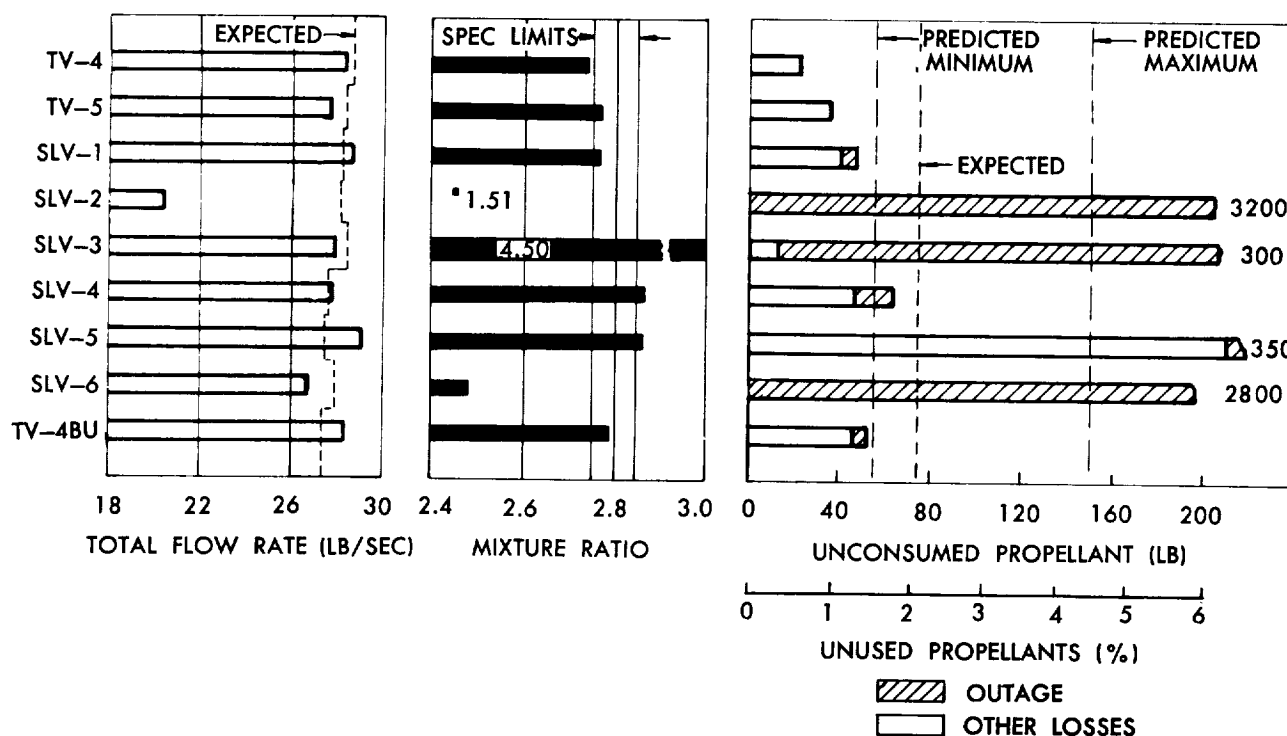


Fig. 59 Second-Stage Propellant Parameters

outages. The high outage of SLV-5 was caused by a forced vortex over the entire liquid surface in the WIFNA tank, induced by the fact that the vehicle was spinning out of control. This allowed helium to enter the feed lines and initiate cutoff while considerable oxidizer remained in the tank. In SLV-6, abnormally low propellant flow rates and burning time caused by the helium regulator failure resulted in extremely high outage.

The 16.7-pound UDMH outage on SLV-4, although rather low, deserves comment because this vehicle was off-loaded to favor the probability of fuel exhaustion. The UDMH load was 12.5 pounds (equivalent to  $1\frac{2}{3}$  seconds burning time) less than that required by the predicted flight mixture ratio. A high oxidizer flow rate in flight caused the mixture ratio to be 4% higher than predicted. No fully satisfactory explanation was found for the high WIFNA flow rate. A hypothesis that the oxidizer filter screens were inadvertently omitted provided a good fit for the telemetered data, but field records and eyewitnesses indicated that the screens were properly installed.

## 6. ENGINE PERFORMANCE

The second-stage engine performance was somewhat less than originally expected, even during the flights

in which no malfunctions occurred. Engine performance can be divided into two main categories: characteristic exhaust velocity ( $c^*$ ), which is a measure of combustion efficiency and injector performance; and thrust coefficient, which is a measure of nozzle efficiency.

**Characteristic exhaust velocity**—The characteristic exhaust velocity on all flights which operated reasonably close to the nominal mixture ratio (except TV-4BU) was about 0.5% low (Fig. 60). This difference is well within the accuracy of both static and flight instrumentation, and some variation in injector performance is to be expected. In some flights, the reduction could be partially accounted for by an increase in flight mixture ratio to a value farther from stoichiometric than the static firing value. However, the fact that the value was low by a similar amount in each of five flights appears to be more than a coincidence.

One possible explanation for an apparent decrease in  $c^*$  during flight was an increase in throat area due to thermal expansion. The acid in the thrust chamber cooling jacket experienced an estimated 150°F temperature rise in flight, as compared with 120°F measured in static firings, because the exhaust gases did not separate from the nozzle walls in flight. Another

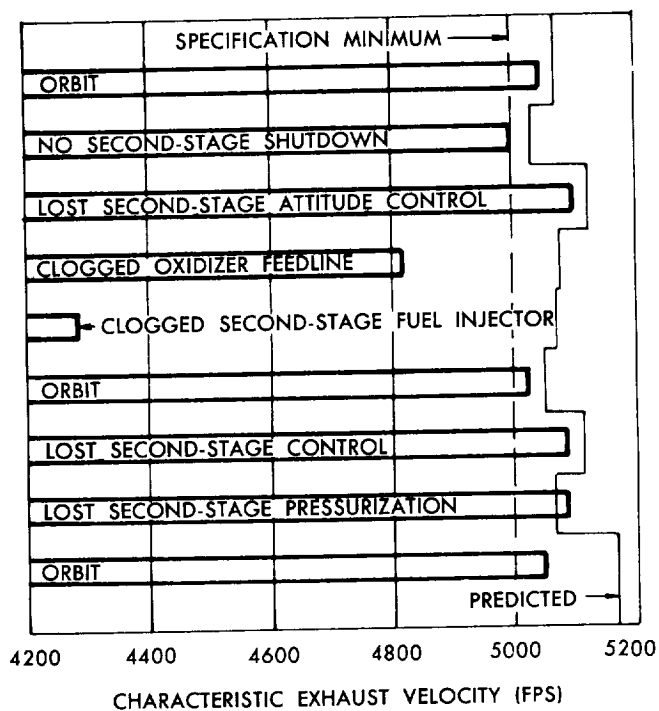
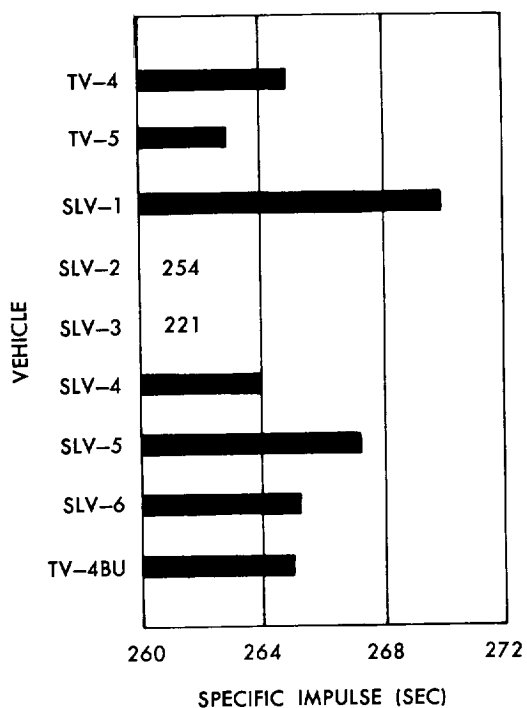
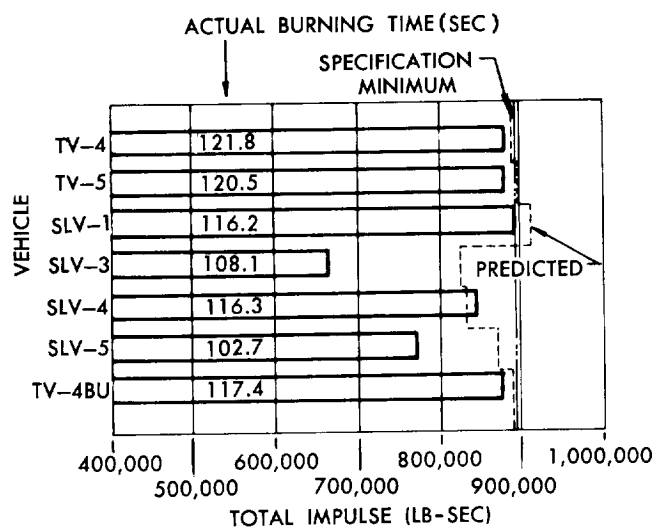
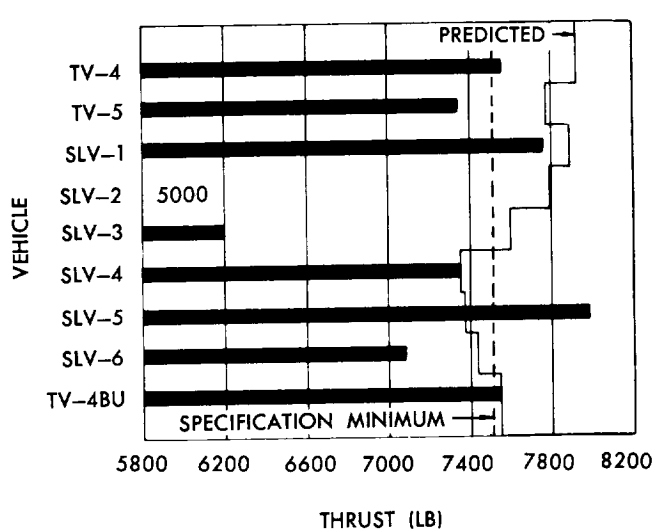


Fig. 60 Second-Stage Performance Parameters

factor that could have contributed to higher thermal expansion in flight was the almost total loss of convective cooling from the thrust chamber outside walls to the ambient air. The effect of thermal expansion was observed during development testing when it was found that an injector fired in a regeneratively cooled thrust chamber had an increase in  $c^*$  of 1 to 2% over that obtained with an uncooled or water-cooled thrust chamber.

The flight  $c^*$  for TV-4BU was more than 2% below the expected value (Ref. 51). System pressures and flow rates were analyzed (in addition to trajectory matching data) in order to verify the accuracy of this result. Static firing records were re-examined to determine if the predicted value of  $c^*$  had been in error. All studies indicated that the prediction was valid and that the flight  $c^*$  was really 2% low. The discrepancy was too great to be accounted for by thermal expansion of the throat, so various malfunctions were considered in an attempt to discover the cause. One assumption, that of a leak from the UDMH injector or injector pressure tap, provided a surprisingly good fit to the data. Such a leak would provide the proper UDMH flow rate to fit the near exhaustion of UDMH evidenced in the shutdown transient, and would also fit the observed injector pressure, which was 11 psi lower than expected. The resultant low UDMH flow rate into the combustion chamber would give a high mixture ratio and low total propellant flow rate, which would account for the apparently low  $c^*$ . If no leak existed, an error must have been made in the analysis of static or flight test data. Instrumentation inaccuracies do not appear to be a sufficient explanation, because the analysis method employs several independent data sources, allowing all parameters to be evaluated within 1%.

**Thrust coefficient**—The first three flights of the second stage all produced appreciably lower velocity increments than expected, despite almost nominal  $c^*$  and the low propellant outages experienced (Figs. 59 and 60). An intensified study (Ref. 53) was made of telemetry, weight, and trajectory data in order to determine the cause of low performance. The thrust coefficient was determined by dividing the best estimate of thrust (from trajectory match and accelerometer data) by telemetered chamber pressure and known throat area. The investigation indicated that the actual thrust coefficient was 1.69, about 3.5% lower than the analytically determined value of 1.75, which had been used for the design. The lower value was further substantiated in the flights of SLV-4 and TV-4BU. Studies made by Aerojet-General of Thor-Able flights and vacuum chamber tests at AEDC indicated a thrust coefficient of  $1.70 \pm 0.02$  for this chamber. A thrust coefficient of 1.69 is indicative of an overall nozzle efficiency of about 92%.

## D. THIRD-STAGE PROPULSION

### 1. GRAND CENTRAL ROCKET COMPANY MOTOR

GCR 33-KS-2800 third-stage motors had five opportunities to fire in flight—on vehicles TV-1, TV-4, SLV-1, SLV-3 and SLV-4. In each of these flights, the motor ignited reliably and performed satisfactorily. A summary of the predicted and delivered performance and weight values for these motors is presented in Table 17.

**Velocity increment**—The horizontal drag-free velocity increment imparted to the payload by the third-stage motor was the only performance item which could be observed with reasonable accuracy. Other performance parameters were calculated from known weights and the observed velocity increment, or were obtained from less reliable indications such as telemetry frequency shifts. The delivered velocity increments were slightly below nominal values for each of these motors, but were greater than predicted minimums. The consistently high nominal predictions are believed to have resulted from lack of information concerning the motor burnout weights. It appears that unburned propellant slivers remained at burnout and reduced the total velocity increments by 100 to 200 fps.

**Specific impulse**—The standard formula used to evaluate solid propellant motor flight performance (see Ref. 54) is:

$$I_{sp} = \frac{\Delta V}{32.17 \ln (M_i/M_b)}$$

where  $I_{sp}$  = specific impulse, seconds

$\Delta V$  = drag- and gravity-free velocity increment, fps

$M_i$  = third-stage mass at ignition

$M_b$  = third-stage mass at burnout.

Substitution of the best estimate of the drag- and gravity-free velocity increment and the ground-measured values of loaded and empty motor weights consistently yielded a calculated flight specific impulse one to four seconds below that predicted from statistical test data (except in the case of the prototype motor for TV-1, Table 17B). This low calculated flight specific impulse was directly attributed to unburned propellant slivers on the order of two to three pounds remaining after burnout under the vacuum condition. These slivers could have been the energy source for the residual thrust discussed below.

**Residual thrust**—Two weeks after the launch of the SLV-4 satellite, the third-stage motor case, which had been separated from the payload after burnout, was found to have an orbit period about four minutes longer than that of the payload. A search of the previous orbits revealed that the same phenomenon had occurred on TV-4, and that the SLV-1 motor case had been reported sighted over Kansas, whereas the payload re-entered the atmosphere below India. The

existence and significance of residual thrust after normal burnout with the solid propellant Grand Central motor was therefore well established.

**Chuffing**—In the summer of 1958, several GCR 33-KS-2800 rocket motors were fired at simulated altitudes of 70,000 to 80,000 feet in a vacuum facility at the Arnold Engineering Development Center (AEDC), Tullahoma, Tennessee. After a motor had apparently burned out, several "chuffs" were observed. Generally, five or six chuffs occurred over a period of about three minutes, each lasting approximately 0.2 second and producing thrust levels as high as 250 pounds. No indications of chuffing could be found in the flight records of Vanguard vehicle TV-1, where the payload was not separated and was instrumented to sense accelerations of this magnitude. It therefore appears that the near perfect vacuum conditions at the third-stage operational altitude would not support the type of chuffing observed in the partial-vacuum tunnel tests.

**Outgassing**—Further studies and some tests with the propellant and motor liner materials showed that these materials decomposed or sublimated under the combined effects of low pressure and high temperature. Calculations indicated that sufficient material remained in the chamber to produce the impulse necessary to explain the observed conditions, and that the major action and impulse would occur during the first 20 minutes after motor burnout when the temperature of

the motor case was highest. These conditions were consistent with the observed relationships between the motor and satellite orbits described above. However, the behavior of the GCR motors after supposed burnout is still not completely understood.

## 2. ALLEGANY BALLISTICS LABORATORY MOTOR

The ABL X248 A2 third-stage motor was used on one Vanguard vehicle, TV-4BU. The motor ignited successfully and operated normally, placing a 52.25-pound payload into orbit. In this case, the payload and expended motor were not separated, resulting in a total satellite weight of approximately 95 pounds. The predicted and delivered performance and weight values are summarized in Table 17.

**Velocity increment**—The horizontal, drag-free velocity increment imparted to the payload by this motor exceeded the predicted value. The X248 was designed so that portions of the rubber insulating liner were consumed during the burning phase. For predicted performance calculations, it was assumed that seven pounds of liner would be consumed. From the flight behavior of the motor, it appears that eight pounds would be a better estimate. The conservative estimate of burnout weight is considered the reason why the nominal predicted velocity increment was exceeded.

**Specific impulse**—The flight specific impulse was calculated in the same manner as for the Grand Central

Table 17. Third-Stage Rocket Motors

VEHICLE	A. Weights (in pounds)				
	INERT PARTS WEIGHT AT IGNITION	WEIGHT EXPULSED AT IGNITION	LOADED PROPELLANTS	ESTIMATED SLIVER LOSS	PAYLOAD WEIGHT <sup>①</sup>
TV-1 <sup>②</sup>			378.8	0	186
TV-4	48.41	0.34	381.2	0-3	4.56
SLV-1	48.27	0.41	382.5	0-3	21.95
SLV-3	47.23	0.43	384.4	0-3	23.91
SLV-4	47.38	0.43	382.3	0-2	23.74
TV-4BU	50.21	0.61	454.6	③	52.25

VEHICLE	B. Performance Comparisons		EFFECTIVE SPECIFIC IMPULSE		VELOCITY INCREMENT <sup>④</sup>	
	BURNING TIME (sec)		(sec)		(fps)	
	Predicted	Actual	Predicted	Actual	Predicted	Actual
TV-1 <sup>②</sup>	33	33	240	242.2		7,375
TV-4	33	34	238	235.8	16,162	15,950
SLV-1	33	32	238	234.7	14,183	14,075
SLV-3	33	33	239.5	238.1	14,066	14,225
SLV-4	33	33	238	236.5	14,190	14,100
TV-4BU	38	37	251	251.2	14,240	14,390

① Includes attachment fittings

② Prototype motor

③ No sliver loss. Estimated liner weight consumed was 8 pounds compared to 7 pounds predicted.

④ Gravity-free velocity increment.

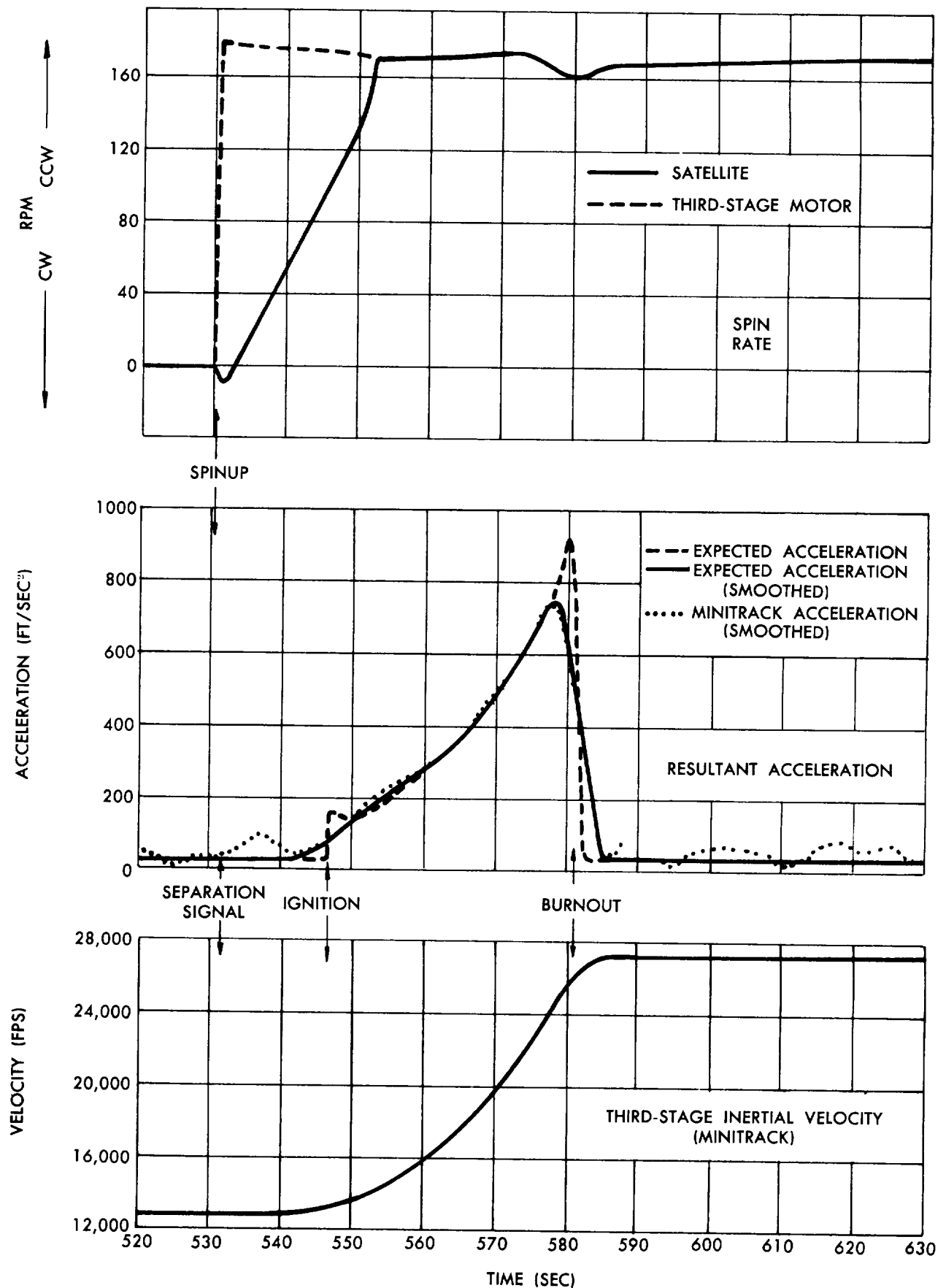


Fig. 61 Time Histories of Velocity, Acceleration and Satellite Spin Rate During Third-Stage Powered Flight, TV-4BU.

motors. Flight results indicated that the effective specific impulse was essentially nominal.

**Outgassing**—Observation of the first TV-4BU orbital period, compared to the periods of succeeding orbits, indicated an increase of the period from 129.4 to 130.2 minutes. The additional impulse required to produce this effect has been attributed to sublimation of the liner material in the motor (outgassing), since the geometry and amount of propellant remaining in the X248 after burnout is believed to make chuffing of this motor almost impossible. Studies indicated that conditions in the motor and the materials remaining were sufficient to provide the impulse necessary to explain the change in orbital period. The minimum impulse required was 200 pound-seconds, which would result in a velocity gain of about 50 fps. An accelerometer kick after payload separation on the first Javelin research vehicle (Honest John, Nike, Nike, X248) is taken as additional evidence of residual thrust with the ABL X248 motor. Thus, residual thrust, which had also previously been observed on the Grand Central motor, seems to be a characteristic of solid propellant motors fired in the space environment.

**Case expansion during burning**—Both longitudinal and diametrical expansion of the X248 motor cases were observed during static firings, but were not considered to be especially significant. Anomalies in the satellite spin rate during the flight of TV-4BU created new interest in case expansion during burning. There was a decided dip in the spin rate of the satellite-motor combination after about 26 seconds of burning (Fig. 61). This dip in spin rate (and partial recovery after burnout) was taken as a strong indication of motor case expansion, which would increase the roll moment of inertia. The presence of a discontinuity at about the same time as portions of the propellant burn-line reached the case liner had not previously been established, since time histories of case deflection during burning had never been made. This expansion could become significant if very precise flight path or spin rate control were required. However, it was not a problem on TV-4BU, as evidenced by the satellite injection angle of less than 0.1 degree from the horizontal.

## E. SEPARATION

### 1. LAUNCH

The launch motions were about as expected for the measured winds and thrust misalignments. Small differences observed were attributed to gusts, unexpected disconnect forces and momentary thrust misalignments.

**Acorn pin bind—fixed launch stand**—During the TV-4 launch, a binding of the quadrant II acorn pin sufficient to overpower the separation spring force

caused the swingaway arm to hang up until a tension force of 2300 pounds pulled the pin free. This resulted in binding of the quadrant II disconnects. The nitrogen, high and then low pressure hydraulic disconnects, respectively, pulled free under a tension load of 300 pounds, about 0.35 second after the acorn pin released. The acorn fittings were redesigned for TV-5 and later vehicles to provide positive centering of the acorn pins; the alignment procedure was revised to preclude lateral motions after the pins were centered.

**Aborted launch—retractable launch stand**—The first attempt to launch a vehicle (SLV-3) from the retractable launch stand was unsuccessful. The engine starting sequence was normal; however, the vehicle settled back on the stand because of a premature shutdown after only about 0.35 inch of vertical motion. The vehicle "bounced" slightly when it hit the launch stand, as a result of the spring action of the stand and vehicle tailcan. No structural damage resulted. Investigation revealed that the shutdown sequence was not initiated by the normal cutoff system but resulted from improper sequencing of the tail plug disconnects (see Chapter VIII, Section G).

Following the SLV-3 first flight attempt, three successful launches were conducted with the retractable launch stand performing excellently and the arms fully retracting before the vehicle had risen 10 inches.

During the SLV-6 launch, however, the retraction of the arms was delayed about 0.4 second, and they were not fully retracted until the vehicle had risen about 23 inches. Examination of motion pictures of the launch stand indicated that the arm releasing mechanism worked properly, but the spring-loaded valve which controls motion of the arms hesitated for 0.4 second about one-third of the way through its 90-degree travel. Excessive clearance between the disc and the housing of the four-way hydraulic valve allowed the disc to wobble and score during repeated operations. The scoring apparently caused sufficient binding to overcome the spring force and to cause the observed delay. This was in no way detrimental to the flight, since the lateral vehicle motions were so small that the engine would have cleared even if the arms had not retracted. The valve was replaced and a spacer was added to decrease the clearance between the disc and the housing, reducing the possibility of scoring the disc. The valve actuating spring was also replaced with a stronger spring as an added precautionary measure.

### 2. FIRST-STAGE SEPARATION

There were nine first- from second-stage separation sequences. Eight of these separations were successful, even though some minor malfunctions did occur. A malfunction during the SLV-5 sequence was the direct cause of that mission failure. A representative (TV-4BU) first- and second-stage thrust variation during

first-stage separation is shown in Fig. 62. First-stage thrust decay was normal for all flights. Initial second-stage thrust buildups are believed to have been normal despite some contrary telemetered data (see Chapter VIII, Section C) from pressure transducers.

**Delayed separation**—The time delay between the TPS separation signal and unplugging of the interstage electrical disconnects was 0.18 second, or about three times longer than expected for TV-4, and 0.3 second, or about five times longer than expected for SLV-5. The telemetered interstage compartment pressure and propulsion system parameters indicated that separation forces of about 15,000 pounds existed. The delay was not understood since extensive efforts to isolate malfunctions in the explosive bolts or their circuitry were fruitless (Chapter VIII, Sections F and G). However, SLV-6 and TV-4BU, wherein the only change was to give the separation signal earlier, or before a dynamic environment had built up, separated promptly.

**Dynamic environment**—All vehicles through SLV-5 had the second-stage engine exhausting into an appreciable back pressure, created by the confines of the interstage compartment prior to stage separation (see Chapter IV, Section E). There were numerous instances of random thrust vector motion during thrust buildup, due to separation in the vacuum exhaust nozzle (Ref. 43). The random thrust vector applied moments on the engine large enough to overcome the servo system and move the engine as much as two degrees on TV-4, against the stop in SLV-3, and hard enough against the stop in SLV-5 to fail the pitch actuator lag (Ref. 49). The primary separation sequence was changed for SLV-6 and up, to be given earlier by TVS<sub>1</sub> (oxidizer valve 27% open) in an attempt to reduce the period over which nozzle flow separation might occur. Precautions were also taken to ensure against excessive and nonuniform accumulation of adhesive used on the nozzle closure, and a check valve (see Chapter VIII, Section I) was installed in the hydraulic system to decrease the rate at which an overpowering force would move the engine.

**Roll transient—SLV-6**—The new early separation system (see Chapter IV, Section E) used for SLV-6 removed the adverse dynamic environment, but was accompanied by rather large pitch, yaw and roll motions; in fact, the rolling motion came near the gyro limit. These motions were probably caused by hinging about the electrical disconnects and tipping due to unequal separation forces. The roll motion was exaggerated by a deficiency of about 40% in second-stage roll jet thrust (see Chapter VIII, Section A). Ensuring a nominal roll jet thrust and placing three guide pins between the first and second stages to prevent hinging about the electrical disconnects resulted in a TV-4BU separation sequence with engine motions

caused solely by engine thrust misalignments and maximum roll excursions only slightly greater than the deadspot setting of  $\pm 3.0$  degrees.

### 3. NOSE CONE JETTISON

The nose cone, which protected the satellite during flight through the atmosphere, was separated from the second stage at 172 seconds after liftoff. Completely successful separation was recorded by two sources of data on all eight vehicles on which separation was initiated. The telemetry system transmitted the initiating signal and also a microswitch signal when the nose cone halves had parted. The Minitrack signal strength and frequency also reacted to the absence of the shielding effect of the nose cone and the unfolding of the satellite antenna.

The second-stage pitch and yaw attitudes were unchanged by the separation of the nose cone, reflecting the symmetry of the separation sequence. However, during the SLV-3 separation sequence, a small counterclockwise roll disturbance about 0.4 second after the separation signal was attributed to a slight binding in one nose cone hinge. Normally, the hinge disengaged 0.7 second after the separation sequence was initiated. Roll control was in no way compromised by this anomaly.

### 4. THIRD-STAGE SEPARATION

The Vanguard third-stage separation sequence was initiated four times by the airborne firing system and once by the ground-based system during the Vanguard program. All resulted in satisfactory separations. The third stages were successfully spun up to at least 178 rpm. Total impulse of the spin rockets was within the specified limits.

**Second-stage spinup**—Exhaust gases from the third-stage spin rockets impinged on the second-stage compartment walls and caused a rolling moment greater than the correcting roll jet moment. This introduced a second-stage roll rate on the order of 10 rpm during third-stage separation. No attempt was made to retard this roll rate on any vehicles because analysis revealed that this spin rate actually increased clearance by more or less averaging out transient disturbances.

**TV-4 premature separation and recontact**—Third-stage spinup for TV-4 was accomplished satisfactorily and all hardware performed normally. However, premature physical separation of the third stage from the spin table occurred, probably because of one or a combination of: vibrations from the spin rockets; pressure buildup underneath the motor by exhaust gases from the spin rockets; and the relatively large attitude error rates. The separation delay time was therefore changed from 3.3 seconds to 1.5 seconds after spin rocket ignition, which prevented recurrence of this premature separation.

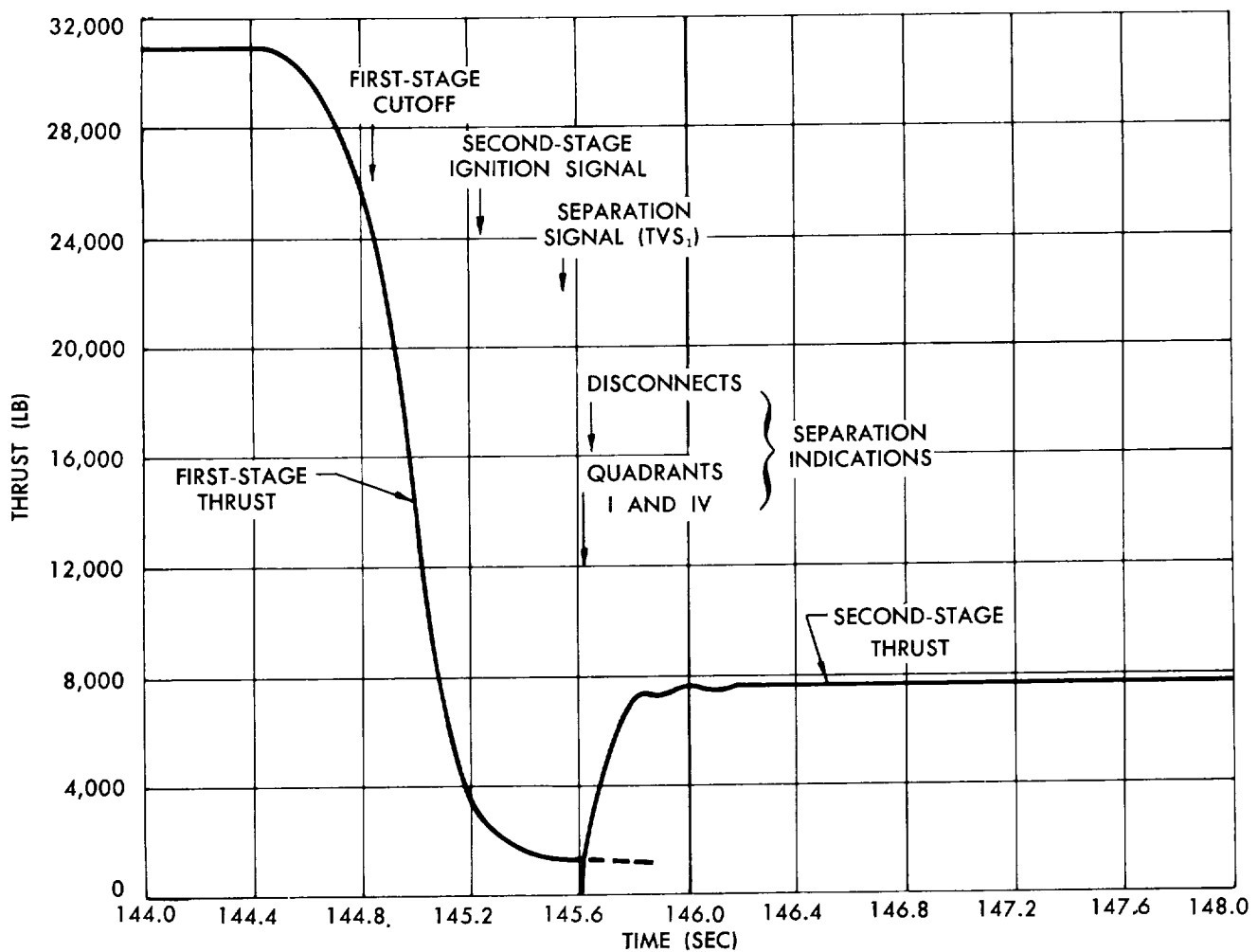


Fig. 62 Representative (TV-4BU) First and Second-Stage Thrust During First-Stage Separation

When the TV-4 pitch/yaw control system was turned off at third-stage spinup, the stuck-open pitch-down tumble jet continued thrusting (see Chapter VIII, Section A). As the third stage spun up, the second stage was also spun (see above). The second stage had rotated more than half a revolution and had developed a wobble of better than one degree because of the continued jet thrusting and the reversal in attitude errors. The third-stage nozzle base hit the second stage just as it was separating, apparently because the premature separation (see above) sufficiently lengthened the time that the third stage was free inside the second to allow the second-stage wobble to cause collision. The collision was not serious since the TV-4 satellite was injected with an angular error of approximately 0.8 degree.

**SLV-4 control cutoff**—On SLV-4, pitch jet actuations (one up and one down) were recorded between 0.10 and 0.15 second after retrorocket ignition, when the control system was normally de-energized. This malfunction was attributed to one set of contacts on the 1.5-second delay relay closing about 0.20 second after the other set. This time difference was within specification and did not affect the stabilization during separation.

**Retrorocket performance**—An increase in the

tipoff rate of the TV-4BU second stage during retrorocket burning (Ref. 51) was believed to have been caused by unbalanced retrorocket forces. The increase in rate could have been caused by a nominal difference between retrorockets. This increase was not detrimental to the point of causing collision between stages. Following the SLV-1 launch, one retrorocket shield was found near the launch site. No adverse effects were noted, as both rockets ignited properly.

## 5. SATELLITE SEPARATION

Every satellite except that of TV-4BU was separated from the burned out third-stage motor to avoid signal interference, to limit the satellite spin rate and/or to orbit a symmetrical body. A spring-loaded device to be actuated after third-stage burnout was supplied with the satellites to provide a relative velocity of about three fps between the payload and rocket.

**TV-4**—The satellite of TV-4 was connected to the third stage by a high friction bearing. The satellite and rocket motor were spinning with no relative rotation between them from four seconds after spinup to satellite separation, 75 seconds later. A slight increase in spin rate during third-stage burning was probably caused by transfer of the angular momentum of the burning gases as they moved from the burn line inward toward

the center through the propellant slots. (The nozzle throat diameter was considerably smaller than the average diameter of the propellant burn line.) There was a sharp decrease in spin rate after separation from the third-stage motor, which has since been attributed to the tie-down strap attaching the satellite to the third-stage motor. This strap, when released, would tend to straighten. The change in its moment of inertia would cause the strap to rotate at a decreased rate and thus tangle in the satellite antenna, resulting in the satellite losing rotational energy.

**SLV-4**—A tumble rate of approximately 15 rpm about an axis slightly off the equatorial plane was superimposed during separation on the existing payload spin rate of less than one rpm about the spin or polar axis. This tumbling was attributed to a disturbing moment resulting from the binding of the separating spring on a sharp ledge. The disturbing moment was particularly damaging because of the unexpectedly low satellite spin rate which resulted when a despin device operated more effectively at altitude than ground calibrations had indicated. A thin metal sleeve was placed in the separation device for SLV-5 and SLV-6 to prevent binding, and the separation spring was restrained to the third stage. A flight shift was also applied to the ground calibration tests of the despin device, based on the measured performance during SLV-3 and SLV-4 flights.

**Post-separation spin drag**—The SLV-4 satellite tumble rate had decayed from 15 rpm to slightly more than 11 rpm in about two weeks of observation. The spin rate about the spin axis also decayed from somewhat less than one rpm to about 0.5 rpm. A similar decay was also noted on the TV-4 satellite. These decays are considered normal and are attributed to the energy dissipated by eddy currents generated in the metallic satellite that is spinning in the earth's magnetic field.

**Time of payload separation**—The TV-4 and SLV-1 payloads were separated from the third stage approximately 27 seconds after burnout. Residual thrust, noted in AEDC wind tunnel tests, raised the possibility of an expended motor being accelerated into collision with the satellite after separation. Satellite separation was delayed for approximately five minutes in the SLV-3 through SLV-6 vehicles, but (see Chapter VIII, Section D) even this did not remove the concern over possible collision from residual thrusting. Accordingly, the TV-4BU burned-out third stage was left attached to the payload since the fiberglass case did not adversely affect the experiments.

## F. ORDNANCE

No failure of any ordnance component is known to have occurred on any Vanguard flight. There was, however, just one instance where ordnance was under

suspicion. SLV-5 experienced a mysterious delay in actual separation of the first stage, and unusually severe flow separation occurred in the second-stage nozzle just after ignition (see Chapter VIII, Section C). The behavior of the vehicle could be explained very conveniently by assuming that actuation of the explosive bolt detonators was delayed for about 250 milliseconds and that the blast doors failed to open, causing excessive back pressure in the interstage compartment. Consideration was given to the possibilities that the separation delay might have been due to overaged detonators, resulting either in a weak detonation or a delay in detonator actuation, and that the blast doors may have failed to open due to weak latchpin squibs or LOX tank ice sealing the doors.

Nearly half of all the E-77 detonators used for first-stage separation were removed from Vanguard stores at Cape Canaveral and returned to Martin-Baltimore for test purposes. These detonators included those of the lot from which the SLV-5 detonators had been taken. Four explosive bolts were sheared, using only one detonator in each bolt, and leaving the opposite bolt cavity empty and not capped. Two annealed explosive bolts were sheared with these detonators. Times to detonation were measured for six of the detonators wired in parallel in a mockup of the vehicle firing circuit. This test was repeated twice. Finally, a bolt was sheared with only one detonator installed and a detonator alone was fired while both were subjected to a vacuum of about  $5 \times 10^{-4}$  millimeters of mercury. The detonators operated normally in all tests.

Blast door latchpins and squibs were similarly returned for tests. Tests included firing squibs alone under adverse conditions, and operating a mockup of the blast door installation with a thick coating of ice around the doors. All squibs and latchpins operated normally, and the blast doors opened.

Based on the test results, it was concluded that the E-77 detonators and latchpin squibs were not likely to have malfunctioned on SLV-5, and that those remaining in Vanguard storage at AFMTC were acceptable for the succeeding flights. Subsequent flight data indicated that these detonators and squibs operated normally. The separation delay on SLV-5 has never been satisfactorily explained.

Prior to flight, two first-stage igniters failed during the entire program. In one instance, the failure was caused by improper installation. In the second case, actual failure of the igniter occurred, apparently because of low order burning of the igniter charge.

## G. ELECTRICAL

A summary of electrical system functions and voltages measured during the Vanguard flight program is given in Table 18.

**Table 18. Electrical System Functions and Voltages\***

	TV-4	TV-5	SLV-1	SLV-2	SLV-3	SLV-4	SLV-5	SLV-6	TV-4BU
Battery Paralleling (time from liftoff)	120.01	120.01	120.1	120.1	120.2	120.25	127.24	127.32	T-60
Second-Stage Arming	120.01	120.01	120.1	120.1	120.2	120.25	127.24	127.32	127.3
First-Stage Cutoff	144.07	140.7	143.5	143.4	140.15	144.11	140.88	144.46	144.85
Method	LPO	FPO	FPO	FPO	LPO	LPO	LPO	LPO	LPO
Second-Stage Ignition	144.25	141.05	143.9	143.97	140.53	144.51	141.17	144.82	145.25
Method	CPS	CPS	CPS	CPS	CPS	CPS	CPS	CPS	CPS
Stage Separation Signal	144.65	141.57	144.25	144.45	140.98	145.03	141.69	145.18	145.55
Method	TPS	TPS	TPS	TVS <sub>2</sub>	TPS	TPS	TPS	TVS <sub>1</sub>	TVS <sub>1</sub>
Stage Separation Actual	144.83	141.64	144.3	145.52	141.03	145.08	142.0	145.28	145.65
Helium Heater Squib Ignition	144.83	141.1	152.0	152.5	146.5	150.5	146.0	145.28	145.65
Nose Cone Separation Signal	172.0	172.05	172.02	172.05	172.21	172.27	172.27	172.28	172.32
Nose Cone Separation Actual	172.1	172.1	172.1	172.1	172.26	172.35	146.54	172.30	172.39
Second-Stage Cutoff	266.07		261.5	152.56	248.59	260.77	243.86		263.07
Method	TPS	TPS	TPS	TPS	Oxidizer Probe	Oxidizer Probe	Oxidizer Probe		Oxidizer Probe
Hydraulic Pump Motor Cutoff	720	720	720		418	418			285
Third-Stage Ignition and Spinup	590.87		553.0		421.02	526.37			530.27
Method	CTC		CTC		Ground	CTC			CTC
Third-Stage Separation Signal	594.5		554.42		Command				
First-Stage Batt. Volt. Limits (d-c volts)	29.3-29.5	27.4-29.0	29.0	29.2-29.5	29.6-29.8	28.0-28.7	28.8	28.8-29.4	531.86
Second-Stage Batt. Volt. Limits (d-c volts)	29.5-29	27.3-28.7	27.9-29.8	27.8-29.3	27.2-28.7	26.1-28.9	27.0-28.8	27.9-29.5	29.6-30
Inverter Voltage Limits (a-c volts)	115.2-115.5	118.8-120.2	115.2	115	114	112-114	115.5	114.4	26-30
									114.1-114.8

\* All units are in seconds except where noted.

LEGEND

CPS—First-Stage Chamber Pressure Sensor.  
 TPS—Second-Stage Chamber Pressure Sensor.  
 LPO—LOX Pump-Out Pressure Sensor.

FPO—Fuel Pump-Out Pressure Sensor.  
 TVS<sub>1</sub>—Oxidizer Main Valve Switch No. 1 (valve 27% open).  
 TVS<sub>2</sub>—Oxidizer Main Valve Switch No. 2 (valve 78% open).  
 CTC—Coasting Time Computer.

**Arming and battery paralleling**—Battery paralleling, first-stage cutoff arming, and second-stage arming in vehicles through SLV-4 were accomplished by a relay in the program timer at approximately 120 seconds after liftoff. For SLV-5 and SLV-6, this time was changed to 127 seconds to give longer first-stage burning in the event that a malfunction caused first-stage cutoff upon arming of the cutoff system. Studies indicated that no adverse effects could result from this change. On the last vehicle, TV-4BU, the flight batteries were paralleled before liftoff, resulting in a more reliable 28-v d-c system, since flight experience had indicated that battery capacity was more than adequate for the additional usage. Battery paralleling, arming and first-stage cutoff operated as planned in every flight.

**Second-stage ignition**—Second-stage ignition was designed to occur when the first-stage chamber pressure sensor operated, as thrust reached the 10% level. A backup was provided by utilizing a one-second timer actuated at cutoff. In all flights, the primary system gave the second-stage ignition signal.

**First-stage separation signal**—In vehicles up to SLV-5, the first-stage separation signal was initiated by TPS when thrust in the second stage reached 70% and was backed up by TVS<sub>2</sub> when the oxidizer valve reached 78% of full open. During the SLV-2 flight, when thrust buildup was slow because of clogged oxidizer screens, TVS<sub>2</sub> initiated the separation signal.

On SLV-6 and TV-4BU, the separation circuitry was changed so that the oxidizer valve opening 27% of full open (TVS<sub>1</sub>) would give the primary separation signal. Use of the TVS<sub>1</sub> signal enabled separation to occur before the interstage compartment pressure reached a level which could adversely affect the sequence.

**Helium heater squib ignition**—The second-stage helium heater squib was designed to ignite when a pressure switch (HPS<sub>1</sub>) sensed that sphere pressure had dropped to  $1400 \pm 50$  psia. Because of a stress corrosion problem on spheres in vehicles through TV-4, the maximum sphere pressure was limited to 1360 psia; as a consequence, actual stage separation was used to initiate squib ignition instead of the HPS<sub>1</sub> switch. On two flights, TV-5 and SLV-6, premature squib ignition occurred when HPS<sub>1</sub> momentarily operated as a result of helium pressure transients. After TV-5, a circuit was added through the interstage disconnects to block squib ignition until actual separation. The squib ignited prematurely on SLV-6 with no adverse effects. Squib ignition was changed to occur at first-stage separation on TV-4BU.

**Second-stage cutoff**—The second stage was designed to cut off when either oxidizer or fuel exhaustion caused chamber pressure to decrease to approximately 130 psia. On TV-5, cutoff was not completed

because the K2 relay did not latch in after being energized by the chattering thrust pressure switch (TPS) (Ref. 44). This was due either to a design deficiency in the relay sequencing (K1-K2) or to an in-flight component malfunction within the relays. However, on SLV-1, oxidizer exhaustion, coupled with unstable burning (see Chapter VIII, Section C) again caused chattering of the TPS switch, resulting in a delayed cutoff and a subsequent rupture between cooling tubes of the thrust chamber. Oxidizer probe circuitry was designed for SLV-2, but was not completely proven on this flight, since cutoff was initiated prematurely by TPS when clogged oxidizer line screens resulted in low chamber pressure. The oxidizer probe circuitry sensed oxidizer exhaustion during the SLV-3 flight and gave a successful second-stage cutoff. For vehicles SLV-4 and up, the redesigned oxidizer probe circuitry sensed exhaustion in either oxidizer feed line independently and gave a more repeatable cutoff.

**Hydraulic pump motor**—Originally the hydraulic pump motor was planned to be de-energized at second-stage cutoff, since hydraulic pressure was not required for the coasting phase of flight. Later studies indicated that second-stage thrust did not decrease to zero for several seconds after cutoff. On TV-4 through SLV-2, the hydraulic pump motor remained energized continuously. A requirement for increased battery hold time caused the hydraulic pump motor to be de-energized at the initiation of the fifth pitch rate for SLV-3 through SLV-6 and at second-stage cutoff plus 20 seconds on TV-4BU. On all vehicles not prematurely terminated, the motor was de-energized as planned.

**Battery voltages**—First- and second-stage flight battery voltages remained within specification limits during all flights except for short periods of time when the limits were exceeded because of incorrect battery preloading (loading the battery for a period of time until the voltage load characteristics became such that voltage was within specification for all foreseeable load conditions). Preloading procedures were revised, but a tendency persisted to under preload to conserve battery capacity. Battery capacity was amply demonstrated on several occasions when unexplained momentary overloads, on the order of 60 amperes, did not adversely affect bus voltage.

**Inverter voltage**—Although the inverter voltage was well within specification limits on all flights, there were instances when the voltage dropped slightly during the flight. The voltage drop was attributed to telemetry demodulator drift, rather than to inverter control system drift since, during qualification testing, the inverter voltage did not drop under similar circumstances.

**B+ power supply**—Plate voltage for the electronic autopilot was provided by a dynamotor and electronic noise filter combination on vehicles TV-3 through SLV-5. However, this system was sensitive to changes

in battery voltage. Any change in battery voltage was reflected through the dynamotor to the plates of the tubes in the amplifiers, and sometimes resulted in fairly large transient engine motions. For instance, on TV-4, at paralleling of first- and second-stage batteries, a 2.9-degree engine transient was recorded in the pitch axis, with 2.5 degrees in yaw. Engine transients of this magnitude were never experienced on later vehicles at battery paralleling because of tighter control of battery preloading techniques. On SLV-3 and SLV-4, no engine transient resulted, while on SLV-5 only 0.5 degree of engine motion was recorded at battery paralleling.

The transformer rectified-regulated B+ power supply, using the inverter as a primary input voltage, was incorporated on SLV-6 and TV-4BU, thereby essentially isolating the amplifier plates from changes in battery voltage. This unit gave reliable performance on the last two vehicle flights, and B+ voltage was maintained well within the specification limits of  $150 \pm 7.5$  volts. There were no engine transients at battery paralleling on the SLV-6 flight and, of course, none on the TV-4BU flight, since the batteries were paralleled prior to launch. Slight second-stage engine motions (on the order of 0.5 degree) were noted during the first-stage separation sequences of SLV-6 and TV-4BU, but these were due to loss of first-stage servo loads at separation and were not considered detrimental to vehicle control.

## H. MECHANICAL

**First-stage roll jets**—The basic first-stage roll jet design was satisfactory in that adequate roll control was maintained on all flights (see Chapter VIII, Section A).

The action of the roll jets during flight showed a friction condition in the control actuation mechanism that increased in severity with altitude. An improved seal of aluminum bronze was used in TV-3 and up to prevent galling which had occurred with the original stainless steel seals due to high exhaust temperatures. Ground tests were made after the SLV-3 flight that duplicated the altitude pressure differential (15 psi) on the jet nozzle cases. Normal deflection of the backup structure (0.030 inch maximum), as the pressure differential across the case increased with altitude, decreased the available clearance between the cam link and torque tube fork and caused binding. The observed flight malfunctions (see Chapter VIII, Section A) were reproduced when the initial clearance setting was reduced below the specified minimum of 0.04 inch. Corrective action consisted of increasing the minimum clearance between the cam link and torque tube fork from 0.04 to 0.06 inch. Roll jet operation on subsequent flights indicated that this corrective action had eliminated linkage binding.

Roll jet response on TV-4BU flight was slightly abnormal in that the up-left jet exhibited high friction during the first 50 seconds of flight. The high friction was probably due to the labyrinth seal rubbing against the turbine exhaust tube temporarily until steady-state heat transfer conditions had been established.

**Third-stage spin mechanism**—The design of the Vanguard third-stage spin mechanism proved to be highly successful and reliable, as indicated by flight performance. Six third-stage rockets were successfully spun up and separated from the second stage; the seventh was an inert rocket that was spun up but not separated in TV-2. The basic spin mechanism was first flight tested on TV-1. The motor-table spin rate after two revolutions was 200 rpm, at which time the motor was released and coasted clear of the vehicle at retro-rocket ignition. Examination of gyro telemetry records indicated that there were no component malfunctions and that the system accomplished a clean spinup and separation in its first flight test. On the flight of TV-2, the spin table and inert motor attained a spin rate of 204 rpm at two revolutions, closely duplicating the successful spinup of the live motor on TV-1. The Vanguard configuration spinups are discussed in Chapter VIII, Section E.

Special low friction bearings were utilized in the satellite forward bearing housing on SLV-1 to minimize the satellite spin rate (requirement was a maximum rate of about 60 rpm). This was done to provide information on the ability of these bearings to produce a low spin rate for the cloud cover experiment. The indicated spin rate from Minitrack data was 53.5 rpm.

## I. HYDRAULIC

The Vanguard first-stage hydraulic system was first flight tested on TV-2. The second-stage hydraulic system was incorporated on TV-3 and later vehicles. Flight results throughout the program verified the hydraulic system designs, and that operation was generally within design limits.

**First stage**—First-stage hydraulic pressure normally varied about a 1600- to 1700-psi nominal value due to the design of the pressure regulator. A maximum flight hydraulic pressure of about 1800 psi occurred on SLV-6 and TV-4BU. On other flights, the pressure was normal. In all cases, the hydraulic system provided adequate pressures to move the engine actuators in response to gyro commands.

A tendency toward a slight hydraulic pressure drop was noted throughout most first-stage flights. For instance, on SLV-1, the pressure gradually decreased from 1720 psi at launch to 1630 psi at first-stage burn-out. This pressure drop was probably due to lowering of the viscosity of the hydraulic fluid from a normal temperature rise in the hydraulic system.

Hydraulic pressure surges were noted during the launch transient on some flights. These surges varied from the 500 psi noted on TV-3BU to 3100 psi on SLV-1. Such surges at launch are characteristic of engine starts and are not considered dangerous. Although the 3100 psi surge noted on SLV-1 was slightly above the proof pressure of the system (2650 psi), it was well below the burst pressure of 4375 psi, and was not considered detrimental.

Noisy telemetering data was obtained on some of the earlier flights, probably because of vibration of the transducer. After the SLV-3 flight, the aluminum tubing to the transducer was replaced by flexible steel hose to reduce the vibration. Also, a damping orifice was added at the transducer to damp out pressure surges. The results of SLV-4 and subsequent flights indicated that the noise level in hydraulic pressure data was reduced by about 50% by these changes.

**Second stage**—Second-stage hydraulic pressure should normally have varied from about 1000 to 1100 psi due to the design of the pressure regulator. The pressure was satisfactorily regulated between the limits of 990 psi on SLV-1 and 1000 psi on SLV-3 during first-stage flight. On several flights, a peculiar drop in second-stage hydraulic pressure at second-stage engine ignition was indicated. At engine shutdown, the pressure indication sometimes returned to the normal level. Investigation revealed that this particular pressure transducer could be made to sense erroneous pressure readings by changing the level and frequency of the

vibration, and also by application of large pressure surges. Proper hydraulic pressures and measurements were obtained on SLV-5, SLV-6 and TV-4BU by consecutively moving the transducer upstream of the accumulator, incorporating a more effective locking device in the system relief valve to prevent shift of the valve adjustment, removing the transducer from the high vibration environment, replacing the steel tubing to the transducer with flexible steel hose and installing a damping orifice at the transducer.

Pressure surges at the actuator of 2800 psi on SLV-3 and at least 3300 psi on SLV-5 indicated large overpowering forces during the starting sequence of the second-stage engine. These overpowering forces on SLV-5 impacted the engine into its stops at a rate of about 146 degrees per second, causing structural failure of the pitch actuator lug and consequent loss of pitch attitude control. A check valve was incorporated into the pressure line to each second-stage hydraulic actuator on SLV-6 and TV-4BU to limit the rate of engine motion induced by externally applied loads to about 20 degrees per second. Therefore, the force with which the engine could impact against its stops when overpowered by external loads could no longer exceed the structural design limitations. Data at second-stage ignition of SLV-6 and TV-4BU indicated that the check valve arrangement operated properly since no large hydraulic pressure surges were evident.

The average steady-state hydraulic pressures during second-stage powered flight are given in Fig. 63.

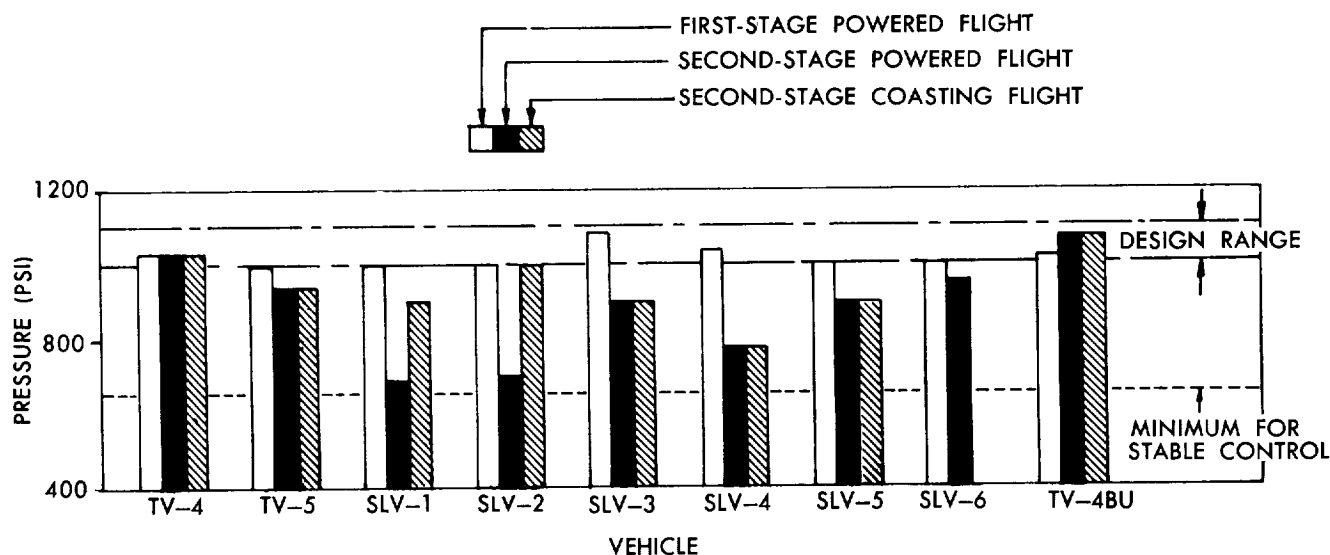


Fig. 63 Average Steady-State Second-Stage Hydraulic Pressure

## J. RANGE SAFETY

The flight of rockets from Cape Canaveral may endanger life and property. Five primary sources of information were used by Air Force range safety personnel during a typical Vanguard operation to ensure that these hazards were held to an absolute minimum. They were an electronic skyscreen system, two optical systems, present position plots supplied from radar, and predicted impact plots supplied from radar. In general, the equipment operated satisfactorily and provided adequate coverage of the flights. Occasionally, however, ground equipment malfunctions (especially TV-0, Ref. 38) gave conflicting and even erroneous data. Range safety personnel invariably interpreted the available information correctly. Operation of the individual systems is described below.

### 1. GROUND SYSTEMS

**Electronic skyscreen**—The electronic skyscreen system (telemetry/ELSSE) was used to indicate deviations from a vertical reference plane and the programming of the vehicle from a vertical position to a down-range direction. A red (destruct) signal was noted on SLV-5 before second-stage burnout, but occurred five seconds after the end of range safety responsibility. No commands were required or sent.

**Optical system**—The Mark 51 is an optical skyscreen system of tracking that is normally the primary source of early track range safety information. Fifteen minutes before the launch of TV-0, the Mark 51 was found to be unfit because of a faulty calibrator. A crash program was believed to have eliminated the difficulty by launch. The system showed red destruct after launch, but range safety personnel properly ignored the indication because of other available information and the prelaunch history. All other Vanguard program flights were indicated to be safe by this system.

The second optical system consisted of an observer using a vertical wire skyscreen. He reported a red condition early in the flight of TV-5 but no action was taken. Later study of theodolite film proved this condition to have been safe.

**Present position plots**—The Range Safety Officer had six present position plots presented on three 2-pen plotting boards. Each board presented a plot of vertical position versus down-range position and vertical position versus cross-range position. Two of the plotting boards were supplied by the XN-1 C-band radar; one board had an expanded scale that covered only the early portion of the flight. The XN-2 C-band radar supplied the remaining board. Coverage by these systems was adequate for all flights and indicated that safety limits were not exceeded.

**Predicted impact point plots**—The predicted impact point plots, an output of a digital program using XN-1 and XN-2 data, were traced by pens on impact prediction maps of the ground plane. There were four predicted impact plotting boards, each of which covered a different portion of the range. These plots were used for both flight termination and command control purposes. No commands or destruct signals were sent on the basis of these plots.

### 2. AIRBORNE SYSTEM

**Command receivers and decoders**—The flight trajectory for all SLV's except SLV-6 required that command control be successively shifted from Cape Canaveral to Grand Bahama Island, San Salvador, and Grand Turk, respectively, in order to assure a signal level above 5 microvolts. Command control was not shifted to Grand Turk for SLV-6 because of its planned northerly flight azimuth. The shift in command control was carried out as planned for all vehicles except for SLV-2 (because of premature second-stage cutoff) and for SLV-5 (where a range discrepancy prevented the shift). There was no necessity for cutoff or destruct commands during any flight. However, the system presumably would have operated successfully if required, since third-stage ground commands were successfully received by SLV-3, SLV-4 and TV-4BU.

On SLV-1, a decision was made to initiate third-stage spinup and ignition by ground command; however, the system never operated. The abnormally severe second-stage shutdown had caused the telemetry transmitter to cease functioning, and perhaps contributed to failure in the second-stage command receiver or its associated circuitry. This failure was of no consequence, since the CTC successfully ignited the third stage. However, on subsequent vehicles, all r-f connectors were Scotch-casted to increase reliability. The adequacy of the command system was demonstrated on SLV-4 and TV-4BU by the reception of third-stage firing commands even while the second stage was rolling after third-stage spinup.

**C-band beacon**—The AN/DPN-48(c) SHF beacon was used on Vanguard to increase the effective tracking range of the AN/FPS-16 C-band radars at Patrick Air Force Base and Grand Bahama Island. Analysis of radar tracking obtained for all vehicles indicated proper tracking beacon operation with only minor dropouts caused by second-stage tumbling on SLV-5 and second-stage vehicle attitude change on SLV-1.

A "beacon steal" condition was observed on the XN-1 AGC record during the flight of SLV-6, which probably resulted from improper synchronization of the XN-1 and XN-2 signals. Arrival of the XN-1 interrogation pulses at the beacon apparently coincided with the times when the beacon was transmitting to XN-2

**Table 19. Satellite Launch Vehicle Instrumentation**

**A. INTERNAL**

*1. First Stage*

NOTE: All measurements on PPM telemetry system, except as indicated by \* (PWM system), or \*\* (both PPM and PWM systems).

<i>Measurement</i>	<i>Range</i>	<i>Measurement</i>	<i>Range</i>
Pitch Motor Deflection**	± 5°	Turbine Exhaust Pressure	0 to 40 psia
Yaw Motor Deflection**	± 5°	Fuel Tank Differential Pressure	0 to 5 psid
Down-Right Roll Jet Position	± 50°	LOX Tank Differential Pressure	0 to 10 psid
Up-Left Roll Jet Position	± 50°	Helium Sphere Pressure	0 to 4500 psi
Fuel Pump Inlet Temperature	0 to 150°F	Hydraulic Pressure	0 to 3000 psi
LOX Pump Inlet Temperature	-300 to -250°F	Turbine rpm*	0 to 36,000
Combustion Chamber Pressure	0 to 700 psia	Instrumentation Battery Voltage	0 to 5 v dc
Fuel Injector Pressure	0 to 1000 psia	T/M Battery Voltage	0 to 32 v dc
LOX Injector Pressure	0 to 1000 psia	Flight Battery Voltage	0 to 32 v dc
Fuel Pump Inlet Pressure	0 to 30 psia	LOX Flow Rate*	0 to 450 gpm
LOX Pump Inlet Pressure	0 to 70 psia	Fuel Flow Rate*	0 to 350 gpm
Peroxide Tank Pressure	0 to 700 psia	Liftoff Signal	On or Off

*2. Second Stage*

NOTE: All measurements on PWM telemetry system.

<i>Measurement</i>	<i>Range</i>	<i>Measurement</i>	<i>Range</i>
Pitch Motor Deflection	± 5°	Ignition Signal (2nd Stage)	On or Off
Yaw Motor Deflection	± 5°	3rd-Stage Spinup Signal	On or Off
Pitch Gyro Error Signal	± 10°	Separation Signal (2nd Stage)	On or Off
Yaw Gyro Error Signal	± 10°	Separation Signal (3rd Stage)	On or Off
Roll Gyro Error Signal	± 10°	Destruct Signal	On or Off
UDMH Feed Line Temperature	0 to 100°F	CW Roll Jets	On or Off
WIFNA Feed Line Temperature	0 to 100°F	CCW Roll Jets	On or Off
Pitch Gyro Torquer Rate	0 to 1.6°/sec	Down Tumble Jet	On or Off
Yaw Gyro Torquer Rate	0 to 1.6°/sec	Up Tumble Jet	On or Off
Hydraulic Pressure	0 to 3000 psig	Right Tumble Jet	On or Off
Combustion Chamber Pressure	0 to 300 psia	Left Tumble Jet	On or Off
UDMH Injector Pressure	0 to 400 psia	Nose Cone Separation	On or Off
WIFNA Injector Pressure	0 to 400 psia	180-sec Backup Timer (0-sec sig)	On or Off
Helium Sphere Pressure	0 to 2000 psig	180-sec Backup Timer (180-sec sig)	On or Off
Propane Tank Pressure	0 to 300 psia	120-sec Signal	On or Off
UDMH Tank Pressure	0 to 400 psia	172 to 190-sec Signal	On or Off
WIFNA Tank Pressure	0 to 400 psia	Computer Spinup Signal	On or Off
3rd-Stage Spinup	0 to 300 rpm	Martin Timer	Contact
Longitudinal Accelerometer	-1 to +6g	WIFNA Flow Rate No. 1	0 to 60 gpm
Flight Battery Voltage	0 to 32 v dc	WIFNA Flow Rate No. 2	0 to 60 gpm
Inverter Voltage	100 to 130 v dc	UDMH Flow Rate	0 to 80 gpm
Instrumentation Battery Voltage	0 to 5 v dc	Velocity (Integrating Accel)	0 to 22,000 fps
Dynamotor Voltage	0 to 200 v dc	Command Rec AGC No. 1	0 to 100,000 μv
T/M Battery Voltage	0 to 32 v dc		

**B. EXTERNAL**

C-band Radar Tracking Data Using Airborne AN/DPN-48 Beacon  
 Phototheodolite and Fixed Camera Tracking Data  
 Trajectory and Impact Range Safety Charts Using Radar Inputs  
 Weight Recorder Data  
 Anemometer Record  
 Motion Picture Film—Both Engineering Surveillance and Overall Coverage  
 Auto-Digital Data Reduction Printouts  
 Weather Data—Ground and Aloft  
 Sequence Recordings

Telemetry/ELSSSE Plots  
 Teledeltos Auto-Reduction Records  
 Radar Function Records  
 Function and Command Records  
 Telemetry Station AGC's  
 Radar Logs  
 Minitrack Doppler Report  
 Minitrack AGC's  
 PWM/FM Telemetry Magnetic Tape  
 PWM/FM and PPM/AM Telemetry Film Time History Records

or recovering from this transmission. According to available data, synchronization of the ground-transmitted interrogation pulses was present prior to flight, with provisions for manual adjustment during flight. The loss of synchronization may have been caused by a transient in line voltage which had the same effects as a manual adjustment. Also, the 48-degree flight azimuth used for SLV-6 resulted in the signal path between XN-1 and XN-2 and the vehicle being considerably different than on previous flights, and may have caused some errors in adjusting the signal spacing. As a result of the "beacon steal" condition, the manual adjustment was changed from a pulse-type to a continuous-type system to eliminate the effects of line voltage transients.

## K. INSTRUMENTATION

A large share of the success of the Vanguard flight analysis effort may be traced directly to the extreme reliability of the telemetry systems throughout the course of the program. There was not a single flight in which the Government-furnished telemetry transmitters failed to function, and about 97% of the programmed measurements were recorded for review. The instrumentation system therefore demonstrated excellent performance and reliability.

**Telemetry antenna systems**—Three telemetry antenna systems were used in the Vanguard program: one each for the PPM/AM system in the first stage and the FM/FM and PWM/FM systems in the second

stage. The PPM/AM system was required to transmit signals for first-stage flight only, while the other systems were required to operate to at least third-stage separation. The FM/FM system was not used after TV-4, which permitted relocation of the PWM/FM antenna system to eliminate the attenuating effects of propane gas from the second-stage roll jets.

On earlier vehicles, dropouts were experienced in the first-stage telemetry signals during the first-stage burnout transient as a result of ionization of exhaust gases. The ionization effect on signal dropout was lessened on SLV-3 and up by reducing the radiating power of the transmitter. On all vehicles, the PWM/FM telemetry coverage extended beyond third-stage separation, except on TV-5, SLV-2, SLV-5 and SLV-6 where vehicle malfunctions prevented the initiation of third-stage ignition.

**Data procurement**—The Vanguard program, by definition, was not to interfere with the military missile program. This caused the project to have a low standing on the AMR priority list, with consequent delays in data procurement (on the order of weeks in the early firings). This condition was circumvented on all vehicle flights after TV-1 through the use of special telemetry processing facilities which had been set up by the VOG to supply quick-look data. The flight analysis effort was supplied with complete sets of data from this source very shortly after each flight.

**Typical instrumentation**—All available flight measurements taken on a typical Vanguard satellite launch are presented in Table 19.



## IX. SIGNIFICANT FLIGHT ANALYSIS TECHNIQUES

The Vanguard program afforded the opportunity to develop several new flight analysis techniques and to reaffirm some well established ones. The following section describes, in brief, the guiding philosophies and some of the more significant techniques that were used.

### A. PHILOSOPHIES

**Automatic data reduction**—Various attempts were made to use automatic digital data reduction equipment, teledeltos, Benson-Lehner film readers and other mechanized equipment. However, the relatively few measurements (about 80), the long flight times (up to 800 seconds) and the selectivity of interest made such attempts inefficient. Experience with the analysis of the flights of 14 vehicles indicated that about three man-weeks was the average time spent in telemetry data reduction, whereas better than a man-year per vehicle was spent in scrutiny and interpretation of the raw telemetry records. All mechanized equipment at the disposal of the program was therefore used only as backup information to the detailed studies by engineering personnel of the continuous telemetry records.

**Flight analysis**—A serious attempt was made in the Vanguard program to have the flight analysis effort perform three functions. These were, in order of importance:

- (1) Improvement in the probability of the success of the next vehicle to be fired by close study of what happened in prior flights.
- (2) Documentation of all efforts and results.
- (3) Measurement of vehicle performance to refine prediction capabilities.

Improvement in the probability of success of following vehicles literally involved looking for trouble whether or not any was known to exist. Obvious areas of work centered on flight failures. Not so obvious areas were exemplified by the ABL third-stage motor case expansion during burning, as deduced from the Minitrack AGC records, and TV-3 gross vibration environment before liftoff as deduced from motion picture comparisons of the way ice was shaken off the LOX tank during the launches of TV-2 and TV-3. This latter study caused a shift of emphasis from the obvious point of failure—a broken fuel line—to happenings before liftoff which were the real causes of the difficulty.

Measurement of vehicle performance to refine prediction was accomplished by utilizing as many independent measurements of the various parameters as were known (e.g., telemetry, external tracking, weight data, etc.). Judicious selection of data chosen to obey known laws, such as allowable variations in characteristic exhaust velocity and thrust coefficient, permitted a "best estimate" type of approach to performance determination. This systems approach invariably uncovered faulty data that would have otherwise been misleading. The overall accuracy for typical measurements was on the order of 1% for propulsion system operations, 0.1 degree for engine and gyro motions, and perhaps 0.2 degree for pitch injection angles.

Every effort was made to prepare as complete a story on the flight of each Vanguard vehicle as was possible, since the Vanguard project recognized the benefit of industry-wide flight analysis liaison. The NASA Vanguard organization, formerly with NRL, gave excellent support to these efforts such as, for example, the authorization of the Guidance and Control Volumes (Refs. 13, 14 and 55) and this Engineering Summary.

**Opinions on optimum instrumentation**—Flight failures are likely in the early stages of a test program. Selected instrumentation and continuous high response time records are essential in the examination and understanding of the rapid transients that invariably accompany flight failures. These selected continuous records with high response are infinitely more valuable in a failure such as those on TV-3BU and TV-5 than many measurements with a frequency response too low to record any data over the extremely short interval of interest.

However, the optimum instrumentation for performance determination consists of as many independent measurements to as high a degree of accuracy as is possible. Commutation of data to increase the scope of measurements is quite acceptable. Use of this type of instrumentation may be increased in the late stages of test programs where flight failures are unlikely but precise performance determination is highly desirable.

### B. TECHNIQUES

**Trajectory match**—A Vanguard trajectory match procedure was developed that used external tracking data as an additional source of information in the

determination of the basic vehicle performance parameters. The technique involved an iterative least-squares solution to minimize the ignition and burnout position and velocity difference between the measured and calculated trajectories by varying the stage thrust, total propellant flow rate and pitch rates. Accurate matching of ignition and burnout conditions allowed an analysis of overall performance parameters, while the deviations between these two points gave an estimate of the quality of the match.

The best available values for all input parameters were used to calculate a first estimate of the flight trajectory. Three additional trajectories were then calculated in which thrust, flow rate and pitch rate were changed to give sensitivity coefficients. The position and velocity differences between the measured and the estimated trajectories at the match points were minimized on a least-squares basis. The solution gave a perturbation on the original thrust, flow rate and pitch rates, from which a new estimated trajectory could be calculated. This trajectory duplicated the match positions and velocities better than the first estimate. Repeating the least-squares fit gave rapidly converging, increasingly accurate matches. Repetitive solutions were necessary because of the nonlinearity of the sensitivity coefficients and nonequivalence of the partial derivative equation when finite increments are used. The basic equations used, in addition to those that comprise the Vanguard 704 program, were:

$$x_{OBS} = x_{TM} + \frac{\partial x}{\partial \dot{\theta}} \Delta \dot{\theta} + \frac{\partial x}{\partial \dot{w}} \Delta \dot{w} + \frac{\partial x}{\partial T} \Delta T + R_x \quad (1)$$

$$y_{OBS} = y_{TM} + \frac{\partial y}{\partial \dot{\theta}} \Delta \dot{\theta} + \frac{\partial y}{\partial \dot{w}} \Delta \dot{w} + \frac{\partial y}{\partial T} \Delta T + R_y \quad (2)$$

$$\dot{x}_{OBS} = \dot{x}_{TM} + \frac{\partial \dot{x}}{\partial \dot{\theta}} \Delta \dot{\theta} + \frac{\partial \dot{x}}{\partial \dot{w}} \Delta \dot{w} + \frac{\partial \dot{x}}{\partial T} \Delta T + R_{\dot{x}} \quad (3)$$

$$\dot{y}_{OBS} = \dot{y}_{TM} + \frac{\partial \dot{y}}{\partial \dot{\theta}} \Delta \dot{\theta} + \frac{\partial \dot{y}}{\partial \dot{w}} \Delta \dot{w} + \frac{\partial \dot{y}}{\partial T} \Delta T + R_{\dot{y}} \quad (4)$$

$$R^2 = (K_x) R_x^2 + (K_y) R_y^2 + (K_{\dot{x}}) R_{\dot{x}}^2 + (K_{\dot{y}}) R_{\dot{y}}^2 \quad (5)$$

$$\frac{\partial R}{\partial \dot{\theta}} = 0, \frac{\partial R}{\partial \dot{w}} = 0, \frac{\partial R}{\partial T} = 0 \quad (6)$$

where

$x, y, \dot{x}, \dot{y}$  = position and velocity coordinates in feet and fps, respectively

$\dot{\theta}$  = pitch rate

$\dot{w}$  = flow rate

$T$  = thrust

$R^2$  is the quantity to be minimized by equation (6),

and subscripts OBS and TM are measured and calculated values, respectively.

The  $K$  values are weighting factors for dimensional consistency. The results obtained were quite satisfactory when these factors were assumed to be 1.

The present solution was based on position and velocities in the pitch plane; however, more refined studies could incorporate azimuth deviations.

**Sea level thrust**—A simple approximation to the early external track of vertically-launched rocket vehicles appears as:

$$\Sigma F_y = \dot{y} = \left( \frac{T - D}{w/g_0} \right) - g \quad (7)$$

Suitable integration between the limits of  $t_1$  and  $t_2$  yields

$$T - D = \frac{\left( \frac{\dot{y}_2 - \dot{y}_1}{(t_2 - t_1)} + g \right) w_1/g_0}{1 + \frac{(t_2 - t_1) |\dot{w}|}{2w_1} + 1/3 \left[ \frac{(t_2 - t_1) |\dot{w}|}{w_1} \right]^2 + \dots} \quad (8)$$

where

$T - D$  = thrust minus drag, pounds

$\dot{y}$  = vertical velocity, fps

$g$  = local gravity, fpsps

$g_0$  = 32.174 fpsps

$w$  = weight, pounds

$\dot{w}$  = propellant flow rate, lb/sec,

and the subscripts 1 and 2 indicate respective times.

Equation (8) is limited by the assumption of no motion off the vertical and constant thrust and specific impulse over the time interval  $t_2 - t_1$ . However, equation (8) was compared with an early track as computed on a 704 program, and found to be applicable (less than 40 pounds error in 28,000 pounds) over the time interval from the end of the starting transient to the insertion of the pitch program at 10 seconds flight time.

The accuracy of the thrust determination is seen to be directly proportional to the accuracy of the vehicle weight measurement. Thrust is relatively insensitive to vehicle velocity since 0.6% or 0.2 fps error in the vertical velocity difference introduces a thrust error of only 30 pounds. Thrust is very insensitive to the weight flow,  $w$ , since 10% error amounts to a thrust error of only 30 pounds. The time interval and local gravity should be accurately determinable. Therefore, the sea level thrust of vertically launched liquid-propellant rocket vehicles may be determined to a quite reasonable degree of accuracy by the use of equation (8).

**Specific impulse**—A somewhat different treatment of the equations of motion from that given in equation ⑦ appears as

$$\frac{a}{g_0} = \frac{T - D}{w} \quad (9)$$

where  $a$  = acceleration along vehicle axis, sensed inside the vehicle.

Suitable integration yields:

$$\frac{T}{|\dot{w}|} = I_{sp} = \frac{D}{|\dot{w}|} - \frac{1}{\frac{g_0}{a} \left[ \frac{d \ln(T - D)}{dt} \right] + d \left( \frac{g_0}{a} \right)} \quad (10)$$

Equation ⑩ is limited by the assumption of one-dimensional motion, where variations in wind (or other forces inclined to the flight path), azimuth deviation, angle of attack, gyro errors, thrust misalignment, etc., cannot be properly accounted for. Equation ⑩ can be reduced to usable form through the further assumptions of constant thrust and zero drag, thus:

$$I_{sp} = - \frac{1}{\frac{d \left( \frac{g_0}{a} \right)}{dt}} \quad (11)$$

Equation ⑪ was found to be a useful first approximation to determine flight specific impulse of the various Vanguard stages, but could not be used as a precise determination, even with exact accelerometer measurements, because of the assumptions required. External track measurements are a potential source of acceleration along the vehicle axis, but should be used (if at all) with extreme care because of the triple differentiation required.

**Orbit injection angle**—A flight path time history of a stable orbit is readily obtainable if the orbital elements are known. Orbital elements of the Vanguard satellites were computed from Minitrack observation at the IBM World Computing Center, Washington, D. C. These elements were used to calculate the flight path time history at about the time of injection.

The flight path angle at the instant of injection is the actual orbit injection angle.

Calculations for the SLV-4 and TV-4BU orbits indicated injection angles of  $-0.02$  and  $-0.05$  degree, respectively, with an error tolerance of  $\pm 0.2$  degree. The high degree of measurement precision was obtainable because the stable character and low decay rate of the orbits permitted numerous observations to be used, and also because the flight path angle varies by only  $\pm 10$  degrees throughout the orbit and is, therefore, relatively insensitive to injection time.

Additional impulse as a result of third-stage outgassing or chuffing would be included in the final orbit. This residual or delayed impulse would tend to increase the perigee altitude on orbits injected near perigee, while decreasing the computed injection angle. A time history of the residual thrust would be required to obtain the actual injection angle.

**Special cases**—A mechanical contrivance, consisting of a rotating commutating disc, was devised to give a controlled intermittent electrical signal. This intermittent signal was fed into the dynamic mockup analog computer in such a fashion as to simulate the observed TV-3BU motor deflections around vehicle breakup. The resultant data provided a major tool in determining the cause and area of structural failure (see Chapter VII, Section D).

A digital program was prepared that accepted telemetered gyro (attitude) time histories to produce resultant vehicle motions. This program was used in the study of the large indicated SLV-3 pitch motions just after third-stage spinup, and was required because the high vehicle roll rate (11 rpm) caused cross-coupling into the pitch and yaw gyro motions which obscured actual vehicle motion.

A method using the observed engine motions and the analytical and laboratory-determined characteristics of the hydraulic system was developed to calculate overpowering loads on the second-stage engine actuator arms. This method predicted structural failure at the time indicated by telemetry in the SLV-5 first-stage separation sequence, and was used in determining the effectiveness of the "fix" for future vehicles.



## X. PROGRAM ACCOMPLISHMENTS

This report is primarily a documentation of the Vanguard satellite launching vehicle. However, a measure of the success of the vehicle is provided by what it accomplished; what it is capable of doing; and what was learned in designing, building and flying it. These program accomplishments are discussed below.

### A. SATELLITE ORBITS

For some time in the future, there will be three instrumented satellites in stable orbits about the earth that were launched by Vanguard vehicles. These orbits are summarized in Table 20.

The TV-4 (1958 Beta One) and SLV-4 (1959 Alpha Two) burned-out third stages that were separated from their payloads are also in orbit. Both rocket motors have approximately the same inclination and perigee altitude as their instrumented payloads, but the outgassing effect described in Chapter VIII, Section D, gave them slightly longer periods and higher apogee altitudes than their payloads.

### B. MISSION CAPABILITIES OF THE FINAL VEHICLE

A realistic performance appraisal, based on flight experience and using the probability approach described

in the Appendix, now confirms that the Vanguard launching vehicle has appreciably greater capabilities than that specified for the original mission (Ref. 56). With the higher performance ABL X248 third-stage motor used in the last vehicle, the Vanguard configuration can place a 100-pound payload into an orbit with an expected perigee of 180 statute miles. Capabilities for precisely-controlled space probe and re-entry missions supplement its original function as a satellite launching vehicle.

Statistical methods applied to input data from acceptance, static and flight firings have been employed to arrive at the expected performance parameters given in Table 21. Probability analyses were used in conjunction with these performance parameters to determine the *expected* and *three-sigma* mission capabilities. The term *expected* mission capability may be interpreted as the most likely performance, or the performance that will be exceeded 50% of the time. The *three-sigma* capability represents mission performance that will be exceeded about 699 out of 700 times.

**Orbital missions**—The payloads that can be placed in orbit from Cape Canaveral, using the normal down-range flight azimuth of 107.5 degrees, with a resulting orbit inclination of about 33.5 degrees, are shown in Fig. 64. The inclination of the orbit to the equatorial

**Table 20. Vanguard Satellite Orbits**

<i>Launching Vehicle</i>	<i>TV-4</i>	<i>SLV-4</i>	<i>TV-4BU</i>
Launch Date	17 March 1958	17 February 1959	18 September 1959
Time, GMT	12:15:41	15:55:02	5:20:07
<i>Injection Conditions</i>			
Time, GMT	12:26:21	16:04:38	05:29:49
Altitude (stat mi)	408	345	318
Velocity (fps)	26,935	26,860	27,195
Flight path angle (deg)	0.8	-0.02	-0.05
<i>Satellite Designation</i>	1958 Beta Two <i>VANGUARD I</i>	1959 Alpha One <i>VANGUARD II</i>	1959 Eta <i>VANGUARD III</i>
<i>Initial Orbit Parameters</i>			
Anomalistic period (min)	134.27	125.82	130.19
Inclination (deg)	34.25	32.85	33.34
Eccentricity	0.190	0.166	0.190
Perigee altitude (stat mi)	410	348	318
Apogee altitude (stat mi)	2460	2060	2330
<i>Orbit Parameters on 9 March 1960</i>			
Anomalistic period (min)	134.04	125.62	130.13
Inclination (deg)	34.02	32.88	33.37
Eccentricity	0.190	0.165	0.189
Perigee altitude (stat mi)	403	348	321
Apogee altitude (stat mi)	2450	2050	2320

NOTE: Small discrepancies among injection, initial perigee and current perigee altitudes are due to inaccuracies in the various data sources and changing orientation of the perigees with respect to the oblate earth.

**Table 21. Expected Performance Parameters**

(PAYLOAD: 100 LB)

		First Stage	Second Stage	Third Stage	Complete Vehicle
Gross Weight at Lift-off	lb	17,822	4393 <sup>③</sup>	608	22,823
Propellant Weight at Lift-off	lb	16,201 <sup>①</sup>	3352 <sup>④</sup>	456	20,009
Weight Consumed for Power	lb	15,965 <sup>①</sup>	3279	463 <sup>⑤</sup>	19,707
Burnout Weight	lb	1,857	1072	145	
Total Propellant Flow Rate	lb/sec	111.2 <sup>①</sup>	27.4		
Thrust—Sea Level	lb	28,000 <sup>②</sup>			
Altitude	lb	30,600 <sup>②</sup>	7343	3100 (average)	
Specific Impulse—Sea Level	sec	252			
Altitude	sec	275	268	252 (effective)	
Mixture Ratio (O/F)		2.15	2.75		
Burning Time	sec	143.6	119.7	38	
Gravity-Free Velocity Increment	fps			11,500	

① Includes 335 lb hydrogen peroxide at lift-off, of which 315 lb are consumed for power at 2.2 lb/sec.

② Does not include roll jet thrust.

③ Includes 33 lb nose cone, separated 172 sec after lift-off.

④ Includes 9 lb starting losses.

⑤ Includes 7 lb liner consumed.

plane can be increased to approximately 48 degrees simply by rotating the launch azimuth, with minor reductions in payload as indicated in Fig. 65. Range safety limitations at Cape Canaveral preclude the use of steeper launch azimuths in either direction. However, if the second stage were yawed during coasting flight, this would effectively “dog-leg” the third-stage flight path and thereby permit the attainment of orbit inclinations up to about 70 degrees, with payload penalties as shown in Fig. 65. A different launch site, where north-south launch azimuths are not restricted by range safety, would permit polar orbits (90-degree inclination) with the slightly reduced payloads shown in Fig. 64.

In cases where precise control of orbit perigee is desired, a trajectory should be selected such that both second-stage apogee and orbit injection altitudes are close to the planned perigee altitude. This flight path would best utilize available vehicle performance, allow maximum injection angle error tolerance and reduce the sensitivity of the perigee to performance variations. The initial portion of the powered flight would be used to achieve the vertical velocity necessary to carry the vehicle to the desired satellite injection altitude. The pitch program would be such that, when the required vertical velocity has been attained, the vehicle's attitude is horizontal. Therefore, additional impulse would increase the velocity at second-stage apogee, but would not appreciably change the injection altitude. For perigees of about 200 miles, the overall accuracy of the existing Vanguard systems would be expected to produce an orbit perigee within  $\pm 20$  miles of that predicted, if the above technique is employed. Payload capability would be approximately 10% less than that

shown in Fig. 64 because of the modified pitch program required during powered flight.

**Space probe missions**—Optimum flight programs were used to determine the maximum apogee that can be reached with different payloads (Fig. 66). The break in the curve is caused by the optimum flight path changing from a low angle, high velocity trajectory for the lighter payloads to a practically vertical flight path for the heavier payloads. The equivalent of the four-pound TV-4 satellite could have been accelerated to escape velocity by the last vehicle of the current Vanguard series.

**Re-entry missions**—The velocities for re-entry trajectories at an altitude of 80 statute miles are given in Fig. 67 as a function of payload. It should be noted that the payloads in Fig. 67B are obtained with the first two stages only. In this case, the precise second-stage attitude control system remains attached to the payload until final separation, providing the capability of controlled attitude changes.

## C. ADVANCES IN THE STATE OF THE ART

The great surge of rocket development in the late 1950's produced many important advances in the state of the art. The manner in which the Vanguard satellite launching vehicle contributed to this progress is summarized below.

### 1. VEHICLE DESIGN

- The Vanguard was the first large rocket to have a launch thrust-to-weight ratio as low as 1.2.

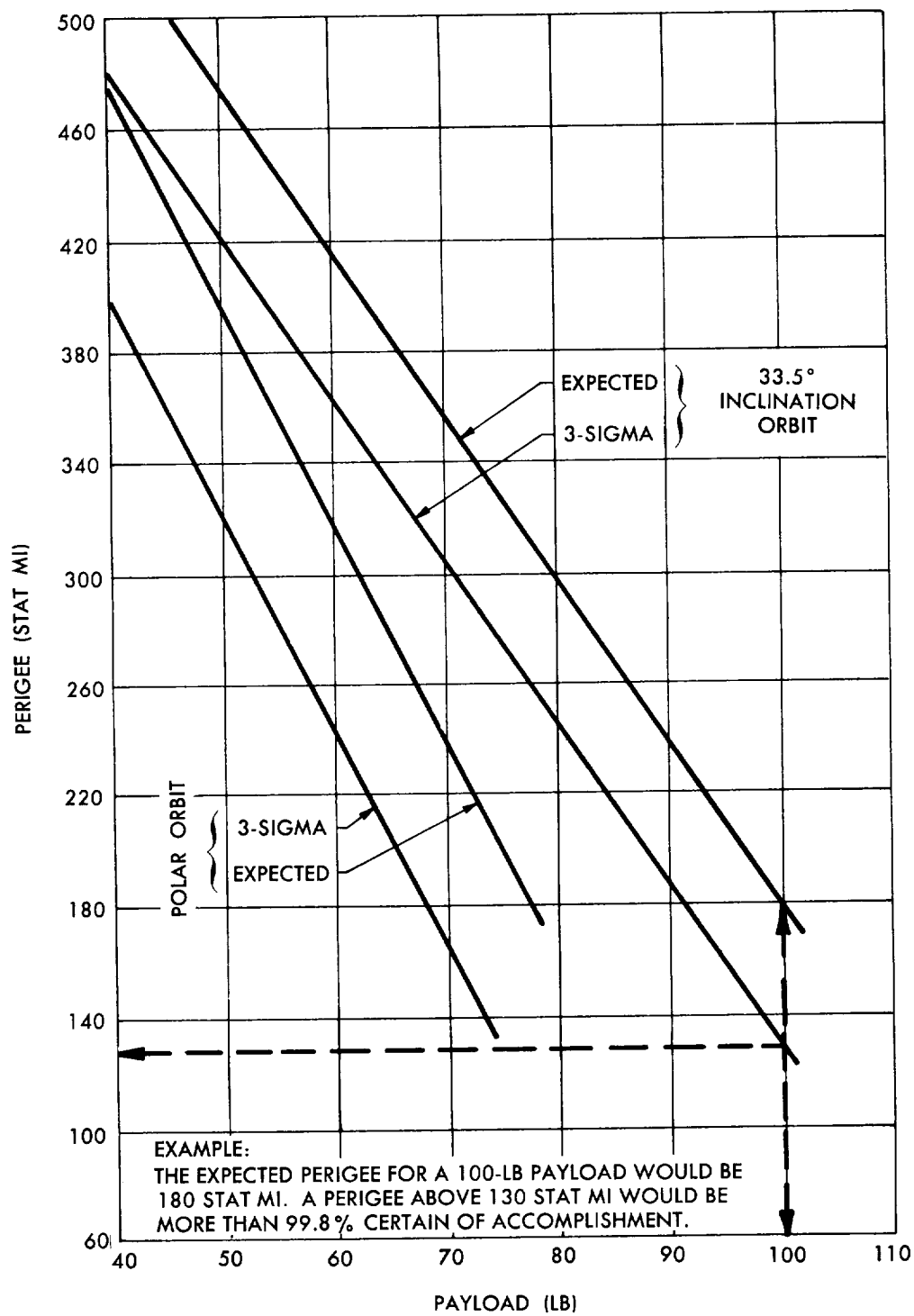


Fig. 64 Payload Capability for Orbital Missions, Using Optimized Flight Programs

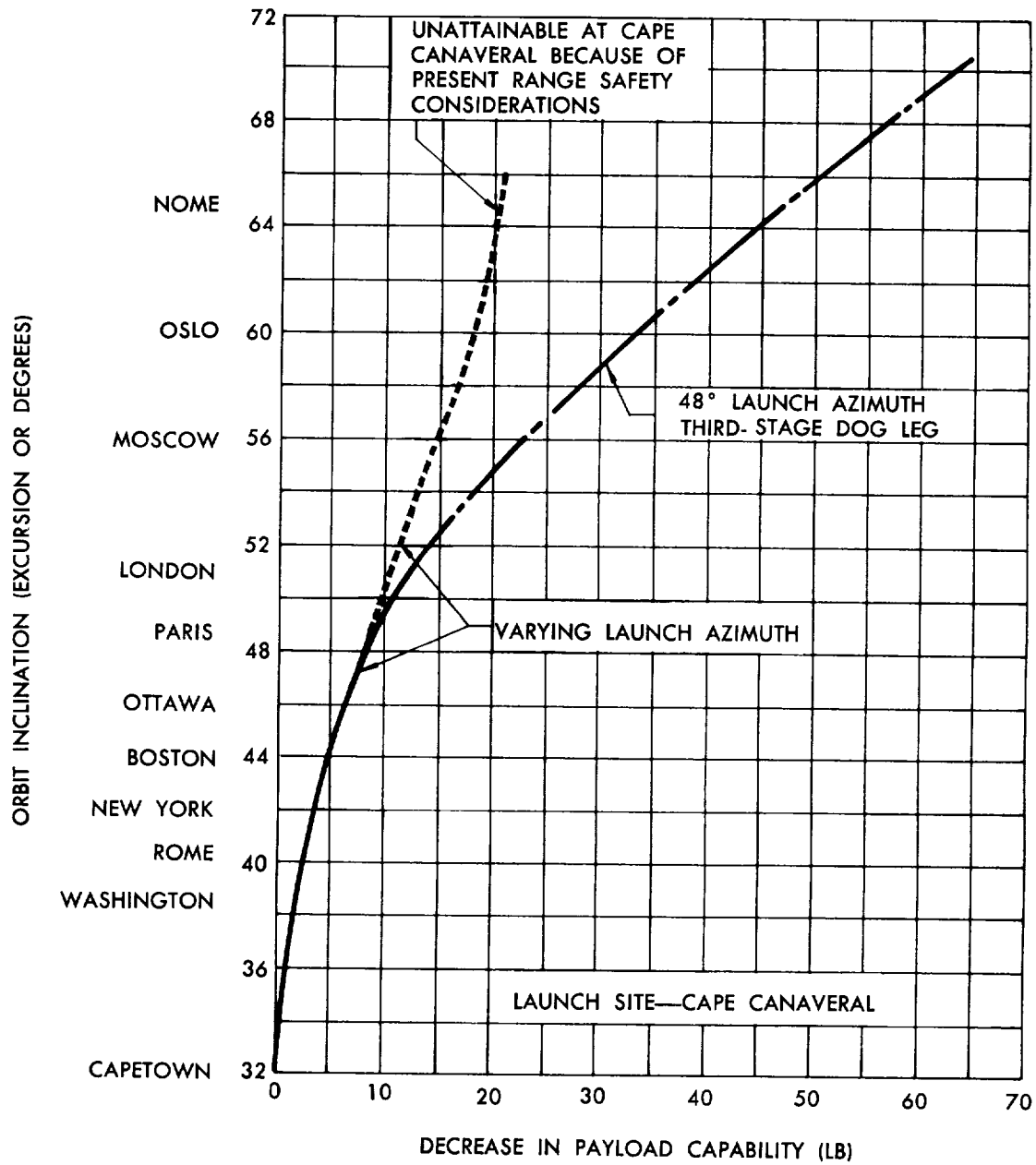


Fig. 65 Approximate Decrease in Payload Capability for Increasing Orbit Inclination

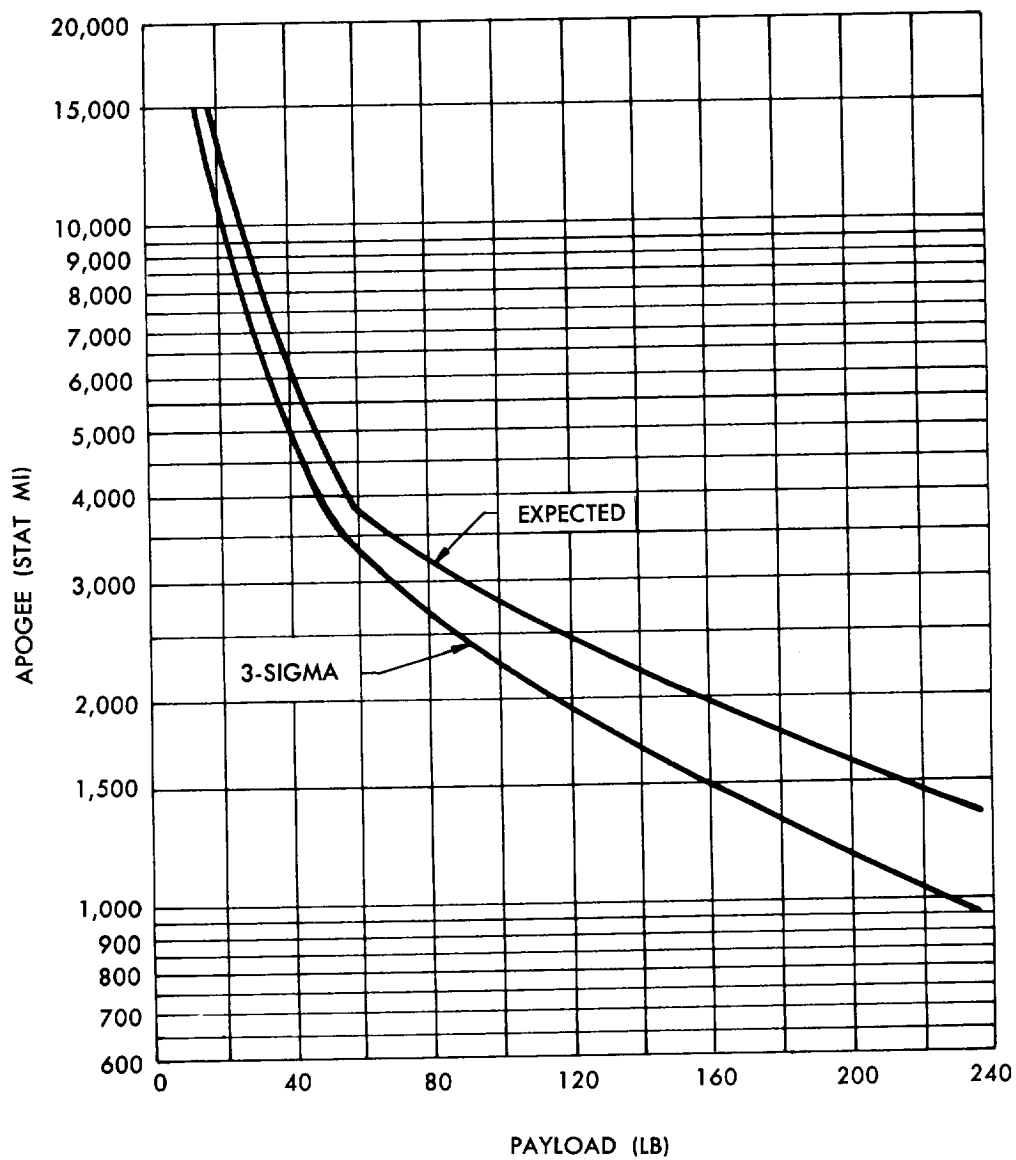
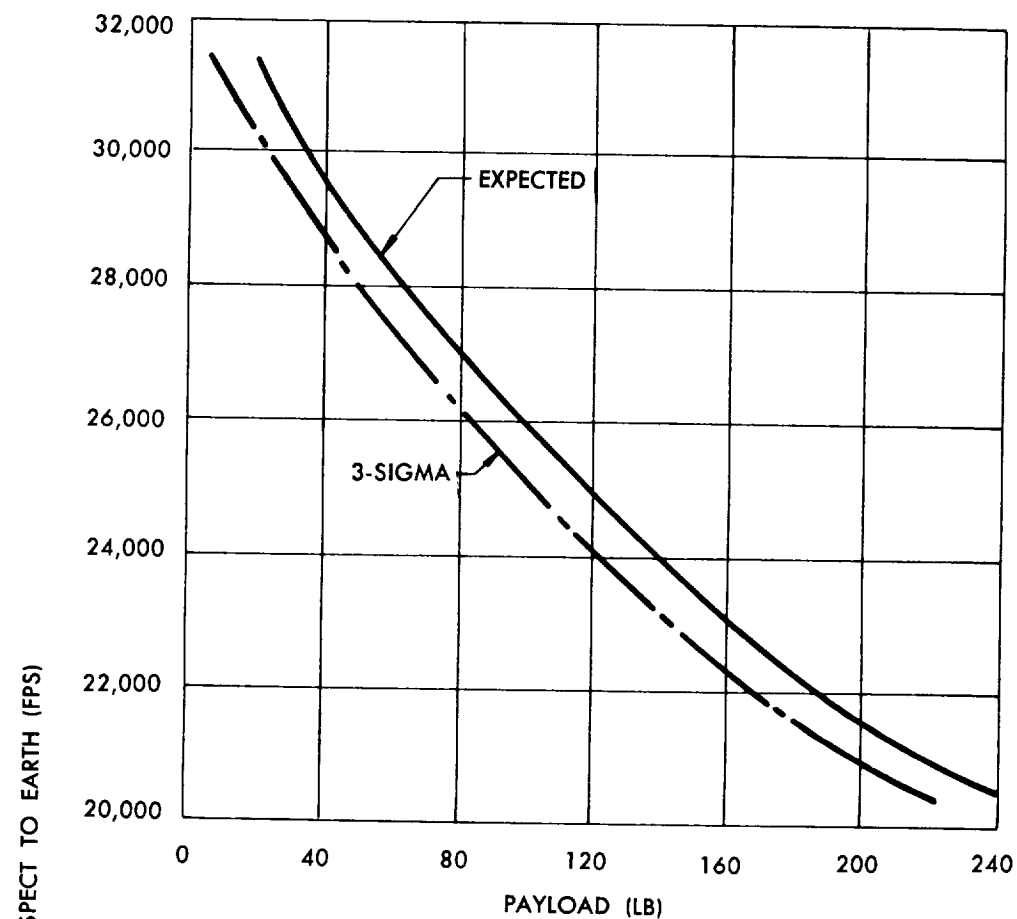
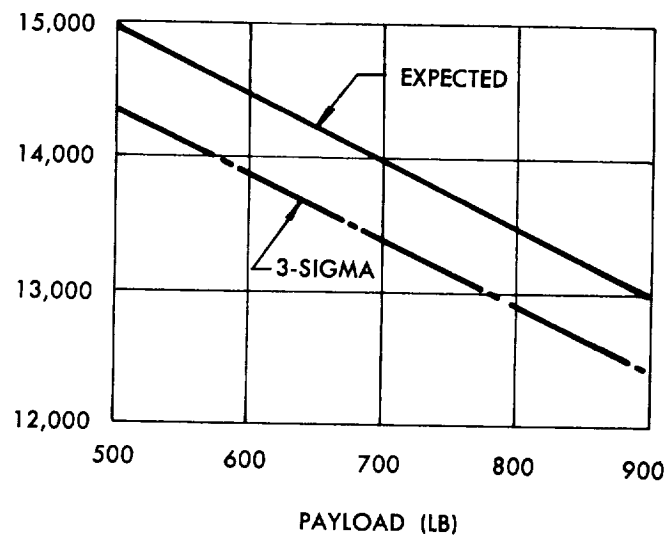


Fig. 66 Vanguard Payload Capability for Space Probe Missions



A. THREE-STAGE PERFORMANCE



B. TWO-STAGE PERFORMANCE

Fig. 67 Payload Capability for Re-entry Missions at an Injection Altitude of 80 statute miles

- The mass ratio was one of the largest of any contemporary vehicle—88% of the launch gross weight was propellant.
- The structural margin of safety was only 25% except in areas affecting personnel safety.
- Structural feedback was incorporated in the structural load analysis and allowed the control system response characteristics to be modified so as to minimize the structural loads. This procedure, called load control, is now being used throughout the rocket industry.
- Submerging the helium sphere in the second-stage tankage increased the structural efficiency by reducing the differential pressures acting on the walls. Heating of the pressurizing helium substantially reduced the maximum sphere pressure required, providing a further saving in structural weight.
- The Vanguard was one of the first rocket vehicles which relied entirely on thrust reactions for stability. There were no stabilizing fins.
- The use of a "strapped-down" gyro platform was originated with Vanguard and has since been adopted for many ballistic missile systems. Other advances were the unusually low gyro drift rate and the use of in-flight roll programming to appreciably and accurately change the flight azimuth.
- The rotatable exhaust jets of the first-stage turbopump provided a unique and efficient source of roll control.
- Low first-stage propellant outage was consistently obtained without the use of an automatic propellant utilization system, primarily because rigid engine calibrations during static firings and precise propellant loading procedures closely identified the propellant mixture ratio realized in flight.
- The third-stage rockets represented significant progress in the design of solid-propellant motors. The rounds were very accurately aligned and balanced. Both the steel GCR and the fiberglass ABL motors had extremely high mass ratios (0.89 and 0.91, respectively). The specific impulse of the ABL motor (251 seconds) is one

of the highest yet achieved by a solid-propellant rocket.

- Two successful stage separation sequences were designed, which allowed the altitude start of the liquid-propelled second stage and the in-flight spinup and separation of the solid-propellant third stage.
- An outstandingly successful C-band radar beacon antenna was developed. This component has since been used on the Thor Able vehicle.

## 2. VEHICLE ANALYSIS

- Elaborate and original analytical techniques were developed to define the dynamics of the spinning third stage, which included consideration of the non-rotating satellites and counter-rotating second stage.
- The flight of TV-3BU allowed a verification of the Vanguard structural design procedures and philosophy through the excellent correlation between the predicted and observed flight failure. However, this technique for design verification is not recommended.
- The significant problem of post-burnout impulse ("outgassing") of solid-propellant rockets was discovered on the Vanguard.
- New work was done in investigating and protecting against wind-induced vehicle oscillations while on the launch stand, and in the development of usable wind shear criteria for rocket flight through the atmosphere.
- The three-dimensional, six-degree of freedom digital trajectory program is one of the most comprehensive in existence, and has been solicited by other agencies.
- The method of post-flight simulation (trajectory match) of the vehicle trajectory to acquire independent quantitative experimental values for propulsion and control system parameters was a unique tool as developed and used by the Vanguard flight analysis team.
- The probability method of performance prediction, though developed too late to affect the Vanguard design, was convincingly demonstrated on the last flight, and is expected to be a most valuable tool on future rocket programs.



## XI. REFERENCES

NOTE: All references are classified Confidential except where noted.

1. "Project Vanguard, A Scientific Earth Satellite Program for the International Geophysical Year", A report to the committee on Appropriations, U. S. House of Representatives, by Surveys and Investigations Staff. Unclassified.
2. Sissenwine, N., "Wind Speed Profile, Wind Shear and Gusts for Design of Vertical-Rising Air Vehicles", USAF Cambridge Research Center Report No. 57, November 1954, Unclassified.
3. Spec. No. NRL-4100-1, "Design Specification for Vanguard Launching Vehicle", (Revised 6-3-59).
4. ER No. 8524, "Vanguard First Series Low Speed Wind Tunnel Test Results", Martin.
5. Nickel, H. and others, "Vanguard Second Series Low Speed Wind Tunnel Test Results", ER No. 8531, Sept. 1956, Martin.
6. Paulos, G., "Transonic Wind Tunnel Test Results", ER No. 8973, Martin, April 1957.
7. "Supersonic Wind Tunnel Test of the Vanguard at the Aberdeen Proving Ground", ER No. 8521, Martin, August 15, 1956.
8. "Supersonic Wind Tunnel Test of 1.75% Vanguard Model", ER No. 8977, Martin, June 1957.
9. Sidwell, C. and Challberg, T., "Aerodynamic Loads for the Vanguard Satellite Launching Vehicle", ER No. 9941, Martin, January 1958.
10. Boehmer, C. and Browne, W. B., "Supplementary Range Safety Report for Vanguard Test Vehicle No. 5 (U)", ER No. 9659, Martin, January 1958.
11. "Aerodynamic Characteristics of Vortex Spoilers", ER No. 8984, Martin, August 5, 1957.
12. "Structural Design Directives, GLM Model 330 (Vanguard)", ER No. 7904, Martin, October 10, 1956.
13. "Vanguard Guidance, Control, Separation, Stabilization Final Report, Volume I,—Systems and Components (U)", ER No. 10299-I, Martin, August 1, 1958.
14. "Vanguard Guidance Control, Separation, Stabilization Final Report, Volume II—Development and Tests (U)", ER No. 10299-II, Martin, December 1, 1958.
15. Engler, T. and Fisher, T., "Ground-Based Third-Stage Firing System for Vanguard Satellite Launching Vehicle No. 1 (U)", ER No. 9959, Martin, May 1958.
16. Spec. No. GLM-924, Development Specification Liquid Propellant Rocket Engine For Vanguard Launching Vehicle (Revised 10-15-58), Martin.
17. Spec. No. E-707, Model Specification, Engine, Rocket Liquid Propellant: XLR (later) X-405 Engine (Revised 6-23-58), General Electric Corporation.
18. Spec. No. GLM-925, Development Specification Propulsion System For Second Stage of the Vanguard Launching Vehicle (Revised 5-18-59), Martin.
19. Spec. No. ATS-L4.164, Model Specification, Propulsion System Package, Liquid Propellant, Model AJ10-37 (Revised 4-19-57), Aerojet-General Corp.
20. Spec. No. GLM-926, Development Specification Solid Propellant Rocket Motor for Third Stage of Vanguard Launching Vehicle (Revised 2-10-59), Martin.
21. Spec. No. GCR-S-350, Model Specification for Third Stage Motor (Revised 3-7-58), Grand Central Rocket Company.
22. Spec. No. NRL-4100-3, Development Specification for a High Performance Solid Propellant Rocket Motor for the Third Stage of Vanguard Launching Vehicle (Revised 9-20-58) NRL.
23. "JATO X248 High Performance Space Rockets", Allegany Ballistics Laboratory, Cumberland, Maryland, November 1, 1959.
24. Spec. No. GLM-1130, Development Specification for Solid Propellant Rocket Stabilization and Retro Motor For Vanguard Launching Vehicle (Revised 9-19-58) Martin-Baltimore.
25. Model Specification For The Production of Prototype Spin and Retro Rockets 1XS50 (Revised 6-3-57) Atlantic Research Corporation.
26. Moore, R. S., Hydraulic Oil Contamination Report. ER No. 10295, Martin.
27. Spec. No. DR-E-586, Qualification Test Specification, Engine, Rocket, Liquid Propellant: XLR (later) X-405 Rocket Engine (Revised 3-20-58) General Electric Corporation.
28. Panagopulos, A. M., "Vanguard Satellite Launch Vehicle First-Stage Pressurization System Test", ER No. 9862, Martin, March 1958.
29. "Vanguard Second Stage Exhaust Gas Impingement on First Stage LOX Tank Dome (Aerojet-General Report No. PG-4784), ER No. 9467, Martin, July 1957.
30. Spec. No. ATR-LQ-18R.001, Propulsion System Package Liquid Propellant Qualification Test for Vanguard Launching Vehicle (Revised 11-2-56) Aerojet-General Corporation.
31. Spec. No. DR-E-585, Acceptance Test Specification, Engine, Rocket, Liquid Propellant: XLR (later) X-405 Rocket Engine (Revised 10-24-57) General Electric Corporation.
32. Spec. No. ATR-LA-18R.001, Acceptance Test Specification, Propulsion System Package Liquid Propellant for Vanguard Launching Vehicle (Revised 2-28-58) Aerojet-General Corporation.
33. Sidwell, C. W., Johnston, J., Rakoske, D., "Range Safety Report Vanguard Test Vehicle No. 4 (U)", ER No. 9654, Martin, November 1957.
34. "Range Safety Data for TV-2", ER No. 9459, Martin, 1957.
35. Yeager, M. and Furth, W., "Estimated Performance of Vanguard Test and Satellite Launching Vehicles, Addendum II", ER No. 8528, II, Martin, February 1958.
36. Furth, W., "Vanguard Satellite Launching Vehicle Estimated Performance (Final)", ER No. 9950, Martin, April 1958.
37. Escher, W. J. D., and Foster, R. W., "A Sequence Diagram Analysis of the Vanguard Satellite Launching Vehicle", Proposed NASA paper, to be published, April 1960.
38. Klawans, B., "Flight Analysis of the TV-0", ER No. 8976, Martin, April 1957.
39. Klawans, B., and Brennaman, C., "Flight Analysis of TV-1", ER No. 9453, Martin, June 1957.
40. Klawans, B. and Brennaman, C., "Flight Analysis of TV-2", ER No. 9470, Martin, December 1957.

41. Klawans, B. and Brennaman, C., "Flight Analysis of TV-3", ER No. 9948, February 1958, Martin.
42. Klawans, B. and Brennaman, C., "Flight Analysis of Vanguard Test Vehicle No. 3BU", ER No. 9955, Martin, April 1958.
43. Klawans, B. and Brennaman, D., "Flight Analysis of Vanguard Test Vehicle No. TV-4", ER No. 9960, Martin, June 1958.
44. Klawans, B. and Brennaman, C., and Michel, F., "Flight Analysis of Vanguard Test Vehicle No. 5", ER No. 10300, Martin, July 1958.
45. Klawans, B., Michel, F. and Moyer, R., "Flight Analysis of Vanguard Satellite Launch Vehicle No. 1", ER No. 10301, Martin, Sept. 1958.
46. Klawans, B., Michel, F. and Moyer, R., "Flight Analysis of Vanguard Satellite Launch Vehicle No. 2", ER No. 10302, Martin, October 1958.
47. Klawans, B., Moyer, R. and Michel, F., "Flight Analysis of Satellite Launch Vehicle No. 3", ER No. 10303, Martin, December 1958.
48. Klawans, B. and Moyer, R., "Flight Analysis of Satellite Launch Vehicle No. 4", ER No. 10304, Martin, April 1959.
49. Moyer, R. and Davis, H., "Flight Analysis of Vanguard Satellite Launch Vehicle No. 5", ER No. 10305, Martin, July 1959.
50. Moyer, R. and Davis, H., "Flight Analysis of Vanguard Satellite Launch Vehicle No. 6", ER No. 10306, Martin.
51. Davis, H., Michel, F. and Murray, O., "Flight Analysis of Vanguard Test Vehicle No. 4-BU", ER No. 10307, Martin, December 1959.
52. Edelen, B. and Bloom, B. H., "Vanguard System Response to Aerodynamic and Internal Excitations (Dynamic Loads)", ER No. 8979, Martin, September 1957.
53. Furth, W., "Estimation of Second-Stage Engine Performance", ER No. 10294, Martin, August 1958.
54. "Determination of Drag-Free Horizontal Burnout Velocity for Vanguard Third-Stage Rocket Motor", Supplemental Report No. 3, Grand Central Rocket Company, 1956.
55. Edelen, D., "Guidance, Control, Separation, Stabilization Final Report, Volume III, Dynamic Analysis", ER No. 10299-III, Martin, September 1958.
56. "Vanguard Space Research Vehicle", ER No. 10786, Martin, June 1959.

## XII. BIBLIOGRAPHY

The following list of documents pertaining to project Vanguard is included for the reader's convenience. These reports are arranged in the following order: A, Martin Engineering Reports; B, Martin Post-Flight Letter Reports; C, Martin Range Safety Reports; D, Martin Miscellaneous Reports (from outside agencies); and E, Vanguard Specifications. Documents referenced in the body of this report (see References, above) are not repeated herein.

All documents are Confidential except where noted otherwise; all titles are unclassified except where noted.

### A. MARTIN ENGINEERING REPORTS

E.R. 8021	"PRELIMINARY GYRO REFERENCE SYSTEM REPORT", The Glenn L. Martin Co., June 6, 1956.	E.R. 8079	"DEADWEIGHT DISTRIBUTION AND MOMENT OF INERTIA FOR TEST VEHICLE NO. 5", The Glenn L. Martin Co., May 1956.
E.R. 8051	"DEADWEIGHT DISTRIBUTION AND MOMENT OF INERTIA", The Glenn L. Martin Co., May 1956.	E.R. 8080	"ANALYSIS AND EVOLUTION OF VANGUARD GUIDANCE SYSTEM", The Glenn L. Martin Co., November, 1956.
E.R. 8068	Phalen, F., "FLIGHT-TEST INSTRUMENTATION REPORT TV-0 THROUGH TV-5 SATELLITE LAUNCH VEHICLES", The Glenn L. Martin Co., August 13, 1956.	E.R. 8219-B	Stanka, M., "VANGUARD STRUCTURAL TEST PROGRAM (FINAL)", January 1958.
E.R. 8069	"PRELIMINARY ELECTRICAL SYSTEM, Model Vanguard", The Glenn L. Martin Co., May 1956, Unclassified.	E.R. 8520	Freeman, P., "PRELIMINARY ANALYSIS OF THE JET CONTROL SYSTEM", The Glenn L. Martin Co., October 1956.
E.R. 8070	Edelen, D., "PROBLEM OF STRUCTURAL FEEDBACK IN A ROCKET", The Glenn L. Martin Co., June 29, 1956.	E.R. 8522	Gray, K. E., "AERODYNAMIC HEATING ANALYSIS OF THE VANGUARD VEHICLES", The Glenn L. Martin Co., September, 1956.
E.R. 8071	Black, F. R. "PRELIMINARY DESIGN AND AN ANALYSIS OF THE PITCH AND YAW POWERED-FLIGHT CONTROL SYSTEM", The Glenn L. Martin Co., June 1956.	E.R. 8523	Bryant, P., "FINAL ANALYSIS: VANGUARD THIRD-STAGE SEPARATION CLEARANCES", The Glenn L. Martin Co., December 1956.
E.R. 8072	"ANTENNA DATA FOR TV-0", The Glenn L. Martin Co., June 29, 1956.	E.R. 8525 & App. A	Ashwell, J. R. & Wentworth, F. L., "ANTENNA DATA FOR TEST VEHICLE NO. 1", The Glenn L. Martin Co.
E.R. 8073	"DEADWEIGHT DISTRIBUTION AND MOMENT OF INERTIA FOR TEST VEHICLE NO. 0", The Glenn L. Martin Co., May 1956.	E.R. 8526	"DEADWEIGHT DISTRIBUTION AND MOMENT OF INERTIA FOR SATELLITE LAUNCH VEHICLE NO. 1 (Second Preliminary)", The Glenn L. Martin Co., September 1956.
E.R. 8074	Haefeli R. C., "INVESTIGATION OF THE FEASIBILITY OF PARACHUTE RECOVERY FOR VIKING NO. 14", The Glenn L. Martin Co., August 8, 1956, Unclassified.	E.R. 8527	"CALCULATED WEIGHT AND BALANCE: SATELLITE LAUNCH VEHICLE NO. 1", The Glenn L. Martin Co., September 1956.
E.R. 8075	"DEADWEIGHT DISTRIBUTION AND MOMENT INERTIA FOR TV-1", The Glenn L. Martin Co., June 7, 1956.	E.R. 8529 & App. A	Ashwell, J. R. & Wentworth, F. L., "ANTENNA DATA REPORT FOR TEST VEHICLE NO. 2", The Glenn L. Martin Co., October 31, 1956.
E.R. 8076	"DEADWEIGHT DISTRIBUTION AND MOMENT OF INERTIA FOR TEST VEHICLE NO. 2", The Glenn L. Martin Co., June 8, 1956.	E.R. 8530 & App. C	Alden, F. A., "FIELD TEST PLAN FOR TV-0", The Glenn L. Martin Co., October 1, 1956.
E.R. 8077	"DEADWEIGHT DISTRIBUTION AND MOMENT OF INERTIA FOR TEST VEHICLE NO. 3", The Glenn L. Martin Co., June 8, 1956.	E.R. 8532	Alden, F. A., "VANGUARD FIELD HANDLING CONCEPT", The Glenn L. Martin Co., Unclassified.
E.R. 8078	"DEADWEIGHT DISTRIBUTION AND MOMENT OF INERTIA FOR TEST VEHICLE NO. 4", The Glenn L. Martin Co., June 1956.	E.R. 8533 & App. A	Ashwell, J. R., "ANTENNA DATA FOR TEST VEHICLE NO. 3", The Glenn L. Martin Co., January 1957.
		E.R. 8534	"TEST PLAN: TV-2", The Glenn L. Martin Co., November 1956.

E.R. 8538	Dingman, E. G., "BASIC PHYSICAL PROPERTIES AT ELEVATED TEMPERATURES OF PYROTEX 9526 D1 ASBESTOS PHENOLIC MATERIAL", The Glenn L. Martin Co., July 3, 1956, Unclassified.	E.R. 8981	Moncure, R., "STRUCTURAL TEST OF VANGUARD SECOND-STAGE FORWARD STRUCTURE", Martin, July 1957.
E.R. 8797	Hurd, Henry, "STRUCTURAL TEST OF FIRST STAGE TAIL CAN", The Glenn L. Martin Co., November 1956.	E.R. 8982	Simpson, A., "STRUCTURAL TEST OF VANGUARD FIRST-STAGE SPACER," Martin.
E.R. 8802	Hurd, H. W., "PRESSURE TEST OF HYDROGEN PEROXIDE TANK", The Glenn L. Martin Co., November 1956.	E.R. 8983	Daniels, Jr., M. R., "STRUCTURAL TEST OF VANGUARD STATIC FIRST STAGE (t = 0 SECONDS)," Martin, May 16, 1957.
E.R. 8819	"PROJECT VANGUARD—BRIEFING FOR SUBCONTRACTORS", The Glenn L. Martin Co., August 13, 1956.	E.R. 8985	Darden, R., "VANGUARD SUMMARY STRESS ANALYSIS", Martin, January 1958.
E.R. 8963	Bryant, J., "ANALYSIS OF GUIDANCE, CONTROL, AND STABILIZATION SYSTEMS", Martin, April 1957.	E.R. 8988	Simpson, A. J., "STRUCTURAL TEST OF VANGUARD STATIC FIRST STAGE (PRE - LAUNCH — TANKS FULL)", Martin, July 1957.
E.R. 8964	Kammeyer, R., "LIQUID OXYGEN SEAL TEST PROGRAM", The Glenn L. Martin Co., January 28, 1957, Unclassified.	E.R. 8989	Moncure, R. A., "THERMAL STRESS INVESTIGATION VANGUARD STATIC FIRST STAGE", Martin, September 1957.
E.R. 8965	"TEST PLAN: TV-3", Martin, December 1956.	E.R. 8990	Woodward, W. G., "STRUCTURAL TEST OF VANGUARD STATIC FIRST STAGE (PRE-LAUNCH CONDITION)", Martin, July 1957.
E.R. 8966	Moncure, R., "STRUCTURAL TEST OF SECTION BETWEEN FIRST STAGE PROPELLANT TANKS", The Glenn L. Martin Co., January 1957.	E.R. 8991	Moncure, R. A., "STRUCTURAL TEST OF VANGUARD STATIC FIRST STAGE (CONDITION t = 70 SECONDS)", Martin, August 1957.
E.R. 8967	Woodward, W. G., "PRESSURE TEST OF FIRST STAGE HELIUM SPHERE", The Glenn L. Martin Co., February 1957.	E.R. 9148-31	Famini, J., "DETERMINATION OF PEEL STRENGTH OF RUBBER SPOILERS BONDED TO A METAL SURFACE WITH JOHNS MANVILLE J-M 351 TAPE", Martin, May 7, 1957, Unclassified.
E.R. 8968	Keithley, H., "DEADWEIGHT DISTRIBUTION AND MOMENT OF INERTIA FOR SATELLITE LAUNCH VEHICLE NO. 1 (FINAL)", Martin, January, 1957.	E.R. 9148-37	Miller, N. B., and Stein, M., "BEARING STRENGTH PROPERTIES OF RIVETED LAP JOINTS OF PYROTEX 9526-D1 (Asbestos-Phenolic) LAMINATE MATERIAL", Martin, Unclassified.
E.R. 8969	Woodward, W., "STRUCTURAL TEST OF SECOND STAGE EQUIPMENT BAY", Martin, June 1957.	E.R. 9148-43	Ivkovich, T. and Famini, J., "AN INVESTIGATION OF THE FEASIBILITY OF USING HEAT RESISTANT PLASTIC LAMINATES AS A ROCKET FLAME SHIELD", Martin, August 13, 1957, Unclassified.
E.R. 8970	Stanka, M., "STRUCTURAL TEST OF VANGUARD FIRST-STAGE PROPELLANT TANKS", Martin, June 1956.	E.R. 9200	"A MOON IS BORN", Martin, Unclassified.
E.R. 8971	Stone, R., "DYNAMIC MOCK-UP TESTS OF VANGUARD FIRST-STAGE ROLL CONTROL JETS", Martin, January 1958.	E.R. 9293	"INSTRUMENTATION LIST FOR TV-1—Measurements to be made on Test Vehicle No. 1", The Glenn L. Martin Co.
E.R. 8972	Kammeyer, R., "DYNAMIC MOCKUP TESTS OF VANGUARD SECOND-STAGE PITCH AND YAW CONTROL JETS", Martin, August 1957.	E.R. 9293-1	"TELEMETRY CHANNEL ASSIGNMENTS FOR TV-1", The Glenn L. Martin Co.
E.R. 8974	Paulos, G., "RESULTS OF WIND TUNNEL TESTS ON VORTEX SPOILERS FOR TEST VEHICLE NO. 2", April 1957.	E.R. 9451	McKeown, A. B., "VANGUARD LIQUID OXYGEN TANK DOME IMPINGEMENT TEST", Martin, July 1957.
E.R. 8978	Woodward, W., "CYCLING AND BURST PRESSURE TEST OF VANGUARD HYDROGEN PEROXIDE TANK", Martin, June 1957.	E.R. 9452 & App. A	Krushinski, W., "ANTENNA DATA FOR VANGUARD TEST VEHICLE NO. 4", Martin, July 1957.

E.R. 9454	Fitzgerald, J., "VANGUARD THIRD-STAGE SPIN AND SEPARATION MOCKUP TESTS", Martin, September 1957.	E.R. 9664	Markarian, D. J., "VANGUARD PROGRAM PLANNING (U)", Martin December 1957.
E.R. 9455	Simpson, A. J., "STRUCTURAL TEST OF VANGUARD HELIUM SPHERES AND PEROXIDE TANK SUPPORTS AND BACKUP STRUCTURES", Martin, August 1957.	E.R. 9665	Moncure, R., "VANGUARD STRUCTURAL TEST SECOND-STAGE PROPANE TANK", Martin, December 1957.
E.R. 9456	Woodward, W. D., "STRUCTURAL TEST OF VANGUARD SPIN TABLE AND FORWARD SUPPORT ARMS", Martin, August 1957.	E.R. 9666	Moncure, R., "VANGUARD STRUCTURAL TEST FIRST-STAGE CHEM-MILLED HYDROGEN PEROXIDE TANK CYCLING AND BURST PRESSURE TEST", Martin, December 1957.
E.R. 9457	Stofega, J., and Simpson, A., "STRUCTURAL TEST OF VANGUARD RE-DESIGNED FIRST-STAGE SPACER", Martin, October 1957.	E.R. 9667	Moncure, R., "VANGUARD STRUCTURAL TEST—FIRST-STAGE RE-DESIGNED LIGHTWEIGHT HELIUM SPHERE PRESSURE TEST", Martin, December 1957.
E.R. 9458	Woodward, W., "STRUCTURAL TEST OF VANGUARD NOSE CONE", Martin, August 1957.	E.R. 9668	Eisenbeis, W. and Moncure, R., "VANGUARD STRUCTURAL TEST NOSE CONE HEAT TEST", Martin, February 1958.
E.R. 9464	Dorn, L. H., and Bruce, R. G., "VANGUARD TEST VEHICLE NO. 2 BACKUP GROUND RESONANCE SURVEY", Martin, October 1957.	E.R. 9669	Moncure, R., "VANGUARD STRUCTURAL TESTS THIRD-STAGE FORWARD SUPPORT ARMS AND SPIN TABLE SUPPORTS", Martin, November 1957.
E.R. 9465	Bruce, R. G., "GROUND RESONANCE SURVEY OF VANGUARD TEST VEHICLE APPLICABLE TO SATELLITE LAUNCH VEHICLES, U", Martin, January 1958.	E.R. 9670	Moncure, R., "VANGUARD STRUCTURAL TESTS—SECOND-STAGE LOWER DOME AND GIMBAL SUPPORT", Martin, November 1957.
E.R. 9466	Freeman, P., and Bryant, J., "ANALYSIS OF THE VANGUARD AUTOPILOT-STRUCTURE STABILITY", Martin, September 1957.	E.R. 9671	Moncure, R., "VANGUARD STRUCTURAL TEST DESTRUCTION TEST OF THE STATIC SECOND-STAGE, CONDITION t = 70 SECONDS", Martin, January 1957.
E.R. 9468	"TEST PLAN: TV-4 AND TV-4BU", Martin, October 1957.	E.R. 9672	Kalinich, A. M., "VANGUARD VEHICLE SHOCK AND VIBRATION ENVIRONMENT", Martin, January 1958.
E.R. 9469	Bloom, B. H., "VANGUARD VIBRATION AND STRUCTURAL TRANSFER FUNCTION ANALYSIS", Martin, November 1957.	E.R. 9791	Noyes, G. D., "VANGUARD REPORT ON FIRST STAGE PRESSURIZATION SYSTEM MOCKUP TEST ACCIDENT", Martin, Unclassified.
E.R. 9494	"FIELD PROCEDURES, VANGUARD TEST VEHICLE NO. 2, VOLUME II", Martin, June 3, 1957.	E.R. 9940	"TEST PLAN: TV-5", Martin, November 1957.
E.R. 9628	"VANGUARD TEST VEHICLE NO. 2—FIELD PROCEDURES—VOLUME III", Martin, July 1957.	E.R. 9942	Fisher, T. A. and Browne, W. B., "LAUNCHING AZIMUTH STUDY FOR VANGUARD TEST VEHICLE NO. 4", Martin, November 27, 1957.
E.R. 9656	Yow, R., "VANGUARD NOSE CONE SEPARATION TESTS", Martin, October 1957.	E.R. 9945	Fisher, T. A., Boehmer, C. B. and Levine, S., "LAUNCHING AZIMUTH STUDY FOR VANGUARD TEST VEHICLE NO. 5 AND SLV'S", Martin, December 18, 1957. (with Addendum I, March 1958).
E.R. 9657	Markarian, D. J., "PROJECT VANGUARD HISTORY AND STATUS OF ENGINEERING EFFORT", Martin, October 1957.	E.R. 9947	Approved by Levine, S., "GROUND BASED THIRD-STAGE FIRING SYSTEM FOR VANGUARD TEST VEHICLE NO. 3", Martin, December 1957. (With Addendum I, April 1958).
E.R. 9662	Drake, J. E. and Packard, R. F., "ANTENNA DATA FOR VANGUARD TEST VEHICLE NO. 5 AND SATELLITE LAUNCH VEHICLES", Martin, December 1957.	E.R. 9949	"LAUNCHING PLAN, VANGUARD SATELLITE LAUNCH VEHICLES", Martin, January, 1958.
E.R. 9663	Parady, J., "DYNAMIC MOCK-UP TESTS OF VANGUARD SECOND-STAGE ROLL CONTROL JETS", Martin, January 1958.		

E.R. 9953	Wong, B. and Crouch, D. S., "ENVIRONMENTAL TESTS OF THE VANGUARD CONTROLS SYSTEM (U)", Martin, June 1958.	E.R. 10626	Maitzen, D., "PROJECT VANGUARD COMPONENTS AND PARTS RELIABILITY REPORT", Martin, November 1958, Unclassified.
E.R. 9957	Engler, T. S. and Fisher, T. A., "GROUND BASED THIRD-STAGE FIRING SYSTEM VANGUARD TEST VEHICLE NO. 4 (U)", Martin, March 1958.	<b>B. MARTIN POST-FLIGHT LETTER REPORTS</b>	
E.R. 9958	Engler, T. and Fisher, T., "GROUND-BASED THIRD-STAGE FIRING SYSTEM FOR VANGUARD TEST VEHICLE NO. 5", Martin, April 1958.	E.R. 8987	"POSTFLIGHT LETTER REPORT, VANGUARD TEST VEHICLE NO. 1", Martin, 10 May 1957.
E.R. 9961	Furth, W., Browne, W. and Kearsley, M., "VANGUARD LAUNCH STAND CLEARANCE", Martin June 1958.	E.R. 9673	"VANGUARD TEST VEHICLE NO. 2 POSTFLIGHT FIELD TEST REPORT", Martin, 7 November 1957.
E.R. 9974	Teague, R., "STUDY OF VANGUARD DELAYED SECOND STAGE IGNITION", Martin, October 23, 1957.	E.R. 9946	"VANGUARD TEST VEHICLE NO. 3 POSTFLIGHT LETTER REPORT", Martin, 14 December 1957.
E.R. 10115-8	Bankard, M. H., "METALLURGICAL INVESTIGATION OF FORGED ROCKET NOZZLE 3RD STAGE ASSEMBLY", Martin, September 29, 1958, Unclassified.	E.R. 9954	"VANGUARD TEST VEHICLE NO. 3S POSTFLIGHT LETTER REPORT, Martin, 15 February 1958.
E.R. 10115-9	Bankard, M. H., "METALLURGICAL INVESTIGATION OF RECOVERED SECOND STAGE TANKAGE SLV NO. 2", Martin, Dec. 4, 1958.	E.R. 9956	"VANGUARD TEST VEHICLE NO. 4 POSTFLIGHT LETTER REPORT", Martin, April 1958.
E.R. 10116-1	Alford, J., "IMPACT TESTING OF NON-METALLIC MATERIALS IN LIQUID OXYGEN", Martin.	E.R. 9962	"VANGUARD TEST VEHICLE NO. 5 POSTFLIGHT LETTER REPORT", Martin, May 1958.
E.R. 10116-17	Alford, J., "STUDY OF MATERIAL AND PROCESS INTEGRITY OF VANGUARD HYDRAULIC AND PROPELLANT SYSTEM PS AND PC COMPONENTS", Martin, July 8, 1958, Unclassified.	E.R. 9964	Arnowitz, L., "VANGUARD SATELLITE LAUNCH VEHICLE NO. 1 FLIGHT LETTER REPORT", Martin, June 1958.
E.R. 10116-34	Irvine, H. C., "STRESS CORROSION CRACKING OF A.I.S.I. 410 CORROSION RESISTANT STEEL", Martin Company, December 17, 1958, Unclassified.	E.R. 10291	Arnowitz, L., "VANGUARD SATELLITE LAUNCH VEHICLE NO. 2, FLIGHT LETTER REPORT", Martin, July 1958.
E.R. 10136	Elfers, W. A., "EQUATIONS DESCRIBING THE MOTION OF THE SATELLITE LAUNCH VEHICLE CONFIGURATION OF PROJECT VANGUARD", Martin, April 15, 1958, Unclassified.	E.R. 10297	Arnowitz, L., "VANGUARD SATELLITE LAUNCH VEHICLE NO. 3 FLIGHT LETTER REPORT", Martin, October 1958.
E.R. 10292	Engler, T. S. and Fisher, T. A., "TRAJECTORY OPTIMIZATION STUDIES FOR MAXIMUM SATELLITE LIFE-TIME", Martin, July 1958.	E.R. 10588	Arnowitz, L., "VANGUARD SATELLITE LAUNCH VEHICLE NO. 4, FLIGHT LETTER REPORT", Martin, February 1959.
E.R. 10293	Boehmer, C. and Fisher, T., "VANGUARD MODIFIED FLIGHT AZIMUTH INVESTIGATION (U)", Martin, September 1958.	E.R. 10589	Arnowitz, L., "VANGUARD SATELLITE LAUNCH VEHICLE NO. 5, FLIGHT LETTER REPORT", Martin, April 1959.
E.R. 10296	Kinports, L. B. and Engler, T. E., "VANGUARD SUPPLEMENTARY SLV TRAJECTORY OPTIMIZATION STUDIES", Martin, September 1958.	E.R. 10590	Arnowitz, L., "VANGUARD SATELLITE LAUNCH VEHICLE NO. 6, FLIGHT LETTER REPORT", Martin, July 1959.
E.R. 10310	Walters, R. C., "VANGUARD PROGRAM ENGINEERING REVIEW", Martin, December 1958.	E.R. 10907	Arnowitz, L., "VANGUARD TEST VEHICLE NO. 4 BU, FLIGHT LETTER REPORT", Martin, October 1959.
		<b>C. MARTIN RANGE SAFETY REPORTS</b>	
		E.R. 8975	Meara, V., "TV-1 RANGE SAFETY REQUIREMENTS", The Glenn L. Martin Co., April 1957.
		E.R. 9460	Kolk, D., "SUPPLEMENTARY RANGE SAFETY INFORMATION FOR VANGUARD TEST VEHICLES NO. 2 & NO. 2 BACKUP", Martin, July 1957.
		E.R. 9461	Kolk, D., "RANGE SAFETY REPORT VANGUARD TEST VEHICLES NO. 3 AND NO. 3 BACKUP", Martin, August 26, 1957.

E.R. 9462	Johnston, J., Walsh, J., and Sidwell, C., "SUPPLEMENTARY RANGE SAFETY INFORMATION FOR VANGUARD TEST VEHICLES NO. 3 AND NO. 3 BACK-UP", Martin.	M.R. 5512-Z-11	Snyder, H. W., "REAC STUDY OF ERROR COMPONENTS IN EULER ANGLES CAUSED BY GYRO CROSS-COUPPLING IN THE VANGUARD MISSILE", Minneapolis-Honeywell Regulator Co., Aeronautical Division, 1 May 1956.
E.R. 9654	Sidwell, C., Johnston, J. and Rakoske, D., "RANGE SAFETY REPORT VANGUARD TEST VEHICLE NO. 4," with Addendum I, Martin, January 1958.	M.R. 5512-Z-12 Through -12q	Delp, R. H., "DEVELOPMENT OF A GYRO REFERENCE SYSTEM FOR MARTIN MODEL 330, Progress Report AD5536-PRI, for period 15 Jan. 1956 through 2 May 1957", Minneapolis-Honeywell Regulator Company, Aeronautical Division.
E.R. 9658	Fisher, T. A., "RANGE SAFETY REPORT VANGUARD TEST VEHICLE NO. 5", Martin, January 1958. (With Addendum I, April 1958).		
E.R. 9943	Fisher, T. A., Engler, T., and Rakoske, D., "RANGE SAFETY REPORT VANGUARD SATELLITE LAUNCH VEHICLES LAUNCH AZIMUTH 107.5°", Martin, February 1958.	M.R. 5512-Z-13	Downing, W., "THREE-AXIS GYRO REFERENCE SYSTEM FOR THE VANGUARD SATELLITE LAUNCHING VEHICLE, FINAL ENGINEERING REPORT", Minneapolis-Honeywell, Aeronautical Division, MH Aero Report 2008-TR2 (AD5536), 31 August 1958.
E.R. 9943-A	Kinports, L. B., "RANGE SAFETY REPORT FOR VANGUARD SATELLITE LAUNCH VEHICLE SLV-6, LAUNCH AZIMUTH 46°", Martin, November 1958.	M.R. 5570-B Through B-15	Colbert, D., "PROGRESS REPORTS IN ACCORDANCE WITH PURCHASE ORDER 46-36633 OF THE GLENN L. MARTIN COMPANY", Air Associates, Inc., Electronic Equipment Division.
E.R. 9944	Engler, T. and Browne, W. B., "SUPPLEMENTARY RANGE SAFETY REPORT FOR VANGUARD SATELLITE LAUNCH VEHICLES", Martin, February, 1958. (With Addendum A, December 1958).	M.R. 5570-C	Harries, W., "DATA ON SATELLITE ORBITS IN CONNECTION WITH PURCHASE ORDER 46-36633 OF THE GLENN L. MARTIN COMPANY, BALTIMORE, MARYLAND", Air Associates, Inc., Electronic Equipment Division, 3 August 1956, Unclassified. Report No. 01-00101.
E.R. 9951	Fisher, T. A. and Engler, T. S., "RANGE SAFETY REPORT VANGUARD SATELLITE LAUNCH VEHICLES LAUNCH AZIMUTH 110°", Martin, February 1958.		
E.R. 10308	Kinports, L. B., Altieri, F. D. and Rakoske, D. T., "RANGE SAFETY REPORT VANGUARD TEST VEHICLE NO. 4-BU", Martin, January 1959.	M.R. 5570-D	"COASTING TIME COMPUTER, Equipment Specification Qualification Test Procedure and Acceptance Test Procedure, February 12, 1957" Air Associates, Inc., Research & Development Division, February 12, 1957.
E.R. 10309	Kinports, L., Furth, W. and Sidwell, C., "SUPPLEMENTARY RANGE SAFETY REPORT FOR VANGUARD TEST VEHICLE NO. 4-BU", Martin, January 1959.	M.R. 5755-D	Williams, J. J., "3 COMPONENT FORCE AND PRESSURE INVESTIGATION ON A 1.75% SCALE VANGUARD VEHICLE AT MACH NUMBERS 1.61, 1.81, 2.0, 2.25, 3.00 and 3.5", University of Southern California, Engineering Center, 3 Dec., 1956. USCEC Report 23-1-17.
<b>D. MARTIN MISCELLANEOUS REPORTS</b>			
M.R. 5090-I	Hubbard, E. C. and Hynden, C. M., "EFFECTS OF THIRD STAGE DISTURBANCES ON THE TRAJECTORY OF THE EARTH SATELLITE VANGUARD", NPG 1543 Naval Proving Ground, Dahlgren, Va. 9 August 1957.	M.R. 5785-L	"VANGUARD LAUNCH, Operations Requirements No. 702", Air Force Missile Test Center, Patrick Air Force Base, Florida, 1 October 1957. OR-702 MT 57-19289.
M.R. 5098-L Through L5	"DEVELOPMENT OF 1XS50 MOTOR", Atlantic Research Corp., period covering May 21, 1956-June 15, 1956, 25 June 1956.	M.R. 5785-N	"VANGUARD LAUNCH", Air Force Missile Test Center, Patrick Air Force Base, Florida, 30 October 1957, OD No. 702, Secret. MT-57-27034.
M.R. 5147-BB	"PLOTTED AND TABULATED DATA FOR THE N.A.M.T.C. SUPERSONIC WIND TUNNEL TEST ON THE 1.75% SCALE MODELS OF THE VANGUARD LAUNCHING VEHICLE", Naval Air Missile Test Center, Point Mugu, California, April 1957.	M.R. 5785-V	"VANGUARD GROUND INSTRUMENTATION TESTS", Air Force Missile Test Center, Cape Canaveral, Florida, 6 Nov. 1957, OD No. 731.

M.R. 5785-W	"VANGUARD LAUNCH, Operations Requirements No. 703", Air Force Missile Test Center, Cape Canaveral, Florida, 28 February 1958. MT 58-8702	M.R. 5823-K	Windsor, R. I., "WIND TUNNEL TESTS OF A 12% MODEL OF THE GLENN L. MARTIN COMPANY VANGUARD MISSILE, MODEL 330, 2nd SERIES", University of Maryland, Aeronautical Laboratory, August 1956.
M.R. 5785-Y	"OPERATIONS REQUIREMENTS NO. 5, VANGUARD TV-0 LAUNCH", Air Force Missile Test Center, Patrick Air Force Base, Florida, 21 September 1956. PAFB 56-16111.	M.R. 5922-B Vol. I & II	Duncan, R. H. and Haas, H. W., "QUADRALOOP ANTENNAS, PART I: The Design and Performance of Quadraloop Antennas; Part II: Telemetering Quadraloop Antennas for Project Vanguard; (Volume I—Unclassified). Volume II—Part III: Command Control Antennas for Project Vanguard; Part IV: The Vanguard TV-3 and TV-4 Antenna Configurations." New Mexico College of Agriculture & Mechanic Arts, Physical Science Laboratory, December 1957.
M.R. 5785-Y-1	"OPERATIONS REQUIREMENTS NO. 7, DETAILED TEST REQUIREMENTS FOR VANGUARD TEST VEHICLE TV-1", Air Force Missile Test Center, Patrick Air Force Base, 19 November 1956. PAFB 56-21368, PCI 5211.		
M.R. 5785-Z	"VANGUARD TV-1 LAUNCH", Air Force Missile Test Center, Florida, 19 November 1956. PAFB 56-21368, OR 700.		
M.R. 5785-Z-1	"VANGUARD TV-2 LAUNCH", Air Force Missile Test Center, Florida, 10 April 1957. MT 57-8861, OR 701.	M.R. 5922-B-1	Duncan, R. H. and Haas, H. W., "RADIO FREQUENCY DIFFUSION BREAKDOWN ANALYSIS MARTIN COMPANY TELEMETRY QUADRALOOP ANTENNA DESIGN PROJECT VANGUARD", New Mexico College of Agriculture and Mechanic Arts, Physical Science Laboratory, April 1958, Unclassified.
M.R. 5785-Z-2	"VANGUARD-GROUND INSTRUMENTATION TESTS", Air Force Missile Test Center, Florida, 4 June 1957, Unclassified. OR 730.		
M.R. 5785-Z-3	"VANGUARD-GROUND INSTRUMENTATION TESTS, Air Force Missile Test Center, Florida, 24 September 1957, Unclassified. OR 731.	M.R. 5935-N	"VANGUARD & VIKING COMPARISON, Glenn L. Martin", Airborne Instruments Laboratory, Inc., Mineola, N. Y., April 1956.
M.R. 5785-Z-5	"VANGUARD TV-1 LAUNCH", Air Force Missile Test Center, Florida, 11 January 1957. MT 57-1675, OD 7.	M.R. 5937-W-19	Darms, F. J., "STRESS REPORT STRUCTURAL COMPONENTS FOR SECOND STAGE OF VANGUARD", Aerojet-General Corporation, Azusa, California, 7 April 1958, Martin P.O. No. E-55-3522.
M.R. 5785-Z-6	"VANGUARD TV-2 LAUNCH", Air Force Missile Test Center, Florida, 7 June 1957. MT 57-25350, OD 701.	M.R. 5937-W-27	Stark, J. K., "APPENDIX I, VANGUARD SECOND STAGE EXHAUST GAS IMPINGEMENT ON FIRST STAGE LOX TANK DOME", Aerojet-General Corp., Azusa, California, Test Series No. D-131-LA and D-137-LA.
M.R. 5785-Z-7	"VANGUARD GROUND INSTRUMENTATION TEST", Air Force Missile Test Center, Florida, 21 June 1957. MT 57-25509, OD 730.	M.R. 5937-W-34	Nicholson, J. and Zernow, L., "LOW TEMPERATURE EXPERIMENTS WITH VANGUARD COMPONENTS", Aerojet-General Corporation, AZUSA, California. Report No. 8074-2.
M.R. 5785-Z-8	"TV-3 TEST PLAN", Air Force Missile Test Center, Patrick Air Force Base.	M.R. 5937-W-35	Nicholson, J. and Zernow, L., "HIGH VACUUM & LOW TEMPERATURE EXPERIMENTS WITH VANGUARD COMPONENTS", Aerojet-General Corporation, Azusa, California, Report No. 8074-1.
M.R. 5785-Z-12	"VANGUARD LAUNCH", Air Force Missile Test Center, Patrick Air Force Base, 17 March 58. MT 58-40742, OD 703.	M.R. 5937-W-39	Goldie, R. L., "SUMMARY REPORT OF STRUCTURAL TESTING OF COMPONENTS FOR SECOND STAGE VANGUARD", Aerojet-General Corp., Azusa, California, 16 July 1958, Martin P.O. No. E55-3522.
M.R. 5785-Z-13	"DATA ACQUISITION AND SUPPORT PLAN FOR PROJECT VANGUARD", Air Force Missile Test Center, Patrick Air Force Base, Florida, 5 November 1956. PCG 22061, PAFB 56-7.857.		
M.R. 5785-Z-14	"TEST REQUIREMENTS HANDBOOK", Air Force Missile Test Center, Patrick Air Force Base, Florida, 1 March 56.		
M.R. 5823-C	Sekscienski, W. S., "WIND TUNNEL REPORT NO. 188—WIND TUNNEL TESTS OF A 12% MODEL of the Glenn L. Martin Vanguard Missile Model 330", University of Maryland, Aeronautical Laboratory, March 1956.		

M.R. 5937-Y-1 Through Y-8	"DEVELOPMENT OF A LIQUID PROPELLANT ROCKET PROPULSION SYSTEM FOR SECOND STAGE OF MODEL 330 VANGUARD LAUNCHING VEHICLE", Aerojet-General Corp., Azusa, California, 30 August 1957, Purchase Order E-55-3522-CP. August 30, 1957 through February 28, 1958.	M.R. 6104-D-2	Drake, W. T., "DEVELOPMENT OF THIRD-STAGE SOLID PROPELLANT ROCKET MOTOR PROJECT VANGUARD", Grand Central Rocket Co., Redlands, California. Letter Contract 56-3509-CP, 14 June 1957, for period 1 March-1 April 1957. MPR No. 15.
M.R. 5958-U	Beiser, L., "INSTRUMENTATION FOR LAUNCHING THE VANGUARD ROCKET", A Lecture to be delivered by L. Beiser on February 24, 1958, over the MILITARY AFFILIATE RADIO SYSTEM (MARS)—Frequency—4030 kc, upper sideband transmission", Polarad Electronics Corporation, Long Island City 1, New York.	M.R. 6104-D-3	Drake, W. T., "DEVELOPMENT OF THIRD-STAGE SOLID PROPELLANT ROCKET MOTOR PROJECT VANGUARD", Grand Central Rocket Co., Redlands, California. Letter Contract 56-3509-CP, 15 July 1957, for period 1 June-1 July 1957. MPR No. 16.
M.R. 6066-II	Escher, W. and Stehling, K., "A METHOD OF IMPROVING THE PERFORMANCE OF THE VANGUARD LAUNCHING VEHICLE BY USING PERCHLORYL FLUORIDE AS THE OXIDIZER FOR THE SECOND-STAGE PROPULSION SYSTEM (CONFIDENTIAL TITLE)", Naval Research Laboratory, Washington, D. C., August 31, 1956. NRL Memo. Rpt. 627.	M.R. 6104-D-4	"DEVELOPMENT OF THIRD-STAGE SOLID PROPELLANT ROCKET MOTOR PROJECT VANGUARD", Grand Central Rocket Co., Redlands, California, Letter Contract 56-3509-CP, 4 October 1957, for period 1 July to 1 August 1957. MPR No. 17.
M.R. 6076-C	"GUIDED MISSILES, ROCKETS AND ARTIFICIAL SATELLITES (INCLUDING PROJECT VANGUARD), A Selected List of Titles", Department of the Army, Army Library, 23 January 1957, Unclassified. Special Bibliography No. 11.	M.R. 6104-D-5	Drake, W. T., "DEVELOPMENT OF THIRD-STAGE SOLID PROPELLANT ROCKET MOTOR PROJECT VANGUARD", Grand Central Rocket Co., Redlands, California. Letter Contract 56-3509, 24 October 1957, for period 1 August to 1 September 1957. MPR No. 18.
M.R. 6087-R-1	"COMPOSITE DESIGN RESEARCH PANEL, MINUTES OF THE TWENTY-SECOND MEETING", The Johns Hopkins University, Applied Physics Laboratory, Applied October 2 and 3, 1956, Thompson Products, Inc., Cleveland, Ohio, Secret. APL-JHU TG 60-23.	M.R. 6104-D-6	Drake, W. T., "DEVELOPMENT OF THIRD-STAGE SOLID PROPELLANT ROCKET MOTOR PROJECT VANGUARD", Grand Central Rocket Co., Letter Contract 56-3509, 7 November 1957, for period 1 September to 1 October 1957, MPR No. 19.
M.R. 6104-A	Hartzell, W. G., "FIELD HANDLING MANUAL FOR SOLID PROPELLANT ROCKET MOTOR GCR 33 KS 2800, FM-350", Grand Central Rocket Company, Redlands, California.	M.R. 6104-D-7	Drake, W. T., DEVELOPMENT OF THIRD-STAGE SOLID PROPELLANT ROCKET MOTOR PROJECT VANGUARD", Grand Central Rocket Co., Redlands, California, Contract 56-3509, for period 1 October to 1 November 1957. MPR No. 20.
M.R. 6104-B	Schoen, R. L., "PERFORMANCE ANALYSIS FOR ROCKET MOTOR 33KS-2800, Manual No. GCR-PA-33-2800", Grand Central Rocket Company, Redlands, California, 25 June 1957.	M.R. 6104-D-8	"DEVELOPMENT OF THIRD-STAGE SOLID PROPELLANT ROCKET MOTOR PROJECT VANGUARD", Final Summary Report, 1 March 1956 to 23 July 1958, Contract 56-3509. GCRCo. Rpt. No. P-0059-58.
M.R. 6104-D-1	Drake, W. T., "DEVELOPMENT OF THIRD-STAGE SOLID PROPELLANT ROCKET MOTOR PROJECT VANGUARD", Grand Central Rocket Co., Redlands, California. Letter Contract 56-3509-CP, 14 June 1957, for period 1 March-1 April 1957. MPR 13.	M.R. 6104-H-1	Hartzell, W. G., "DEVELOPMENT OF THE 33KS 2800 ROCKET MOTOR FOR PROJECT VANGUARD", Grand Central Rocket Co., Redland, Redlands, California.
		M.R. 6104-R	PROPOSAL NO. 1290 TO THE MARTIN COMPANY FOR AN IMPROVED VANGUARD THIRD STAGE ROCKET ENGINE", Grand Central Rocket Co., Redlands, California, 2 August 57.
		M.R. 6126-U	Fargo, E. L., "PROPOSED PHOTO-RECORDING AND RECOVERY SYSTEM FOR VANGUARD TEST VEHICLES", Goodyear Aircraft Corp., Akron, Ohio, 26 September 1956. GER-7726 S/1.

M.R. 6133-E-2	"PROJECT VANGUARD REPORT NO. 16", Progress through April 15, 1957, Naval Research Laboratory, Washington, D. C., May 1, 1957, (Not releasable to foreign nationals), NRL 4950.	M.R. 6133-E-18	"PROJECT VANGUARD REPORT NO. 19, PROGRESS THROUGH JUNE 30, 1957", Naval Research Laboratory, Washington, D. C., August 6, 1957. NRL Report 5010.
M.R. 6133-E-3	By Project Vanguard Staff, "PROJECT VANGUARD REPORT NO. 17, Progress Through May 31, 1957", Naval Research Laboratory, Washington, D. C., July 10, 1957. Not releasable to foreign nationals. NRL 4980.	M.R. 6133-E-19	Simas, V. R., "PROJECT VANGUARD REPORT NO. 24, MINITRACK REPORT NO. 4, THE SATELLITE TELEMETRY RECEIVER SYSTEM", Naval Research Laboratory, Washington, D. C., January 20, 1958, Unclassified, NRL Report 5065.
M.R. 6133-E-7	Hagen, J. P., "VANGUARD TV-3 OPERATIONS PLAN", Naval Research Laboratory, Washington, D. C., 15 November 1957.	M.R. 6133-E-20	Simas, V. R. and Bartholomew, C. A., "PROJECT VANGUARD REPORT NO. 23, MINITRACK REPORT NO. 3, RECEIVER SYSTEM", Naval Research Laboratory, Washington, D. C., December 6, 1957, Unclassified, NRL Report 5055.
M.R. 6133-E-8	Escher, J. D., Freeland, J. E., Schmidt, F. R., "A METHOD OF IMPROVING THE PERFORMANCE OF THE VANGUARD LAUNCHING VEHICLE BY COOLING THE SECOND-STAGE PROPELLANTS BELOW AMBIENT TEMPERATURE", Naval Research Laboratory, Washington, D. C., Vehicles Branch Project Vanguard, January 16, 1957. NRL Memo. Rpt. 631.	M.R. 6133-E-21	Escher, J. D. and Foster, R. W., "THE VANGUARD SEQUENCE DIAGRAM, A GRAPHICAL METHOD OF PRESENTING COMPLEX SYSTEM OPERATION, PROJECT VANGUARD REPORT NO. 31", Naval Research Laboratory, Washington, D. C., August 15, 1958, Unclassified.
M.R. 6133-E-9	"PRELIMINARY REPORT ON THE VANGUARD TV-3S FLIGHT MALFUNCTION", Naval Research Laboratory, Washington, D. C., February 13, 1958. NRL Memorandum Report 783.	M.R. 6133-E-24	Hepler, D. S., "PROJECT VANGUARD REPORT NO. 35, MINITRACK REPORT NO. 6, THE VANGUARD SATELLITE COMMAND RECEIVER", Naval Research Laboratory, Washington, D. C., September 30, 1958, Unclassified, NRL Report 5217.
M.R. 6133-E-10	"VANGUARD TV-5 OPERATIONS PLAN", Naval Research Laboratory, Washington, D. C., 20 February 1958.	M.R. 6133-E-25	"TEST REQUIREMENTS VANGUARD", Naval Research Laboratory, Washington, D. C., 1 August 1956.
M.R. 6133-E-11	"PROJECT VANGUARD REPORT NO. 30, PROGRESS THROUGH DECEMBER 31, 1957", Naval Research Laboratory, Washington, D. C., March 27, 1958. NRL Report 5113.	M.R. 6133-E-26	"VANGUARD TEST PLAN TEST VEHICLE NO. 2 (TV-2)", December 19, 1956, Naval Research Laboratory, Washington, D. C.
M.R. 6133-E-13	"VANGUARD SATELLITE LAUNCHING VEHICLES OPERATIONS PLAN", Naval Research Laboratory, Washington, D. C., 15 April 1958.	M.R. 6133-E-27	"PRELIMINARY TEST PLANS FOR VANGUARD LAUNCHING OPERATIONS", Naval Research Laboratory, Washington, D. C., November 14, 1955.
M.R. 6133-E-14	Blake, R. E. and Oleson, M. W., "PROJECT VANGUARD REPORT NO. 26, PRELIMINARY PHASES OF THE VANGUARD VIBRATION PROGRAM", Naval Research Laboratory, Washington, D. C., May 13, 1958, NRL Report 5102.	M.R. 6133-E-28	"VANGUARD TV-4 OPERATIONS PLAN", Naval Research Laboratory, Washington, D. C., 1 January 1958.
M.R. 6133-E-15	"PROJECT VANGUARD REPORT NO. 4, PROGRESS THROUGH APRIL 15, 1956," Naval Research Laboratory, Washington, D. C., May 3, 1956. NRL Report 4748.	M.R. 6133-E-31	"NRL PARTICIPATION IN THE CSAGI ROCKET AND SATELLITE CONFERENCE", Naval Research Laboratory, Washington, D. C., September 30 to October 5, 1957, by Vanguard Staff, January 5, 1959, Unclassified.
M.R. 6133-E-16	"PROJECT VANGUARD REPORT NO. 5, PROGRESS THROUGH MAY 15, 1956", Naval Research Laboratory, Washington, D. C., June 2, 1956. NRL Report 4767.	M.R. 6133-E-32	"VANGUARD TEST PROGRAM", Naval Research Laboratory, Washington, D. C., 2 July 1956.
M.R. 6133-E-17	"PROJECT VANGUARD REPORT NO. 6, PROGRESS THROUGH JUNE 15, 1956", Naval Research Laboratory, Washington, D. C., June 28, 1956. NRL Report 4800.	M.R. 6133-E-33	"VANGUARD TEST PROGRAM", Naval Research Laboratory, Washington, D. C., 2 July 56.

M.R. 6139-J	Di Girolamo, A., "STANDARD OPERATING PROCEDURE FOR BALANCING LOW ROTATIONAL ROCKET MOTORS WITH THE DYNAMIC UNBALANCE TEST INSTALLATION", Hercules Powder Company, Allegany Ballistics Laboratory, Unclassified.	M.R. 6150-Z-55	Freeman, P., "THE VANGUARD CONTROL SYSTEM DEVELOPMENT PROGRAM", May 1956, Unclassified.
M.R. 6148-P-5 Through D-29	"PROJECT VANGUARD 1st STAGE PROPULSION, Progress Reports from March 1957, to November 1958 to The Martin Company", General Electric, Flight Propulsion Laboratory Dept.	M.R. 6154	Price, R. P., "VANGUARD SATELLITE PROGRAM TIMER, SIXTH MONTHLY PROGRESS REPORT FOR NRL CONTRACT NONr-1817(00), Glenn L. Martin Co., P.O. 36-67802, for period 31 December 1956 through 31 January 1957", Designers for Industry, Inc., Cleveland, Ohio, 20 February 1957.
M.R. 6150-Z-40	Howell, R. L., "A SATELLITE BEACON STATION", Massachusetts Institute of Technology (Awarded second place in the Martin sponsored Vanguard Essay Contest), Unclassified.	M.R. 6154-A Through R	McDonald, H., "VANGUARD SATELLITE PROGRAM TIMER", Progress Reports, Designers for Industry, Inc., Cleveland 9, Ohio, P.O. 36-67802-CP.
M.R. 6150-Z-41	Mechtly, E., "A TECHNIQUE FOR INCREASING A SATELLITE'S ENERGY-WEIGHT RATIO", Penn State, 3rd place—Martin sponsored Vanguard Essay Contest, Unclassified.	M.R. 6259 Through 6259-E	"MAGNETIC AMPLIFIER AUTOPILOT", Vickers, Inc., Vickers Electric Division, Glenn L. Martin P.O. 46-5876-CP, Contract NON(r)1817(00), Unclassified.
M.R. 6150-Z-42	Beaubien, D. J., "AN EARTH SATELLITE RADIO TRACKING SYSTEM EMPLOYING LOW LEVEL DETECTION", 4th place—Martin sponsored Vanguard Essay Contest, Unclassified.	M.R. 6193-V	"THREE DIMENSIONAL TRAJECTORY WITH ROTATING, OBLATE EARTH", Martin, revised May 1959, Unclassified.
M.R. 6150-Z-43	Covert, E. E., "EARTH SATELLITES: AN ESSAY", Massachusetts Institute of Technology, 5th place—Martin sponsored Vanguard Essay Contest, Unclassified.	M.R. 6193-X	"SATELLITE DATA HANDBOOK, PROJECT VANGUARD", Martin, March 1956, Revised January 1957, Unclassified.
M.R. 6150-Z-44	Gebelein, R. J., "HUMAN LONGEVITY AS IT RESTRICTS MAN'S REACH INTO OUTER SPACE AND POSSIBLE GRAVITATIONAL EFFECTS BEARING ON THE PROBLEM", University of Rochester, 6th place—Martin sponsored Vanguard Essay Contest, Unclassified.	QT-D1-1	"VANGUARD SATELLITE PROGRAM TIMER INTERIM REPORT QUALIFICATION TEST NRL CONTRACT NONr-1817(00) THE MARTIN CO. P.O. 36-67820-CP", Designers for Industry, Inc., Cleveland 9, Ohio, 13 September 1957.
M.R. 6150-Z-45	Ulbrich, E. A., "PRETESTING SATELLITE COMPONENTS IN AN ELECTRO-MAGNETIC ACCELERATOR", University of New Mexico, 7th place—Martin sponsored Vanguard Essay Contest, Unclassified.	QT-D1-2	"VANGUARD SATELLITE PROGRAM TIMER. FINAL QUALIFICATION TEST REPORT FOR NRL CONTRACT NONr-1817(00) The Martin Co. P.O. 36-67802", Designers for Industry, Inc., Cleveland 9, Ohio, 29 January 1958.
M.R. 6150-Z-46	Stoffel, R. J., "OPERATION M.O.P. (MAN, OXYGEN, AND PLANT)", University of Missouri, 8th place—Martin sponsored Vanguard Essay Contest, Unclassified.	QT-G6-1 Through 6	"VANGUARD TEST NO. 83 QUALIFICATION TEST NO. 1", Grand Central Rocket Company, Redlands, California.
M.R. 6150-Z-47	Kittlitz, R. G., Jr., "LIQUID PROPELLANTS IN THE DESIGN OF THE VANGUARD SATELLITE VEHICLE", University of Mississippi, 9th place—Martin sponsored Vanguard Essay Contest, Unclassified.	QT-G6-7	Lambert, B. L., QUALIFICATION TEST REPORT FOR THE 33KS 2800 THIRD STAGE SOLID PROPELLANT ROCKET MOTOR VANGUARD LAUNCHING VEHICLE FOR THE MARTIN COMPANY", Grand Central Rocket Company, Redlands, California, 15 March 1958, Prime Contract No. NONr-1817(00).
M.R. 6150-Z-48	Barth, C. A., "A PERMANENT EARTH SATELLITE PROGRAM", U.C.L.A., Dept. of Physics, 10th place—Martin sponsored Vanguard Essay Contest, Unclassified.	QT-M6-3	"REPORT OF TESTS ON DGG52-B VANGUARD GYROSCOPE ASSEMBLY INERTIAL REFERENCE", Minneapolis-Honeywell, Aeronautical Division, March 25, 1958.

## E. VANGUARD SPECIFICATIONS

Inspection and Procedure Manual For Spin and Retro Rockets 1XS50 (Revised 6-3-57). Atlantic Research Corporation.

Specification No. X241A1 Model Specification for Model X241A1 Motor (Undated). Allegany Ballistics Laboratory.

Specification No. 3090-1 and 3090-1A Model Specification, Controls Test Equipment (Revised 12-13-57). Polarad Electronics Corporation.

Specification No. 3090-2, Qualification Test Specification, Controls Test Equipment (10-1-56) Polarad Electronics Corporation.

Specification No. 3090-3, Acceptance Test Specification, Controls Test Equipment (10-2-56). Polarad Electronics Corporation.

Specification No. 3090-2A/3A, Qualification Test and Acceptance Test Specification, Controls Test Equipment. (Revised 9-6-57). Polarad Electronics Corporation.

Specification No. 3090-4 and 3090-4A, Model Specification for Unit Tester for Controls Test Equipment (Revised 5-10-57). Polarad Electronics Corporation.

Specification No. 3090-5, Qualification Test Specification For Unit Tester For Controls Test Equipment (Revised 8-7-57). Polarad Electronics Corporation.

Specification No. 3090-6, Acceptance Test Specification For Unit Tester For Controls Test Equipment (Revised 8-6-57). Polarad Electronics Corporation.

Specification No. RD-24821, Equipment Specification, Coasting Time Computer (Revised 1-31-58). Electronic Communications, Inc.

Specification No. RD-24822, Qualification Test Specification, Coasting Time Computer (Revised 11-19-57). Electronic Communications, Inc.

Specification No. RD-24823, Acceptance Test Procedure, Coasting Time Computer (Revised 1-31-58). Electronic Communications, Inc.

Specification No. DFI-1-2592, Model Specification for Program Timer (Revised 10-7-57). Designers For Industry.

Specification No. DFI-2-2592, Qualification Test Specification for Program Timer (Revised 10-17-57). Designers For Industry.

Specification No. DFI-3-2592, Acceptance Test Specification for Program Timer (Revised 10-17-57). Designers For Industry.

Specification No. ES12048-10, Inspection and Installation Specification for Tester Console D-UG458A-1 (Revised 9-9-57). Minneapolis-Honeywell Regulator Co.

Specification No. ES-12048-12, Inspection and Installation Engineering Specification for Launching Calibrator System (6-12-57). Minneapolis-Honeywell Regulator Co.

Specification No. ES-12048-16/16A, Inspection and Installation Engineering Specification for D-GG52A Gyroscope Assembly (Revised 8-29-57). Minneapolis-Honeywell Regulator Co.

Specification No. 893/893-1, Acceptance Test Specification for the Gyroscope Assembly, Inertial Reference, Three Axis, Type D-GG52B, and For Associated Ground Test Equipment (Revised 7-23-58). Minneapolis-Honeywell Regulator Co.

Specification No. R-ED-891/891-1, Model Specification, Gyroscope Assembly Type D-GG52B (Revised 12-17-57). Minneapolis-Honeywell Regulator Co.

Specification No. R-ED-740/740-1/740-2, Model Specification Gyroscope Assembly, Type D-GG52A (Revised 5-29-57). Minneapolis-Honeywell Regulator Co.

Specification No. R-ED-762/762-1/762-2, Qualification Test Specification for Gyroscope Assembly, Type D-GG52A, and For Associated Ground Test Equipment (Revised 5-29-57). Minneapolis-Honeywell Regulator Co.

Specification No. R-ED-766/766-1, Acceptance Test Specification, Gyro Assembly, Inertial Reference, Three Axis, Type D-GG52A, and For Associated Ground Test Equipment (Revised 5-3-57). Minneapolis-Honeywell Regulator Co.

Specification No. GCR-IPM-33KS2800, Inspection Procedure Manual For Third Stage Motor (Revised 12-11-57). Grand Central Rocket Company.

Specification No. NRL-4100-2, Design Specification For Vanguard Antennas (Revised 9-20-58). NRL.

Specification No. GLM-1064, Development Specification, Three Axis Gyro Reference for Vanguard Launching Vehicle (Revised 9-15-58). Martin-Baltimore.

Specification No. GLM-1082, Design Data Requirements For Vanguard Launching Vehicle, (Revised 4-24-59). Martin-Baltimore.

Specification No. GLM-1123, Technical Data Requirements For Solid Propellant Rocket Motor For Vanguard Launching Vehicle (Revised 9-19-58). Martin-Baltimore.

Specification No. GLM-1125, Sub-System Specification For Guidance and Control of Vanguard Launching Vehicle (Revised 11-13-58). Martin-Baltimore.

Specification No. GLM-1126, Specification for Static and Flight Structure for the Vanguard Launching Vehicle (Revised 8-20-56). Martin-Baltimore.

Specification No. GLM-1131, Technical Data Requirements For Solid Propellant Rocket Stabilization and Retro Motor For Vanguard Launching Vehicle (Revised 9-19-58). Martin-Baltimore.

Specification No. GLM-1135, Rocket Stands For First and Second Stage Engines (Revised 9-19-58). Martin-Baltimore.

Specification No. GLM-1182, Controls Test Equipment For Vanguard Launching Vehicle (Revised 9-15-58). Martin-Baltimore.

# APPENDIX:

## PROBABILITY METHOD OF PERFORMANCE PREDICTION

The initial Vanguard performance estimates were based on the trajectories generated by nominal or specification values of parameters. Tolerance limits for these parameters were necessary, since the mission objective specified a minimum perigee that must be achieved for the most adverse combination of vehicle tolerances, barring malfunction (Ref. 3). The actual flight performance of non-malfunctioning Vanguard vehicles consistently exceeded both the minimum (adverse combination of extreme tolerances) and the nominal (adverse combination of expected tolerances) predicted performance. There was no justification to increase estimates or decrease tolerances on individual system parameters to rectify this discrepancy.

A more realistic approach appeared to be one which considered the combinations of tolerances from a probability aspect. The method was developed and accurately predicted the performance of the last Vanguard vehicle (Fig. A-1). The probability method was also used to "posthumously" predict the expected second-stage apogee altitude and velocity of all Vanguard vehicles which achieved successful second-stage powered flight. The previous minimum, nominal and maximum predicted performances and the actual vehicle performance are compared with this "expected" performance in Fig. 43 (see Chapter VI, Section D). Figure A-2 compares the expected orbit injection conditions of the three orbiting satellites with the actual injection conditions and the previous nominal vehicle performance.

### A. METHOD AND TERMINOLOGY

#### 1. VEHICLE SYSTEM PARAMETERS

The parameters which govern the operation of the pertinent individual vehicle systems are called vehicle system parameters. They include mixture ratio tolerances, loading errors, starting and stopping losses, trapped propellants, tankage volumes, propellant specific gravities, gyro drift and misalignments, aerodynamics and others. Complete statistical descriptions of the system parameters are usually unavailable, especially in the design stage. However, estimates of the mean values and some knowledge as to the correlations and deviations of the vehicle system parameters are usually available, since they are necessary in any tolerance analysis.

#### 2. INPUT PARAMETERS

Input parameters are used directly by the computational facilities in generating a trajectory. They include stage weights, amounts of propellant consumed, flow rates, specific impulse, pitch program, timing, staging and sequencing. The input parameters are calculated from the system parameters and are often complicated non-linear functions of the system parameters. For example, the amount of propellant consumed is a function of mixture ratio, propellant loading errors, starting and stopping losses, trapped propellants, flow rates and tankage volumes.

The probability distributions of the input parameters could be obtained by considering all possible combinations of the vehicle system parameters. This, in general, would require an infinite number of individual computations. Approximate methods which may be used are discussed below.

**Discrete distribution method**—Each system parameter tolerance is divided into a finite number of equally probable values of the parameter. Consequently, the number of different combinations of system parameters is finite and the statistical properties of the resulting input parameters can be estimated in a finite number of computations.

**"Monte Carlo" method**—If the number of different system parameter combinations sufficient to give the desired input parameter accuracy is too large to consider all possible combinations by the discrete distribution method, the "Monte Carlo" method may be used to select, at random, a representative sample of combinations. Repeated "Monte Carlo" sampling within strata of values can yield increasingly refined estimates, while variations in the vehicle system parameter distributions used give an idea of the amount of error in the resulting input parameter distributions.

The mean values, standard deviations and correlations of the input parameters were found to be relatively insensitive to the probability distribution of vehicle system parameters, provided that the mean, standard deviation and correlations of the assumed distribution of vehicle system parameters was the same as the actual distribution. A summary of the input parameters, their mean values and standard deviations for TV-4BU is given in Table A-1.

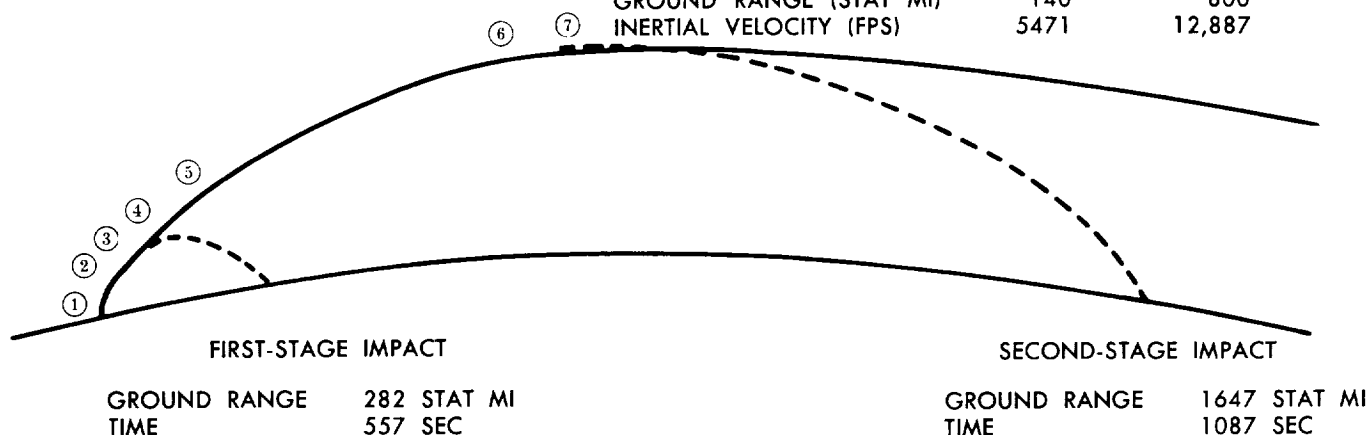
	TIME (SEC)	ALTITUDE (STAT MI)	GROUND RANGE (STAT MI)	EARTH VELOCITY (FPS)	INERTIAL VELOCITY (FPS)
① LAUNCH	0	0	0	0	1,343
② MAXIMUM DYNAMIC PRESSURE (587 PSF)	74.6	6.86	1.38	1,292	2,156
③ FIRST-STAGE BURNOUT	142.5	38.8	26.1	6,021	7,004
④ NOSE CONE SEPARATION	172.0	63.2	52.2	6,956	8,008
⑤ SECOND-STAGE BURNOUT	262.5	150.1	187	13,525	14,727
⑥ THIRD-STAGE IGNITION	545.8	316.8	776	11,513	12,893
⑦ THIRD-STAGE BURNOUT (INJECTION)	583.8	316.6	887	25,750	27,129

#### SATELLITE ORBIT

APOGEE 2211 STAT MI  
PERIGEE 311 STAT MI  
PERIOD 127.9 MIN  
ECCENTRICITY 0.191

FIRST-STAGE APOGEE	SECOND-STAGE APOGEE
-----------------------	------------------------

TIME (SEC)	289	556
ALTITUDE (STAT MI)	101	322
GROUND RANGE (STAT MI)	140	800
INERTIAL VELOCITY (FPS)	5471	12,887



**Fig. A-1 Expected Vanguard Performance — TV-4BU (52-1/4-lb Satellite)**

### 3. TRAJECTORY PARAMETERS

The trajectory parameters include any and all of the individual items which comprise the trajectory, such as: stage ignition and burnout time, velocity, and position; apogee time, altitude, and velocity; flight path angle; dynamic pressure; indicated velocity; and, in general, the trajectory time-position history. The expected value of a trajectory parameter is the arithmetic mean of all of the values generated by the expected distribution of the input parameters. Either a discrete distribution or the "Monte Carlo" method could be used to obtain a representative sample of the input parameters; however, a simpler method is available. The mean, standard deviation and correlations of most trajectory parameters may be evaluated directly through the use of sensitivity coefficients.

**Sensitivity Coefficients**—Sensitivity coefficients are the partial derivatives which relate a change in an input parameter from its mean to the resulting change

in a trajectory parameter, whether or not such a singular change of input parameter is physically realizable. Most of the sensitivity coefficients were found to be essentially constant, and the trajectory parameter change due to system parameter changes could be adequately represented by the summation of input parameter changes times their sensitivity coefficients. Some trajectory parameter deviations from the mean trajectory due to a standard deviation (one-sigma) change in input parameters from their mean values are given in Table A-1.

**Expected Trajectory Parameters**—The arithmetic mean or "expected" input parameters will generate the arithmetic mean or "expected" trajectory parameters if the sensitivity coefficients are constants. Those trajectory parameters whose sensitivity coefficients are nonlinear functions must be obtained through use of techniques such as the discrete distribution or "Monte Carlo" methods.

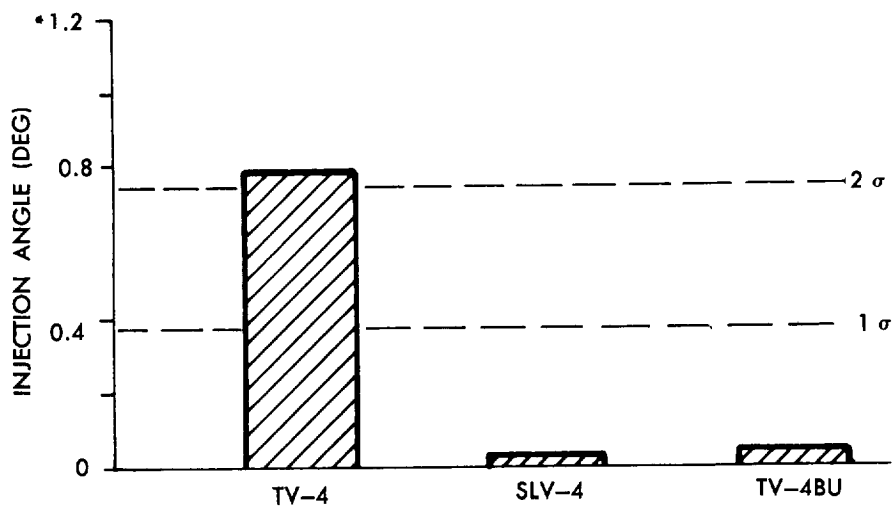
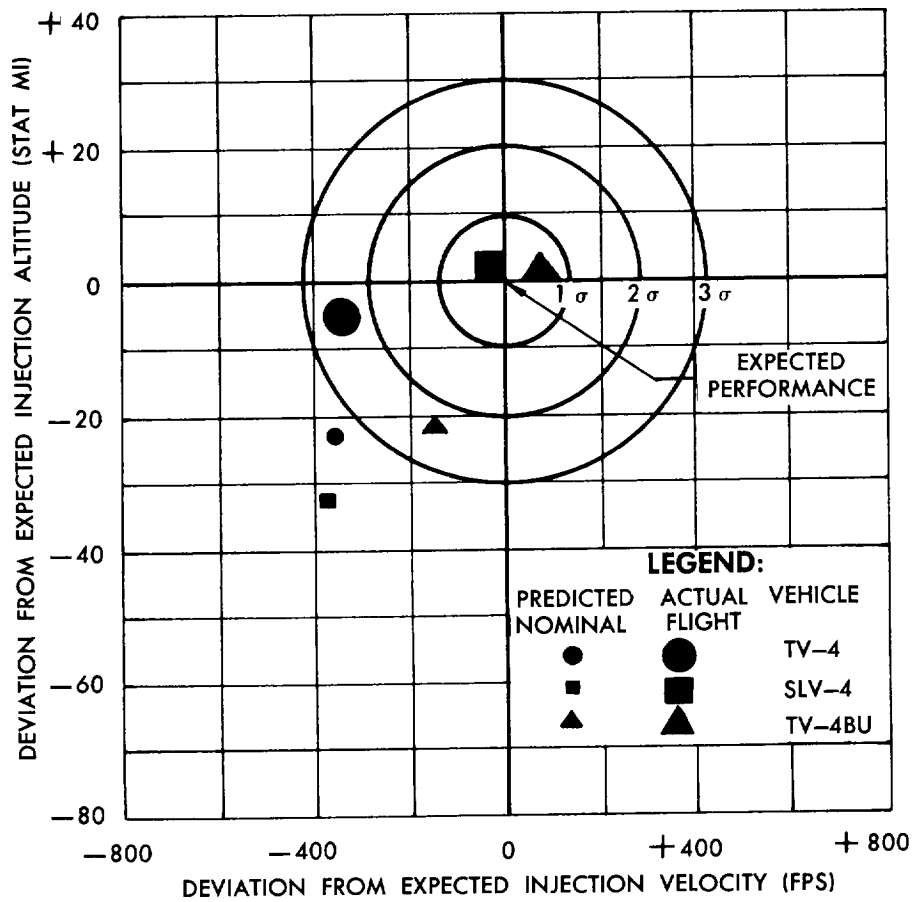


Fig. A-2 Comparison of Orbit Injection Conditions

**Table A-1. TV-4BU Trajectory Parameter Sensitivity to Changes in Input Parameters**

INPUT PARAMETERS	MEAN VALUE	STANDARD DEVIATION	INJECTION CONDITIONS					Orbit Period (min)	Orbit Apogee (stat mi)	
			Altitude (stat mi)	Velocity (fps)	Angle (deg)	Time (sec)	Range (stat mi)			
PROPULSION										
Gross Weight (lb)										
First Stage	17,979	74.6	— 6.3	— 20.1	—0.05	— 4.1	—10.1	—1.11	— 53.8	
Second Stage	4,405	9.1	— 2.5	— 25.5	—0.02	— 2.3	— 6.3	—0.80	— 40.9	
Propellant Consumed (lb)										
First Stage	16,060	93.4	+ 7.5	+ 78.2	—0.07	+ 7.9	+21.2	+1.47	+131.0	
Second Stage	3,295	14.2	+ 3.0	+ 62.8	—0.01	+ 5.2	+14.3	+1.72	+ 89.4	
Specific Impulse (sec)										
First Stage	251①	1	+ 4.1	+ 9.7	+0.04	+ 2.4	+ 5.8	+0.67	+ 31.8	
Second Stage	271	1	+ 2.0	+ 20.8	+0.02	+ 2.0	+ 5.6	+0.72	+ 36.8	
Third Stage	251	1	0	+ 59.6	0	0	+ 0.1	+1.32	+ 69.4	
Flow Rates (lb/sec)										
First Stage	110.7	0.545	+ 4.7	— 33.6	+0.10	— 0.6	— 2.5	—0.18	— 14.6	
Second Stage	27.4	0.40	+ 3.4	— 28.0	+0.13	— 1.7	— 3.9	—0.22	— 15.2	
Burning Time (sec)										
Third Stage	38	1	0	0	—0.01	+ 1.0	+ 2.9	0	0	
Thrust Misalignments (deg)										
First Stage	0	0.1	— 0.3	+ 9.0	+0.01	— 0.2	+ 0.4	+0.15	+ 9.0	
Second Stage	0	0.1	— 2.4	+ 30.2	+0.05	— 0.2	+ 2.1	+0.37	+ 23.2	
CONTROL SYSTEM										
Gyro Drift (deg/sec)	0	0.00025	+ 0.7	— 1.2	+0.05	0	— 0.5	—0.12	— 3.3	
Gyro Error (deg)	0	0.08	+ 1.1	— 18.6	+0.05	0	— 1.1	—0.30	— 15.1	
Program & Vibration	0	②	— 1.3	+ 17.0	—0.19	0	+ 2.0	+0.20	+ 13.2	
AERODYNAMIC										
Drag		+10%	— 3.0	— 5.3	—0.00	— 2.3	— 5.3	—0.45	— 21.3	
Wind	0	Spec	+ 2.1	— 76.3	—0.16	+ 0.2	— 8.8	—1.83	— 78.3	
STANDARD DEVIATION ③			± 10.1	± 141	± 0.37	± 10	± 28	± 3.1	± 177	
MAXIMUM DEVIATION ④			± 32	± 420	± 0.95	± 19	± 67	± 8.8	± 429	
TV-4BU TRAJECTORY PARAMETERS (50-lb Payload)										
	Expected		317	27,084	+0.1	584	888	127.8	2211	
	Actual		317	27,193	—0.05	582	884	130.2	2326	

① Sea level specific impulse.

② Varies with pitch rate—approximately 4 to 10 x 10<sup>-4</sup> deg/sec.

③ All parameters are essentially uncorrelated except gross weight and propellant consumed weight. First-stage correlation coefficient is 0.798, second-stage is 0.666.

④ Maximum deviation of one-sigma vehicles.

**Standard deviation**—The linearization of trajectory parameters with respect to input parameters allows a direct evaluation of the standard deviation (one-sigma change) of the trajectory parameters from the correlation and variances of the input parameters. The standard deviation of the trajectory parameters may be expressed by the equation:

$$\sigma_Y^2 = \sum_{i,j} Y_i Y_j \rho_{ij} = \sum Y_i^2 + 2 \sum_{i>j} Y_i Y_j \rho_{ij}$$

where:

$\sigma_Y$  = standard deviation of the trajectory parameter, Y

$Y_i$  or  $Y_j$  = change in the trajectory parameter, Y, due to a one-sigma change in input parameter i or j

$\rho_{ij}$  = the correlation coefficient between the input parameter i and the input parameter j.

**Correlation Coefficients**—Correlation coefficients are an indication of how different variables are inter-related. The Vanguard input parameters were found to be essentially uncorrelated, except for the stage liftoff weights and the propellants consumed for power. (The correlation of an input parameter with itself is, of course, one.)

**Probability**—The large number of independent variables involved should make those trajectory parameters which can be linearized tend toward a Gaussian distribution.

## B. APPLICATIONS OF THE PROBABILITY DESCRIPTION OF MISSILE PERFORMANCE

The probability method of describing performance presents a realistic analysis of the overall performance

of a large number of systems. The methods are applicable in many areas, but the translation of these mathematical identities into engineering terms is only as good as the converse translation. The Vanguard program revealed many areas where the probability description of vehicle performance could be profitably applied. Some of these areas are presented.

**Mission requirements**—Mission requirements should be phrased in terms that reflect the indeterminateness of the performance. Requirements that a trajectory parameter “be as large as possible” or “shall exceed” a certain minimum are not desirable. For example, should all vehicles whose system parameters are within a three-sigma or six-sigma range of their mean value meet the mission requirement? The probability description is particularly amenable to the type of specification which maximizes the probability of one or more trajectory parameters being between certain limits. The probability of mission success is increased by this realistic attitude, as against basing the design on the performance of a relatively improbable vehicle.

**Guidance system and trajectory optimization**—The determination of the “optimum” guidance system parameters (pitch rates, insertion times, etc.) is implemented by the probability description. That value of the parameter which maximizes the sigma contour tangent to the mission requirement will be the optimum value of the parameter. The type of trajectory flown also may be adjusted to minimize the deviation from the expected.

Often the accurate attainment of one or more trajectory parameters is of utmost importance. Vernier corrections, based on extensive ground-based observations of the trajectory, would be obtained at the expense of payload. A reasonable idea as to the possible (or probable) corrections required would minimize dead weight due to an overly conservative initial design.

**System controls**—Certain additional system controls could significantly decrease the probable performance variations. For instance, had the Vanguard program required it, more accurate flow rate control would have significantly decreased the possible performance variation. The weight penalty of such a device versus the weight penalty involved for comparable accuracy with a ground-controlled vernier system could be objectively compared by means of the probability approach.

**Reliability**—Estimates or limits for the probability of mission success, assuming no system malfunction, may be combined with system reliability data, which indicate the probability of catastrophic malfunction, to give an idea of the probability of mission success. This overall probability of success may be used to quantitatively compare proposed changes or alternate designs.

**Backup systems**—The addition of redundant systems to avoid catastrophic malfunction has a depressing effect on vehicle performance due to the additional weight involved. The increased reliability of the complete system should overshadow the weight penalty. The overall probability of mission success with and without the backup system allows a quantitative comparison of the systems.

**Range safety**—The predicted trajectory parameter limits must be large enough to include all possible nonmalfunctioning vehicles, but stringent enough to allow early detection of any trajectory deviations caused by component failure. The probability method of performance prediction allows a summation of absolute values of the deviations which represents the maximum deviation possible for a given class of vehicles. Table A-1 presents the maximum possible deviations of vehicles with one-sigma input parameters. These deviations correspond roughly to three times the predicted one-sigma deviation.

## C. SUMMATION

The probability approach is applicable during most phases of missile development. In the preliminary design, it encourages specifications which maximize the probability of success rather than requiring a conservative, low-probability vehicle to be the design criterion. The necessity for backup systems, safety devices and auxiliary guidance schemes for increasing accuracy and reliability can be recognized before the systems are finalized. During the development phase, the types and scopes of qualification programs can be evaluated, since a measure of their relative importance is available. Throughout the program, the trade-off between payload and performance margin of safety may be expressed in quantitative terms. Refinements of analyses and accumulations of pertinent data may be incorporated as they become available. The precision requirements of future missile and space missions will demand a quantitative estimate of the probability of success, which this method can provide.





**SINGLE COPY ONLY**